UCRL-11317

University of California

Ernest O. Lawrence Radiation Laboratory

INORGANIC MATERIALS RESEARCH DIVISION

ANNUAL REPORT, 1963

Berkeley, California

DISCLAIMER

Research and Development

UCRL-11317
UC-2 General Misc.
and Progress Report
TID-4500 (27th Ed.)

UNIVERSITY OF CALIFORNIA

Lawrence Radiation Laboratory
Berkeley, California

AEC Contract No. W-7405-eng-48

INORGANIC MATERIALS RESEARCH DIVISION
ANNUAL REPORT, 1963

March 25, 1964

Printed in USA. Price $3.50. Available from the
Office of Technical Services
U. S. Department of Commerce
Washington 25, D.C.

INORGANIC MATERIALS RESEARCH DIVISION
ANNUAL REPORT, 1963

Contents

INORGANIC MATERIALS RESEARCH DIVISION

ANNUAL REPORT, 1963

Leo Brewer, Division Head
Alan W. Searcy, Associate Division Head

Lawrence Radiation Laboratory
Department of Chemistry, Department of Mineral Technology
Department of Chemical Engineering and Department of Nuclear Engineering

March 25, 1964

GENERAL INTRODUCTION

This report contains statements of current staff research interest, descriptions of research recently completed, and list of publications and theses of the past year by members of the IMRD staff. This introductory section briefly presents information concerning IMRD personnel and developments during the past year which may serve to place the operations in perspective.

At the end of the 1963 calendar year, the Inorganic Materials Research Division, LRL, had been in operation for nearly 4 years. The number of principal investigators whose research is supported through the Division had reached 27, and the number of graduate students actively engaged in the research program stood at approximately 120.

During the first 4 years of operation of the Inorganic Materials Research Division, 34 M.S. and 50 Ph.D. degrees were awarded to students whose research was supported through the Division.

The Division has maintained an active program for exchange of information with scientists in different disciplines and with scientists from other institutions. Approximately 25 young Ph.D. men were engaged in our research program on 1- to 3-year postdoctoral appointments.

Professors Harold S. Johnston, Edward A. Grens, and John S. Newman have joined the Division staff of principal investigators for limited terms of approximately 3 years. Professors Grens and Newman are new members of the Department of Chemical Engineering. Professor Johnston of the Department of Chemistry is internationally known for his outstanding studies in the kinetics of gas-phase reactions. Dr. Johnston will make use of the outstanding design and shop facilities of the Lawrence Radiation Laboratory in developing a new apparatus for detection of reactive intermediates of reactions in shock tubes, flash tubes, etc., at levels of 10^{12} molecules per cc, by measuring the decay constant of absorbed light in an optical cavity.

Dr. Lawrence Himmel transferred from our Division at the end of 1963 to the Lawrence Radiation Laboratory at Livermore and Professor Dudley R. Herschbach left the Division and the University to accept a position as Professor of Chemistry at Harvard University.

Professor Norman Phillips was awarded a Guggenheim Fellowship for a year of study at Oxford University.

Professor Richard Fulrath was presented the Ross Coffin Purdy Award by the American Ceramic Society.

Professor John Chipman, who recently retired as Chairman of the Metallurgy Department at MIT, spent a month as a consultant to the Division on problems in metallurgical thermodynamics. Professor Harry Bloom of the University of Tasmania spent approximately three months of his sabbatical leave on a part-time appointment with our Division. Dr. Sadakichi Kitajima, Assistant Professor from Kyushu University, has also been visiting us and doing a research study of preferential work-hardening phenomena in metals.

Dr. Victor F. Zackay has completed most of the arrangements for the second International Materials Symposium to be sponsored by the Laboratory. This symposium, to be held June 15-18, 1964, is on the topic, "High-Strength Materials."

During the 1963 calendar year there were 80 contributions to the regular technical literature and many additional papers were published as UCRL reports. Among the publications of the year were two books:

Gareth Thomas and Jack Washburn, Electron Microscopy and Strength of Crystals (Interscience Publishers, Inc., New York, 1963).

Ralph Hultgren with Raymond L. Orr, Philip E. Anderson, and Kenneth K. Kelley, Selected Values of Thermodynamic Properties of Metals and Alloys (John Wiley & Sons, Inc., New York, 1963).

Additional books by IMRD staff members were:

Earl Parker, editor, Materials for Missiles and Spacecraft, University of California Engineering and Science Extension Series, (McGraw-Hill Book Company, Inc., New York, 1963).

Bruce Mahan, Elementary Chemical Thermodynamics (W. A. Benjamin, New York, 1963).

An informal ground-breaking ceremony for a new laboratory building to house the expanded operations of the Division was held in June. At the time that this report went to press, construction of the building was proceeding on schedule, and the building is expected to be ready for occupancy in November of 1964.

PRINCIPAL STAFF MEMBERS

December 31, 1963

Leo Brewer	Division Head
Alan Searcy	Associate Division Head
Ira Pratt	Assistant Division Head
T. H. Chenoweth	Business Officer

Robert E. Connick

John E. Dorn

Richard M. Fulrath

Ralph Hultgren

William L. Jolly

George Jura

Bruce N. Mahan

Rolf H. Muller

Rollie J. Myers

Donald R. Olander

Edwin F. Orlemann

Earl R. Parker

Joseph A. Pask

Norman E. Phillips

Otto Redlich

Charles Sederholm

Gareth Thomas

Charles W. Tobias

Jack Washburn

Victor F. Zackay

Edward A. Grens

Harold S. Johnston

John S. Newman

Thomas H. Pigford

ADDITIONAL STAFF MEMBERS

1. M. Adamson
2. G. Blue
3. O. Boedtker*
4. D. Budworth*
5. J. Cashion*
6. Y. Chang*
7. M. Child*
8. R. Cooper
9. D. Fiat
10. L. Finegold
11. L. Finnie
12. M. Fluendy*
13. G. Gilbert
14. S. Gokhale
15. R. Goodrich
16. C. Hallada*
17. R. Hasty*
18. L. Himmel*
19. Y. Ishida
20. S. Kitajima
21. M. Lambert
22. R. Langston
23. B. Lichter
24. J. Link
25. K. Maguire*
26. D. Meschi
27. B. Meyer
28. A. Mukherjee
29. R. Muller
30. Y. Oishi
31. M. Onillon*
32. R. Orr
33. M. Pickus
34. S. Ray
35. A. Rosen
36. G. Rosenblatt*
37. L. Toth
38. W. Worrell

* Completed IMRD association during 1963

GRADUATE STUDENTS DURING 1963

1. G. Ahlers
2. A. Ahmadieh
3. S. Antolovich
4. A. Atallah
5. T. Atkins
6. M. Barry
7. E. Barrish
8. R. Batt
9. H. Bell
10. W. Bell
11. J. Birely
12. B. Blank
13. S. Blank
14. E. Blatt
15. M. Borom
16. M. Villena-Blanco
17. G. Brabson
18. P. Brooks
19. R. Busch
20. J. Camahort
21. T. Carlton
22. R. Carpenter
23. T. Cass
24. C. Cheng
25. A. Chutjian
26. S. Copley
27. J. Cross
28. O. Dabbousi
29. S. Dahlgren
30. A. Das
31. G. Das
32. G. DePoorter
33. D. Dickson
34. R. Duerst
35. N. Durai Raghavan
36. R. Eberhart
37. A. Falick
38. J. Ferretti
39. R. Fleck
40. W. Gardner
41. V. Goel
42. S. Gross
43. M. Guinan
44. R. Gunn
45. S. Gupta
46. L. Hagan
47. R. Hamilton
48. F. Harper
49. P. Hart
50. Y. Hashimoto
51. D. Hasselman
52. R. Hauge
53. R. Herm
54. J. Ho
55. J. Hoffer
56. G. Horvath
57. L. Hsu
58. R. Ivanetich
59. M. Jacobson
60. O. Johari
61. J. Johnston
62. M. Judkins
63. V. Kannan
64. K. Kennedy

65. D. Koenig
66. R. Kortzeborn
67. R. Krakowski
68. P. Kroopnick
69. G. Kwei
70. Y. Lee
71. D. Levy
72. M. Lim
73. C. Lindahl
74. T. Lusebrink
75. D. Maher
76. A. Marchetti
77. J. Masse
78. W. Mathews
79. D. McCain
80. P. McKinney
81. C. Merideth
82. D. Messier
83. D. (Monahan) Meyer
84. A. Miller
85. J. Mitchell
86. R. Moon
87. M. Moseman
88. J. Mote
89. J. Muirhead
90. G. Murty
91. D. Nason
92. J. Neumann
93. R. Newmark
94. A. Nunes
95. S. Ng
96. M. Nicol
97. P. Nicholson
98. R. Nolder
99. J. Norris
100. J. Papazian
101. A. Pasternak
102. P. Patel
103. C. Peltzer
104. J. Person
105. P. Petroff
106. D. Phillips
107. J. Poksheva
108. D. Porter
109. L. Posey
110. D. Pratt
111. S. Rajnak
112. K. Ravi
113. W. Roser
114. R. Rossi
115. P. Roy
116. F. Rufeh
117. K. Savage
118. N. Senozen
119. R. Shannon
120. Y. Shen
121. M. Shetlar
122. R. Sigal
123. J. Smith
124. C. Souers
125. J. Spencer
126. O. Stansfield
127. W. Stark
128. J. Strudel
129. Sister G. Thompson
130. J. Thunen
131. L. Van Torne
132. G. Vellaikal

133. R. Villagrana
134. R. Walsh
135. C. Washburn
136. M. Wells
137. K. Wilson
138. C. Young
139. R. Zare

I. CHEMISTRY

A. INORGANIC CHEMISTRY

1. NUCLEAR MAGNETIC RESONANCE STUDIES OF COMPLEX IONS

Elaine C. Blatt and Robert E. Connick

Nuclear magnetic resonance techniques on O^{17} have proven invaluable in the measurement of the very high rates of water exchange from paramagnetic transition-metal cations.[1] In the studies of complex ions, the resonance method is proving equally versatile.

The complex ion studies were undertaken in order to provide more information about the interactions in the electronic systems of the coordination complexes. Upon the change of constituents of the first coordination sphere of a complex ion, an effect was observed on the water exchange rate which can be related to the influence of ligands in bonding. Of the aquo-cations whose water exchange rate has been measured in this Laboratory, ferric[2] and nickelous[1] ions at room temperature have water exchange rates that are slower than the transverse relaxation of O^{17} caused by the paramagnetic ions. Thus, the broadening of the bulk O^{17} resonance is a direct measure of the chemical exchange rate. A detailed investigation of the ferric chloride system has been conducted at room temperature. The line widths of O^{17} in solutions of varying free chloride concentration can be analyzed to yield characteristic values for the contributions to the relaxation of the O^{17} from interaction with various chloride complexes. These values are sums of the relaxation rates resulting from different processes by which a water molecule is removed from the bulk solution and involved in a complex ion, i.e., direct water-water replacement, or replacement of chloride ligand by a water molecule. In all cases, unless a temperature-dependence study shows otherwise, these characteristic numbers yield only lower limits to the various reaction processes involved. Cogent arguments are available in favor of an interpretation of the line widths as a direct measure of chemical exchange rates. These are given in more detail in a publication now in preparation. A temperature study on the O^{17} in ferric chloride solutions is contemplated, but the value of such an experiment is diminished by the lack of information on the heats of complexing of the higher chloro complexes. Even the room temperature results are subject to serious uncertainties because of the possible errors in the literature values for the equilibrium quotients.

---

1. T. J. Swift and Robert E. Connick, J. Chem. Phys. 37, 307 (1962).
2. Edward E. Genser, Studies of Fast Exchange Reactions by the Use of Nuclear Magnetic Resonance (Thesis), UCRL-9846, January 1962.

Relative to the rate of water exchange on the aquo ferric ion, the first chloro complex appears to exchange waters about twice as fast. The contribution from the reaction whereby water replaces chloride on the monochloride complex is very small.[3] In the dichloro- and trichloro-complexes such information is not available. For the composite rate of all possible paths for water to be removed from the bulk of the solution, the best fit to the NMR data yields the following: dichloro-complex, about three times as fast as aquo ion: and trichloro-complex, perhaps thirty times as fast as aquo ion.

Although the water exchange rate is so much higher than the rate of replacement of chloride by water in the monochloro-complex, in 3 M chloride and 0.1 M ferric where the higher complexes are present, the chloride exchange rate as measured by NMR of Cl^{35} seemed to indicate that the chloride ions were exchanging at least as rapidly as the water molecules would be in a solution of the same composition. Perhaps a chloride-chloride exchange reaction is more favored than a water-chloride replacement reaction. Investigation of the Cl^{35} resonance at lower free chloride concentration seems to hint at a sharp dependence of the chloride exchange rate on free chloride concentration. A study of the effect of temperature on a 0.015 M Fe(III), 1 M Cl^- solution shows no evidence of a decrease of the relaxation rate up to 85°C, and in fact shows a significant increase in rate, which would reinforce the idea that the Cl^{35} transverse relaxation is being controlled by chemical exchange. More accurate measurements will be carried to 100°C. The very large quadrupole moment of Cl^{35} might allow an interpretation of the Cl^{35} spectra to include interactions, decreasing the relaxation time, which are not contributed by scalar coupling, the mechanism that we are attributing to the bonding between ferric ion and O^{17} in the complex. Ionic interactions might affect the chlorine resonance more markedly than the O^{17} resonance. Measurements of the longitudinal relaxation time on Cl^{35} would give valuable information on this subject.

In the case of the aquo-nickelous ion, a bendover was observed in the plot of T_{2p}, the relaxation time due to the paramagnetic ion versus the reciprocal of the absolute temperature.[1] This bendover was attributed to a region where the chemical exchange rate was becoming too fast to allow sufficiently satisfactory relaxation during the time spent in the first coordination sphere. Ignoring the probable changes in the relaxation power of the nickelous core upon complexing with ligands other than water, one might expect that the water exchange rate would be fast enough in some complexes to bring us to the region where the relaxation rate is the slow step at room temperature. It is interesting to note that a solution containing the first nickelous ammonia complex produces a larger line width for O^{17} than a comparable nickelous aquo solution, but when the complexing with ammonia is increased the line width narrows. Perhaps the higher nickelous complexes with ammonia exchange waters too fast to allow sufficient relaxation, even at room temperature. A study of the effect of varying temperature in this system is planned for the near future. Heats of complexing are available,

3. R. E. Connick and C. P. Coppel, J. Am. Chem. Soc. 81, 6389 (1959).

and we expect to correlate this work with data on N^{14} resonance available from another Laboratory.[4] A chemical shift is noticeable in the O^{17} work on nickelous-ammonia. Preliminary work indicates a frequency dependence for the transverse relaxation time, consistent with that found in aquo-nickelous ion.[1]

4. John P. Hunt and H. W. Dodgen, Washington State University.

2. THE TEMPERATURE DEPENDENCE OF THE TRANSVERSE RELAXATION TIME OF O^{17} IN AQUEOUS SOLUTIONS CONTAINING CUPRIC IONS

Charles W. Merideth and Robert E. Connick

The temperature dependence of the transverse relaxation time of O^{17} in aqueous solutions containing cupric ions has been studied previously in this Laboratory.[1] This earlier study was carried out in order that the rate of exchange of water molecules from the first coordination sphere could be measured. The results seemed to lead to two conclusions. First, very low temperatures will be required in order to reach the region where the relaxation will be governed by the slowness of chemical exchange. Secondly, it was postulated that there are two possible paths by which the water molecules exchange. On the assumption that the cupric ions have a coordination number of six and that the structure of the molecule is a distorted octahedron (owing to the Jahn-Teller configurational distortion), it was postulated that below approximately 80°C the axial molecules were providing the exchange path and above 80°C the equatorial water molecules were beginning to exchange. This conclusion was based on a slight bendover observed in the plot of $\ln T_{2p}$ vs $1/T°A$ for Cu(II) near 100°C.

In the present study the temperature range of the previous study was extended in order that the two above conclusions would be examined more closely. The temperature range covered here was from -55°C to 150°C (compared to 0°C to 100°C in the previous work). The high-temperature region was made accessible by using sealed glass sample tubes designed to withstand the pressures generated by the aqueous solutions when heated. The subzero temperatures were obtained by use of eutectic solutions of perchloric acid and water. It has been shown that at 42.7% solution of perchloric acid freezes at approximately -55°C.[2] The temperatures were controlled over the entire range within at least 1° by using the Varian EPR temperature-control unit that has been modified for the Varian Wide-Line NMR Spectrometer.

The high-temperature results of the present study show no evidence of the bendover in the plot of $\ln T_{2p}$ vs $1/T°A$ for Cu(II) that was observed in the previous work.[1] Thus the postulate that the equatorial water molecules

1. T. J. Swift and R. E. Connick, J. Chem. Phys. 37, 307 (1962).
2. Langhorn H. Brickwedde, J. Res. Nat. Bur. St. C 42, 309 (1949).

are beginning to exchange in the temperature region above 80°C has to be discarded. The results of the present work indicate that the same mechanism of exchange must be operative above and below 80°C. However, the hypothesis that it is the axial molecules (believed to be less tightly bound than the equatorial water molecules) which are exchanging still appears to be a good one. This will offer an explanation of why the observed rate of exchange of the water molecules from the first coordination sphere of Cu(II) is several orders of magnitude greater than the rates observed for most of the other metal ions studied in the previous work.[1] It is still possible that this new region, where the equatorial water molecules begin to exchange directly with the bulk water, may exist--but at a very high temperature. The results of this study indicate that at 150°C we may still be quite far from this region. There is also a good possibility that the equatorial waters participate in the relaxation through inversion of the octahedron, rather than by direct exchange.[1]

In preliminary measurements the low-temperature data revealed two very interesting results that may require a closer analysis of this region. First, the observed line width of O^{17} in 42.7% perchloric acid is the same as it is in pure water within experimental error. However, the line width of O^{17} in the 42.7% solution of perchloric acid in the presence of Cu(II) (1.0×10^{-3} M) is about twice as broad at 25°C as it is in pure water in the presence of the same amount of the paramagnetic ion. This effect must be checked.

The second interesting observation made in the low-temperature region is that the system may be on the threshold of the region where the relaxation is controlled by the slowness of chemical exchange. Complete analysis of the data has not been carried out to verify this point, and no definite conclusions can yet be drawn.

The present work shows conclusively that the bendover observed in the high-temperature region of the previous work was spurious and does not in fact exist in the range from 0°C to 150°C. Also, the data indicate that it may be possible to reach the region where the relaxation is controlled by the slowness of chemical exchange at very low temperatures by using a perchloric acid–water eutectic solution.

3. COORDINATION NUMBERS OF BERYLLIUM AND ALUMINUM IONS IN AQUEOUS SOLUTIONS AND THE RATE OF EXCHANGE OF THE BOUND WATER

Daniel N. Fiat

With a method proposed by Jackson, Lemons, and Taube[1] the coordination numbers of beryllium and aluminum ions in aqueous solutions were determined by means of NMR.[2] Addition of cobaltous perchlorate to the solutions of aluminum or beryllium ions shifted the O^{17} NMR signal of the free water to a low field, whereas the signal of the bound water was not shifted

1. Jackson, Lemons, and Taube, J. Chem. Phys. 33, 553 (1960).
2. R. E. Connick and D. N. Fiat, J. Chem. Phys. 39, 1349 (1963).

appreciably. The coordination numbers of the ions were calculated from the relative areas of the free to the bound water signals and the composition of the solutions, and were found to be 4.0±0.2 for the Be^{++} ions and 6.0±0.2 for the Al^{+++} ions at room temperature.

The form of the absorption curves and their temperature dependence revealed quite different exchange rates and mechanisms of relaxation for the two ions.

The absorption signals of the bound and of the free water of the Be^{++} and Al^{+++} solutions were overlapping, but if Lorentzian could be resolved. For the Al^{+++} ion this was found to be the case, but in the Be^{++} the resolved curves were asymmetric and broadened, indicating exchange broadening. The temperature dependence of the width of the line (Fig. IA.3-1) and of the relative shift of the bound to the free water (Fig. IA.3-2) confirm this indication. It is seen that for the Be^{++} ions the width of the line increases as a function of temperature, whereas for the Al^{+++} it decreases. We must conclude that for the Be^{++} ions the exchange rate contributes significantly to the line width. For the Al^{+++} ions there is no indication of exchange broadening even up to 80°C, but at higher temperatures this effect appears to be setting in.

The decrease in the shift of the bound relative to the free water as a function of temperature for the Be^{++} ions in agreement with the above explanation, as increase in the rate of exchange should cause the lines to approach each other.

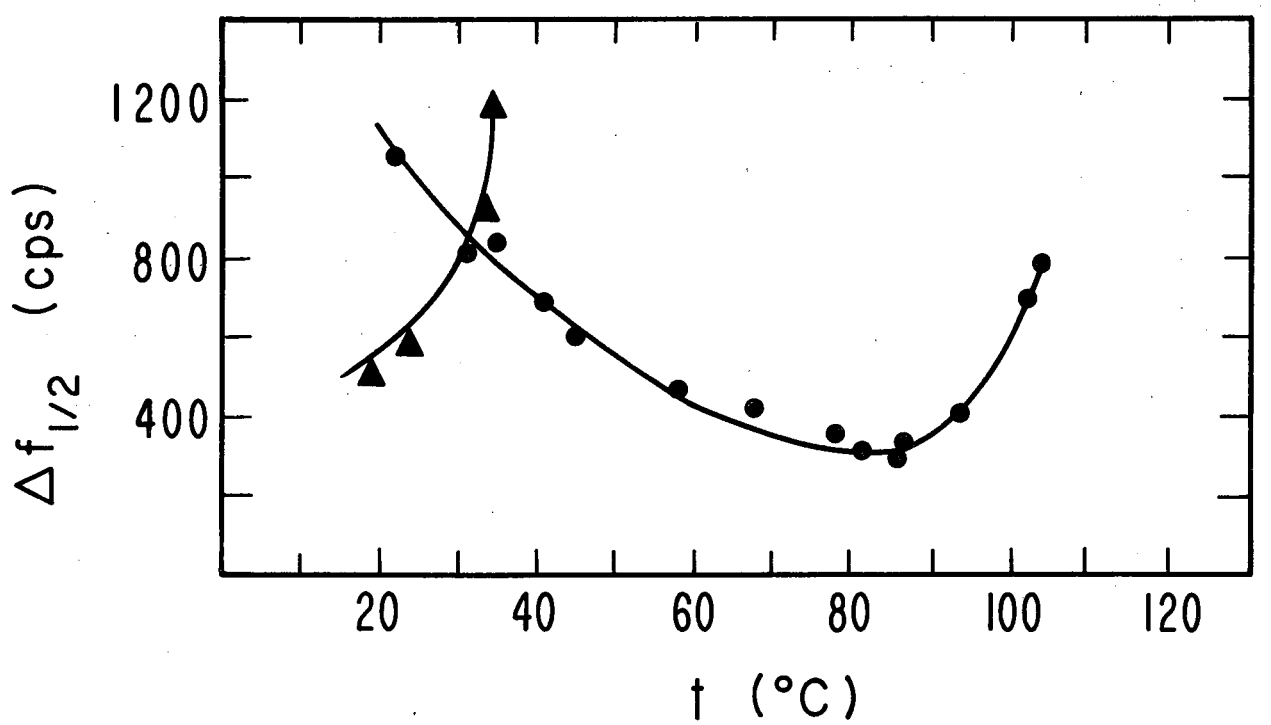

MUB-2857

Fig. IA. 3-1 The width at half height of O^{17} absorption signals as a function of temperature for water bound to Al^{+++} and Be^{++} ions.

○ Solution composition in millimoles: $AlCl_3$, 2.60; H_2O, 91.0; $HClO_4$, 0.812; $Co(ClO_4)_2$, 0.396.

△ $BeCl_2$, 4.868; H_2O, 86.47; $HClO_4$, 1.72; $Co(ClO_4)_2$, 0.520.

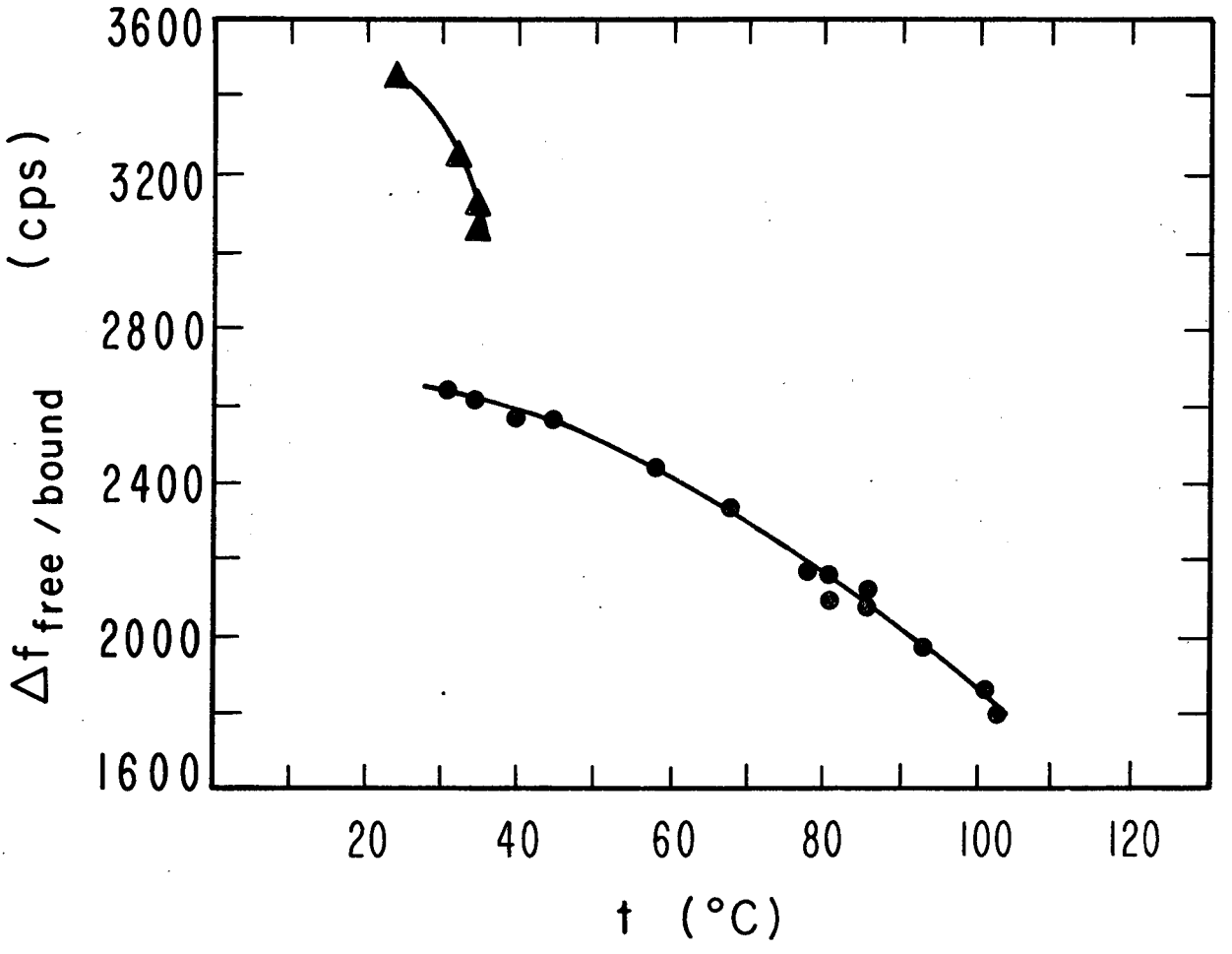

MUB-2858

Fig. IA. 3-2 The shift of the free water relative to the bound as a function of temperature.

○ Solution composition in millimoles: $AlCl_3$, 2.60; H_2O, 91.0; $HClO_4$, 0.812; $Co(ClO_4)_2$, 0.396.

△ $BeCl_2$, 4.868; H_2O, 86.47; $HClO_4$, 1.72; $Co(ClO_4)_2$, 0.528.

4. HYDROLYTIC POLYMERIZATION IN Cr(III) SOLUTIONS

Sister Gertrude Thompson and R.E. Connick

A blue species isolated from refluxed solutions of Cr(III) has been identified as a dimer of the form $Cr_2(OH)_2^{4+}$ or Cr_2O^{4+}.[1,2,3] Rate studies of the decomposition of this species have been carried out in acid solutions of varying concentration (0.005 M to 7 M) at 25.00 (±.05), 35.50(±.05), and 45.00(±.05)°C. In the solutions of lower acid concentration, a constant ionic strength of $\mu = 2.00$ has been maintained with either sodium or lithium perchlorate.

The kinetics of the decomposition indicate a two-step process and point to the existence of an intermediate complex. It is postulated that this species is a singly bridged complex, $Cr_2(OH)^{5+}$. Attempts to isolate the material on an ion-exchange column have been unsuccessful, but a green band of higher charge than the dimer-- i.e., resting higher on a column than the dimer-- can be detected in solutions known to contain large quantities of intermediate. A spectrum of the intermediate species in concentrated perchloric acid has been obtained ($\epsilon_{590} = 17.2$, $\epsilon_{420} = 22.3$ at the maxima).

If the blue dimer is added to concentrated perchloric acid (70%) and left for several half lives, very significant concentrations of the intermediate are formed. The rate at which this species re-forms the dimer can be followed as a function of hydrogen ion concentration, either by merely diluting the solution or by partially neutralizing the acid with a solution of sodium bicarbonate.

ESR and magnetic susceptibility measurements at room temperature have been made of freshly prepared (a) monomer, $Cr(H_2O)_6^{3+}$; (b) dimer $Cr_2(OH)_2^{4+}$, and (c) a green species isolated from refluxed solutions and believed to be a trimer, $Cr_3(OH)_4$. The g values determined for these species are 1.980, 1.976 and 1.942, and the susceptibilities 3.90, 3.71, and 3.54 (Bohr Magnetons), respectively. A magnetic susceptibility measurement in high acid concentration (11.5 M) and therefore of the intermediate only has also been made, yielding a value of 3.32 B.M. Measurements of magnetic susceptibility of the stable species at varying temperatures (0 to 50°C) are being made at present.

Determination of the freezing-point lowering in eutectic mixtures of $HClO_4$ and H_2O (41.7% $HClO_4$) has been undertaken for the three stable species, $Cr(H_2O)_6^{3+}$, $Cr_2(OH)_2^{4+}$ and $Cr_3(OH)_4^{5+}$. Previously Ardon and Lineberg[4] did such measurements for $Cr(H_2O)_6^{3+}$ and for what they thought was

1. James E. Finholt, Chemistry of Some Hydrolyzed Cr(III) Polymers (Thesis), UCRL-8879, April 1960.
2. J. A. Laswich and R A. Plane, J. Am. Chem. Soc. 81, 3564 (1959).
3. M. Ardon and R. A. Plane, J. Am. Chem. Soc. 81, 3197 (1959).
4. M. Ardon and A. Lineberg, J. Phys. Chem. 65, 1443 (1961).

the dimer, although the solution may have contained some intermediate. Since the blue species readily equilibrates at room temperature with the intermediate in solutions of comparable acidity (5.5 M), confirmation of the dimeric character of the intermediate can be deduced from the observation that the freezing-point lowering of pure dimer and dimer-intermediate mixtures has the same value. To insure the presence of dimer alone, a solution is injected into chilled perchloric acid solution (-10°C). Freezing-point lowering measurements on the green species, supposed to be a trimer, are also being carried out.

A fine crystalline powder is thrown down when a concentrated solution (4 M) of the dimer is added to perchloric acid (70%). On standing, further crystallization takes place and larger crystals, which x-ray analysis confirm as $Cr(H_2O)_6(ClO_4)_3$, are formed. The first fine powder gives a rather more complex and decidedly different pattern from that of $Cr(H_2O)_6(ClO_4)_3$. Single crystals of this material large enough for x-ray work have not yet been produced. A solution of the material has a spectrum like that of the dimer.

A determination of the equilibrium constant of the reactions

$$2Cr^{3+} + 2H_2O = Cr_2(OH)_2^{4+} + 2H^+ \qquad (1)$$

and

$$3Cr^{3+} + 4H_2O = Cr_3(OH)_4^{5+} + 4H^+ \qquad (2)$$

has been carried out in solutions of constant ionic strength (μ = 1.00) at 50.00(±05)°C, by an ion-exchange technique. Solutions are equilibrated until a constant pH value has been obtained, then chilled rapidly, and separated on a column of Dowex 50WX4 resin by elution with a 0.5 M calcium perchlorate solution. The concentration of all chromium species can be obtained, and the pH of the solutions is measured at the temperature of equilibration.

5. ANIONIC CHLORO-COMPLEXES OF RUTHENIUM(III)

Martyn G. Adamson

An attempt is being made to obtain good crystalline samples of the relatively insoluble salts of the higher (anionic) chloro-complexes of Ru(III) with the cations of cesium, rubidium, potassium, and possibly barium. Inspection under a microscope of the reddish-brown precipitate formed by adding 1 M cesium chloride to stock solutions of Ru(III) in 6 M HCl reveals that it consists of many small needle-like crystals. This solid, presumably $Cs_2[RuCl_5 \cdot H_2O^{2-}]$ is fairly soluble in 6 M HCl. The possibility that $[RuCl_4(H_2O)_2^-]$ also forms reasonably insoluble salts with certain alkali or alkaline earth metal cations--e.g., Cs^+ or Ba^{2+}-- is also being investigated. X-ray crystallography on pure crystalline specimens of the $RuCl_4^-(x)$ and $RuCl_4^-(y)$ salts would confirm which was the cis-isomer and which was the trans-isomer.

6. PROTON MAGNETIC RESONANCE SPECTRA OF SILYLPHOSPHINE, SILYLARSINE, GERMYLPHOSPHINE, AND GERMYLARSINE*

J. E. Drake+ and W. L. Jolly

The chemical shifts and coupling constants for these hydrides have been measured and interpreted.

* Abstract of paper in J. Chem. Phys. 38, 1033 (1963).
+ Now at Chemistry Department, University of Southampton, Southampton, England.

7. THE PREPARATION OF VOLATILE HYDRIDES IN AN ELECTRIC DISCHARGE

Sudarshan D. Gokhale and William L. Jolly

Techniques have been developed for the preparation of high-molecular-weight hydrides in an electric discharge, and for their separation and isolation by gas chromatography. These methods have been used for the preparation of the two isomers of tetrasilane, Si_4H_{10}, and the two isomers of Si_2PH_7. These isomers have been unambiguously identified by their NMR spectra, and, where possible, by their infrared spectra and chemical properties.

8. THE SYMMETRICAL DEFORMATION FREQUENCIES OF METHYL, SILYL, AND GERMYL GROUPS*

William L. Jolly

The symmetrical deformation frequencies of the MH_3 groups in compounds of the type H_3M-X (where M = Si or Ge, and where X may be bound to other atoms) increase with increasing electronegativity of the atom X. These correlations and the similar correlation for methyl groups may be explained in terms of the repulsions between the M-H bonding electrons and the electrons in the valence orbitals of the X atom (in particular, the M-X bonding electrons and any nonbonding electrons on the X atom).

* Abstract of paper in J. Am. Chem. Soc. 85, 3083 (1963).

9. THE REACTION OF BOROHYDRIDE WITH FERRICYANIDE

Lydia S. Hsu and William L. Jolly

The kinetics of the reaction of ferricyanide with borohydride (in the concentration ranges, for both reactants, of 0.1 to 0.5 M) has been studied in alkaline aqueous solution at room temperature. The reaction was found to be catalyzed by glass surfaces. This catalysis, however, can be avoided by using wax-coated surfaces. The rate of change of the hydroxide ion concentration was found to be first order in both ferricyanide and borohydride and independent of the hydroxide ion, at least in the high pH region, with a rate constant of 4.93×10^{-4} $M^{-1}min^{-1}$. This result is different from that found by Freund[1] for very dilute buffered solutions of ferricyanide and borohydride. Under the conditions of Freund's experiments, no glass catalysis was observed.

1. T. Freund, J. Inorg. Nucl. Chem. 9, 246 (1959).

10. ABSORPTION SPECTRA OF CALCIUM-AMMONIA SOLUTIONS*

Calvin Hallada+ and William L. Jolly

It was observed that, for concentrations up to 0.025 M at -45° and for wavelengths in the region of 15 000 Å, calcium obeys Beer's Law in liquid ammonia. The molar extinction coefficients are twice those for alkali metal solutions; consequently it is clear that two moles of solvated electrons are produced per gram-atom of calcium dissolved. Conductivity studies indicated that the boundary between the one-phase and two-phase regions on the ammonia-rich side of the Ca-NH_3 phase diagram lies at 0.013 M at -64° and 0.032 M at -45°.

* Abstract of paper in Inorg. Chem. 2, 1076 (1963).
+ Now at Conductron Corporation, Ann Arbor, Michigan.

11. CONVENIENT METHODS FOR PREPARING $S_3N_2Cl_2$ AND S_4N_3Cl*

William L. Jolly, Keith D. Maguire+, and David Rabinovich‡

When a suspension of ammonium chloride in S_2Cl_2 is refluxed, the principal reaction products are NSCl and HCl:

$$NH_4Cl + 2S_2Cl_2 \longrightarrow 3S + NSCl + 4HCl.$$

The vapors of S_2Cl_2 and NSCl react to form $S_3N_2Cl_2$:

$$2NSCl + S_2Cl_2 \longrightarrow S_3N_2Cl_2 + SCl_2.$$

By refluxing $S_3N_2Cl_2$ with carbon tetrachloride, S_4N_3Cl may be prepared:

$$3S_3N_2Cl_2 \longrightarrow 2S_4N_3Cl + SCl_2 + Cl_2.$$

The compounds NSCl, $S_3N_2Cl_2$, and S_4N_3Cl are useful intermediates for the preparation of other sulfur-nitrogen compounds.

* Abstract of paper in Inorg. Chem. 2, 1304 (1963).
+ Now at Pennsalt Chemical Corporation, King of Prussia, Pennsylvania.
‡ Now at Chemistry Department, San Jose State College, San Jose, California.

12. FOUR NEW METHODS FOR THE PREPARATION OF NSCl*

Keith D. Maguire+, Jerry J. Smith, and William L. Jolly

Glemser[1] has reported that NSCl may be prepared by the pyrolysis of $(NSCl)_3$. We report four additional methods for preparing NSCl.

The equations for these reactions are

$$S_2Cl_2 + 2N \longrightarrow 2NSCl \text{ (mechanism not yet clear)}, \quad (1)$$

$$NH_4Cl + 2S_2Cl_2 \longrightarrow 3S + NSCl + 4HCl, \quad (2)$$

$$3S_3N_2Cl_2 \longrightarrow 2S_3N_2Cl + 2NSCl + SCl_2, \quad (3)$$

$$S_3N_2Cl_2 + Cl_2 \longrightarrow 2NSCl + SCl_2 \quad (4)$$

* Abstract of paper in Chem. & Ind., 1589 (1963).
+ Now at Pennsalt Chemical Corporation, King of Prussia, Pennsylvania
1. O. Glemser and H. Richert, Z. anorg. allgem. Chem. 307, 313 (1961).

13. THE CHEMISTRY OF SULFUR-NITROGEN COMPOUNDS

Millagros Villena-Blanco+, Keith D. Maguire‡, and William L. Jolly

The reaction between gaseous ammonia and sulfur chlorides (S_2Cl_2 and SCl_2) has been studied under various conditions of temperature, flowrate of ammonia, concentration and type of sulfur chloride, solvent, and duration or run, for the purpose of determining the optimum conditions for the preparation of S_4N_4 and S_7NH. Adsorption-column chromatography on alumina and silica gel columns was employed for the quantitative separation of the reaction products.

S_4N_4 is reported[1] to react with dry hydrogen chloride to yield a red adduct of composition $S_4N_4 \cdot 4HCl$ which is readily converted to S_4N_3Cl. A further adduct $S_4N_4 \cdot HCl$ is also reported.[2] The reaction between S_4N_4 and dry hydrogen chloride was examined in order to determine what adducts are formed and to determine the overall stoichiometry of the reaction. The establishment of a definite stoichiometry is made difficult by the fact that the intermediate products S_3N_2Cl and S_4N_3Cl react slowly with HCl. However, we believe the limiting reaction to be

$$S_4N_4 + 8HCl \longrightarrow 2NSCl + 2NH_4Cl + 2SCl_2.$$

+ Now at Department of Chemistry, University of California, Riverside, Calif.
‡ Now at Pennsalt Chemical Corporation, King of Prussia, Pennsylvania.
1.A. G. MacDiarmid, Nature 164, 1131 (1949).
2.M. Becke-Goehring, Ergebnisse und Probleme der Chemie der Schwefelstickstoffverbindungen (Akademie-Verlag, Berlin, 1956).

14. SOME REACTIONS OF P_2Cl_4*

Charles B. Lindahl+ and William L. Jolly

Diphosphorus tetrachloride, with a lone pair of electrons on each phosphorus, can react as a monofunctional and difunctional Lewis base.

Nickel carbonyl and P_2Cl_4 can react at 0° to form a series of compounds the relative amounts of which depend upon the relative ratios of the reactants and the CO pressure in the reaction vessel. A large excess of $Ni(CO)_4$ reacts with P_2Cl_4 to form the yellow-white solid $P_2Cl_4 \cdot 2Ni(CO)_3$. At carbon monoxide pressures less than 0.3 atm, this material decomposes at 0°. With roughly equal molar amounts of P_2Cl_4 and $Ni(CO)_4$, a yellow solid of approximate empirical formula $P_2Cl_4 \cdot Ni(CO)_2$ is formed. A polymeric structure, $[P_2Cl_4 \cdot Ni(CO)_2]_x$, with terminal groups of P_2Cl_4 or $Ni(CO)_3$ is suggested for this material. Large excesses of P_2Cl_4 react with $Ni(CO)_4$ to form a yellow-brown solid, $(P_2Cl_4)_2 \cdot Ni(CO)_2$. If the CO pressure in the reaction vessel does not build up to 0.7 atm by the evolution of CO during the formation of this compound, the compound continues to react slowly with P_2Cl_4 to yield compounds approaching the compositions $(P_2Cl_4)_3NiCO$ and $Ni(P_2Cl_4)_4$ until the CO pressure does reach 0.7 atm. Experiments with PCl_3, P_2Cl_4, and $Ni(CO)_4$ show that P_2Cl_4 can replace PCl_3 in PCl_3-$Ni(CO)_x$ compounds, and that in mixtures of PCl_3 and P_2Cl_4 with $Ni(CO)_4$ most of the reaction is due to P_2Cl_4. Thus, P_2Cl_4 is a better Lewis base than PCl_3, in agreement with an argument based on the inductive effect.

* Partial abstract of Charles B. Lindahl, Chemistry of Diphosphorus Tetrachlorides (Ph.D. thesis), UCRL-11189, Jan. 1964.
+ Now at Eastman Kodak Corporation, Rochester, New York.

Diphosphorus tetrachloride does not react, or reacts only extremely slowly at 0° with $Fe(CO)_5$, $Cr(CO)_6$, or $Mo(CO)_6$.

With BBr_3 at 0°, P_2Cl_4 reacts to yield PBr_3, BCl_3, mixed boron and phosphorus chloro-bromo-trihalides, and phosphorus subhalides. Boron trichloride and BF_3 do not react with P_2Cl_4 at 0°, in agreement with the known Lewis acid trend $BBr_3 > BCl_3 > BF_3$.

Diphosphorus tetrachloride reacts with B_2H_6, causing decomposition producting H_2, BCl_3, $BHCl_2$, and yellow-orange solids indicative of phosphorus subhalides or subhydrides.

Because P_2Cl_4 has vacant low-energy d orbitals on each phosphorus, it is also a potential Lewis acid. No reaction was observed between P_2Cl_4 and C_2H_4, C_2H_2, or C_3F_6 at 0° or room temperature. However, a reaction between P_2Cl_4 and trimethylamine at temperatures of 0 and -78° produces large quantities of yellow-orange nonvolatile solids. The apparent products of the reaction are $PCl_3 \cdot N(OH_3)_3$ and phosphorus.

Thus, P_2Cl_4 undergoes reaction both as a Lewis acid and as a Lewis base. However, all reactions except the reaction with $Ni(CO)_4$ involve rupture of the phosphorus-phosphorus bond in P_2Cl_4.

B. CHEMICAL THERMODYNAMICS

1. ELECTRONIC SPECTRA OF DIATOMIC GASES

Leo Brewer, Beat Meyer, Jerry Smith, and Martin D. Shetlar

The calculation of entropies and the use of radiative lifetimes to obtain transition probabilities and absorption coefficients requires knowledge of the ground state and low-lying electronic states of high-temperature molecules.

A correlation of known electronic states of diatomic molecules with molecular orbital configurations allows the prediction of relative excitation energies of the low-lying electronic states when the bonding is due to s and p electrons. A variety of sources of electronic spectra is being studied to extend this correlation.

Studies of the spectrum of Se_2 have established the ground state as $^3\Sigma$ instead of the previously accepted $^1\Sigma$ state, and clarifications of features of SO, S_2, and Te_2 have been obtained.[1]

Analysis of emission bands from active nitrogen flames containing sulfur compounds has shown that several reported band systems of NS are portions of a single band system. These observations allow prediction of energies of additional electronic states of NS.

Study of perturbations in several C_2 band systems has provided better estimates of the energies of yet unobserved low-lying levels of C_2.

1. This work is a joint effort with Professor R. F. Barrow of Oxford University.

2. RADIATIVE LIFETIMES OF EXCITED ELECTRONIC STATES

Leo Brewer, Robert A. Berg, Gerd M. Rosenblatt, and Lucy G. Hagan

The apparatus[1] for measurement of radiative lifetimes in the range of 10^{-5} to 10^{-9} second has been applied to fluorescent solids,[1] to organic compounds,[2] and to the v' = 26 level of the $B^3\pi$ state of gaseous iodine.[3] Its use has now been extended to gaseous sodium and other atoms[4] and additional organic compounds.[5]

1. L. Brewer, C. G. James, R. G. Brewer, F. E. Stafford, R. A. Berg, and G. M. Rosenblatt, Rev. Sci. Instr. 33, 1450 (1962).
2. S. J. Strickler and R. A. Berg, J. Chem. Phys. 37, 814 (1962).
3. L. Brewer, R. A. Berg, and G. M. Rosenblatt, J. Chem. Phys. 38, 1381 (1963).
4. Work done by John Link and Ara Chutjian.
5. Work done by Robert Walsh.

Gaseous I_2 has been successfully studied in a molecular beam,[3] and the method is being extended to molecular beams of the high-temperature molecules LaO and CN.

Measurements of absolute absorption and emission intensities of C_2 and CN spectral features in the King furnace[6] have been combined with estimates of equilibrium partial pressures in the King furnace to calculate radiative lifetimes. When directly measured radiative lifetimes become available for these molecules, the calculations can then be reversed to obtain accurate values of the equilibrium concentrations and free energies and enthalpies of formation of C_2 and CN.

6. Lucy G. Hagan, The Absolute Intensity of C_2 Swan Bands (Ph.D. Thesis), UCRL-10620, March 1963.

3. THERMODYNAMIC COMPILATIONS

Leo Brewer, Gollakota R. Somayajulu, Elizabeth Brackett, and Gerd M. Rosenblatt

Methods have been developed[1,2] for the prediction of low-lying electronic states of gaseous diatomic and triatomic molecules and have been used to assist in the critical evaluation and compilation of thermodynamic data for the gaseous metal dioxides[3] and dihalides.[4] A similar critical evaluation of high temperature vaporization data and consistent estimation of partition functions has been done for the gaseous metal monoxides. The application of these data to high temperature purification procedures has been illustrated for removal of oxygen from metals.[5]

1. L. Brewer, in Proceedings of Robert Welch Foundation Conference, November, 1962.
2. L. Brewer and M. S. Chandrasekhariah, Free Energy Functions for Gaseous Monoxides, UCRL-8713, April 1959.
3. L. Brewer and G. M. Rosenblatt, Chem. Rev. 61, 257 (1961).
4. L. Brewer, G. R. Somayajulu, and E. Brackett, Chem. Rev. 63, 111 (1963).
5. L. Brewer and G. M. Rosenblatt, Trans. AIME 224, 1268 (1962).

4. METAL PHASE DIAGRAMS

Leo Brewer

A preliminary evaluation of the fundamental electronic factors that can be correlated with thermodynamic stability of metal phases has been published.[1] The Engel theory of metals was used to relate the structures and stability of metallic phases through the use of bonding concepts that are successful in describing the chemical behavior of conventional materials. The theory has been extended to predict the structures of the possible phases and their maximum composition ranges for the various combinations of thirty transition metals. The results are presented in text, tables, and in the form of multicomponent phase diagrams.[2] These diagrams are being used to guide choices of compositions for superconductivity studies.

---

1. L. Brewer, Thermodynamic Stability and Bond Character in Relation to Electronic Structure and Crystal Structure, in Electronic Structure and Alloy Chemistry of the Transition Elements, Ed. Paul A. Beck (Interscience Publishers, Inc., New York, 1963).
2. L. Brewer, Prediction of High Temperature Metallic Phase Diagrams, UCRL-10701, July 1963; to be published in Proceedings of High Strength Conference, Berkeley, June 1964.

C. SOLID-STATE CHEMISTRY AND PHYSICS

1. THERMODYNAMICS OF THE SUPERCONDUCTING TRANSITION IN RUTHENIUM

Russell H. Batt and Norman E. Phillips

The absence of an isotope effect in the transition temperature T_c of ruthenium has raised the possibility that the superconductivity of transition metals may be produced by a mechanism other than the electron-phonon interaction. For this reason, the evaluation of the parameters characterizing the superconducting state is of particular interest. We have made heat capacity measurements on a sample of ruthenium from 0.28°K to above 1°K. The data are shown in Fig. IC.1-1. The superconducting state electronic heat capacity C_{es} follows a typical exponential temperature dependence, $C_{es}/\gamma T_c = 8.12 \exp(-1.40\ T_c/T)$, as shown in Fig. IC.1-2. The various parameters determined by the measurements fit the usual correlation with T_c/Θ, where Θ is the Debye temperature, suggesting that the electron-phonon interaction plays the same role as in other superconductors.

2. THE HEAT CAPACITY OF IRON-TITANIUM ALLOYS

Russell H. Batt and Norman E. Phillips

For dilute solutions of iron in titanium the iron atoms carry a local moment but the transition temperature, as measured by magnetic methods, is increased over that in pure titanium. This behavior is the opposite of that observed in nontransition metals, and has been interpreted as showing that the mechanism producing superconductivity in titanium is different from that in the nontransition metals. We have measured the heat capacity of a 1% solution of iron in titanium from 0.3°K to 20°K. The data suggest that only a small part of the sample becomes superconducting at the transition temperature observed by magnetic methods, and that the bulk of the sample has a transition temperature lower than that of pure titanium. Most of the sample thus behaves in the same way as nontransition metals.

3. LATTICE HEAT CAPACITY OF SUPERCONDUCTING MERCURY AND LEAD

Norman E. Phillips, Marcel H. Lambert, and William R. Gardner

The heat capacities of mercury and lead have been measured at temperatures below 1°K in both normal and superconducting states. Within the experimental accuracy no discrepancy in lattice heat capacity of the kind reported in indium was observed. The heat capacity data for indium are interpreted as showing that no observable change in Debye-Waller factor should be expected at the superconducting transition.

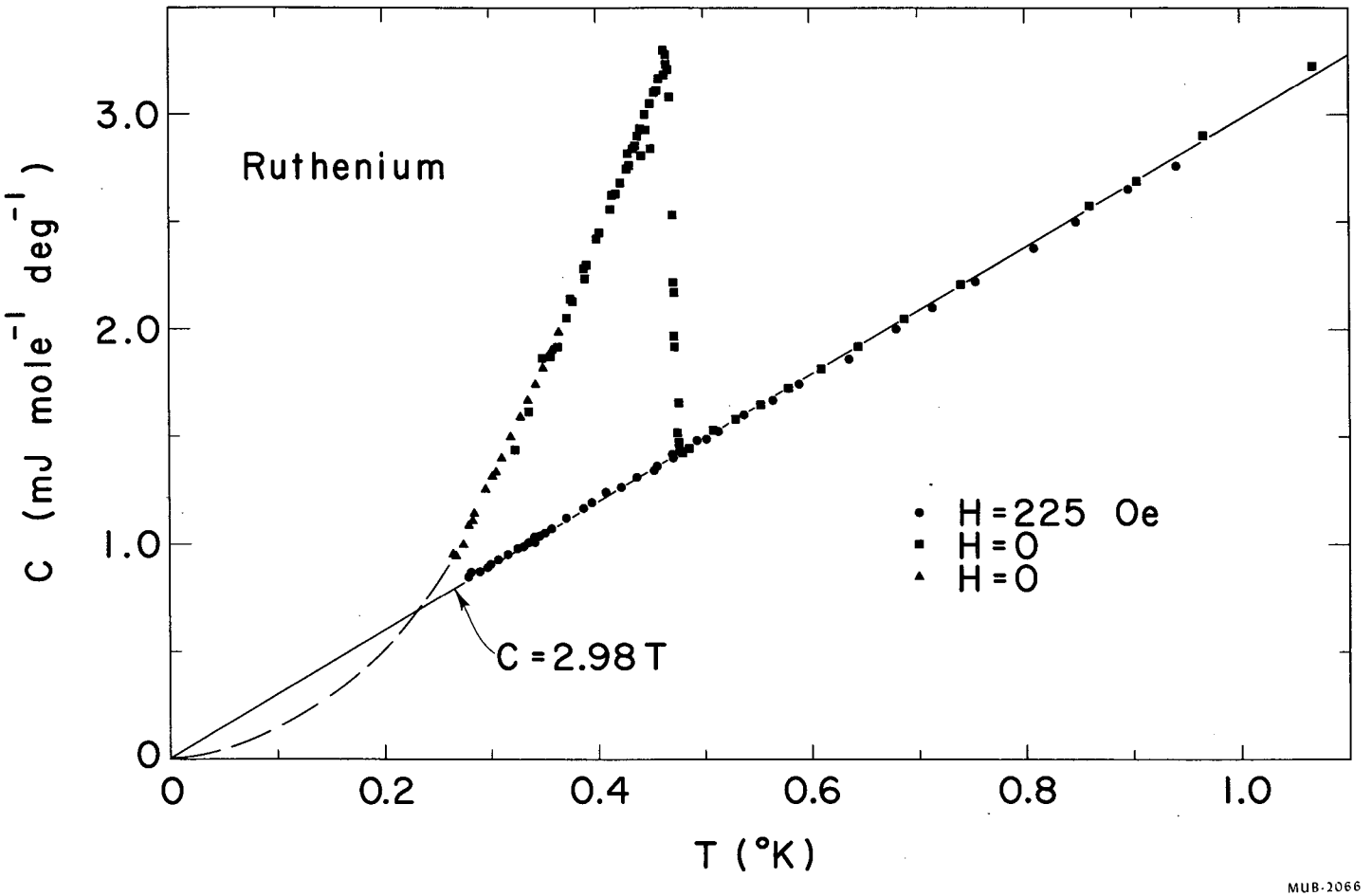

Fig. IC. 1-1 The heat capacity of ruthenium.

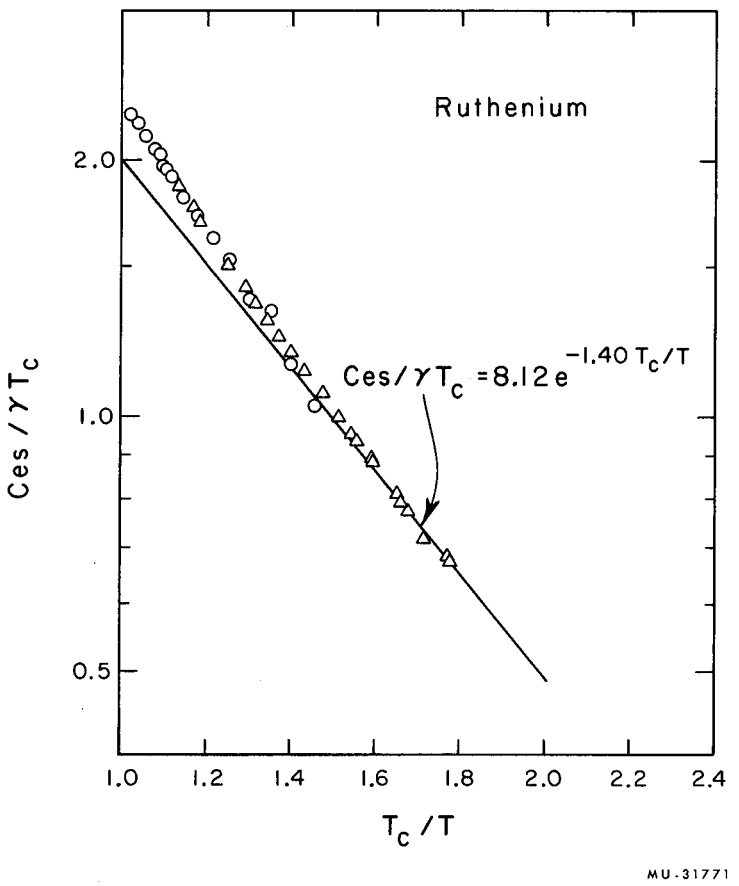

Fig. IC. 1-2 The superconducting state electronic heat capacity of ruthenium.

4. HEAT CAPACITY OF THE γ PHASE OF He^4*

Guenter Ahlers†

About two years ago Vignos and Fairbank reported a new solid phase, identified as the γ phase, in He^4,[1] and soon thereafter Schuch and Mills established that this phase has a body-centered cubic (bcc) structure.[2] Recently Grilly and Mills established the PVT relations for the transition from the α to the γ phase, and from the α and γ phases to the liquid.[3] The α phase in He^4 has a hexagonal close-packed (hcp) structure. Both an hcp and a bcc structure also exist in He^3, and the heat capacity of both of these phases has been measured by Heltemes and Swenson for this isotope.[4] The Debye Θ of the bcc phase was found to be about 20% smaller than that of the hcp phase at the same density, the isotope effect on Θ was observed to be only slightly larger than the $m^{0.5}$ ratio in the hcp phase, and an anomaly of unknown origin was found in the heat capacity of the bcc phase. The work presented here was undertaken primarily to determine if a similar difference in the lattice heat capacity of the two phases also exists in He^4, to determine the isotope effect in the bcc phase, and to see if a similar anomaly exists in the heat capacity of γ-He^4.

In order to measure the heat capacity, temperature increments of (1 or 2) $\times 10^{-3}$ K had to be used. It was nonetheless possible to obtain a precision of the order of 1% in the heat capacities by using a germanium thermometer which was calibrated against the vapor pressure of He^4. The molar volume was inferred from the α-to-liquid or γ-to-liquid transition temperature and the data of Grilly and Mills.[3]

Some of the experimental results in the α phase and most of the results in the γ phase are presented in Fig. 1. Within experimental accuracy, the Debye Θ of the α phase decreases linearly with increasing temperature over the temperature range covered here. The Debye Θ of the γ phase is 16.9°K. One set of measurements on the α phase was made at a molar volume of 19.87 cc, at which direct comparison with existing data is possible. The data presented here agree well with those of Keesom and Keesom,[5] but differ from those of Webb, Wilkinson, and Wilks[6] by about 12% in the heat capacity. The heat

---

* Abstracted from Guenter Ahlers, Phys. Rev. Letters 10, 439 (1963).
† Now at Bell Telephone Laboratories, Murray Hill, New Jersey.
1. J. H. Vignos and H. A. Fairbank, Phys. Rev. Letters 6, 265 (1961).
2. A. F. Schuch and R. L. Mills, Phys. Rev. Letters 8, 469 (1962).
3. E. R. Grilly and R. L. Mills, Ann. Phys. (N.Y.) 18, 250 (1962).
4. E. C. Heltemes and C. A. Swenson, Phys. Rev. Letters 7, 363 (1961).
5. W. H. Keesom and A. P. Keesom, Physica 3, 105 (1936).
6. F. J. Webb, K. R. Wilkinson, and J. Wilks, Proc. Roy. Soc. (London) A214, 546 (1952).

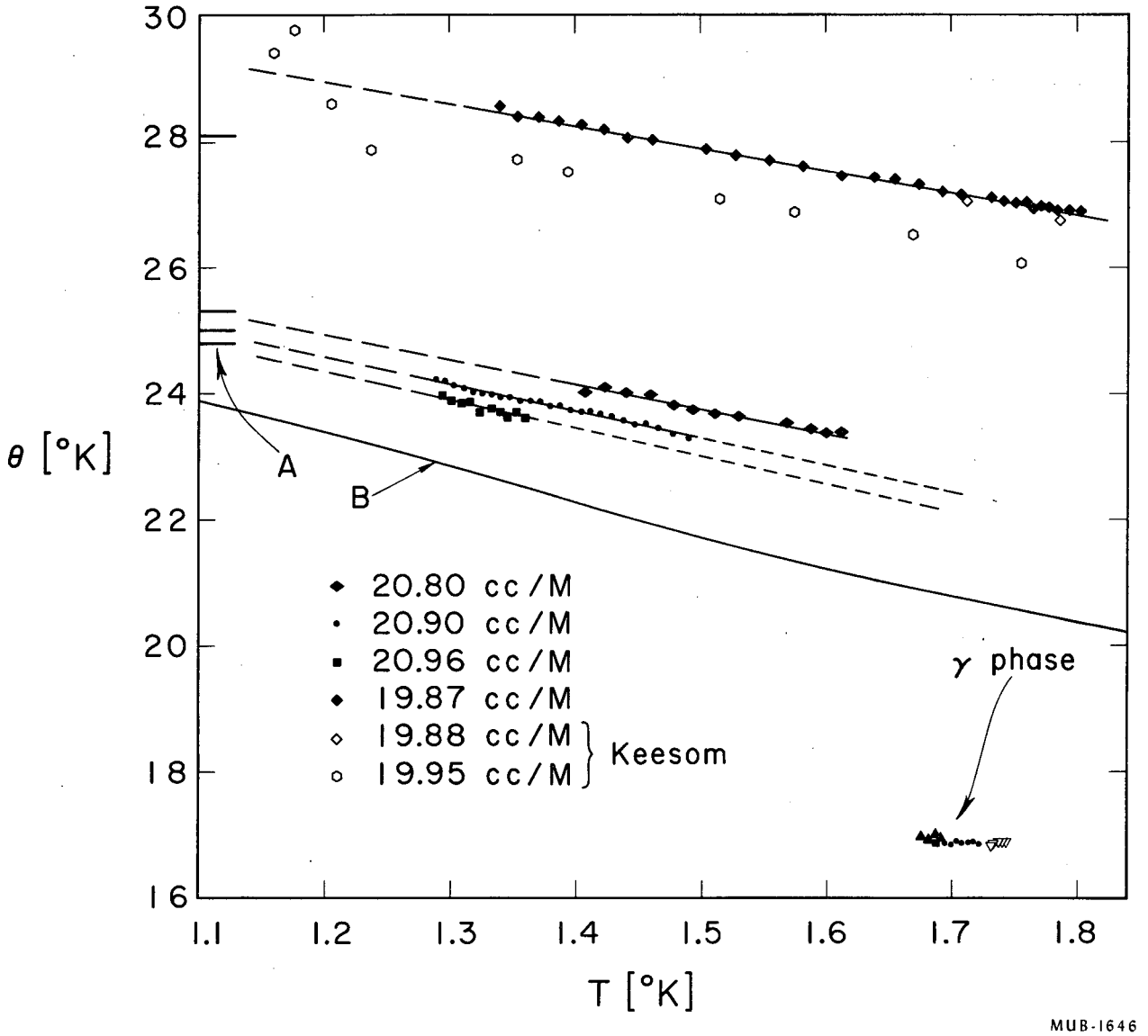

Fig. IC. 4-1 Debye theta vs temperature for the α and γ phases of solid He^4.

A indicates the values obtained by Heltemes and Swenson for the volumes of He^4, used in this experiment and

B indicates the Debye Θ calculated from Heltemes and Swenson's total heat capacity for bcc He^3 at 20.9 cc/mole.

capacity of solid He^4 has also been measured by Dugdale and Simon[7] and by Heltemes and Swenson.[4] However, Dugdale and Simon's data are at smaller molar volumes, and comparison is difficult. Heltemes and Swenson's data include the molar volume range studied here, but are supposedly reliable only below 1.1°K. Thus comparison is again not straightforward. Since the Θ values reported herein are temperature-dependent and extend only down to 1.3°K or $(T/\Theta) \approx 0.052$, an extrapolation to 1.1°K or $(T/\Theta) \approx 0.044$ must be made. Comparison with Debye Θ values of other substances on which accurate measurements are available over a large temperature range shows that a linear extrapolation in this relative temperature range is not likely to be in error by more than 1 or 2%. This type of extrapolation agrees well with Heltemes and Swenson's data at 20.9 cc/mole, but differs from their data by 4% in Θ at 19.87 cc/mole.

In order to compare the Debye Θ values of the α and the γ phases at the same molar volume, again an extrapolation is necessary because the two-phase temperature range at constant volume is about 0.2°K. Extrapolation from $(T/\Theta) \approx 0.060$ to $(T/\Theta) \approx 0.067$ must be made in this case, and again a linear extrapolation for the α phase is not likely to introduce a prohibitive error. This extropolation yields a difference between the Debye Θ values for the two phases of 24%, which is about the same as that found in He^3 for the phases of the same crystal structures. It therefore appears that the larger lattice heat capacity of the bcc phase is not a peculiarity of He^3, but rather that it is associated with the structure of the lattice. Whereas the uncertainties in the above comparison are rather large, there is a definite indication that the Debye Θ ratio for the bcc phases of the helium isotopes is larger than that indicated by simple theory.

An anomalous contribution to the heat capacity of bcc He^4 such as that reported for He^4 was not observed in this work.

At present neither the data on He^3 nor those on He^4 are sufficient to establish clearly the relative magnitudes of possible anomalous and lattice contributions to the heat capacity of the bcc phases of the two isotopes. In He^4 there is not much hope for improvement because of the natural limitations set by the existence range of the phase. The bcc phase of He^3 can perhaps be studied more thoroughly, and one would hope that more precise data over a larger temperature range would shed some light on the problem.

Considerable information was gained during this work on the detailed behavior of He^4 along the various phase boundaries. In particular, the difference between the λ point in the liquid at the melting line and the upper triple point was found to be 10×10^{-3}°K, in agreement with Vignos and Fairbank[1] and in disagreement with Grilly and Mills.[3] Work on the α-γ two-phase region is still in progress, and a comprehensive report on all the work will be given elsewhere.

7. J. S. Dugdale and F. E. Simon, Proc. Roy. Soc. (London) A218, 291 (1953).

5. λ ANOMALY IN THE HEAT CAPACITY OF SOLID HYDROGEN AT SMALL MOLAR VOLUMES

Guenter Ahlers [+] and W. H. Orttung[‡]

Apparatus for the determination of properties of solid hydrogen at volumes between 15 and 23 cc/mole has been described,[1] and results of measurements on the λ anomaly in the heat capacity of solid hydrogen containing large concentrations of orthohydrogen reported for molar volumes from 15.8 to 22.6 cc. The λ temperature was found to vary with intermolecular separation R as R^{-5}, with a small contribution from a higher exponent. This is in agreement with the expected relative contributions of electric quadrupole and valence interactions to the intermolecular potential. The relative contribution of the λ anomaly to the total anomalous entropy was estimated. The λ anomaly was found to have at least two distinct peaks.

+ Now at Bell Telephone Laboratories, Murray Hill, New Jersey.
‡ Now at Department of Chemistry, University of California, Riverside, California.

1. Guenter Ahlers, Some Properties of Solid Hydrogen at Small Molar Volumes (Ph.D.Thesis), UCRL-10757, January 1964.

6. NUCLEAR SPIN ORDERING IN ADSORBED He^3 *

Marcel H. Lambert

This report presents specific-heat data for He^3 adsorbed on zeolite in the temperature range 0.1 to 1.4° K (Fig. IC.6-1). The results indicate that the nuclear spin entropy is substantially removed at 0.2°K, and emphasize the importance of exchange effects at high densities.

---

* Abstract of Phys. Rev. Letters 12, 67 (1963).

7. THE HYPERFINE AND ELECTRONIC HEAT CAPACITIES OF γ MANGANESE

James C. Ho and Norman E. Phillips†

For the ferromagnetic metals iron,[1] cobalt,[2,3,4] and nickel,[5] the

---

† Alfred P. Sloan Research Fellow.

1. S. S. Hanna, J. Heberle, G. J. Perlow, R. S. Preston, and D. H. Vincent, Phys. Rev. Letters 4, 513 (1960).
2. V. Arp, D. Edmonds, and R. Petersen, Phys. Rev. Letters 3, 212 (1959).
3. A. C. Gossard and A. M. Portis, Phys. Rev. Letters 3, 164 (1959).
4. Y. Koi, A. Tsujimara, T. Hihara, and T. Kushida, J. Phys. Soc. Japan 17, Suppl. B1, 96 (1962).
5. R. L. Streever, Phys. Rev. Letters 10, 232 (1963).

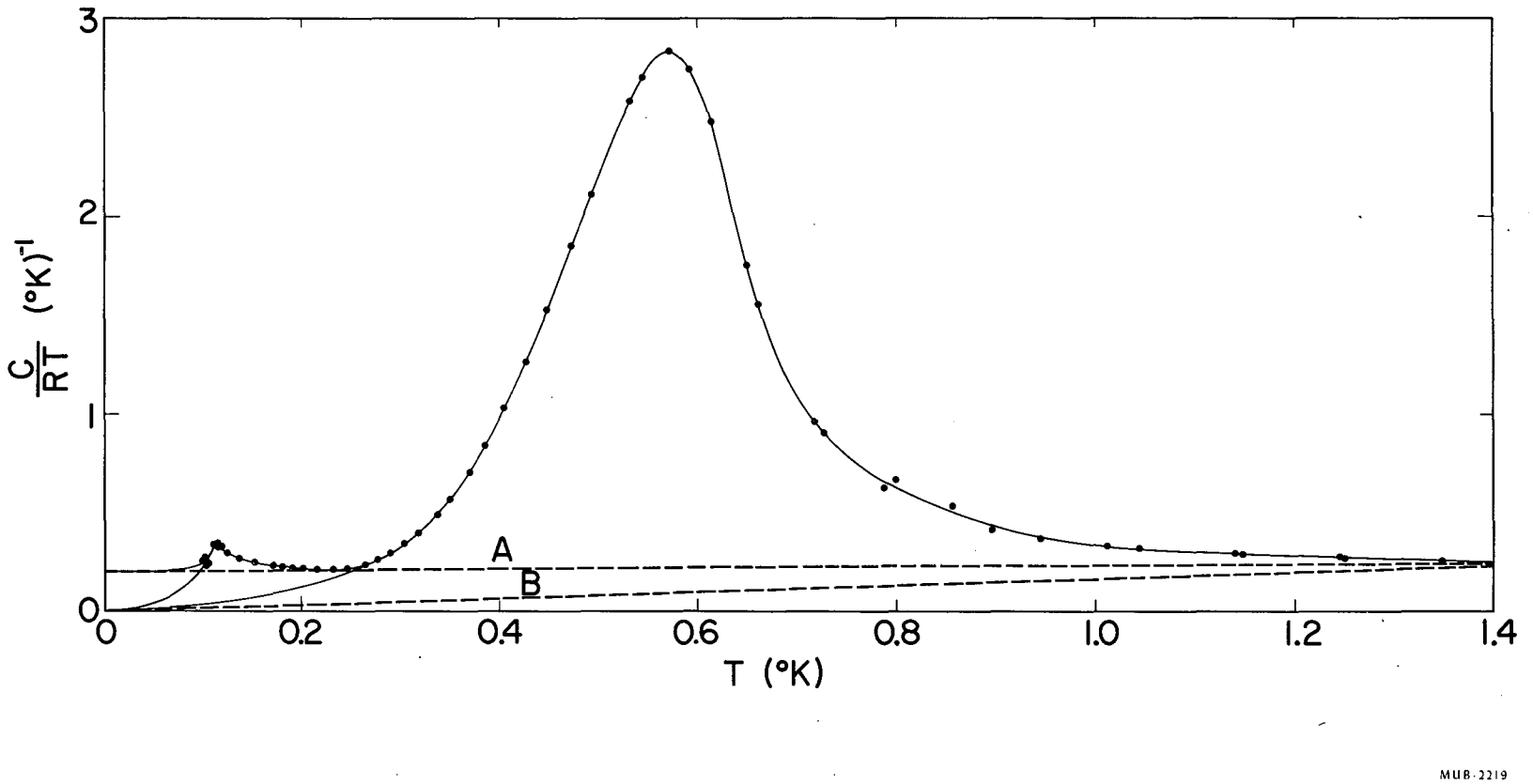

Fig. IC. 6-1 Specific heat of He^3 adsorbed on Zeolite.

magnetic hyperfine fields H_e are known and have been the subject of several theoretical investigations.[6,7,8] Further progress toward understanding the relative importance of the different contributions to H_e seems to depend on its measurement in a variety of situations. We have therefore made a calorimetric determination of H_e in the antiferromagnet, γ manganese. In iron, cobalt, and nickel, H_e is approximately equal to the calculated negative contribution from exchange polarization of the core electrons.[7,8] In γ manganese, H_e is much smaller in magnitude (more positive) than the calculated core polarization term, suggesting the presence of positive contributions that do not exist (or are smaller) in the ferromagnetic metals.

The γ manganese crystal is face-centered tetragonal[9] with $c/a = 0.95$. Ions with $n_{eff} = 2.4$ are aligned parallel to the c axis to produce a magnetic structure in which each ion has eight antiparallel nearest neighbors and four parallel neighbors at a slightly greater distance.[10,11]

The sample was prepared by electrolytic deposition under conditions known to produce the γ phase,[12] and the absence of α-phase material was confirmed by x-ray examination. The heat capacity was measured[13] over the range 0.066 to 4.2°K, with an estimated accuracy of 1% above 1°K and 2% below 1°K. As shown in Fig. IC.7-1, the experimental points fit the equation

$$C(\text{mJ mole}^{-1}\ \text{deg}^{-1}) = 0.055\ T^3 + 9.20\ T + 0.264\ T^{-2}, \qquad (1)$$

in which the terms on the right are, respectively, the lattice, electronic, and hyperfine heat capacities. The electronic heat capacity differs appreciably from the value deduced from measurements on copper-manganese alloys.[14] Comparison of the hyperfine heat capacity with the equation[6]

$$\frac{C}{R} = \frac{1}{3}\,\frac{I+1}{I}\left(\frac{\mu H_e}{kT}\right)^2 \qquad (2)$$

gives $|H_e| = 65$ kOe. The overestimate of $|H_e|$ arising from the neglect of

6. W. Marshall, Phys. Rev. 110, 1280 (1958).
7. D. A. Goodings and V. Heine, Phys. Rev. Letters 5, 370 (1960).
8. R. E. Watson and A. J. Freeman, Phys. Rev. 123, 2027 (1961).
9. Z. S. Basinski and J. W. Christian, J. Inst. Metals 80, 659 (1951).
10. G. E. Bacon, I. W. Duncan, J. H. Smith, and R. Street, Proc. Roy. Soc. (London) A241, 223 (1957).
11. D. Meneghetti and S. S. Sidhu, Phys. Rev. 105, 130 (1957).
12. D. Schlain and J. D. Prater, Trans. Electrochem. Soc. 94, 58 (1948).
13. Below 1°K, temperature measurements were based on a Curie law for the susceptibility of cerium magnesium nitrate. In other respects the apparatus was similar to that used in earlier experiments [N. E. Phillips, Phys. Rev. 114, 676 (1959)] and will be described more completely in another paper (H. R. O'Neal and N. E. Phillips)
14. J. E. Zimmerman and H. Sato, J. Phys. Chem. Solids 21, 71 (1961).

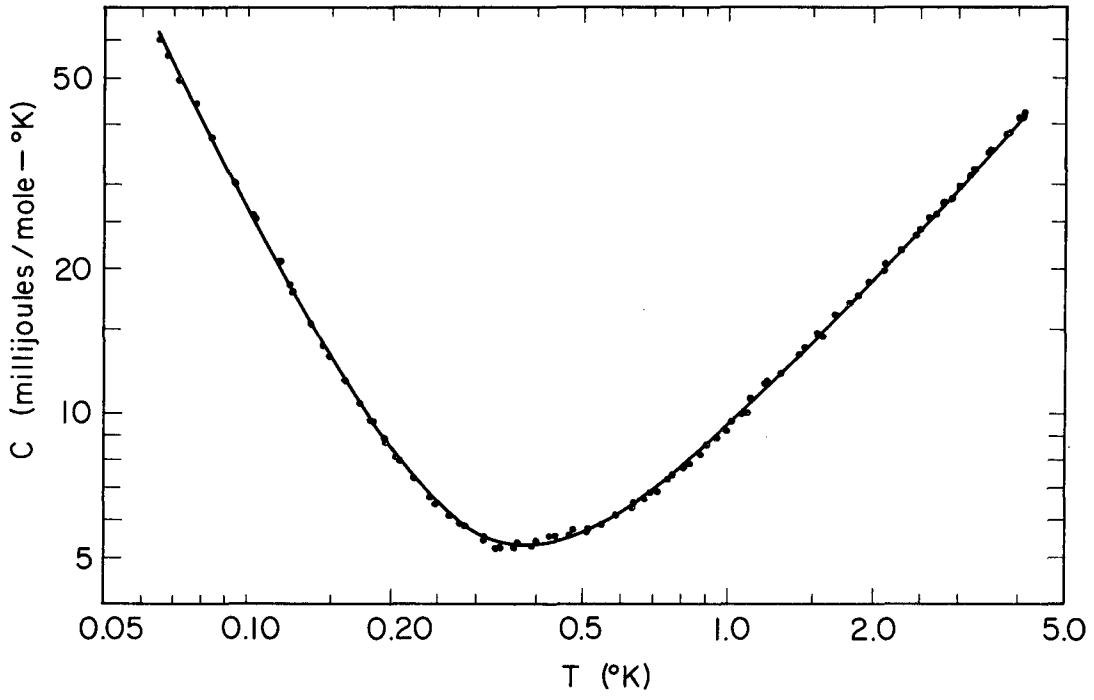

Fig. IC. 7-1 The heat capacity of γ-manganese. The curve represents the equation $C = 0.055\ T^3 + 9.20\ T + 0.264\ T^{-2}$.

electric quadrupole splitting in Eq. (2) is shown to be less than 8% of the absence of a measurable T^{-3} term in the heat capacity, and comparison with other metals suggests that it is not significant.

In the notation used by Marshall,[6]

$$H_e = H_\ell + H_a + H_c \ , \qquad (3)$$

where H_ℓ is the field produced at a nucleus by dipoles at other lattice sites; H_a is associated with electrons localized on the same nucleus (it includes a contribution, H_{core}, from exchange polarization of the s electrons of the core, which is in the direction opposite to the magnetic moment--i.e., negative); H_c is the contact interaction with 4s electrons, including the effects of admixture of 4s functions into the orbitals of the magnetic electrons and exchange polarization of electrons in the 4s band. Each of these effects give a positive contribution to H_c. However, in ferromagnets, an antiferromagnetic polarization of the 4s electrons accompanies the mixture of 4s functions into the 3d band and tends to cancel the contribution.[15]

By neglecting the slight tetragonal distortion and using sums of dipole fields for cubic arrays,[16] we have estimated H_ℓ = -7.7 kOe. Since our experiment does not determine the sign of H_e, $H_e - H_\ell$ = -57 or + 73 kOe. In Table IC.7-I, these values are compared with the corresponding quantities for iron, cobalt, and nickel.

Table IC.7-I Observed hyperfine fields H_e and local field contributions H_ℓ. An estimated core polarization contribution (see reference 8), $H_{core} = -126\, n_{eff}$, is included for comparison. All fields are in kOe. For manganese and hcp cobalt the sign of H_e is not determined by the experiments.

Metal	Reference	H_e	H_ℓ	$H_e - H_\ell$	$-126 n_{eff}$
Mn	This work	± 65	-7.7	-57, +73	-300
Fe	1	-330	0	-330	-280
Co(hcp)	4	228	≈0	228	-217
Co(fcc)	3	-213	0	-213	-217
Ni	5	- 80	0	- 80	- 77

15. P. W. Anderson and A. M. Clogston, Bull. Am. Phys. Soc. 6, 124 (1961).
16. L. W. McKeehan, Phys. Rev. 43, 913 (1933).

The negative sign of H_e in iron, cobalt, and nickel shows the dominance of H_{core}. Theoretical estimates of H_{core} give values comparable to H_e and not large enough in magnitude to compensate for the expected positive contributions.[7,8] Calculations by Watson and Freeman[8] gave $H_{core} \approx -126\ n_{eff}$, in reasonable agreement with values obtained from data on salts of the divalent ions (including manganese) and approximately equal to the total H_e in iron and cobalt. The recently redetermined value of H_e in nickel[5] is also very close to the predicted H_{core}. As noted by Watson and Freeman, the agreement between H_e and the calculated H_{core} is more readily understood in view of the suggestion by Anderson and Clogston[15] that part of the positive 4s contribution to H_e is self-cancelling. However, it appears that the estimated H_{core} for iron, cobalt, and nickel is more likely to be too small than too large. For γ manganese the same estimate gives $H_{core} = -300$ kOe, showing that the calculated H_{core} is too large or that the other contributions are at least 250 kOe more positive than in the ferromagnetic metals.

It is not clear how the difference between ferromagnetic and antiferromagnetic ordering would affect the 4s contribution. The partial cancellation noted by Anderson and Clogston in ferromagnetic metals occurs in the space average of the 4s spin density and, apparently, the contributions to H_e do not necessarily cancel. The positive contribution associated with a net unpairing of "free" 4s electron spins in a ferromagnet[6] would be absent in an antiferromagnet.

Another effect that may contribute to the apparent difference in behavior between γ manganese and the ferromagnetic metals is the exchange polarization of 3s electrons on one ion by 3d electrons on neighboring ions. The core polarization in an ion with net 3d spin $\uparrow$ is a consequence of the spin dependence of the exchange interaction of a core electron with the 3d electrons. The 2s electrons are "inside" the 3d shell and the result is to produce a net $2s\downarrow$ density at the nucleus and a negative contribution to H_e. The 3s electrons are "outside" the 3d shell and produce a positive contribution of smaller magnitude. The sensitivity of the 3s polarization to the 3d spin density in the outer region of the ion[7] and the amplitudes of the Hartree-Fock orbitals at half the nearest neighbor distance suggest that the difference between ferromagnetic and antiferromagnetic ordering might have a substantial effect on H_{core}. In a ferromagnet the $3d\uparrow$ spin density on neighbors may tend to counteract the inward attraction of the $3s\uparrow$ electrons, making H_{core} more negative and improving agreement between experiment and theory. In an antiferromagnet the effect of nearest neighbors would be reversed and H_{core} would be made less negative.

8. HYPERFINE HEAT CAPACITIES OF MANGANESE-COPPER ALLOYS

James Ho and Norman E. Phillips

The heat capacities of cubic manganese-copper alloys have been measured below 1°K. At present it is not possible to separate the contributions of the copper and manganese nuclei to the hyperfine heat capacity, but it is hoped that further experiments will accomplish this. On the assumption that the copper contribution is negligible, the value of $|H_e|$ at manganese nuclei varies from 65 kOe in pure manganese to 370 kOe in dilute solutions. This variation is much greater than the change in local moment on

the manganese ions, suggesting that interaction between manganese ions or conduction electron polarization is important in determining H_e.

9. THERMODYNAMICS OF METALS UNDER PRESSURE

George Jura

One of the objectives of the high-pressure program is the determination of the thermodynamic properties of materials under high pressures. Except for very special cases--namely, hydrogen at helium temperatures--no direct measurement of a high-pressure thermal property of any solid has been made. The difficulty in these measurements is that the heat capacity of the container is much larger than the heat capacity of the system under consideration. Also, the heat leak is very large. We believe that in metals these difficulties can be solved in the following manner.

The resistance of a metal can be determined as a function of the temperature, thus the temperature can be determined by a resistance measurement. If a pulse of electrical energy is passed through the sample, the sample is heated. The energy in the pulse can be measured, and the rise in resistance (temperature) can be measured. If the pulse is of sufficiently short duration, and if the resistance measurement is made rapidly enough, then the average heat capacity between the original and final temperature may be determined. By using various starting temperatures, these data can be differentiated and the actual heat capacity determined as a function of the temperature and pressure of the sample. Calculations of the thermal conductivity of silver chloride show that, in 2 microseconds, less than 1% of the heat will be conducted away from the sample if the temperature rise of the sample is about 200°C. In order to raise the temperature of the sample this much, the pulse must have an energy of about 0.2 joule, delivered in less than 1 μsec.

The resistance measurement is easily completed in the alloted time. The problems of switching and obtaining a sufficiently large pulse of energy in the necessary time have not yet been solved. It is hoped that the electrical problems will be solved within the next six months.

10. HEAT CONDUCTIVITY OF INSULATORS UNDER PRESSURE

George Jura

This measurement is a byproduct of our early attempts to determine the heat capacities of metals. We have found, after heavily pulsing a metal sample, and then following the resistance as a function of time, that the temperature decay is controlled by the temperature of the medium rather than the sample. By placing probes at various positions with respect to the sample, it is possible to determine the temperature gradient in the insulator. By measuring the energy input in a steady state it becomes possible to determine the flow of heat through the insulating material. If these measurements could be carried out over a sufficiently wide range of temperatures, it would become possible to approximate--among other quantities--the Debye temperature of the insulator.

11. RESISTANCE MEASUREMENTS

George Jura

There is a continuing interest in resistance measurements. Reliable measurements can now be made, and if necessary with an accuracy of 0.01%. The major effort at present is directed toward an extension of the working-temperature range from 77°K to about 600°K. In order to obtain higher temperatures it has been necessary to use more complex pressure devices than Bridgman anvils. By using resistive heating we have reached a temperature of at least 1400°K, with no ill effects on the anvils. The volume of material under study is less than in conventional design, nevertheless, it is large enough to make good sample measurements.

The technique of internal heating will also be a definite asset in the study of phase transformation under pressure. Thus far preliminary studies of iron and bismuth have been made. The iron transition has been difficult to study under nearly hydrostatic conditions, as the transformation would start sometimes at a pressure of 160 kbars and at times over 200 kbars. (Even when the transition has been as highly overdriven, the transition would still take about 50 kbars to be completed). Preliminary measurements using internal heating give a sharp transition at about 110 kbars.

The bismuth 6-8 transition has also been surveyed. Here by judicious heating it has been possible to transform the material to the two-phase region and actually watch one of the phases grow at the expense of the other. With this technique, the preliminary value for this transition is 80 kbars, as compared with the previously determined 88 kbars.

12. MÖSSBAUER MEASUREMENTS UNDER PRESSURE

George Jura

The two determinations of the Mössbauer effect under pressure, for Dy^{161} and Fe^{57}, show the importance of this technique in high-pressure studies. In iron, the experiments became impossible when the data became the most interesting when the iron started to transform to the high-pressure phase. The first experiments did not permit us to conclude studies of the magnetic nature of the high-pressure phase.

Studies of the geometry and containing rings are progressing. These studies will enable us to make determinations at higher pressures. Use of higher temperatures will enable us to determine the spectrum of iron after it has been completely transformed to the high-pressure phase. This in turn will enable us to determine the magnetic properties of the high-pressure form. There also will be an attempt to make these determinations as a function of temperature as well as pressure. In general, when a Mössbauer nucleus is available, it will be possible in many cases to determine the magnetic properties of the material under study as a function of interatomic distance. These results could be important in the understanding of the ferromagnetic state.

In the Dy^{161} work, we found that under certain circumstances placing

the sample under pressure induced the formation of a high-resolution spectrum. The development of a hyperfine structure and the increase in the separation of lines with pressure developed an increasingly complex fine structure to a pressure of 50 kbars. Above this pressure no further resolution of the spectrum occurred. It is our belief that it was the absorber that limited the resolution. We are now building a system whereby the absorber can be maintained at any temperature down to helium temperatures. This method, which will be of value for many systems, will be tested with a solution of gold in iron.

D. ELECTROCHEMISTRY

1. A STUDY OF THE OXIDATION AND REDUCTION OF THE In, In(+3) COUPLE AT A MERCURY ELECTRODE AS A FUNCTION OF pH IN PERCHLORATE MEDIA

Wayne Mathews and E. F. Orlemann

Solutions 1M in $NaClO_4$ containing 5×10^{-4} M In(+3) with pH varied from 1 to 3.7 were investigated by using a hanging-mercury-drop electrode system.

In one family of experiments the applied potential was linearly cycled with time from 0 to -1.4 V (vs S.C.E.) at frequencies varying from 10 to 0.02 cycles per second. As the voltage sweeps from 0 to -1.4 V, the current voltage curve shows the reduction of In(+3) species; in the return sweep from -1.4 to 0 V, the current voltage curve shows the oxidation of In accumulated in the Hg surface. Alternatively current-voltage curves for the reduction of In(+3) were recorded with a single, time-varied linear potential sweep from +0.2 V to -1.4 V. Comparable studies of the oxidation of In amalgam were made by accumulating In in the Hg drop at -1.4 V followed by single time-varied linear potential sweeps from -1.4 to +0.2 V.

In all cases the oxidation of In amalgam was characterized by a single current-voltage wave with a peak potential at -0.5 V that was independent of the applied potential frequency from 0.02 to 10 cps. No evidence of intermediate oxidation states was obtained. The oxidation waves were also independent of pH from 1 to 3.7, showing that the mechanism of oxidation is independent of the In(+3) species present in solution. The cyclic experiments showed no evidence of an In(+3) species characteristic of the oxidation process.

The current-voltage curves for the reduction of In(+3) in these solutions are characterized by two waves, one at a peak potential of -0.55 V and a second one at -1.2 V (vs S.C.E.). At any given frequency of the linear potential sweep the ratio of the height of the -0.55 V wave to that of the -1.2 V wave increases with increasing pH. The In(+3) species reduced at -1.2 V is presumably the aquo-ion. The species reduced at -0.55 V is, an undefined hydroxy In(+3) species. When the pH is around 2 the relative heights of the two In(+3) reduction waves is dependent on the frequency of the applied single-sweep potential. The -0.55 V reduction wave is predominant at low frequencies, and the -1.2 V wave is predominant at high frequencies. This observation, due to a time-dependent conversion of the aquo-ion to the hydroxy species, suggests possible dimerization to account for the relatively slow rate.

2. A STUDY OF THE OXIDATION AND REDUCTION OF THE In, In(+3) COUPLE AT A MERCURY ELECTRODE AS A FUNCTION OF CHLORIDE ION CONCENTRATION IN PERCHLORATE MEDIA

Wayne Mathews and E. F. Orlemann

Solutions 5×10^{-4} M in In(+3) at pH = 1, covering a chloride ion concentration range from 10^{-5} to 1 M, were prepared by using $NaClO_4$ to maintain a constant ionic strength of unity. The reduction of In(+3) at a hanging mercury drop and the oxidation of In amalgam were studied by using a linearly time-dependent applied potential as described in Section ID.1 of this report.

Under all conditions the oxidation of In amalgam is characterized by a single current voltage wave at -0.5 V peak potential, independent of the frequency of the applied potential. No evidence of intermediate oxidation states was obtained. The peak potential shifts to more negative potentials with increasing chloride ion concentration. No evidence for the production of an In(+3) species characteristic of In amalgam oxidation was obtained.

Reduction of the In(+3) shows two waves, one at -1.3 V, the other at -0.55 V. The latter first appears at a chloride ion concentration of 0.001M and becomes increasingly important as the chloride ion concentration is increased. At chloride ion concentration from 0.01 to 0.1 M the height of the -0.55 V wave relative to the -1.3 V wave decreases as the frequency of the applied potential increases. The aquo-indium ion is presumably the species reduced at -1.3 V. An undefined chloride ion species is reduced at -0.55 V. The rate of interconversion of these species occurs with a half life of around 10 to 30 seconds.

3. DISTRIBUTION OF ELECTROCHEMICAL REACTION RATES IN A FISSURE-TYPE PORE

Rolf H. Muller

An approach to understanding the complex behavior of porous electrodes consists in a detailed analysis of the behavior of a single pore.[1] For this purpose a fissure formed by two segmented flat electrodes facing each other at typical pore diameters was built. The distribution of current into the depth of this single pore was measured using a redox system of ferriferrocyanide in KOH. Because of cold flow of the bonding material, however, the two segmented electrodes could not be brought to the desired distances in the order of 10 μ. If construction of a newly designed assembly can be completed successfully, its possible applications will include gas discharge and electrodeposition reactions, where the pore geometry continually changes as the reaction proceeds.

---

1. Edward A. Grens, Dynamic Analysis of a One-Dimensional Porous Electrode Model (Ph.D. Thesis), University of California, Berkeley, Sept. 1963.

4. THICKNESS MEASUREMENT OF TRANSPARENT FILMS BY LIGHT INTERFERENCE*

Rolf H. Muller

Fizeau interference fringes and interference colors have long been used as a convenient means for determining optical film thicknesses.[1] The different methods based on light interference in thin films have more recently been reviewed in monographs, such as those by Mayer,[2] Heavens,[3] or Wolter.[4] The observations are usually made with unpolarized light at normal incidence. This technique, if applied to transparent films on metal surfaces, results in pictures of very low contrast, where interference fringes or colors are difficult to recognize. The reason for this failure lies in the high reflectance of the film-metal interface as compared with the air-film interface. Thus, only a partial extinction results under conditions of destructive interference (Rayleigh criterion[5]). This situation can be greatly improved by simple procedures which do not seem to be treated in the literature, although Tolansky has discussed the influence of polarization on the appearance of silver-modified Newton rings.[6] The method is based on the dependence of reflection and refraction on angle of incidence and direction of polarization. A theoretical analysis shows that particular angles of incidence exist for light polarized parallel ($\parallel$) and normal ($\perp$) to the plane of incidence under which the amplitudes of the interfering waves are matched. Experiments have confirmed the dependence of the interference phenomena on angle of incidence and mode of polarization, and have yielded saturated, easily identifiable interference colors under the conditions determined for amplitude matching.

For the air-film interface the reflection and refraction coefficients are obtained from the Fresnel equations. (The sign convention employed in recent texts, such as Stone[7] and Françon,[8] are used here.) The reflection coefficient for the film-metal interface is calculated with the equation given by König,[9] modified for contact with the film of refractive index n_1.[10]

---

* Abstract of paper accepted for publication by J. Opt. Soc. Am.

1. P. Drude, The Theory of Optics (Dover, New York, 1959).
2. H. Mayer, Physik dunner Schichten (Wiss Verlagsges, Stuttgart, 1950), p. 53.
3. O. S. Heavens, Optical Properties of Thin Solid Films (Academic Press, New York, 1955), p. 103.
4. H. Wolter, Optik dunner Schichten, in S. Flugge, ed., Encyclopedia of Physics, Vol. 24 (Springer-Verlag, Berlin, 1956), p. 528.
5. S. Tolansky, An Introduction to Interferometry (Longmans, Green, London, 1955), p. 39.
6. S. Tolansky, Multiple-Beam Interferometry (Clarendon Press, Oxford, 1949), p. 40.
7. J. M. Stone, Radiation and Optics (McGraw-Hill Book Co., Inc., N.Y., 1963) p. 397
8. M. Françon, Interference, diffraction et polarisation, in S. Flugge, ed., Encyclopedia of Physics, Vol. 24 (Springer-Verlag, Berlin, 1956), p. 391.
9. W. Konig, Elektromagnetische Lichttheorie, in Handbuch der Physik, Vol. 20 (Springer-Verlag, Berlin, 1928), p. 242.
10. W. Voigt, Nachr. Ges. Wiss. Gottingen, Math.-Phys. Kl., 259 (1902).

For the complex refractive index of the metal surface,

$$n = n_2(1-i\ \chi_2), \qquad (1)$$

the bulk values for tungsten, nickel, and silver are used,[11,12] representing typical metals of low, medium, and high reflectance.

Of special interest is the amplitude ratio of the interfering waves $R_0/\Sigma R_n$. In Fig. ID. 4-1 this quantity is plotted as a function of the angle of incidence ϕ for a film of refractive index 1.365 on tungsten, nickel, and silver. At the "optimum angle of incidence," $\phi_{||}$, where the ratio of -1 is reached, complete destructive interference is expected in a film of very low thickness with light polarized parallel to the plane of incidence. Complete destructive interference with $\perp$ light is obtained under another "optimum angle of incidence," $\phi_{\perp}$, with an additional optical path length in the film of $\lambda/2$. The amplitude ratio plotted in Fig. ID.4-1 with a positive sign indicates constructive interference at very low film thickness. The results of computations for the three metal surfaces covered with films of three difference refractive indices are given in Table ID.4-I.

Experiments were conducted with a film of refractive index 1.365 (3.4 N aqueous solution of KOH) on nickel. As predicted by the computations and shown in Fig. ID.4-2, the interference fringes from $\perp$ polarization were found to remain qualitatively the same but increase in contrast with increasing angle of incidence. The fringes from $||$ polarization, on the other hand, being the same as those of $\perp$ at normal incidence, decrease in contrast as ϕ increases until they vanish at Brewster's angle ϕ_p (where no reflection occurs at the film-air interface). For angles of incidence above ϕ_p they increase in contrast with increasing ϕ while their fringe pattern is complementary to the $\perp$ pattern. In this region of ϕ the use of unpolarized light markedly reduces the picture contrast. At an angle of incidence intermediate between $\phi_{\perp}$ and $\phi_{||}$ (77.5°) satisfactory results could be obtained with both polarizations (Fig. ID.4-2). Intensity minima and certain interference colors could visually be identified to less than ±0.05 μ film thickness.

For quantitative interpretations, only the interference minima and maxima in the case of monochromatic illumination, or certain characteristic interference colors in the case of white light, can be used in practice. Since their appearance is associated with different film thicknesses under the two modes of polarization it is desirable to use both simultaneously, thus obtaining twice the number of contour lines on a given film .

Refinements of the theoretical analysis are under consideration to include the exact phase change upon metallic reflection and the frequency dependence of the optical constants.

---

11. Handbook of Chemistry and Physics (Chemical Rubber Publishing Co., Cleveland, Ohio, 1956), p. 2703.
12. Landolt-Börnstein, 2, p. 905, Berlin (1923), Eg 1, p. 468, Berlin (1927).

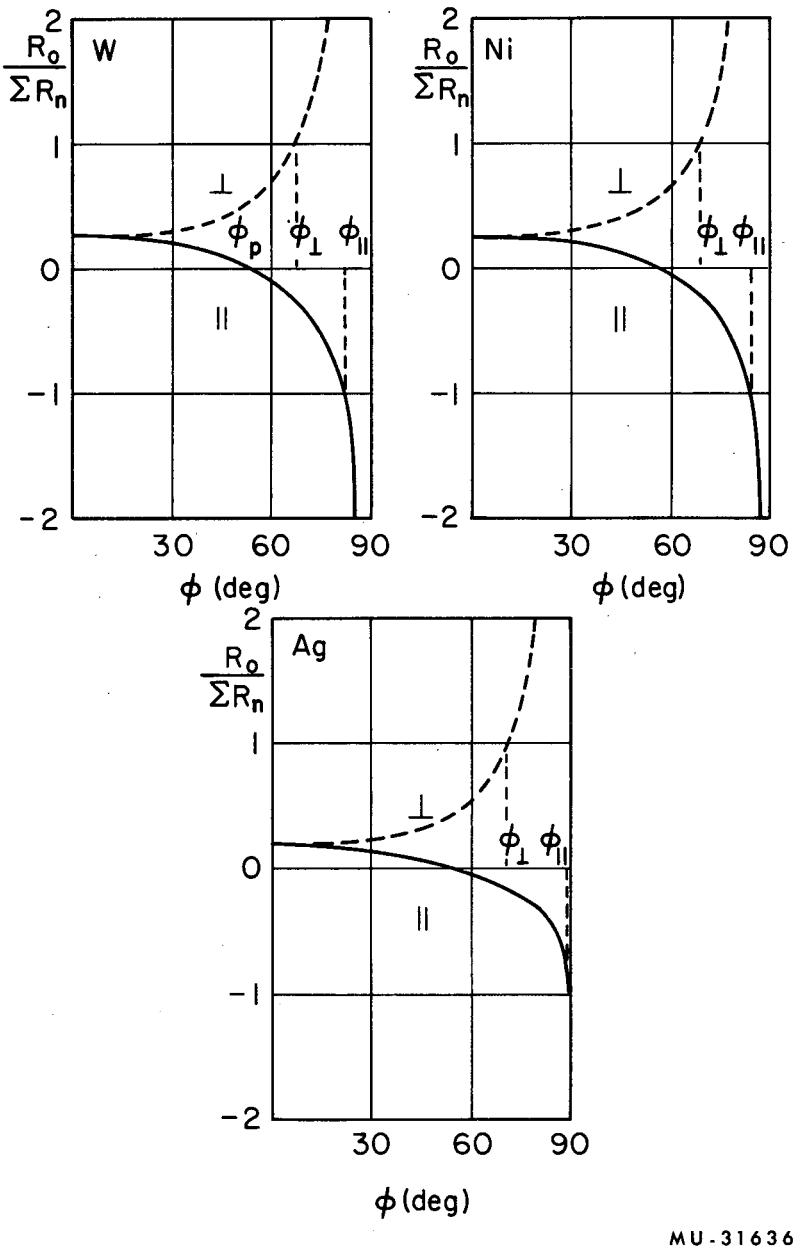

Fig. ID. 4-1 Amplitude ratio of interfering waves reflected by a transparent thin film (n_1 = 1.365) on different metal surfaces.

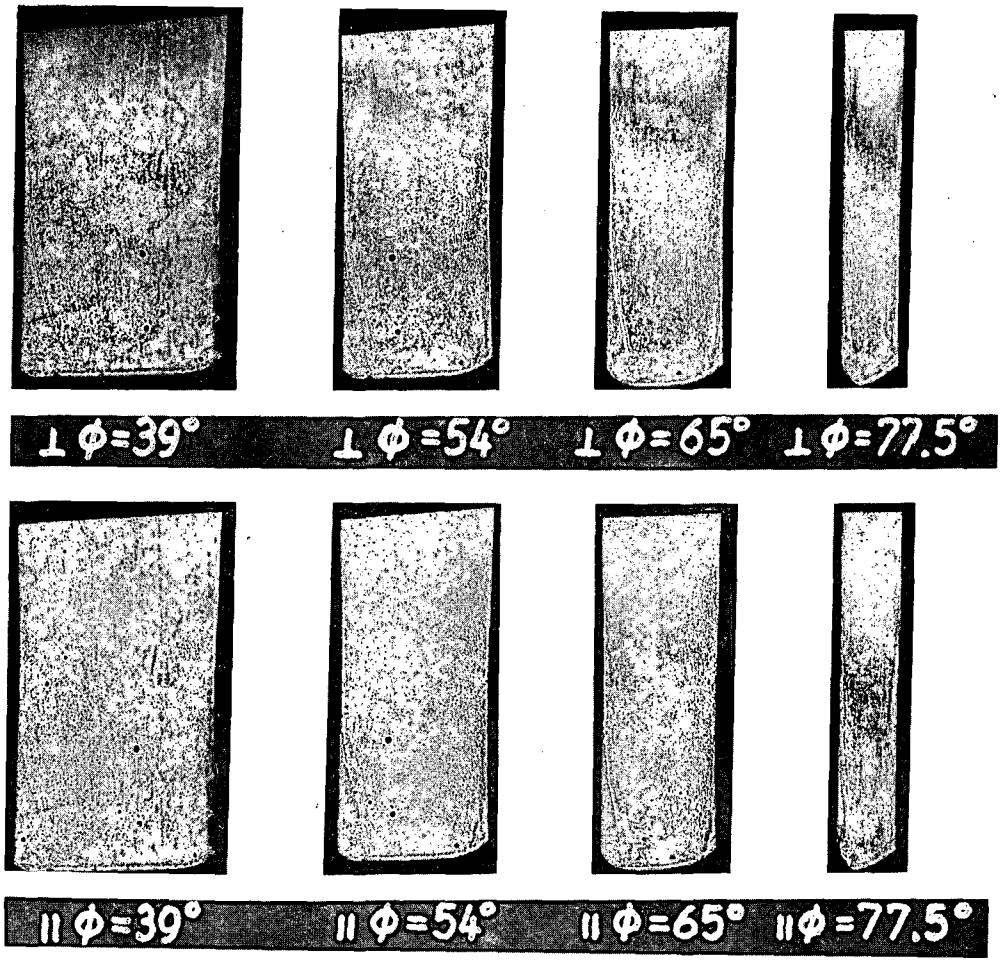

Fig. ID. 4-2 Appearance of a film of 3.4 n KOH solution (n_1 = 1.365) on a polished, optically flat nickel plate. Interference fringes of equal thickness are shown as a function of angle of incidence φ and mode of polarization (⊥ or ||) in parallel sodium light.

Table ID.4-I. Optimum angles of incidence, $\phi_{\perp}$ and $\phi_{\parallel}$, for the observation of transparent thin films on different metal surfaces with Na light polarized normal ($\perp$) and parallel ($\parallel$) to the plane of incidence.

Metal Surface	Film Refractive Index, n_1	$\phi_{\perp}$ (deg)	$\phi_{\parallel}$ (deg)
W	1.200	75	82
W	1.365	67	82
W	1.500	61	82
Ni	1.200	75	84
Ni	1.365	68	84
Ni	1.500	63	84
Ag	1.200	76	89
Ag	1.365	71	89
Ag	1.500	66	89

5. ELECTROLYTE FILMS ON METAL SURFACES*

Rolf H. Muller

Liquid films extending beyond the apparent liquid-solid-gas interface have long been suspected to exist on gas-consuming electrodes,[1] and attention to their importance for the mass transfer in gas diffusion electrodes has recently been drawn by Will.[2] An analysis for porous electrodes by Rockett[3] has supported the concept of an electrolyte film inside pores. An important parameter for understanding the processes occurring in such an electrolyte film is its thickness. If the electrochemical charge transfer takes place in the film, its thickness will affect mass transfer and ohmic potential drop, and thus influence the spatial distribution of the reaction.

The direct observation of liquid films on metal surfaces is difficult because of their sensitivity to most types of probes. Optical techniques have the advantage of allowing a continued observation with a minimum disturbance to the object. By use of light-interference techniques particularly developed for this study,[4] the thickness of liquid films formed by partial withdrawal of polished flat surfaces from aqueous solutions has been measured for several systems as a function of time. A typical result obtained on a rectangular nickel electrode (1.7 cm wide, 3 cm high) is shown in Fig. ID.5-1 for two different heights x above the liquid level. At time zero the liquid in the cell (3.4 M KOH) is rapidly lowered and cathodic reduction of oxygen is initiated under a constant current (100 μ A). Down to a thickness of about 1 μ, where surface effects become noticeable, the film thinning follows the relationship (inverse square root of time) expected from a consideration of viscous and gravitational forces only. A stationary film thickness is first reached in the upper parts of the electrode (after 2.5 hr at x = 1.4 cm), and considerably longer times are necessary in the lower parts (8 hr at x = 0.4 cm). After these periods, electrolyte films have been found in other experiments to remain unchanged over several weeks.

The thermodynamic stability of electrolyte films on vertical electrodes is due to a lower surface energy of the wet than of the dry metal surface. One should therefore expect a spontaneous film formation on a dry electrode upon partial immersion. The inability to observe this process, currently under study, may be due to adsorption phenomena or surface contamination, to which film formation is extremely sensitive.

---

* Abstract of paper to be presented at Spring Meeting, 1964, Electrochemical Society.

1. W. R. Grove, Phil. Mag. 21, 417 (1842).
2. F. G. Will, J. Electrochem. Soc. 110, 145, 152 (1963).
3. J. A. Rockett, Paper presented at Electrochemical Society Meeting, New York, October 2, 1963.
4. Rolf H. Muller, Light Interference in Transparent Thin Films on Metal Surfaces (UCRL-10963, July 1963), submitted to J. Opt. Soc. Am.

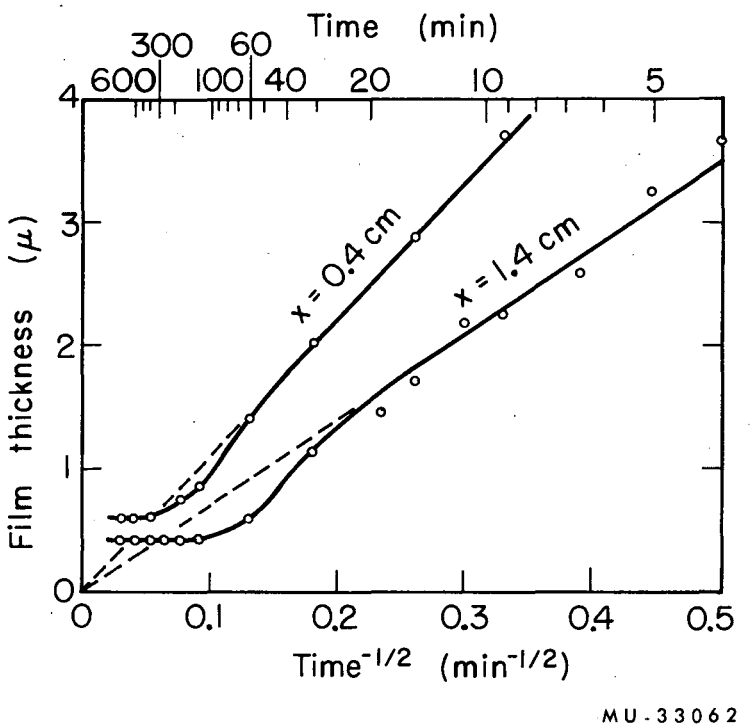

Fig. ID. 5-1 Formation of an electrolyte film on a polished nickel surface after withdrawal from the liquid. (3.4 n KOH, x = height above liquid level).

6. MOLAL VOLUMES OF ELECTROLYTES*

Otto Redlich

The variation of the volume with the concentration was derived from the theory of Debye and Hückel in 1931 and reviewed in 1940. Although the facts have been quite plain since then, numerous authors did not accept the theoretical limiting law, presumably because the textbook of Harned and Owen proposed an obviously wrong value for the limiting slope. The correct slope has recently been confirmed by experimental work of Owen and co-workers. A final, clarifying discussion was considered to be appropriate.

---

* Abstract of a note published J. Phys. Chem. 67, 496 (1963) and a review scheduled for Chem. Revs., June 1964.

7. COMPLEXES OF NEODYMIUM CHLORIDE IN AQUEOUS SOLUTIONS

Otto Redlich and Diane Meyer†

Since some divalent metal ions form intermediate ions, the existence of ions of the types $NdCl^{++}$ or even $NdCl_2^{+}$ may be suspected. Extinction coefficients have not furnished any evidence for such ions. The spectrum of Nd^{+++} solutions is independent of the concentration in water and in $HClO_4$ (up to 10 M). It varies, however, in a fairly complicated manner in a series of mixtures containing c moles HCl and (10-c) moles $HClO_4$ per liter. The results are tentatively interpreted as indicating a sequence of complex ions from $Nd(H_2O)_6^{+++}$ to $NdCl_6^{---}$.

---

† Now at Massachusetts Institute of Technology, Cambridge, Mass.

8. EQUATION OF STATE

Otto Redlich, Robert Gunn, and Max Jacobson

In thermodynamic calculations for chemical reactions, distillation, extraction, and other processes, one needs fugacity coefficients if the pressure is high or even moderate. For good reasons fugacity coefficients are always derived from an equation of state. Since integrations and differentiations are involved, an algebraic equation is practically indispensable. An equation suggested in 1949 was found to be surprisingly good in view of the fact that it contained only two parameters. Yet, it was by no means entirely satisfactory. Pitzer and his co-workers demonstrated that three individual parameters are practically sufficient for a good representation. The older equation has been improved by a term containing Pitzer's "accentric factor." Moreover, a satisfactory combination rule for the representation of mixtures without additional parameters has been established.

Lack of information of fugacity coefficients has seriously limited technical calculations, particularly in the petroleum industry, where high-pressure

operations are frequent and where precise advance calculations are quite important. The proposed computer program, after being thoroughly checked, is expected to furnish satisfactory information up to high pressures (perhaps 1000 atm) in a very convenient manner.

9. EVALUATION OF CURRENT DISTRIBUTION IN ELECTRODE SYSTEMS BY HIGH-SPEED DIGITAL COMPUTERS*

Jack A. Klingert, Scott Lynn,+ and Charles W. Tobias

In the absence of significant concentration gradients, the distribution of potential in electrolytic cells can be satisfactorily described by the Laplace equation. Because of severe mathematical difficulties in the past, analytical solutions have been obtained only for a few simple cell configurations. In other fields of application it is well known that the finite-difference form of the Laplace equation by iterative procedure is ideally suited for numerical solution by digital computers. The method is suitable for handling any arbitrary two-dimensional cell geometry and allows consideration of realistic overpotential behavior.

A brief description is given of the elementary mathematical relations involved and of the iterative procedure employed in machine computations. By use of this technique, the primary and secondary current density distributions were evaluated for the outside corner of an electrode which is a model representative of cell geometries commonly employed in industry. The effects of the variations of geometric and overpotential parameters are demonstrated. The results obtained indicate that the numerical technique employed is eminently suitable for rapid and accurate evaluation of current-density distributions for realistic models.

---

* Abstract of paper in Electrochem. Acta, 9, 297 (1964).

+ Research Laboratories, Western Division, Dow Chemical Company

10. PHYSICAL PROPERTIES OF Ca-NH_3 SOLUTIONS*

Wa-She Wong and Charles W. Tobias

The following measurementswere performed at -40°C, -45.5°C, and -51°C:

(a) conductivity of dilute Ca-NH_3 solutions,
(b) density of Ca-NH_3 solutions,
(c) viscosity of dilute Ca-NH_3 solutions and liquid NH_3.

In the two-liquid-phase region, the specific conductance of the dilute phase is constant at constant temperature. However, in the one-liquid-phase region, the specific conductance decreases as concentration of Ca decreases. This produces a break in the curve of the specific conductance vs overall concentration (Fig. ID.10-1), which occurs at a concentration corresponding to that of the saturated dilute phase (Table ID.10-I).

Density measurements were used to determine the phase separation of Ca-NH_3 solutions in the concentrated region. In the two-liquid-phase region, the density and concentration of each phase are constant at constant temperature, with the overall density depending only on the relative amounts of both phases present. In the one-liquid-phase region, the density of the solution changes with the concentration of Ca. If the overall density is plotted against the overall concentration of Ca, a break in the curve is again obtained (Fig. ID.10-2), which indicates the concentration at which the phase separation occurs (Table ID.10-I).

The temperature coefficient of conductivity of dilute Ca-NH_3 solutions is 3.1% per degree at -45.5°C. A comparison of this with the temperature coefficient of viscosity of liquid NH_3 (-1.64% per degree) indicates that the temperature coefficient of conductivity of dilute Ca-NH_3 solutions is not only due to the viscosity change but is also governed by the degree of dissociation.

The density of Ca-NH_3 solutions is less than that of liquid NH_3 at all concentration. The excess volume of the concentrated Ca-NH_3 solutions in the one-liquid-phase region has been calculated and is plotted in Fig. ID.10-3. The excess volume of Ca-NH_3 solutions is considerably larger that that of alkali-metal-ammonia solutions,[1] and it decreases rapidly as concentration of Ca increases.

* Contract No. N123(62738) 23531A, Technical Report No. 8.

1. P. Marshall and H. Hunt, J. Am. Chem. Soc. 77, 5016 (1955).

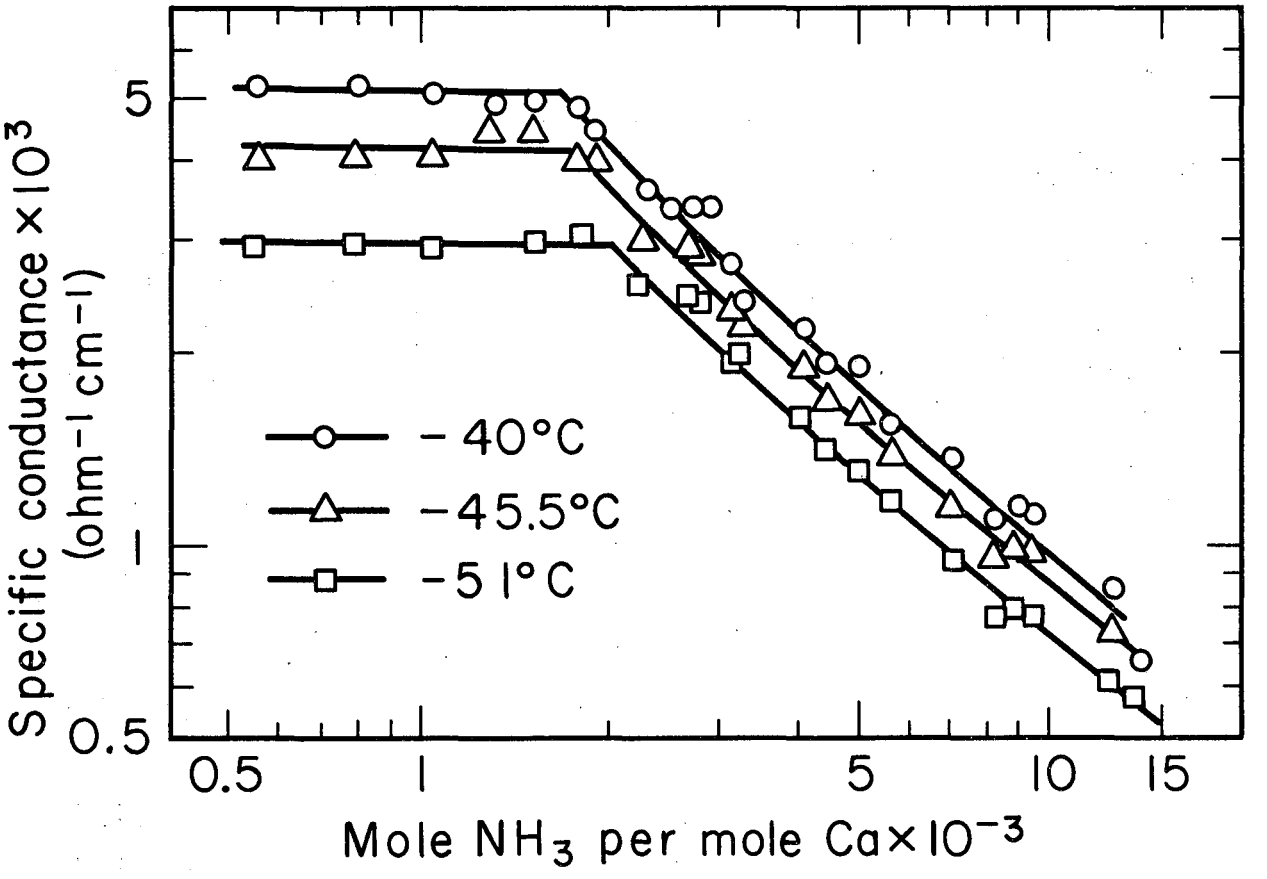

MUB-2801

Fig. ID. 10-1 Specific conductance of Ca-NH_3 solutions.

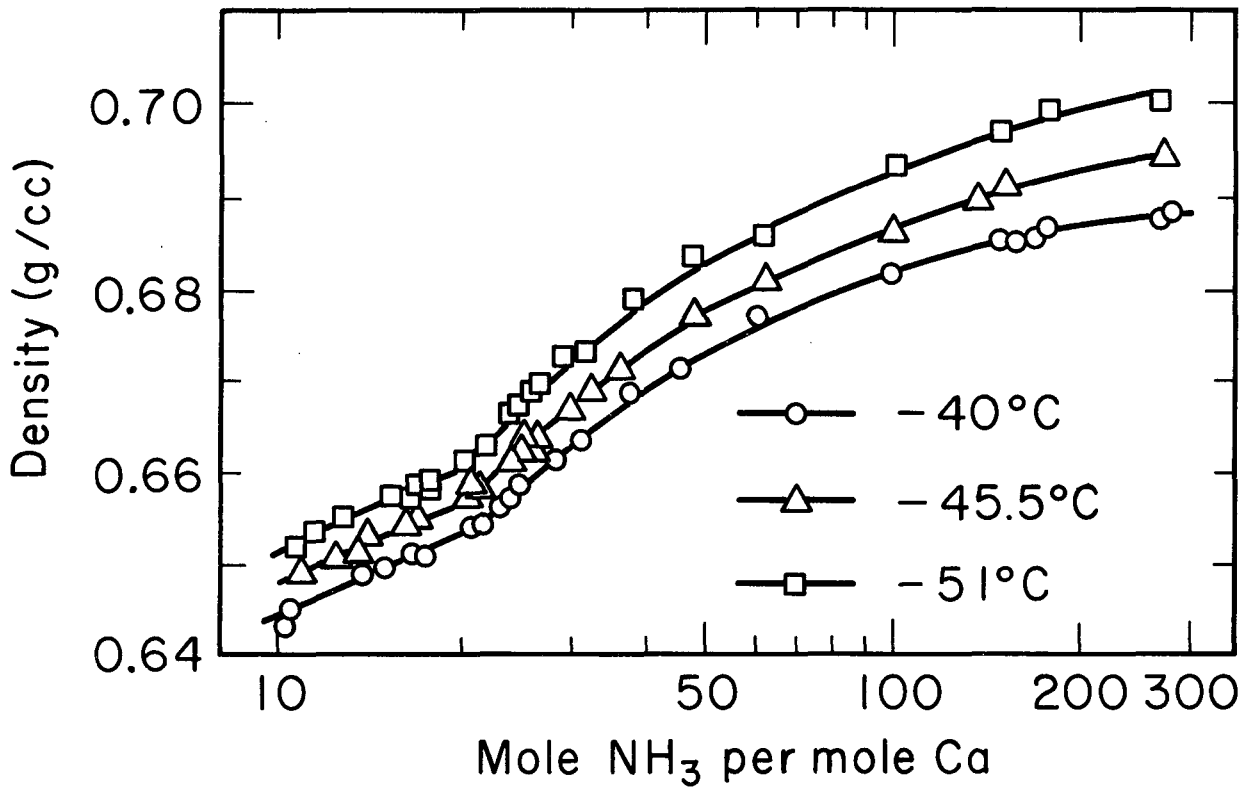

MUB-2800

Fig. ID. 10-2 Overall density of Ca-NH_3 solutions.

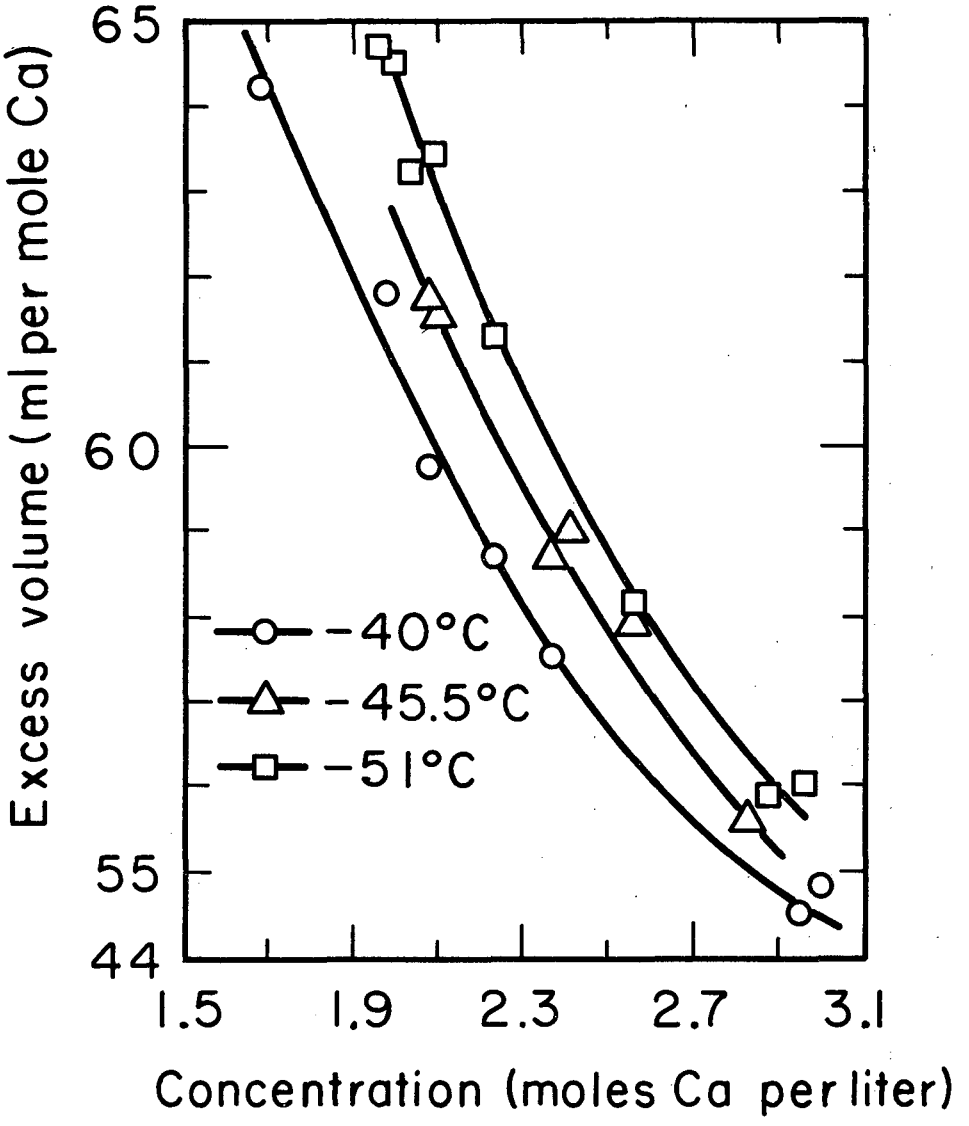

Fig. ID. 10-3 Excess volume of Ca-NH_3 solutions.

TABLE ID.10-1
CONCENTRATION OF DILUTE AND CONCENTRATED Ca-NH_3 SOLUTION
IN THE TWO-LIQUID-PHASE REGION

Temperature (°C)	Concentration of Dilute Phase		Concentration of Concent'd. Phase		Experimental Method	Source of Data
	Mole NH_3 / Mole Ca	Mole Ca / liter	Mole NH_3 / Mole Ca	Mole Ca / liter		
-32.5	199	0.1987	10.1		Vapor pressure measurements	Kraus[a]
-40	1600	0.0253	21.1	1.667	Conductivity	
-45.5	1700	0.0235	19.7	1.747	and density	Present Work
-51	1950	0.0212	18.9	1.822	measurements	
-45		0.032			Conductivity	Hallada
-64		0.013			measurements	and Jolly[b]

[a] C. A. Kraus, J. Am. Chem. Soc. 30, 653 (1908).

[b] C. Hallada and W. L. Jolly, J. Inorg. Chem. 2, 1076 (1963).

11. DYNAMIC ANALYSIS OF A ONE-DIMENSIONAL POROUS ELECTRODE MODEL*+

Edward A. Grens II and Charles W. Tobias

A one-dimensional model is developed to represent flooded porous electrodes in which there is no bulk flow of electrolyte in the pores. In this representation the pore configuration is ignored and the entire electrode treated as a homogeneous macroscopic region of electrolyte with distributed current and species sources. Mass transport in the electrolyte by diffusion and migration is considered. No assumptions of uniformity of electrolyte conductivity or composition are made. The model is capable of incorporating electrode reaction overpotential expressions of quite arbitrary nature.

Analysis of the model is conducted by numerical techniques to furnish descriptions of electrode behavior for both steady-state and transient operation. Performance characterization includes electrode overpotential and current and concentration distributions as functions of current drain and system parameters. The computational procedure is implemented on digital computing machinery.

Examples are investigated based on the cadmium anode in 5 N KOH and on the ferriferrocyanide electrode in 2 N NaOH. In these samples overpotential relationships incorporating both forward and reverse reaction terms are used and the inadequacies of approximations to these relationships are demonstrated.

* Supported by NASA Research Grant NSG 150-61.

+ Abstract of Edward A. Grens II, Ph.D. Thesis, September 1963 (also Space Sciences Laboratory Technical Report, Series No. 4, Issue No. 55), University of California, Berkeley.

12. A MODEL FOR ANALYSIS OF POROUS GAS ELECTRODES

Edward A. Grens II

A model has been developed for the analysis of the behavior of porous gas electrodes in which the reactant gas is supplied to the reaction sites at the pore walls by diffusion through a film of electrolyte covering the walls. This treatment includes consideration of the influence of dissolved gas diffusion, local overpotential, and removal (by diffusion and migration) of ionic reaction products, as well as electric current transport in the film. It yields predictions of electrode overpotential and of current distribution along the pore walls. The existence of a uniform film of electrolyte, wetting the pore interior and extending a long distance beyond the intrinsic meniscus in the pore, is assumed.

Previously published investigations using similar models, notably the recent work of Will,[1] are based upon a local reaction rate controlled exclusively by reactant supply (equilibrium reaction). This case is valid only so long as the rate of dissolved gas diffusion through the film is equivalent to a current density that is small compared with the exchange current density

1. F. G. Will, J. Electrochem. Soc. 110, 152 (1963).

of the reaction in question---a condition that may not be satisfied in many cases (e.g., the O_2 electrode in pores of micron dimensions). The present study seeks to describe these cases and predict their behavior.

In this investigation, the film is taken as a region of electrolyte in which the transport of ionic species (and current) is in only one significant direction. Subject to assumptions of constant transport parameters, an analog solution technique is developed. Approximate analytical solutions are also derived which are valid for cases of low current drain. Results are presented for the example of the oxygen electrode in 30% KOH.

13. EVALUATING THE EFFECTIVE RESISTANCES OF DIAPHRAGMS OR ELECTROLYTIC SEPARATORS*

Robert E. Meredith and Charles W. Tobias

It is shown that diaphragms or electrolytic separators, such as those commonly made of cloth or fibrous asbestos, can be approximated by a model comprised of rods which are randomly oriented in a two-dimensional lattice. The effective resistances of various arrangements of rods are measured and compared with the data for cloth, asbestos, and spun glass. The theory of electrical potential is employed to derive expressions that relate the effective resistance of such diaphragms to their porosity and to the conductivity of the dispersing solution.

---

* Abstract of paper published in J. Electrochem. Soc. 110, 1257 (1963)(Based on Robert E. Meredith, Studies on the Conductivities of Dispersions (Ph. D. Thesis), UCRL-8667, July 1959).

14. THE EFFECT OF BUOYANCY FORCES ON FORCED CONVECTION IONIC MASS TRANSFER AT HORIZONTAL PLANAR ELECTRODES* +

Robert G. Hickman and Charles W. Tobias

The effect of buoyancy forces on ionic mass transfer to electrodes in a horizontal flat duct were studied experimentally with both laminar and turbulent bulk flow. Copper electrodes and an acidified cupric sulfate electrolyte were used in obtaining mass transfer data by the technique of limiting currents. The ranges of the significant dimensionless groups covered in the experiments were as follows:

---

* Partially supported by Contract No. Da36-039 SC-89153

+ Extracted from Robert G. Hickman, Ph.D. Thesis, December 1963.

$$10^5 < \text{Gr (Grashof number)} < 10^{12},$$
$$75 < \text{Re (Reynolds number)} < 7000,$$
$$600 < \text{Sc (Schmidt number)} < 12\,000,$$
$$0.05 < \frac{d}{L}\left(\frac{\text{duct diameter}}{\text{electrode length}}\right) < 20.$$

With turbulent bulk flow, buoyancy forces were found to have a negligible effect on the mass-transfer process in the range of variables covered.

With laminar bulk flow, buoyancy forces can induce secondary flows near the electrode interface in the form of roll cells or even turbulence if the Grashof number is sufficiently high. Either of these free convective secondary flows can dominate the mass transfer process. Average mass transfer coefficients for laminar bulk flow may be predicted by estimating which of the two convective modes (forced or free) controls the mass transfer process, and then using the existing correlating equation appropriate to the controlling mode. If

$$\log(\text{Gr}) \geq 2.964 + \log(\text{Re}),$$

the process is dominated by free convection; otherwise forced convection dominates.

The data were compared with the equation of Norris and Streid for forced-convection-dominated system, and that proposed for free-convection-dominated systems, by Fenech and Tobias,[1] where Nu' is the mass transfer Nusselt number:

$$\text{Nu}' = 1.85\,(\text{Re Sc } d/L)^{1/3},$$
$$\text{Nu}' = 0.19\,(\text{Gr Sc})^{1/3}.$$

The average deviation of all the data from the appropriate correlating equation was 7% when so treated.

Other experiments were performed to obtain local mass transfer rates. These showed the transition in the direction of flow from forced convection control to free convection control as a function of the Reynolds and Grashof numbers. The influence of the secondary convective flows on the deposition profiles transverse to the direction of flow was also investigated.

---

1. E. J. Fenech and C. W. Tobias, Electrochimica Acta, 2, 311 (1960).

15. DESIGN PRINCIPLES FOR ANNULAR-BED ELECTROCHROMATOGRAPHY*

Ray M. Hybarger, Charles W. Tobias, and Theodore Vermeulen

A cylindrically symmetric arrangement is proposed for an electrochromatograph, in order to eliminate thermal bed-face effects. Theoretical analysis

---

* Abstract of paper published in Ind. Eng. Chem. Process Design Develop. 2, 65 (1963).

of the thermal and electrical behavior of a simplified model has been made. For a given geometry and a specified separation, the following relations apply: The product of residence time and applied voltage is constant. At relatively long residence times, power input is proportional to the maximum temperature rise in the unit; at any preset power input, the maximum allowable concentration then becomes proportional to the square of the residence time. These relations can be used to maximize the separation capacity of any given unit.

16. INVESTIGATION ON IONIC DIFFUSION AND MIGRATION BY A ROTATING-DISC ELECTRODE*+

Stanley Luverne Gordon and Charles W. Tobias

Contributions of migration to ionic mass transport require consideration of the interdependence of the transference number of the reacting ion and its concentration which varies within the mass transfer boundary layer.

The hydrodynamic model of the rotating-disk electrode is chosen for the purpose of developing quantitative methods for the evaluation of the contribution of migration to the overall mass transport rate.

When all ionic diffusivities are equal and a large excess of supporting electrolyte is present in the bulk electrolyte, the potential gradient across the boundary layer is constant. For this case, an analytical solution for the limiting current is obtained.

When the concentration of the supporting electrolyte is comparable to that of the reacting ionic species, the potential gradient may not be assumed constant. Since for this condition one cannot obtain an analytical solution, it is proposed that the arithmetic average of the potential gradient in the bulk solution and at the electrode-electrolyte interface may be used in the estimation of the effective transference number of the reacting species.

Anodic and cathodic limiting currents were measured for equimolar potassium ferriferrocyanide (0.01 to 0.20 molar) in sodium and in potassium hydroxide (0.0 to 3.7 molar). By application of the correction developed for the migrational contribution, it is shown that the Stokes-Einstein parameter, $\frac{D\mu}{T}$, for the ferri- and ferrocyanide ions depends on the ionic strength, Γ, only very slightly:

$$\frac{D\mu}{T}\,(\text{ferri}) = (0.234 + 0.0014\,\Gamma) \times 10^{-9}\ \frac{\text{cm}^2}{\text{sec}}\ \frac{\text{poise}}{^\circ\text{K}}\ ,$$

$$\frac{D\mu}{T}\,(\text{ferro}) = (.187 + 0.0034\,\Gamma) \times 10^{-9}\ \frac{\text{cm}^2}{\text{sec}}\ \frac{\text{poise}}{^\circ\text{K}}\ ,$$

with standard errors of estimate of 0.005 and 0.007, respectively.

---

*Partially supported by Contract No. DA36-039 SC-89153.

+ Stanley Luverne Gordon (M.S. Thesis), May 1963.

Values of the parameter $\frac{D\mu}{T}$ obtained for either pure ferricyanide or ferrocyanide are within 6% of those obtained for solutions containing supporting electrolyte, after the correction for the migrational contribution (up to 20%) is applied.

17. TEMPERATURE MAXIMA IN COUNTERCURRENT HEAT EXCHANGERS WITH INTERNAL HEAT GENERATION*

E. A. Grens II and R. A. McKean†

In countercurrent heat exchange equipment where heat is being generated in a process steam being cooled, maxima can exist in the temperature profiles. These maxima may far exceed temperatures that would have been reached without cooling and are not necessarily accompanied by high outlet temperature. The conditions favoring this phenomenon are discussed and its importance cited. The special case of uniform heat generation in a process steam is analyzed in detail. Two examples are presented.

---

* Abstract from Chem. Eng. Sci. 18, 291 (1963).

† At Union Oil Company of California, Union Oil Center, Los Angeles, Calif.

E. PHYSICAL CHEMISTRY

1. THE EFFECT OF CONCENTRATION DRIVING FORCE ON LIQUID-LIQUID MASS TRANSFER*

Donald R. Olander and L. B. Reddy†

The enhancement of the rate of mass transfer due to concentration driving force-induced interfacial turbulence has been investigated in several typical liquid-liquid systems.

The three solvent pairs studied were isobutanol-water, 85 volume % tributyl phosphate (TBP) in n-hexane-water, and 85 volume % tributyl phosphate in carbon tetrachloride-water. Nitric acid was the solute in all three systems. The experiments were conducted in an unbaffled stirred-vessel extractor operated as a steady state continuous flow device. The stirring speed was 72 rev/min for all experiments.

For all the systems, transfer from the organic to the aqueous phase was unstable. The overall mass-transfer coefficient increased sharply by factors of 1.5 to 4 as the driving force was increased. Transfer from aqueous to organic phase was stable, except for the TBP-n-hexane system in which the mass-transfer coefficient increased at high driving forces. The transfer coefficient was found to depend only on the concentration driving force, except for the TBP-hexane system in which it appeared to be a function of concentration level as well as of driving force.

The results were consistent with the qualitative features of Marangoni instability, although several aspects of the data could not be explained on this basis.

---

* Abstract of a paper to be published in Chem. Eng. Sci. 19, 67 (1963).
† Now at Kennametal Inc., Fallon, Nevada.

2. THE MECHANISM OF EXTRACTION BY TRIBUTYL PHOSPHATE-N-HEXANE SOLVENTS* PART II. NITRIC ACID EXTRACTION

Donald R. Olander and M. Benedict†

The kinetics of extraction of nitric acid by tributyl phosphate-n-hexane solvents has been investigated in a stirred-vessel transfer cell.

---

* Abstract of a paper published in Nuc. Sci. Eng.
† Now at Department of Nuclear Engineering, Massachusetts Institute of Technology, Cambridge, Massachusetts.

Elucidation of a possible slow step in the extraction process due to the complexing reaction $HNO_3 + TBP \longrightarrow HNO_3 \cdot TBP$ was of particular interest.

The criteria used to determine the mechanism were

(a) The effect of temperature.
(b) The effect of stirrer speed.
(c) Comparison of the mass-transfer coefficients to those of nitric acid in a nonreacting solvent.
(d) Comparison of the mass-transfer coefficients to those predicted by a previously developed correlation for two-component, two-phase systems.

On the basis of these criteria, the kinetics were found to be controlled by purely diffusional processes.

The mechanism proposed involves mass transfer of the nitric acid through the aqueous film, rapid and complete conversion to the complex at the interface, and transfer of the complex to the organic phase. This last step constitutes the major portion of the overall resistance, although resistance in the aqueous phase also constitutes a small fraction of the total. No effect of a slow chemical conversion was found. At high acid levels, the transfer process was accelerated by a factor of 2 to 3 by the phenomenon of interfacial turbulence, arising probably from the Marangoni effect.

3. A MODIFIED MODEL OF STIRRED-VESSEL MASS TRANSFER*

Donald R. Olander

The model of stirred-vessel mass transfer previously presented[1] has been amended to account for transfer in the core region. In addition to the two-region picture, a modified single-region model, in which the return flow to the interface occurs in a region close to the vessel wall, is also described. Both the corrected two-region and the single-region models show good agreement with data from transfer cells with no separators at the interface. The recent data of Loosemore and Prosser,[2] in which the interface was partially blocked, were also in reasonably good agreement with theory if transfer in the core region of the interface is included.

---

* Abstract of a paper to be published in Chem. Eng. Sci.

1. D. R. Olander, Chem. Eng. Sci. 18, 123 (1963).
2. M. J. Loosemore and A. P. Prosser, Chem. Eng. Sci. 18, 555 (1963).

4. HIGH FLUX SOLID-LIQUID MASS TRANSFER*

A. S. Emanuel† and Donald R. Olander

The effect of large concentration gradients upon the rate of mass transfer from a rotating disk has been measured experimentally and compared with theory. Measured rates were found to agree with numerical solutions of the variable property, finite interfacial velocity diffusion equation. The data were also compared with approximate perturbation and integral solutions of the diffusion equation. The systems investigated were benzoic acid, potassium bromide, sucrose, and copper sulfate in water. Variations in density, viscosity, and diffusivity and the existence of a diffusion-induced interfacial velocity can result in differences between the constant property, zero interfacial velocity, and the actual Sherwood numbers as large as a factor of two.

* Abstract of a paper to be published in Intern. J. Heat Mass Transfer.
† Now at Atomics International Division, North American Aviation, Canoga Park, Calif.

5. TRANSPORT PROPERTIES OF LIQUID METALS

Alan Pasternak and Donald R. Olander

The few available data on diffusivities in liquid metals have been tentatively correlated by a modified form of absolute rate theory which had previously been applied to ordinary liquid solvents.[1] The method represents an improvement of the Stokes-Einstein relation in that the interaction between solute and solvent can now be taken into account. Interactions of the simple dispersion type are incorporated into the theory by a term involving the viscosities of the pure metal components.

All available data agree satisfactorily with the analytical model except for the diffusion coefficients involving uranium as one component. The discrepancy may lie in the fact that the viscosity of uranium has not been measured, and the common empirical estimations of liquid metal viscosities may not be applicable to the actinide elements.

In order to resolve the question of uranium diffusion coefficients, a capillary viscosimeter has been constructed to measure the viscosity of uranium in the range 1130 to 1200°C. Because of the corrosive nature of liquid uranium, the device is constructed of tantalum metal. To avoid errors due to corrosion-induced alteration of the capillary geometry, the viscosimeter is used as a relative rather than an absolute measuring device. The unknown viscosity is obtained by comparing the efflux time to those of standards such as tin and copper.

1. D. R. Olander, A.I.Ch.E.J. 9, 207 (1963).

6. A LAMINAR JET APPARATUS FOR THE STUDY OF HIGH-TEMPERATURE GAS-LIQUID REACTIONS

Jose L. Camahort and Donald R. Olander

The precisely controlled and known hydrodynamics of a laminar jet of liquid passing through a gas phase makes a contacting device based on this principle useful in studying high-temperature gas-liquid reactions. Similar designs have been used for studying low-temperature aqueous systems,[1,2] but considerable modifications were required before fused salts or liquid metals could be handled.

The present design consists of a nickel reaction vessel approximately 10 in. high and 4 in. in diameter, which is divided into two sections by a nickel plate pierced by a 1-mm orifice. The molten salt is fed to the upper section from a feed tank and is maintained at a constant head by a level controller. The jet existing from the orifice leaves the reaction section via a 2-mm capillary tube and is collected in a receiving tank.

The dynamic characteristics of absorption into the jet produced by this apparatus have been checked by measuring the diffusivity of CO_2 in water with the equipment. The 5% agreement between the measured and literature values of the diffusion coefficient indicate that an ideal jet is in fact produced.

1. P. Raimondi and H. L. Toor, A.I.Ch.E.J. 5, 86 (1959).
2. W. Manogue and R. L. Pigford, A.I.Ch.E.J. 6, 494 (1960).

7. STUDIES OF MOLECULAR STRUCTURE USING NMR TECHNIQUES

Charles H. Sederholm

In this Laboratory, high-resolution NMR techniques are being used to study the structure of molecules. In addition, correlations are being found between the structure of molecules and their NMR spectra.

A thorough study of the factors influencing fluorine-fluorine coupling constants has led to the conclusion that the direct overlap of nonbonding electrons around the two nuclei being coupled is as important to fluorine-fluorine coupling constants as are the bonding electrons in the molecule. The spin information carried by the bonding electrons is reduced as the electronegativity of the other atoms attached to the molecule is increased.

Measurements of fluorine NMR spectra over a wide temperature range have resulted in two types of information. Barriers to internal rotation in several halogen-substituted ethanes containing at least one fluorine atom have been determined, and some correlation has been established between the barrier heights and the size of the halogen substituents. The time-weighted average approximation for chemical shifts and coupling constants has been tested in several compounds, and it has been demonstrated that solvent effects can cause serious exceptions to this approximation. The effect solvents have on coupling constants is being further investigated.

Proton geminal coupling constants are predicted to vary with the H-C-H bond angle. For a normal tetrahedral angle the coupling constant is predicted to be and is generally found to be roughly 8 to 12 cps. In several four-membered ring compounds the geminal coupling constant has turned out to be quite small; on the order of 2 to 3 cps. Geminal coupling constants in four-membered rings are being further investigated to determine which factors affect their size.

8. NMR FLUORINE-FLUORINE COUPLING CONSTANTS

Charles H. Sederholm

A thorough study of F-F coupling constants has resulted in a reasonably complete picture of the factors influencing the magnitude of these coupling constants. We believe that magnetic spin information is transmitted both by the direct overlap of the electronic clouds of the atoms being coupled (through space coupling), and by indirect coupling through bonding electrons (through-the-bonds coupling).

Experimental data to support our belief that a large amount of the F-F coupling comes about as a result of the direct overlap of the electronic clouds of the atoms being coupled is shown in Fig. IE.8-1. Here for a group of perfluoro compounds we have made the assumptions that: (a) there is no through-the-bonds coupling, and (b) through-space coupling is zero if the two fluorine atoms are at a distance greater than 2.72Å. The first assumption is discussed below. The latter is based on the fact that vicinal F-F coupling constants in perfluorocarbons are typically zero. On the basis of these assumptions, coupling constants are plotted vs distance between the two fluorine atoms under consideration. This correlation shows that as the distance gets smaller, and the electronic overlap gets larger, the coupling constant increases. Each point on this plot corresponds to the data for many compounds.

In a four-membered ring compound in which two nonequivalent CF_3 groups can be either on the same side of the ring or on opposite sides, the coupling constant for the cis compound is large (approx. 12 cps), while the coupling constant for the trans compound is near-zero. See Fig. IE.8-2. Again, our interpretation is that only through-space coupling is active here, and hence the coupling is large only when the two fluorine atoms get close to each other.

The magnitude of the indirect coupling through the bonds is affected by the electronegativity of other atoms in the molecule. In Fig. IE.8-3, for a group of halogen-substituted ethanes, vicinal fluorine-fluorine coupling constants are plotted vs the sum of the electronegativity of the other atoms attached to the carbon skeleton. A good correlation is found. It should be noted that the results of this correlation predict that the through-the-bonds vicinal coupling constant in perfluorocarbon compounds should be nearly zero, as was assumed above.

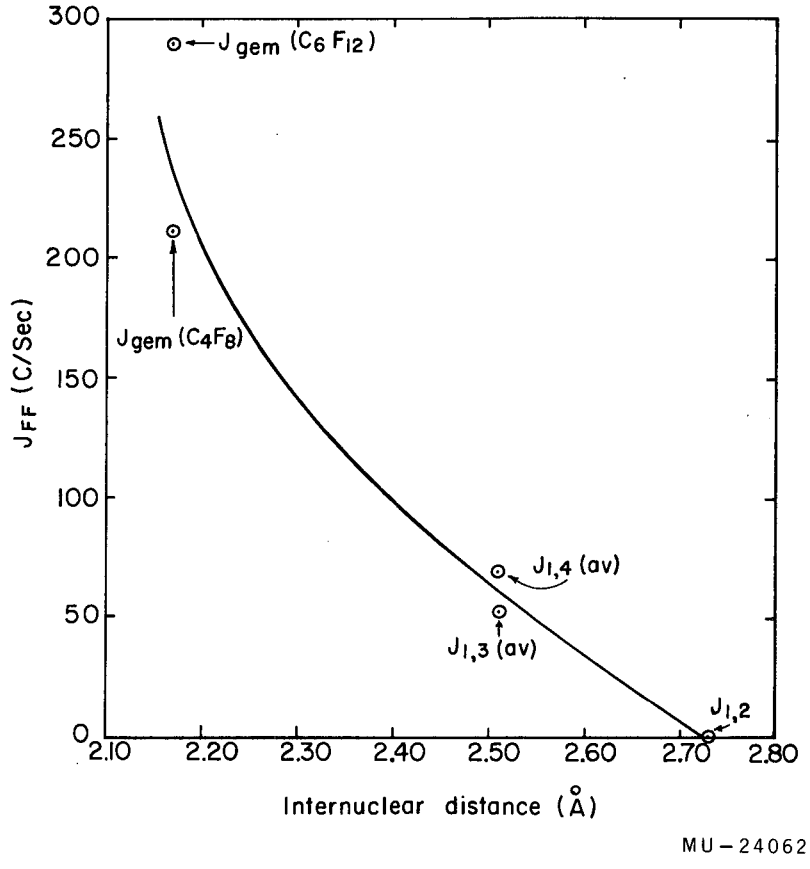

Fig. IE. 8-1 Plot of F^{19} spin coupling constants as a function of internuclear distance between interacting nuclei.

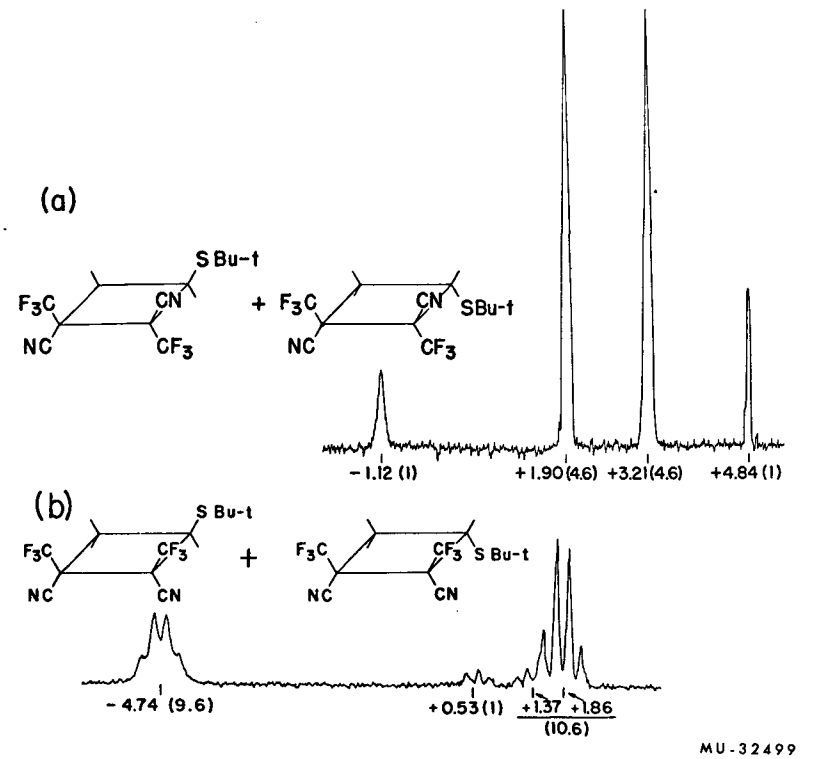

Fig. IE. 8-2 F^{19} NMR spectra of cyclobutane diastereomer mixture.

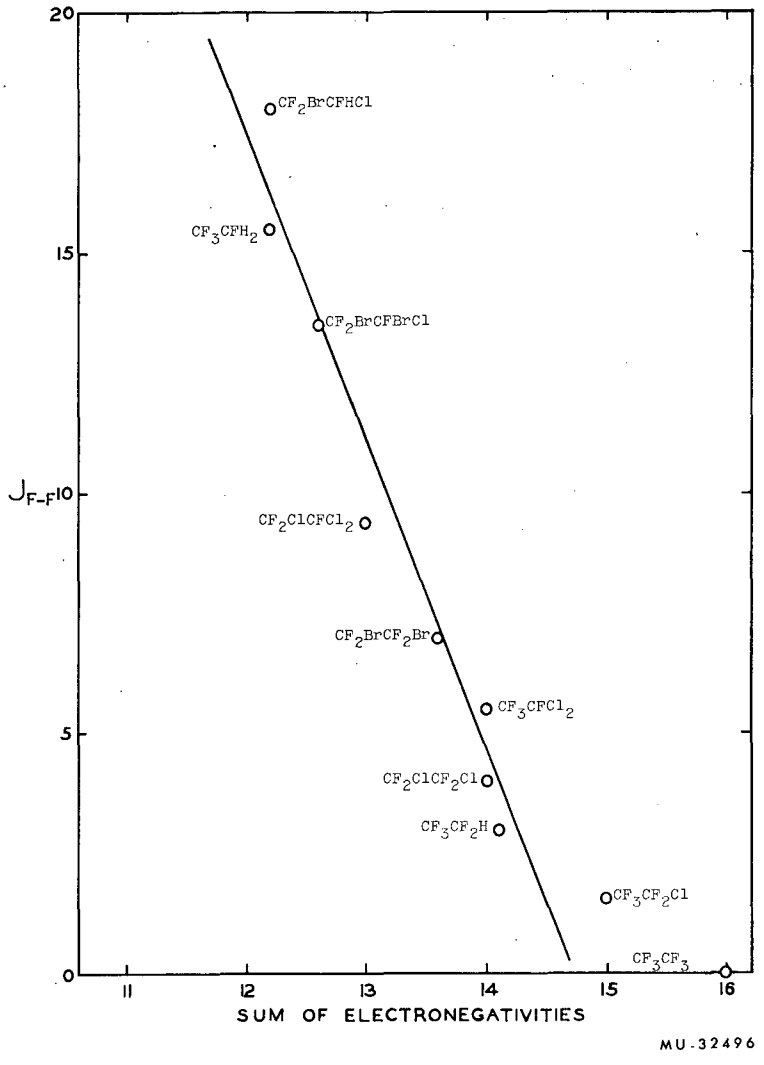

Fig. IE. 8-3 Plot of J_{F-F} vs sum of electronegativities of substituents in ethanes.

9. SOLVENT EFFECTS ON F-F COUPLING CONSTANTS

Charles H. Sederholm

Some F-F coupling constants vary considerably with temperature. This temperature dependence could come about as a result of exciting vibrational and rotational modes of a molecule, or could also come about as a result of temperature-dependent solvent effects. In an effort to show that the second is not negligible we have investigated the low-temperature spectrum of CF_2Br-$CFBrCl$ in a variety of solvents. The temperature was sufficiently low so that the individual rotamers could be observed. It was found that the observed coupling constants for a single rotamer at a single temperature could be altered by several percent by a change in the solvent.

The spectrum of bromotrifluoroethylene was also taken in a variety of solvents at room temperature. Again, all of the coupling constants were observed to vary with the solvent by a few percent.

10. REACTION KINETICS BY PARAMAGNETIC RESONANCE

Bruce H. Mahan and Rollie J. Myers

Electron paramagnetic resonance permits the direct observation of gaseous free radicals, and can be used to study the rates of their chemical reactions. There are no completely satisfactory measurements of the rates of

$$O + \dot{O} + Ar \rightarrow O_2 + Ar,$$

$$N + N + Ar \rightarrow N_2 + Ar,$$

and $$H + H + Ar \rightarrow H_2 + Ar,$$

and we intend to determine the rate constants for these reactions within the next year. They are of particular interest because the potential energy surfaces are well known, and the rate data can be interpreted theoretically.

As a second part of the program, metathetical free-radical reactions will be studied. For example,

$$H + O_2 \rightarrow OH + O$$

and $$O + H_2 \rightarrow OH + H$$

are reactions in which both product and reactant radicals can be detected. This allows a more certain determination of reaction mechanisms and rate constants in these potentially more complicated systems, and in some cases gives rate information that cannot be obtained by any other technique.

11. KINETICS OF ELECTRON REACTIONS

Bruce H. Mahan

By using microwave cavity resonance techniques, it is possible to measure the concentration of gaseous thermal electrons. This method can be used to study the kinetics of the elementary reactions of electrons. For example,

$$e + NO_2 + Ar \rightarrow NO_2^- + Ar, \qquad (1)$$

$$e + N_2O \rightarrow N_2 + O^-, \qquad (2)$$

and

$$e + NO^+ \rightarrow N + O \qquad (3)$$

are three different types of reactions that gaseous electrons undergo. Reaction (1) is presently under investigation. It is of practical interest because NO_2^- is an important negative ion in the upper atmosphere. The theoretical analysis of such a reaction in which the de Broglie wave length of the electron is large compared with the extent of the fields of the molecules is possible, and indicates that the data can be analyzed to give a limit for the lifetime of the electron on NO_2 in the process

$$e + NO_2 \rightarrow (NO_2^-)^*,$$

$$(NO_2^-)^* \rightarrow NO_2 + e.$$

The energy dependence of reactions (2) and (3) can be interpreted in terms of the potential energy surfaces for reactants and product molecules. Thus we plan to make such measurements on these and a variety of other small molecules and ions in which the potential energy surfaces are expected to be of simple form.

12. THE DISSOCIATION ENERGY OF Cs_2^+ BY A PHOTOIONIZATION METHOD

Yuan-tseh Lee and Bruce H. Mahan

Experiments on the photoionization of cesium vapor in a space charge detector by Mohler, Foote, and Chenault[1] have shown that in addition to the predicted ionization beyond the absorption series limit there is some ionization by line absorption.

Subsequent studies by Mohler and Boeckner[2] established that the ionization by line absorption involves the production of an excited atom and the subsequent collision of the excited atom and a normal atom, i.e.,

1. Mohler, Foote, and Chenault, Phys. Rev. 27, 37 (1926)
2. Mohler and Boeckner, Bureau of Standards Journal Research 5, (RP 186).

$$Cs^* (np) + Cs = Cs_2^+ + e.$$

Independent kinetic studies by Freudenberg[3] suggested, from the observation and temperature dependence of ionization current due to the 4555-Å line, that the dissociation energy of Cs_2^+ is 1.05 eV, much higher than the dissociation energy of Cs_2 (0.45 eV).

Recent investigations by Barrow[4,5] by a spectroscopic method furnished the following values of dissociation energies of Li_2^+, Na_2^+, K_2^+:

	$De(M_2)$	$De(M_2^+)$	$De(M_2^+)-De(M_2)$
Li	1.20	1.63	0.43 eV
Na	0.76	1.01	0.27 eV
K	0.51	0.76	0.25 eV

Owing to the low concentration of diatomic species in the vapor of heavy alkali metals, spectroscopic determinations of dissociation energy of Cs_2^+ and Rb_2^+ are not available. Because there seems to be a large gap between Freudenberg's value for Cs_2^+ and the value that might be extrapolated from the general behavior of alkali metals obtained by the spectroscopic method, it seemed worthwhile to carry out the excited-cesium-atom reaction by direct measurement of ionization current of cesium by line absorption, thereby avoiding the possible complications of the space charge detector.

Preliminary experiments were carried out by detecting with a vibrating-reed electrometer the ionization current under steady illumination with the cesium pressure of 10^{-2} to 10^{-1} mm Hg. These experiments showed that it is impossible to detect such a small signal current, because of the high level of background current due to thermal electron emission from the collecting electrode. In order to pick up the small signal current buried in the high background current, we arranged to chop the incident light and to detect the signal by a lock-in amplifier which is composed of a narrow band-width tuned amplifier and phase-sensitive detector.

In preliminary experiments carried out at 288°C and at a vapor pressure of 10^{-1} mm Hg, we have been able to measure Cs_2^+ current for the absorption lines shorter than 3612 Å with signal-to-noise ratio greater than 25. On the basis of these results, we can conclude that the bond energy of Cs_2^+ is 0.6 ± 0.1 eV, which is more nearly in accordance with the results for the other alkali metals than is the value of Freudenberg.

3. Freudenberg, Physik 67, 417 (1931).
4. Barrow, Travis, and Wright, Nature 4732, 141 (1960).
5. Robertson and Barrow, Proc. Chem. Soc. 329 (1961).

13. MECHANICS OF ATOM RECOMBINATION

Bruce H. Mahan

There have been several attempts[1,2,3] to calculate the rate constant for the recombination of atoms according to the three-body collisional mechanism

$$A + A \rightleftharpoons A_2^* \quad \text{(for K)},$$

$$A_2^* + M \longrightarrow A_2 + M \quad \text{(for } k_c\text{)}.$$

The equilibrium constant K for the formation of unbound atom complexes can be calculated reliably by statistical mechanics. Commonly, k_d is set equal to $\langle P \rangle Z$, where Z is the bimolecular collision rate, and $\langle P \rangle$ is the average probability that a collision of M with the A_2^* complex will lead to a bound molecule. The usual procedure has been to set $\langle P \rangle$ equal to unity, in the absence of any other information. In this note we show how the conservation laws alone can be used to obtain a more refined estimate of the deactivation probability.

Figure IE.13-1 is a velocity vector diagram for two recombining atoms (particles 1 and 2) and an inert deactivator M (particle 3). At any separation r, the relative speed g_{12} of particles 1 and 2 is

$$g_{12}(r) = \left[g_{12}^2(\infty) - \frac{2\varphi}{\mu_{12}} \right]^{1/2},$$

where φ is the (negative) potential energy of particles 1 and 2. If particle 1 undergoes an impulsive collision such that the resulting relative speed g_{12} is less than $(-2\varphi/\mu_{12})^{1/2}$, the atoms become bound. Therefore, a "deactivation sphere" of radius $(2\varphi/\mu_{12})^{1/2}$ can be drawn with the tip of $\underset{\sim}{v}_2$ as the origin. If the collision of atom 1 with M is such that the final velocity vector $\underset{\sim}{v}_1'$ falls within the deactivation sphere, particles 1 and 2 are bound.

The effect of the 1-3 collision is to rotate the relative velocity vector $\underset{\sim}{g}_{13}$ about the center-of-mass vector $\underset{\sim}{V}_{13}$. The final vecloity vector $\underset{\sim}{v}_1'$ will lie somewhere on the surface of this "collision sphere," whose radius is $g_{13}m_3/(m_1+m_3)$. If there is a hard-sphere interaction between the particles 1 and 3, their scattering is isotropic, and the collision sphere is uniformly populated with final velocity vectors. In these circumstances, the fraction of collisions that lead to deactivation is just the fraction of the area of the collision sphere that lies within the deactivation sphere. Although this

1. C. B. Kretschmer and H. L. Peterson, J. Chem. Phys. 39, 1772 (1963).
2. S. W. Benson and J. Fueno, J. Chem. Phys. 36, 1597 (1962).
3. D. L. Bunker, J. Chem. Phys. 32, 1001 (1960).

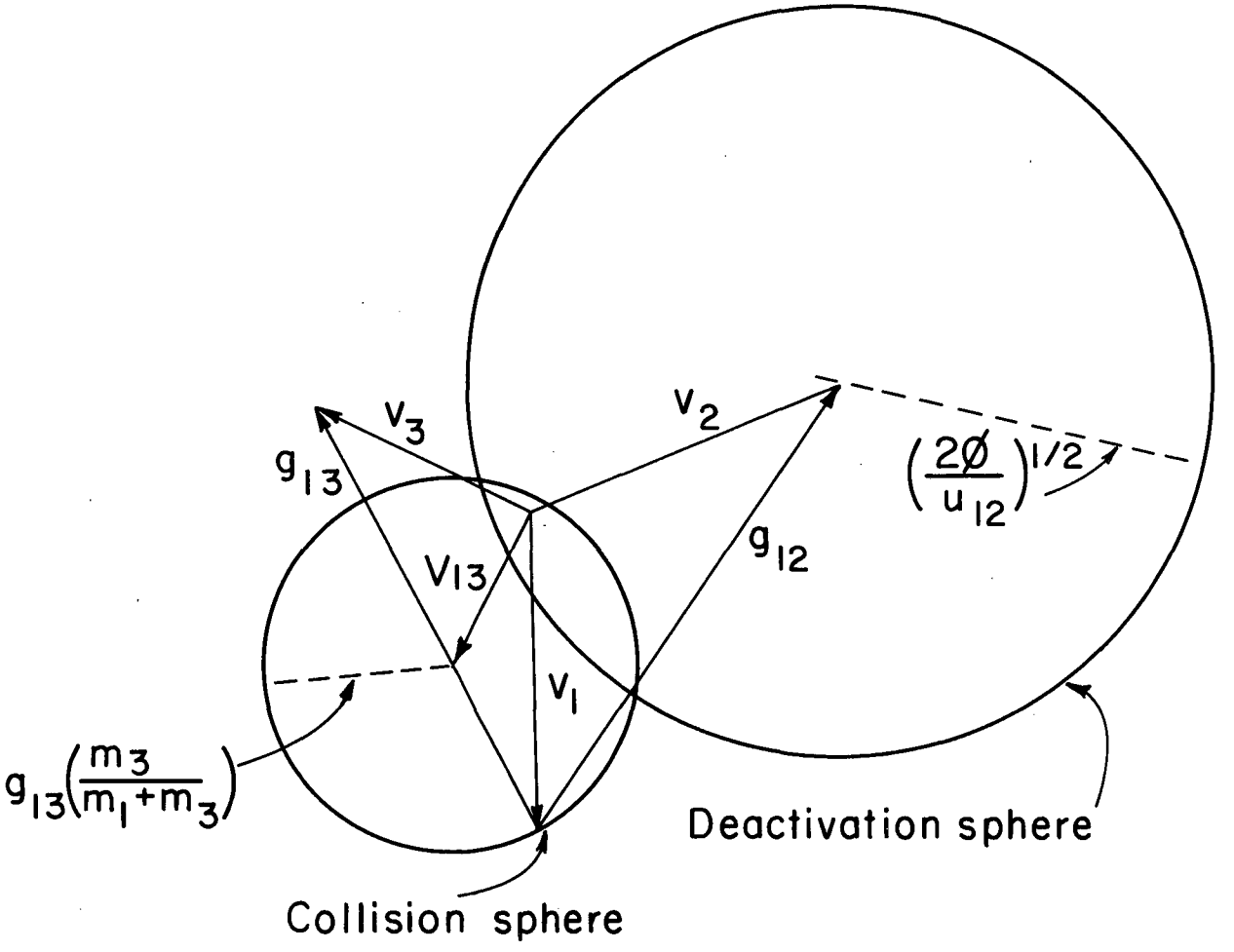

MUB-2791

Fig. IE. 13-1 Velocity vector diagram for atom combination.

fraction is easily expressed in terms of the velocity vectors, proper averaging over the magnitudes and directions of the velocities to obtain $\langle P \rangle$ is very difficult. However, it is possible to conclude that when the separation of the atoms is small, so that $(-2\varphi/\mu_{12})^{1/2} \gg g_{12}(\infty)$, $\langle P \rangle \approx 1$. It is also true that for $|\varphi| < kT$, $\langle P \rangle < 0.1$. Consequently we can decide that in order for deactivation to occur two atoms must be close enough so that $|\varphi| > kT$. This provides a practical criterion for a three-body rate calculation.

14. RECOMBINATION OF GASEOUS IONS. I.*

Bruce H. Mahan and James C. Person+

The rate at which gaseous NO^+ and NO_2^- neutralize each other has been measured in a variety of gases over a relatively large pressure range. In the limit of low pressures of inert gas, the neutralization process is a bimolecular electron transfer reaction,

$$NO^+ + NO_2^- \xrightarrow{k_o} \text{neutrals}.$$

The measured value of k_o is 2.1×10^{-7} cc per ion sec, which means that any two ions that come within 25 Å of each other undergo charge transfer.

At pressures of inert gas in the range of 0.01 to 1 atm, most ions are neutralized by a three-body recombination process,

$$NO^+ + NO_2^- \xrightarrow{k_1} (NO^+NO_2^-)^*,$$
$$(NO^+NO_2^-)^* \xrightarrow{k_2} NO^+ + NO_2^-,$$
$$(NO^+NO_2^-)^* + M \xrightarrow{k_3} (NO^+NO_2^-) + M \longrightarrow \text{neutrals}.$$

Here $(NO^+NO_2^-)^*$ is a pair of ions close to each other, but with enough energy to separate, and $(NO^+NO_2^-)$ is a pair of ions in bound orbit which will eventually bring them close enough for charge transfer to occur. The value of k_1 has been found to be $1.7 \pm 0.5 \times 10^{-6}$ cc per ion sec. This means that any two ions closer to each other than 140 Å are susceptible to collisional deactivation by a third body M. At these distances the negative potential energy of the ions is approximately equal to 4 kT. It would appear then that the requirement for susceptiblity to deactivation is that the kinetic energies of the ions be noticeably greater than the average thermal energy. If an ion is moving faster than the average neutral, it is more likely to lose than to gain energy upon a collision.

---

* Abstract of paper submitted to J. Chem. Phys.

+ Now at Argonne National Laboratory, Argonne, Illinois.

The relative values of k_3 were measured for a variety of inert gases, and are given below.

He	1.00	N_2	5.2±1.1
H_2	1.4±0.4	Ar	3.6±0.8
D_2	1.5±0.4	Kr	4.3±1.0
		Xe	6.8±1.5

These values are consistent with the larger collision cross sections of the heavier molecules, and with the limitations imposed on energy transfer by the law of conservation of momentum.

15. RECOMBINATION OF GASEOUS IONS. II.*

Bruce H. Mahan and James C. Person+

The mechanics of a three-body collision involving two gaseous ions and a neutral atom are discussed, and a method for calculating the rate at which ions are deactivated into bound orbits is presented. The relative efficiencies of various gases in promoting ion recombination are calculated, and found to be in satisfactory agreement with the experimental values found in Part I of this series. The details of the mechanics show that deactivation efficiency increases with the mass of the neutral molecule, and decreases with the relative kinetic energy of the ion pair.

* Abstract of article submitted to J. Chem. Phys.
+ Now at Argonne National Laboratory, Argonne, Illinois.

16. RECOMBINATION OF GASEOUS IONS. III.*

Terry S. Carlton and Bruce H. Mahan

In an earlier publication, Mahan and Person showed that the mechanism of the mutual neutralization of gaseous ions involves two parallel processes. One of these is a bimolecular electron transfer reaction,

$$A^+ + B^- \xrightarrow{k_o} \text{neutrals.}$$

The other is esentially J. J. Thomson's three-body ion recombination reaction,

* Condensation of UCRL-11134 (November 1963), submitted to J. Chem. Phys.

$$A^+ + B^- \xrightarrow{k_1} (A^+B^-)^*,$$
$$(A^+B^-)^* \xrightarrow{k_2} A^+ + B^-,$$
$$(A^+B^-)^* + M \xrightarrow{k_3} (A^+B^-) + M \longrightarrow \text{neutrals}.$$

In this note we report values of k_o measured in three different systems: (a) a photoionized mixture of NO and SF_6, in which the principal ions are probably NO^+ and SF_6^-, (b) a photoionized mixture of benzene and SF_6, in which the principal ions are $C_6H_6^+$ and SF_6^-, (c) photoionized iodine vapor, in which I_2^+ and I^- are prevalent. The values of k_o were obtained by measuring the low-pressure limit of α, which is defined by

$$-\frac{dA^+}{dt} = \alpha\,(A^+)(B^-).$$

Three different inert gases were used in each system. The results are contained in Table IE.16-I.

Table IE.16-I. Results of k_o Measurements.

System	$kx10^7$ (cc/ion sec)
NO-SF_6-He	1.95 ± 0.1
NO-SF_6-Ar	2.0 ± 0.15
NO-SF_6-Xe	1.5 ± 0.15
C_6H_6-SF_6-He	1.8 ± 0.2
C_6H_6-SF_6-Ar	1.75 ± 0.15
C_6H_6-SF_6-Xe	1.35 ± 0.15
I_2-He	1.5 ± 0.2
I_2-Ar	1.2 ± 0.2
I_2-Xe	1.0 ± 0.2

The results seem to be rather insensitive to the chemical nature of the ions. This is in accordance with the idea that the electron states involved in the electron-transfer process are Rydberg states, whose nature is similar in all systems. The slightly smaller values of k_o obtained when Xe is present in the system are thought to be caused by ion-induced dipole complexes between the ions and the polarizable xenon atoms.

* Condensation of UCRL-11134, (November 1963) submitted to J. Chem. Phys.

17. ELASTIC SCATTERING OF CHEMICALLY REACTIVE MOLECULES*

Dudley R. Herschbach+ and George H. Kwei+‡

The angular distribution and the velocity dependence of the total elastic scattering cross section are calculated for a potential which presents a deep "chemical well" at small distances and van der Waals well at large distances. A two-body central force model and semiclassical mechanics are used. It is found that the chemical well suppresses much of the wide-angle scattering and under suitable conditions may introduce several special effects, including "multiple rainbows" and "chemical orbiting" in the angular distribution and "beats" in the undulatory velocity dependence of the total cross section.

---

* Abstract of a paper in Proceedings of the Third International Conference on Collision Processes (North-Holland Publishing Co., Amsterdam, 1963) (also UCRL-11178, January 1964).

+ Present address: Department of Chemistry, Harvard University, Cambridge, Massachusetts.

‡ Woodrow Wilson Foundation Predoctoral Fellow, 1961-63.

18. TESTING OF DIATOMIC POTENTIAL ENERGY FUNCTIONS BY NUMERICAL METHODS

John K. Cashion+

An accurate and efficient numerical method for solving the radial Schrödinger equation for diatomic molecules has been employed in two tests relating to approximate potential functions. First, quantitative estimates have been made of the errors in the approximate eigenvalue equation derived by Pekeris for the rotating Morse oscillator. Secondly, as an example of testing a potential function for which no analytic solution is known, the eigenvalues of the Clinton potential have been compared with those of Morse and with experiment.

---

* Abstract of J. Chem. Phys. 39, 1872 (1963) (also UCRL-10643, May 1963).

+ Present address: Department of Chemistry, Harvard University, Cambridge, Massachusetts.

19. CALCULATION OF INTENSITY DISTRIBUTION IN THE VIBRATIONAL STRUCTURE OF ELECTRONIC TRANSITIONS: THE $B^3\Pi_{o^+_-u} - X^1\Sigma_{o+g}$ RESONANCE SERIES OF MOLECULAR IODINE.*

Richard N. Zare†

Franck-Condon overlap integrals have been calculated which predict within experimental error the intensity distribution of the 60 measured lines in the visible fluorescence spectrum of molecular iodine, $B^3\Pi_{o+u}(v' = 15, 16, \text{or } 26) \rightarrow X^1\Sigma_{o+g}(v'' = 0 \text{ to } 69)$. Rydberg-Klein-Rees potentials were used for both electronic states, and exact vibrational eigenfunctions were obtained by direct numerical solution of the radial Schrödinger equation, including vibration-rotation interaction. The electron transition moment was assumed to be independent of internuclear distance. Overlap integrals derived in the same way for Morse potentials fail to give even qualitative agreement with experiment for lines with $v'' \gtrsim 10$. Because of the rapid oscillation of the vibrational wave functions for high v' and v'', a shift in the potential of only 0.002 Å is found to alter appreciably the calculated intensity distribution; thus the agreement obtained provides a very severe test of the RKR potentials and the Franck-Condon principle. The radiative lifetime of the B state has also been calculated from the absolute intensity of a single line and the integrated intensity of the band system, and the results compare favorably with direct lifetime measurements.

*Abstract of a paper in J. Chem. Phys. 40, 1934 (1964). (Also UCRL-11110, October 1963, and UCRL-10925, November 1963).
† National Science Foundation Predoctoral Fellow, 1961-63. Present address: Department of Chemistry, Harvard University, Cambridge, Massachusetts.

20. EMPIRICAL EVALUATION OF THE LONDON POTENTIAL ENERGY SURFACE FOR THE H + H_2 REACTION*

John K. Cashion† and Dudley R. Herschbach†

An empirical potential surface for the hydrogen exchange reaction is derived from the simplest form of the London approximation (neglecting overlap), by evaluating the Coulomb and exchange integrals from the potential curves for the $^1\Sigma_g^+$ and $^3\Sigma_u^+$ states of H_2. This procedure gives an activation energy of 8.9 ± 1.2 kcal/mole. The potential surface has a single saddle point, and the H_3 complex is linear and symmetrical, with a bond length of 0.96 A. Simple, explicit formulas for the activation energy and the vibrational force constants are also obtained. The results emphasize the important contribution from the triplet repulsion between the end atoms with parallel spins in the complex.

* Abstract of a paper to be published in J. Chem. Phys. (also UCRL-11171, January 1964).
† Present address: Department of Chemistry, Harvard University, Cambridge, Massachusetts.

21. INFLUENCE OF VIBRATIONS ON MOLECULAR STRUCTURE DETERMINATIONS. III. INERTIAL DEFECTS*

Dudley R. Herschbach† and Victor W. Laurie‡

The relationships among various types of moments of inertia and vibration-rotation corrections are developed from general theory, with emphasis on the qualitative physical features and the quantities that may be calculated without knowledge of anharmonic force constants. The inertial defects of planar triatomic and tetratomic molecules and nonplanar molecules with a plane of symmetry are considered, and it is found that simple approximations, which depend mainly on the one or two modes of lowest frequency, give results within 10 to 20% of the experimental values. The application of inertial defect corrections in structure analysis is illustrated for the calculation of HH distances in CH_2Cl_2, SiH_2F_2, and CH_3CXO molecules (X = H, F, Cl, Br).

* Abstract of a paper to be published in J. Chem. Phys. (Also UCRL-11208, Nov. 1963).
† Present address: Department of Chemistry, Harvard University, Cambridge, Massachusetts.
‡ Present address: Department of Chemistry, Stanford University, Stanford, California.

22. VIBRATION-ROTATION INTERACTION FACTORS FOR DIATOMIC MOLECULES CALCULATED BY NUMERICAL METHODS*

John K. Cashion†

The influence of vibration-rotation interaction on transition probabilities for diatomic molecules has been studied through numerical solution of the Schrödinger radial equation. The numerical method described is readily applicable to any choice of potential and dipole moment functions for the molecule, its accuracy considerably exceeds the requirements of practical applications, and it is very economical in terms of computer-time requirements. Its use is demonstrated here in two applications. First, it has been used to check the accuracy of the approximate formulae for the F factors of a rotating Morse oscillator with a linear dipole moment function, derived by Herman, Rothery, and Rubin. It was found that their formulae were very accurate for $\Delta v = 1$ transitions, but that the two formulae given by them for the first and second overtones could introduce errors of several percent at moderate J values. Secondly, quadratic and cubic terms were added to the dipole moment function in order to estimate the sensitivity of F factors to changes in this function. The results indicate that for all transitions in which $\Delta v > 1$, the higher terms can have considerable significance. For example, F factors for the lines R(19) and R(20) of the 3-0 band of LiH were changed by factors of more than 3 when the dipole moment function employed was carried from a linear to a cubic approximation in a Taylor's series expansion.

* Abstract of a paper submitted to J. Chem. Phys. (also UCRL-10644, July 1963).
† Present address: Department of Chemistry, Harvard University, Cambridge, Massachusetts.

23. SEMICLASSICAL ANALYSIS OF WEAKLY INELASTIC MOLECULAR COLLISIONS*

Mark S. Child†

The deflection angles for weakly inelastic vibrational and rotational transitions are shown to be simply related to the classical deflection angles for elastic scattering conditions. The position of the crossing point, at which the values of the initial and final Lagrangian are equal, plays an important role in the discussion, and expressions are derived for these points for different types of transition. Allowance is made for the fact that the effective translational potential energy may depend on the vibrational states of the members of the system.

* Abstract of a paper submitted to Molecular Physics (also UCRL-11135, November 1963)

† Present address: Department of Chemistry, Glasgow University, Scotland.

24. PARAMAGNETIC RESONANCE IN LIQUID AMMONIA

Donald H. Levy and Rollie J. Myers

The study of the paramagnetic resonance spectra of organic negative ions in solution allows one to obtain the isotropic hyperfine coupling constants, which are a measure of the interaction between the unpaired electron and any magnetic nuclei in the molecule. The measured proton hyperfine coupling constant of a proton bonded to a carbon atom in a π-electron system has been related approximately to the π-electron spin density on this carbon atom, and consequently these coupling constants provide an excellent check on any theoretically derived wave function.

Formerly only rather large aromatic conjugated molecules could be reduced to form the paramagnetic negative ion. This was unfortunate, since only roughly approximate calculations could be performed on such complicated molecules although very good experimental data could be obtained. The *in situ* electrolytic reduction technique developed by Maki and Geske[1] offered the possibility of observing steady-state concentrations of less stable but theoretically more simple radical anions. Unfortunately, with the usual solvents, this technique has serious limitations. The high electrolysis potentials necessary to produce the more unstable radicals often preferentially reduce the more reactive solvents. Moreover, all the solvents used have relatively high freezing points, and the possibility of prolonging the lifetime of unstable species by cooling is thus eliminated.

It has long been known that the alkali metals dissolve readily in liquid ammonia to produce blue paramagnetic solutions. Although the exact nature of the paramagnetic species is still open to considerable question, the species is known to be a powerful reducing agent. We have electrolyzed solutions of the tetralkyl ammonium iodides and alkali metal iodides in liquid ammonia and produced a species with properties extremely similar to

1. D. H. Geski and A. H. Maki, J. Am. Chem. Soc. 82, 2671 (1960).

the species that exists in the alkali metal ammonia solutions. This species appeared potentially useful as a reducing agent for organic molecules, and a study of organic radical anions produced electrolytically in liquid ammonia was undertaken.

Butadiene has been the subject of several theoretical calculations,[2] and its spectrum is of considerable interest. A 0.01 M solution of butadiene in liquid ammonia was electrolyzed at 25 V. Tetramethyl ammonium iodide was used as the supporting electrolyte. The resulting spectrum is shown in Fig. IE.24-1. The hyperfine coupling constant associated with the protons attached to carbon atom 1 was found to be 7.617±0.005 gauss, and that associated with the proton attached to carbon atom 2 was 2.791±0.007G. The full line width between points of maximum slope was 0.32 G and the g value was equal to 2.0026. When the electrolysis voltage was turned off the spectrum decayed, following a first-order rate law with rate constant equal to 0.36 sec^{-1}. The line width appeared to be independent of the temperature of the sample.

In order to compare the experimental coupling constants with theoretical calculations it is necessary to obtain the unpaired spin densities. Inasmuch as the quantity Q in McConnell's equation is difficult to determine experimentally, we shall compare only the relative spin densities by defining the quantity $R=A_1/A_2$. The experimental value of R is 2.729. The simple molecular orbital theory of Huckel predicts a value of R=2.61, in excellent agreement with experiment. Recently Sovers and Kauzmann[3] have modified the simple Huckel theory by mixing in d atomic orbitals on the carbon atoms. This modification predicts an R = 2.9. Unfortunately the more elaborate self-consistent field calculations have given less accurate results. The ab initio calculation of Parr and Mulliken[2] predicts R=1.9. This calculation was done for the neutral butadiene molecule (four π electrons), and in order to predict the R of the negative ion one must assume that the unpaired electron goes into the lowest unpaired π orbital without significantly perturbing the π system. A more correct calculation was performed by Goodman, but unfortunately gave even poorer results. Goodman calculated the molecular orbitals of the negative ion directly (five π electrons) and thus took into account the perturbation of the closed shell caused by the fifth electron. His calculation predicts R=1.6.

A solution of nitrobenzene was electrolyzed at 1.0 V. The spectrum of the nitrobenzene negative ion is well known, and the ion itself has formerly been prepared by both chemical reduction and electrolytic reduction in acetonitrile solution. The coupling constants in ammonia solution are

2. R. G. Parr and R. S. Mulliken, J. Chem. Phys. 18, 1338 (1950).
3. O. Sovers and W. Kauzmann, J. Chem. Phys. 38, 813 (1963).

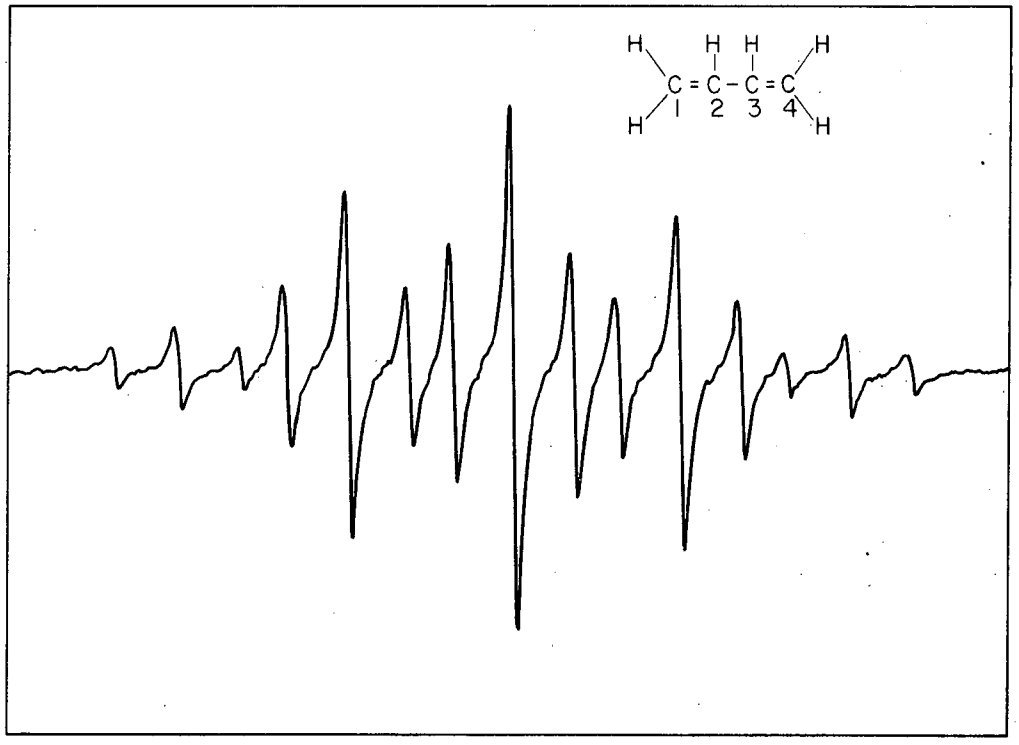

Fig. IE. 24-1 The paramagnetic resonance spectrum of butadiene radical-anion. The derivative of the absorption spectrum is shown as a function of the magnetic field.

A_{ortho}=3.44, A_{meta}= 1.09, A_{para}=3.90, and A_N=11.47. These coupling constants are similar to those obtained by reduction in the other media with slight solvent shifts in the direction noticed previously in polar solvents. By far the most dramatic solvent effect noticed in the course of this work was in the electrolysis of cyclooctatetraene. This molecule had formerly been reduced by Strauss and Frankel,[4] using chemical reduction. They had observed that the chemical reduction produced primarily the di-anion and that so little of the mono-anion was produced that it was difficult to obtain a spectrum. In liquid ammonia the mono-anion is by far the most prevalent species, and a very strong spectrum was observed. The proton coupling constant was 3.278 ±0.004 gauss. This is slightly shifted from the value measured by Strauss and Frankel.

The symmetric molecule 2,3 dimethyl butadiene was electrolyzed. At lower voltages the line width was similar to that of butadiene, but when the electrolysis voltage was increased the line width decreased to 0.099 gauss and a well resolved spectrum was obtained. The spectrum produced showed small splittings which could be explained by assuming that the molecule contained three different kinds of protons. The coupling constant associated with the methyl protons was 1.200±0.002 gauss, and the two different coupling constants associated with the end protons were 7.033±0.003 and 7.241±0.003 G. Of course there was no way to determine which coupling constant was associated with the cis protons and which with the trans. The g value was 2.0020. By use of the above parameters and assumption of Lorenzian line shape, a theoretical spectrum was calculated and shown to be identical with the experimental spectrum. The spectrum was calculated on an IBM 7094 and the output plotted on a Cal-Comp plotter.

4. H. L. Strauss, T. J. Katz, and G. F. Fraenkel, J. Am. Chem. Soc. 85, 2360 (1963).

25. HIGH-TEMPERATURE MICROWAVE SPECTROSCOPY

James S. Muirhead and Rollie J. Myers

High-temperature microwave apparatus has been extensively tested. (The original equipment for this experiment was assembled by John Howe). The vapor of a number of molecules heated from 400 to 1000°C has been examined. The molecule AgCl was very seriously examined, but no microwave lines for this substance were observed. It is quite probable that AgCl vapor decomposes while in contact with our apparatus, but we have little direct evidence for this decomposition. On the other hand, the decomposition of AgI in our apparatus can be readily observed. A very good signal-to-noise ratio could be obtained for KCl, and rotational transitions can be obtained from the $v = 6$ excited vibrational state. From what we know of other high-temperature microwave spectrographs, our sensitivity is among the best that has been obtained. As presently designed the cell should be satisfactory for the study of most high-temperature diatomic molecules with dipole moments.

Some effort was made to observe the microwave lines of $PbCl_2$. Recent molecular beam deflection measurements have confirmed that this molecule has

a dipole moment, and it should have a microwave spectrum. The situation is complicated by the fact that two chlorine isotopes will produce nuclear quadrupolar hyperfine interaction, and also that lead has a large number of isotopes. Both these factors will reduce the intensities of any observable microwave transitions for $PbCl_2$. At this time we have not been able to observe any lines due to $PbCl_2$. It is quite probable that despite our good sensitivity for diatomic molecules we still lack the very high sensitivity necessary to detect triatomic molecules. The major factor limiting our sensitivity is the low transmission of the microwave cell. By changing the design of the cell it should be possible to correct this low microwave transmission and obtain sufficient sensitivity to observe the spectrum of $PbCl_2$ and similar molecules.

Since our cell is constructed largely out of high-grade alumina and platinum, it might be possible to study either fluorides or oxides in the vapor. Our present work on these interesting species has not been successful because of attack by the melts upon our crucibles. If a metal or boron nitride is substituted for our present crucibles it may be possible to study fluorides and perhaps oxides in the vapor. As the cell is presently designed it should be quite suitable for thermodynamic studies involving the alkali halides, and such studies are presently being planned.

26. POWER SATURATION IN PARAMAGNETIC RESONANCE

Douglas C. McCain and Rollie J. Myers

The S-band 200-watt spectrometer has now been completely assembled. It was not possible to complete this spectrometer until late this year, when more space became available. Only preliminary work has been completed with this instrument, but it has operated at nearly full power level. We plan to measure the spin-lattice relaxation times of several transition metal complexes. A variety of experiments are possible with the high microwave fields that can be produced with this instrument, and it should be possible to do electron-nuclear double resonance studies of paramagnetic ions in solution.

27. THE MICROWAVE SPECTRA OF UNUSUAL MOLECULES

Peter M. McKinney and Rollie J. Myers

The microwave spectra of CH_3OSiH_3 and IF_5 have been given a preliminary examination. The first molecule is particularly interesting because it is now well known that SiO bonds are linear or nearly linear. Both the bond angle and barriers to internal rotation are of particular interest for CH_3OSiH_3. The IF_5 molecules is one of the very interesting class of interhalogen molecules. This molecule probably has a pyramidal structure, and the iodine atom is presumed to be close to the base. A complete microwave assignment should settle these points and establish accurate structures for both molecules.

28. THE HYPERFINE COUPLING CONSTANTS AND RATES OF EXCHANGE FOR $C^{13}N^-$ WITH THE AXIAL AND EQUATORIAL POSITIONS IN $Cr(CN)_5NO^{-3}$

J. Brock Spencer and Rollie J. Myers

It has been recently reported[1,2] that the magnetic hyperfine interaction of C^{13} is observable in the paramagnetic resonance spectrum of aqueous solutions of $Cr(CN)_5NO^{-3}$. It seemed probable that this interaction was due only to the equatorial CN^-, but the possible axial coupling remained unknown. In a preliminary report of the exchange with $C^{13}N^-$ we too were unable to differentiate between the axial and equatorial positions.[3] We have now been able to prepare the complex by exchange with C^{13} substituted primarily in the axial position and by synthesis with every cyanide substituted by $C^{13}N^-$. Both the hyperfine interaction and the rates of exchange of the axial and equatorial positions have now been clearly resolved.

Samples of $K_3Cr(CN)_5NO$ were synthesized by utilizing NaCN enriched to 55% in C^{13} isotope.[4] The largest hyperfine splitting in the paramagnetic resonance spectrum of $Cr(CN)_5NO^{-3}$ should arise from the species[5] containing Cr^{53}, N^{14}, and five C^{13}. In the X-band spectrum of the enriched sample, clearly resolved lines occur 62.4 gauss above and below the center of the spectrum. Since these lines must be due to a combination of axial and equatorial C^{13} hyperfine interaction, this splitting can be combined with the previously assigned Cr^{53}, N^{14} and C^{13} equatorial splittings[1,2] to yield a value of 8.55 ± 0.4 gauss for the axial C^{13} coupling constant.

A prominent hyperfine line can also be observed between the C^{12} and the expected equatorial C^{13} lines when the complex is exchanged in solutions containing nearly equal amounts of C^{13}-enriched CN^- and HCN. Direct measurement of this line gives 8.93 ± 0.2 gauss for the axial C^{13} coupling constant. Our values can be compared to the 8.43 ± 0.2 gauss reported by Kuska and Rogers[6] from a resolution of the complex pattern observed for both axial and equatorial C^{13} substitution. A summary of our coupling constants is given in Table IE.28-I.

In the temperature range 60 to 100°C the exchange with $C^{13}N^-$ can be observed without decomposition of the complex. We have followed the decrease

---

1. R. G. Hayes, J. Chem. Phys. 38, 2580 (1963).
2. I. Bernal and S. E. Harrison, J. Chem. Phys. 38, 2581 (1963).
3. J. B. Spencer and R. J. Myers, presented before the Inorganic Division of the American Chemical Society 144th National Meeting, Los Angeles, April 1963.
4. W. P. Griffith, J. Lewis, and G. Wilkinson, J. Chem. Soc., 872 (1959).
5. There is no observable hyperfine interaction from the N^{14} in the CN^-; Cr^{53} is 9.5% abundant.
6. H. A. Kuska and M. T. Rogers (we would like to thank Professor Rogers for sending us a prepublication copy of their work).

in the signal due to unsubstituted complex and the increase in the signal resulting from equatorial C^{13} substitution while the samples were held at constant temperature in the microwave cavity of a paramagnetic resonance spectrometer. In solutions ranging from 0.015 to 0.035 f in complex and 0.1 to 0.2 f in NaCN(55% in C^{13} isotope) we followed the adjacent lines for unsubstituted and C^{13} equatorial-substituted complex for the Cr^{53} species until approximately 50% of the complex was substituted with one $C^{13}N^-$. These experiments were conducted in the nearly complete darkness of the cavity. In separate experiments no pronounced light catalysis, as reported for other cyanide complexes,[7] was observed.

Table IE.28-I. Hyperfine Coupling Constants.

	(gauss)
$A(Cr^{53})$	18.39±0.05
$A(N^{14})$	5.27±0.05
$A(C_e^{13})$	12.64±0.2
$A(C_a^{13})$	8.80±0.3

These exchange data were fitted by rate laws on the assumption of first order in unsubstituted complex and zero order in total CN^- concentration. An integrated rate law was used which took into account the possible substitution of the axial and one of the four possible equatorial CN^-. The total rate constant ka + 4ke can be directly obtained from the decrease in the unsubstituted complex, and the equatorial rate constant ke can be evaluated by successive approximation from the growth of the equatorial C^{13} signal. At 75°C we obtain $ka = 1 \times 10^{-4}$ sec^{-1} and $ke = 7 \times 10^{-6}$ sec^{-1}. Over the range of temperature we get $\Delta H^{\ddagger}_a = 33.5\pm4$ kcal/mole, $\Delta S^{\ddagger}_a = 18\pm8$ eu, $\Delta H^{\ddagger}_e = 30.5\pm4$ kcal/mole, and $\Delta S^{\ddagger}_e = 5\pm8$ eu. In the solutions prepared by adding NaCN to neutral solutions of the complex the ratio ka/4ke = 4±2 over the full range of temperature.

The apparent large positive value for $\Delta S^{\ddagger}_a$ indicates that the activated complex for axial exchange is a protonated species.[8] The formation of $HCr(CN)_5NO^{-2}$ by the removal of the proton from HCN could contribute about 40 eu to the apparent entropy of activation. When exchange experiments are conducted in acidified solutions so that both CN^- and HCN have nearly equal concentrations, the axial rate is accelerated. In this case, as previously mentioned, a line due to axial substitution becomes prominent before the equatorial line is clearly observable. It seems probable that the formal charge of +1 on the NO group makes the axial CN^- more likely for protonation than the more adjacent equatorial CN^-. Our data indicate the possibility, however, that the equatorial exchange is also partly acid-catalyzed.

The similar values for the N^{14} and both C^{13} coupling constants do not give any clear contradiction or support to the bonding scheme proposed for

7. A. G. MacDiarmid and N. F. Hall, J. Am. Chem. Soc. 76, 4222 (1954).
8. We would like to thank professor R. E. Connick for suggesting this possibility to us.

these complexes.[9] The axial CN^- is more liable to exchange in aqueous solution, primarily because of greater protonation at this position, and the enthalpies of activation are equally large for both positions. The theory for the isotopic hyperfine interaction in these compounds is necessarily complex, and both the signs of the coupling constants and the anisotropic terms should be determined before a serious effort is made to explain the axial and equatorial coupling constants in terms of bonding.

---

9. H. B. Gray, I. Bernal, and E. Billig, J. Am. Chem. Soc. 84, 3404 (1962).

II. METALLURGY AND SOLID-STATE BRANCH

A. MICROSTRUCTURE AND PHYSICAL PROPERTIES

1. CLUSTERING OF VACANCIES AND HARDENING*

Gareth Thomas and Jack Washburn

Consideration is given to the clustering of vacancies, the factors involved in their precipitation, annihilation, and the manner in which vacancies induce hardening. The number, kind, and morphology of quenching defects (dislocations formed after vacancy clustering) is a function of material, composition, and quenching conditions. The absence of dislocation loops in various regions inside the grains is probably due to plastic deformation during quenching. In general, precipitation of vacancies in solid solutions is hindered as a result of vacancy trapping by solute atoms. The extent of such trapping depends on the solute atom-vacancy binding energy, and small amounts of impurities may provide sites for heterogeneous precipitation. Although stacking-fault energy determines in a general way the type of defect formed (i.e., perfect or imperfect loops or tetrahedra of stacking faults), the activation energy required to convert one type of defect to another is a very important factor to be considered if the occurrence of defects having dimensions outside those predicted from defect energies is to be understood. The possibility of dissociated prismatic loops may also account for the size and stability of loops in certain metals.

The effect of impurity atoms on vacancy climb of dislocations can be studied by hot-stage experiments in the electron microscope. This technique enables one to estimate the impurity-vacancy binding energy E_b. For example, experiments on Al-Mg alloys permitted determination of a value of E_b of 0.1 to 0.4 eV. This technique is being extended to other systems.

In copper it has been shown by small-angle scattering of x-rays that excess vacancies cluster at 20°C to form small voids. These result in a marked hardening of the crystal, and also in changes in the strain-hardening behavior. Only at higher aging temperatures are defects formed that are large enough to be clearly detected by transmission electron microscopy.

---

* Abstract of paper presented at AIME Symposium on Point Defects, Dallas; published in Rev. Mod. Phys. 35, 992 (1963)(UCRL-10674, February 1963).

2. PHASE TRANSFORMATIONS IN Nb INVOLVING INTERSTITIALS*

Lenon I. Van Torne and Gareth Thomas

A homogeneous phase transformation of bcc Nb to an fcc crystal structure, probably NbO but containing some C and N also, has been observed by transmission electron microscopy, both in thin foils and in bulk specimens containing ≈ 0.5 at. % interstitials, after suitable aging treatments. The transformation proceeds in thin foils at 600°C in a matter of seconds by the following sequence: (a) ordering in Nb with interstitials taking up $\frac{11}{22}0$, and $00\frac{1}{2}$ lattice sites, (b) formation of a precipitate in alternate layers (≈50 Å thick) of Nb and NbO with the transforming region bounded by a prism of {110} Nb, (c) growth to a perfect "NaCl" structure corresponding to NbO but probably containing C and N, also, (d) recrystallization and possible disorder of NbO. See Figs. IIA.2-1 and 2.

In thin foils (1000 Å thick) the crystallographic features of the transformation are observed to be

$$[001]\text{Nb} \;||\; [001]\text{NbO},$$

$$[011]\text{Nb} \;||\; (111)\text{NbO}\ .$$

The habit planes are four variants of {101}Nb, but only those inclined at less than 90° to the foil surface operate. See Figs.IIA.2-3 and 4.

In bulk specimens the habit planes are observed to be {021}Nb, which is in accord with the crystallographic theory for martensitic transformations. The difference in observed habit planes in bulk and thin foil specimens is attributed to the lack of constraints in the latter, where the transformation dilatations can be accommodated elastically by foil buckling. However, these dilatations are observed to be accommodated in bulk specimens by dislocations generated at the precipitate-matrix interfaces.

---

* Abstract of paper in Acta Metallurgica, in press (UCRL-10956, October 1963).

3. MICROTWINNING IN EXPLOSIVELY DEFORMED COPPER AND COPPER ALUMINUM ALLOYS

Om Johari and Gareth Thomas

Nolder and Thomas studied the substructures in shock-loaded nickel and for the first time reported that when a particular value of pressure (350 kbar) was reached a cell structure was no longer observed and the mechanism of deformation changed to microtwinning.[1] Similar results have been found in explosively deformed copper and Cu-Al alloys.[2] In Cu, twinning was observed after a pressure of 28 kbar was applied. The cell size observed prior to twinning was found to be nearly 0.15 μ, as was found for Ni.[1]

---

1. R. Nolder and G. Thomas, Acta Met., 12, 227 (1964).
2. O. Johari and G. Thomas (UCRL-10932 Rev.).

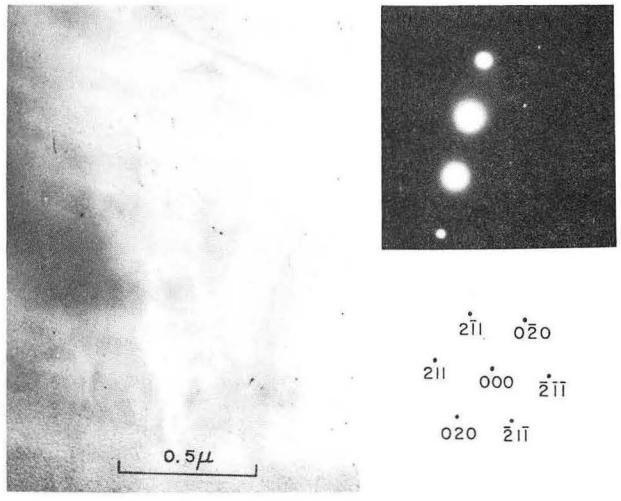

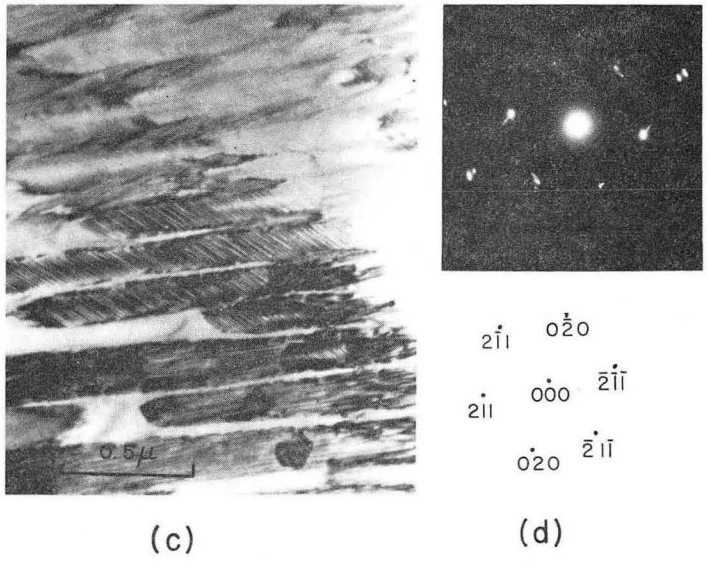

ZN-4257

Fig. IIA. 2-1 (a) [$\bar{1}02$] Nb foil in the initial state.

(b) Diffraction pattern of (a); orientation is not exactly [$\bar{1}02$] owing to slight rotation of crystal about [020] with respect to incident electron beam.

(c) The same field of view as (a) after two electron beam pulses of 40 μA at 1 sec/pulse. Note alternate layers of Nb-NbO-Nb-NbO, with the transforming region confined to a prism of {110} Nb.

(d) Diffraction pattern of (c). Note the intensity spikes on the primary reflections due to a relaxation of the laue conditions in directions perpendicular to the habit planes ($0\bar{1}1$) Nb and (011) Nb.

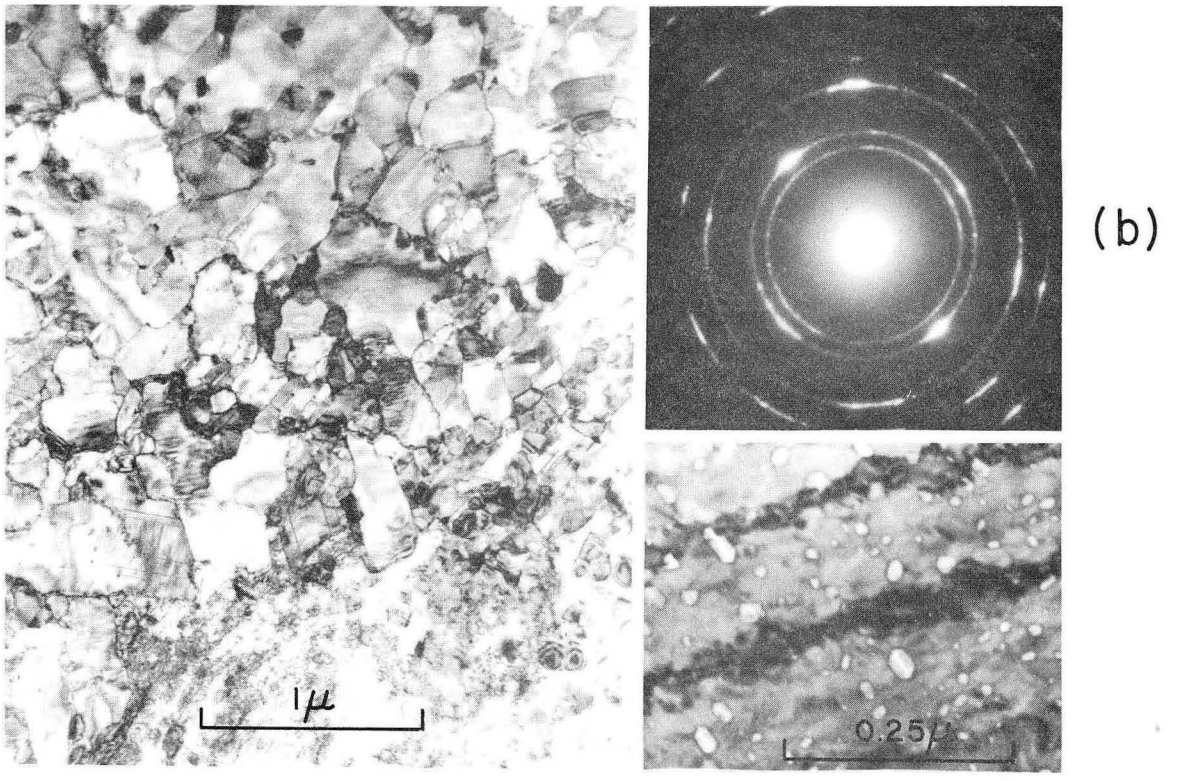

Fig. IIA. 2-2 (a) Recrystallization of the transformation product at 1000°C in the electron microscope heating stage. Note the preferred orientations of the nuclei.

(b) Diffraction pattern of (a): the sequence of rings corresponds to an fcc structure.

(c) Further growth of the crystals shown in (a).

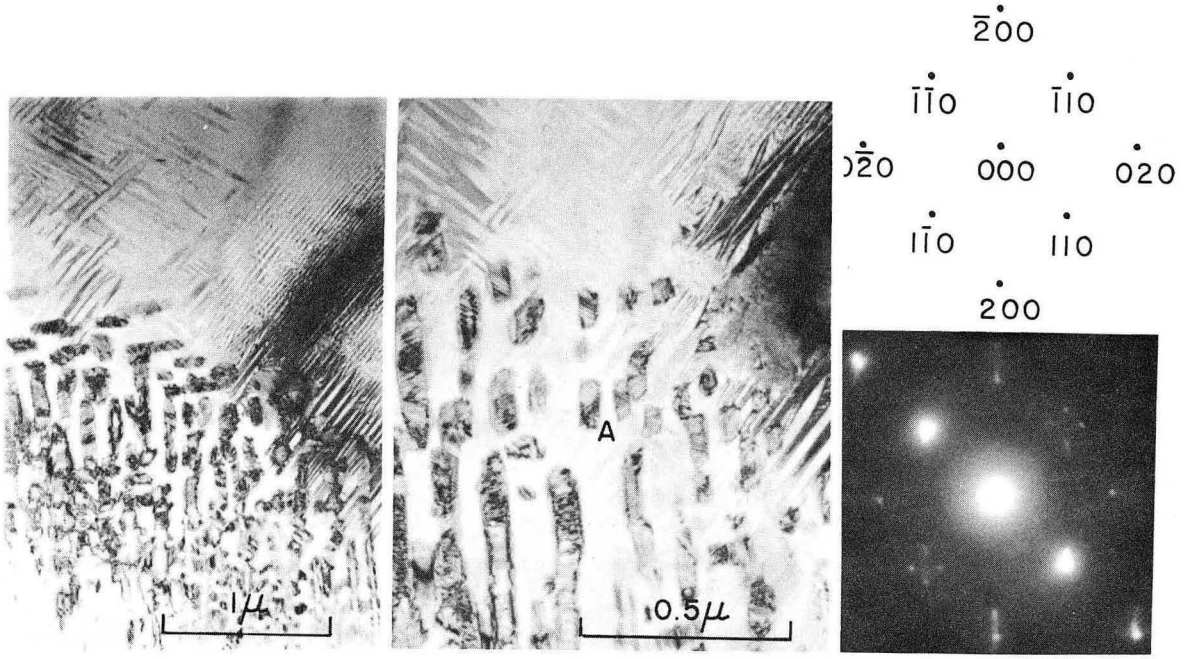

Fig. IIA. 2-3 (a) An [001] Nb crystal in the process of transformation after three electron beam pulses. Note the presence of two boundary prisms which are possible in this orientation.

(b) A magnified view of the prisms formed by the four operating {110} Nb habit planes. Compare observed structure at A with sketches in Fig. IIA. 2-4.

(c) [001] Nb diffraction pattern of region where prisms have formed. Note the presence of intensity spikes on primary reflections due to {110} Nb habit planes within the Nb matrix.

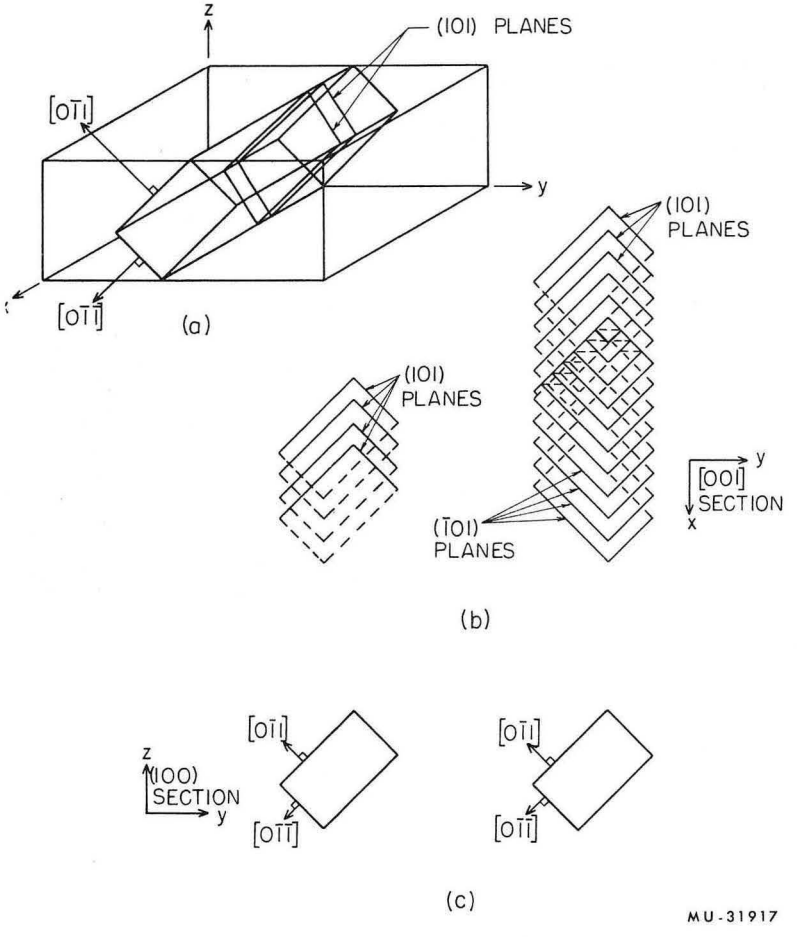

Fig. IIA. 2-4 Sketches showing how the structure observed in Fig. IIA. 2-3b can arise from intersections and overlap of the four operating habit planes.

It was proposed by Nolder and Thomas, using Venable's model,[3] that the onset of twinning and the critical pressure should depend on stacking-fault energy; it is the purpose of these experiments to investigate this model by using Cu-Al alloys of known stacking-fault energy. The important indications to date are:

(a) The critical pressure for onset on twinning is found to decrease with a decrease in stacking fault energy (Fig. IIA. 3-1), as is expected.
(b) It is found in nearly all cases that explosively deformed foils have a very high tendency to polygonize in the electron beam despite measures to minimize heating effects.
(c) In alloys deformed at pressures lower than the critical, cell structures are not always observed.
(d) The substructure at pressures higher than the critical pressures in explosively deformed copper mostly consists of microtwinning (Fig.IIA.3-1). It is found in the alloys that the structure tends to be heavily faulted and possible some other complex process is simutaneously taking place.
(d) Our results on copper did not quantitatively agree with those on nickel. We attribute this difference to the fact that in the two cases the mode of deformation and shapes of specimens were much different (in Ni 3-in.-diam. slabs 1/4 in. thick, for Cu 0.5 -in.- diam. 2-mil-thick sheets). By using specimens of thickness of the order of 1/4 to 3/8 in. we are investigating whether the size factor is important.

We are grateful to Dr. D. Munson of Sandia Corporation for kindly explosively deforming the specimens.

3. J. Venables, in Deformation Twinning, ed. by R. E. Reed-Hill (Gorden & Breach, 1964). (In press).

4. STRUCTURE AND PROPERTIES OF TD-NICKEL†

Manfred von Heimendahl* and Gareth Thomas

TD-nickel is a dispersion-strengthened alloy of nickel with 2 volume % ThO_2 made by means of powder metallurgy. The alloy offers high-temperature stability due to the very high melting point of ThO_2. Some structure-property investigations have been reported earlier.[1,2] This work describes results of a detailed transmission electron microscopy study of annealed and deformed TD-nickel, and the alloy is compared to pure (99.99%) Ni. The following states have been investigated: (i) as extruded; (ii) 60% cold rolled sheet, made from the extruded bar; (iii) as (ii), but additionally annealed in vacuum 2.5 h at 900°C; (iv) annealed like (iii) but additionally deformed by tensile deformation up to 10%. Results The as-extruded material, which is

† This work has been completed and has been submitted to Trans. AIME (UCRL-11260).
* NATO Postdoctoral Fellow on leave from Institut für Metallkunde der Bergakademie Clausthal.
1. F. J. Anders, G. B. Alexander, and W. S. Wartel, Metal Prog. 82,88 (1962).
2. D. K. Dorn and S. F. Marton, Powder Metallurgy (Interscience, New York, 1960) p. 309-342.

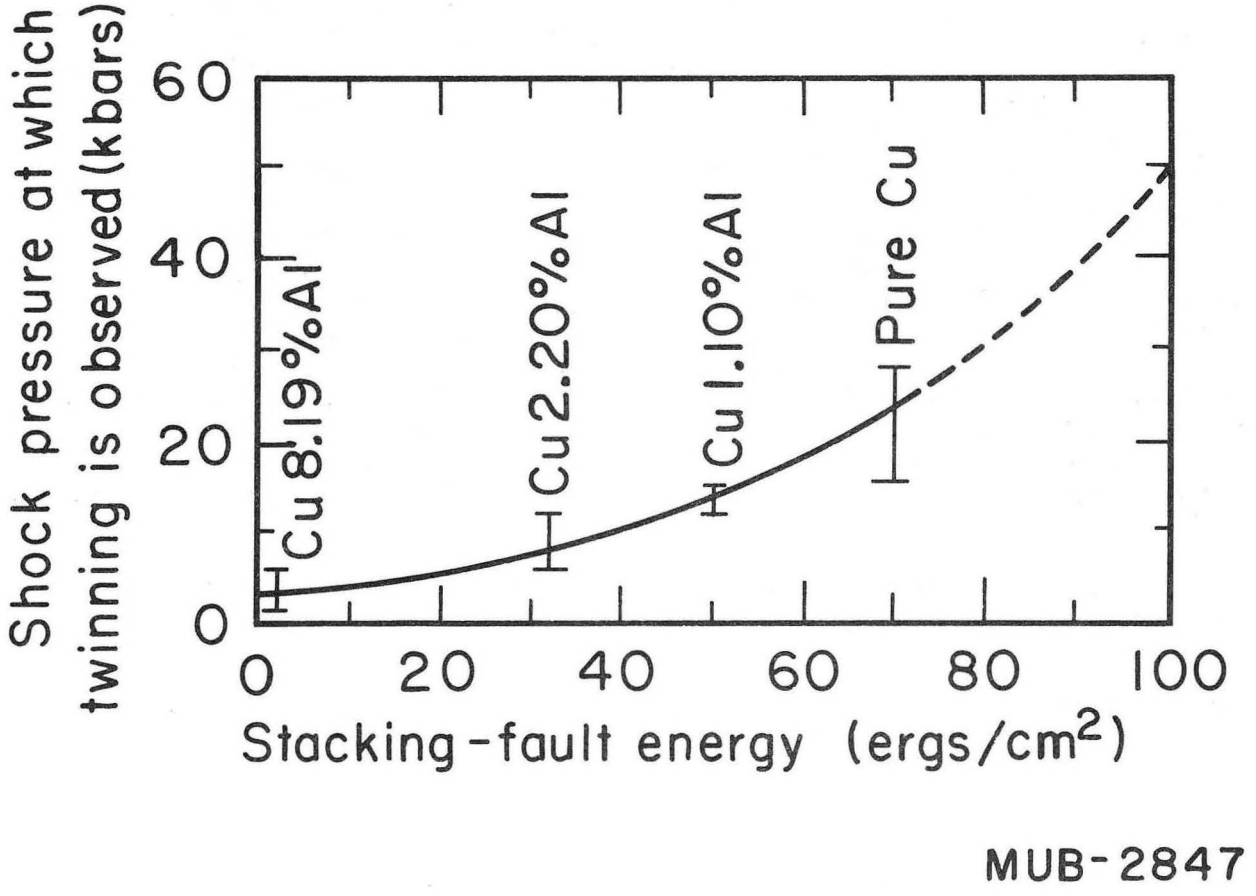

Fig. IIA. 3-1 The upper kbar values for which twinning is observed and the lower kbar values showing no twinning are plotted vs stacking-fault energy. For 8.2% Al-Cu alloy, no observations were made below 6 kbar.

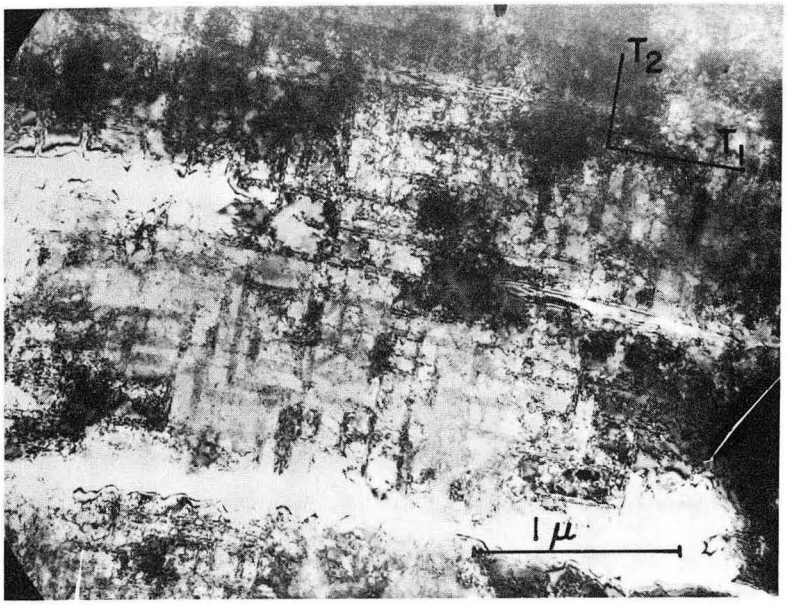

(a)

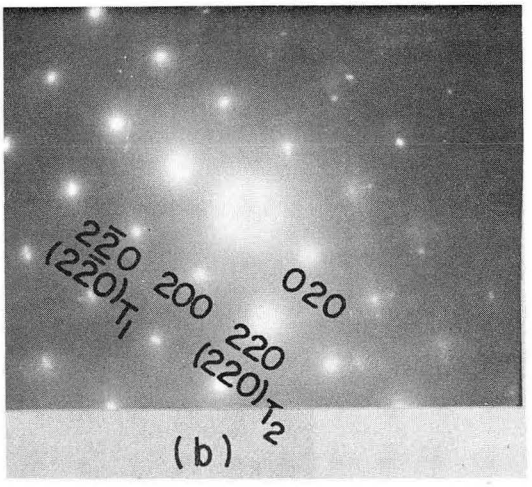

(b)

ZN-3925

Fig. IIA. 3-2 (a) Electron micrograph showing twin structure in explosively deformed copper specimen at 200 kbar pressure. Note the fringe contrast at twin interfaces, the high dislocation density in areas away from twins and preferential etching of twinned material. The foil orientation is (001) and the twins are on {111} planes and appear as traces in ⟨110⟩ directions.
(b) Diffraction pattern corresponding to above figure.

important for many technical applications, consists of extremely small grains (average grain size 1 μ) and exhibits low-angle grain boundaries as well as large grain boundaries. The annealed alloy (2.5 h, 900°C) has a grain size of about 5 to 10 μ. The size and distribution of the ThO_2 particles can be seen from Fig. IIA.4-1. The particles are roughly spherical and exhibit dark contrast. The size of the particles is not uniform and the diameters vary between 100 and 1600 Å. This result is shown much more clearly by transmission microscopy than by an earlier carbon-extraction replica study.[1] Selected area diffraction-pattern analysis was in agreement with the known structure data of the ThO_2 structure from the ASTM file (cubic, a = 5.600 Å). Many ThO_2 particles are covered even by the smallest diffraction aperture, so mostly very weak spotty rings appear from the particles. A characteristic feature of annealed Td-nickel is the appearance of many very narrow annealing twins (Fig.IIA.4-1). The boundaries of these twins are quite jagged, owing to the presence of the particles. This indicates that the twin growth has been influenced to a great extent by the particles. For comparison, micrographs of annealed pure nickel showed no twins in the (small) visual field of the electron microscope. Very large twins (100 μ) were observed under the light microscope.

In the deformed specimens, the dislocation-particle interaction has been studied. The particles act as hard obstacles to moving dislocation lines, which are pinned by the particles and bow out between them. With increasing stress, the dislocations do not loop off from the particles, leaving concentric (glissile) loops, but rather they tangle around the particles, or try to avoid the particles by cross slip. Sometimes elongated prismatic loops are formed. Such loops may be clearly seen in Fig.IIA.4-2. This micrograph also shows tangling of the dislocation lines. Other photographs reveal the importance of the fine-scale annealing twins in the deformation process: many dislocations are seen near the twin interfaces, which may act as sources as well as obstacles for the dislocations.

After larger deformations the dislocations appear to cross-slip more profusely. The result is the tangled structure of dislocations and finally a more or less well-developed cell structure. After 10% tensile deformation a cell structure is present in some, but not all, areas of the samples. The average cell size has been determined to be about 0.3 μ, and this cell size is apparently governed by the spacing of the largest particles. For comparison pure nickel of the same treatment (10% tensile deformation) was studied: here the cell size was much larger, between 0.5 and 3 μ, average 1 μ. But it must be kept in mind, that the grain size of this pure Ni was also extremely large (100 to 300 μ). Finally, in the case of cold rolled TD-Ni, the cell structure was very pronounced (cell size 0.5 μ). We are presently comparing TDNi with pure Ni of similar grain size.

Acknowledgment

Financial assistance from the German Academic Exchange Service is acknowledged (M.V.H.).

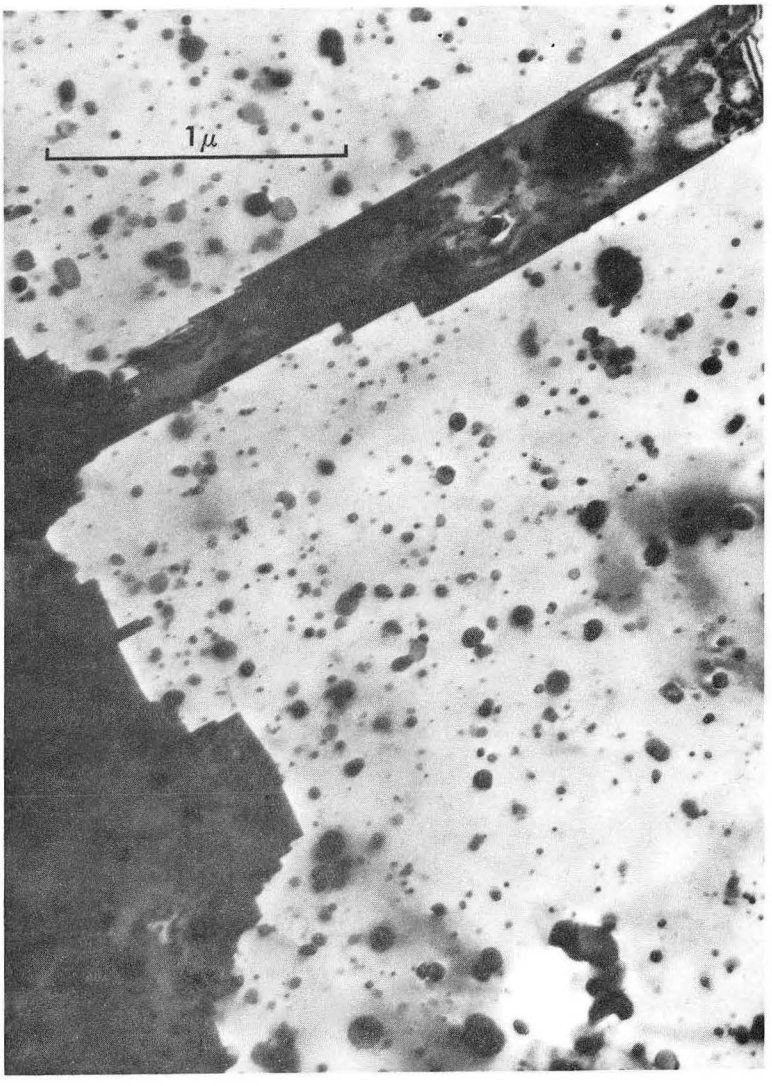

ZN-4235

Fig. IIA. 4-1 Annealed TD-nickel (2.5 h, 900°C).

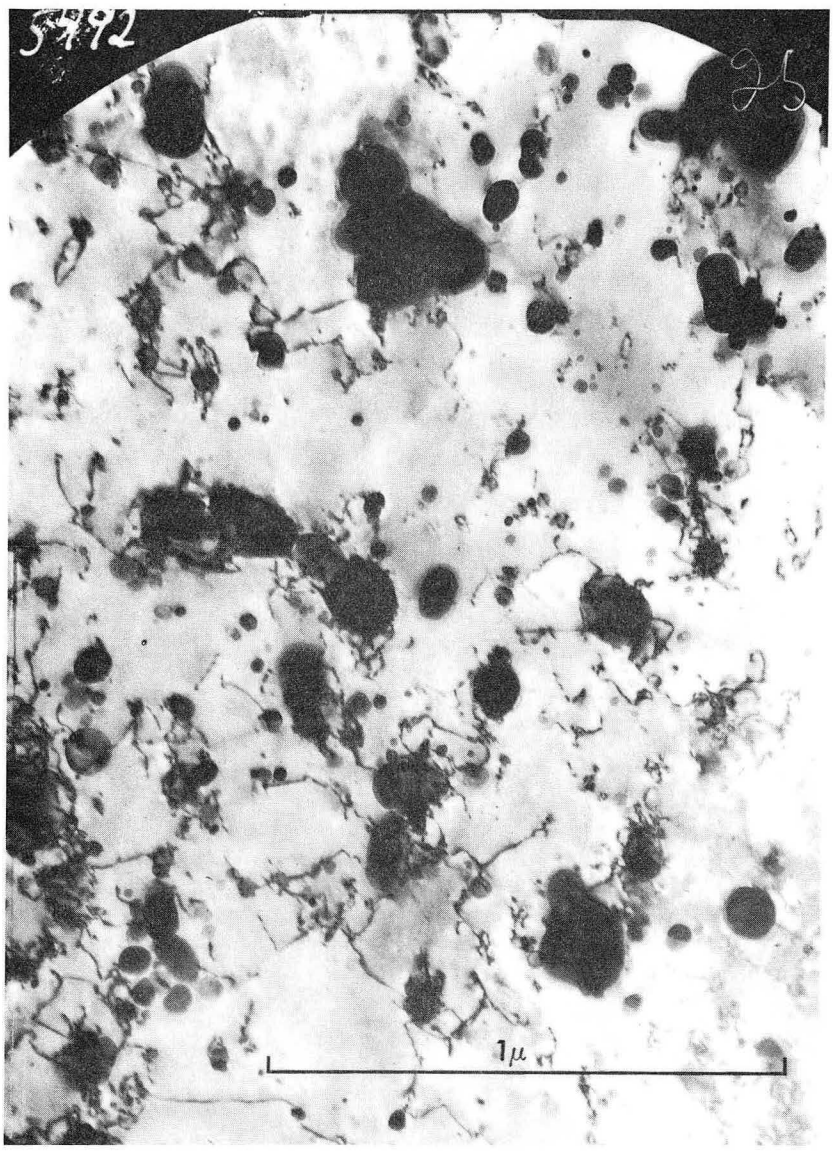

ZN-4236

Fig. IIA. 4-2 TD-nickel, annealed plus 2% plastic strain.

5. PRECIPITATION AND DISLOCATION NUCLEATION IN QUENCH-AGED Al-Mg ALLOYS*

Alf Eikum and Gareth Thomas

Small precipitates have been observed in thin foils prepared from bulk Al-5% Mg and Al-6.5% Mg alloys after quenching followed by aging at 100°C. The precipitates, concluded to be an intermediate form of Mg_2Al_3, apparently nucleate only when a critical supersaturation of both Mg atoms and vacancies exists in the specimen. The vacancy denuded zone between colonies of prismatic dislocation loops and grain boundaries is one good example of regions where the critical supersaturation can occur.

A high stress is associated with the precipitates that can be relaxed by the punching out of rows of prismatic dislocation loops. This has been observed directly in the electron microscope. An example is shown in Fig. IIA.5-1. A comparison of the experimental results with the theory of Bullough and Newman enables one to estimate the critical shear stress for prismatic glide. The value obtained is $3.4 \times 10^{-4} G$ (where G is the shear modulus).

Some general observations on the nature of the precipitation and the generation of dislocation loops are discussed.

---

* Abstract of paper in Acta Metallurgica, in press (UCRL-10968, October 1963).

6. SLIDE RULE METHOD FOR INDEXING ELECTRON DIFFRACTION PATTERNS*

Walter R. Roser and Gareth Thomas

It is important to have a rapid and convenient method for indexing electron diffraction patterns, because of the large number of patterns that must be taken in order to obtain the maximum information from the electron microscope. An ordinary 10-in. slide rule has been adapted by adding scales of reflecting planes so as to allow the direct indexing of diffraction patterns from the measured distances of spots from the origin of the pattern.

Practical Applications. A patent inquiry is being made through the Atomic Energy Commission. The technique has wide application for all people working with crystalline materials.

---

* Abstract of paper submitted to Rev. Sci. Instr. (UCRL-11136, January 1964).

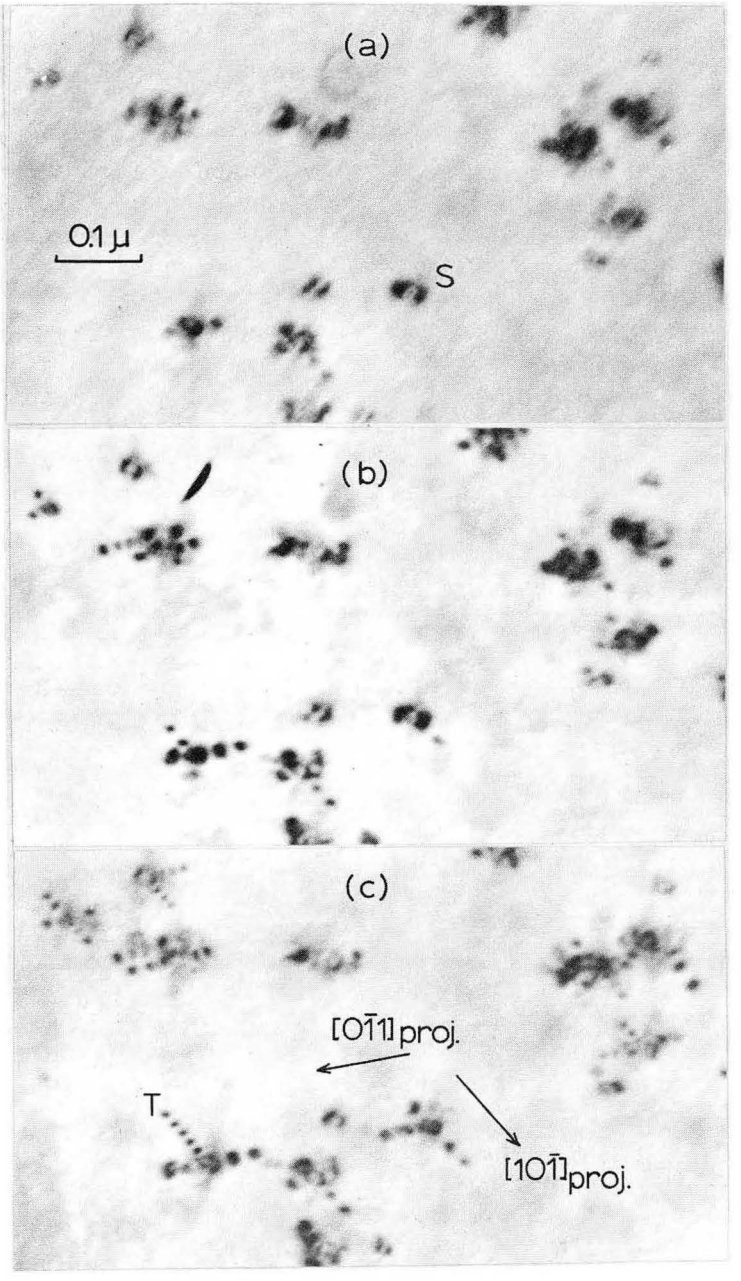

ZN-3959

Fig. IIA. 5-1 A punching sequence observed directly in the microscope, showing (a) precipitate at S exhibiting coherency strain contrast, (b) a single small loop punched out at S, (c) a second larger loop and another row at S, and a row of five loops at T. Foil prepared from Al-6.5 wt % Mg after quenching from 550°C into iced brine, and aging 100 h at 100°C.

7. ANALYSIS OF ELECTRON DIFFRACTION PATTERNS CONTAINING TWIN REFLECTIONS IN ISOMETRIC CRYSTALS*

Om Johari and Gareth Thomas

During the analysis of twinning in explosively deformed copper it was felt that an easier method is needed to solve the electron diffraction patterns. By using general crystallographic principles it was derived that a point p,q,r becomes a point PQR by twinning about an axis [hkℓ] in such a way that the following matrix for transformation is obeyed:

$$\begin{matrix} \frac{h^2-k^2-\ell^2}{h^2+k^2+\ell^2} & \frac{2hk}{h^2+k^2+\ell^2} & \frac{2h\ell}{h^2+k^2+\ell^2} \\ \frac{2hk}{h^2+k^2+\ell^2} & \frac{k^2-h^2-\ell^2}{h^2+k^2+\ell^2} & \frac{2k\ell}{h^2+k^2+\ell^2} \\ \frac{2h\ell}{h^2+k^2+\ell^2} & \frac{2k\ell}{h^2+k^2+\ell^2} & \frac{\ell^2-h^2-k^2}{h^2+k^2+\ell^2} \end{matrix}$$

The relations can be reduced to simple forms, as shown below, for {111} twinning in fcc metals,

$$P = \frac{-hp + 2kq + 2\ell r}{3h} ,$$

$$Q = \frac{2hp - kq + 2\ell r}{3k} ,$$

$$R = \frac{2hp + 2kq - \ell r}{3\ell} ;$$

and for {112} twinning in bcc metals

$$P = -p + \frac{(hp + kq + \ell r)h}{3} ,$$

$$Q = -q + \frac{(hp + kq + \ell r)h}{3} ,$$

$$R = -r + \frac{(hp + kq + \ell r)\ell}{3} .$$

It was shown that this method, when combined with stereographic projection and electron microscopy (particularly dark-field studies), is extremely useful in studies of twinned structures. In Fig.IIA.7-1 the stereographic analysis (a) and expected diffraction pattern (b) and the actual diffraction pattern (c) are shown for twinning on (111) planes of a crystal in (110) matrix orientation.

---

* Condensation of paper in Trans. AIME, in press (UCRL-11094, October 1963).

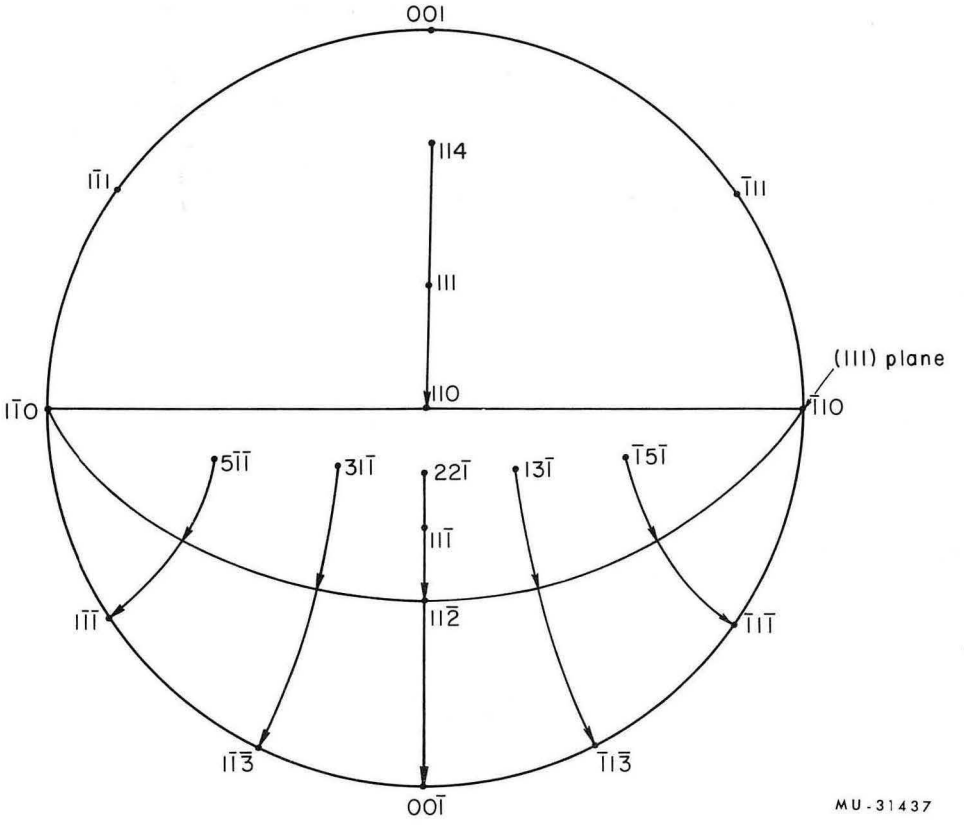

Fig. IIA. 7-1 Stereographic analysis of diffraction pattern.

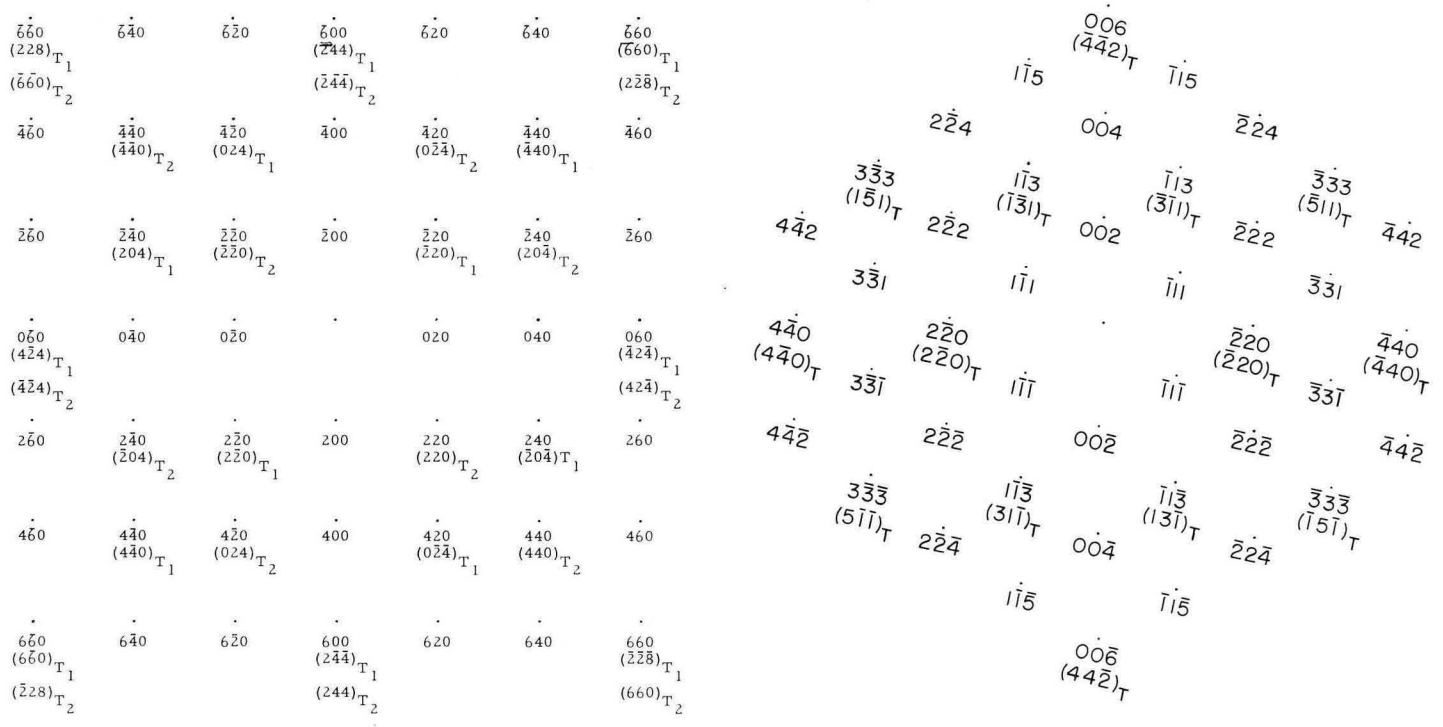

Fig. IIA. 7-2 Diffraction pattern expected from twinning on the (111) plane for (110) orientation. The orientation of twinned crystal becomes $(\bar{1}\bar{1}4)$. No extra spots appear and the spots from the twinned material overlap those from the matrix.

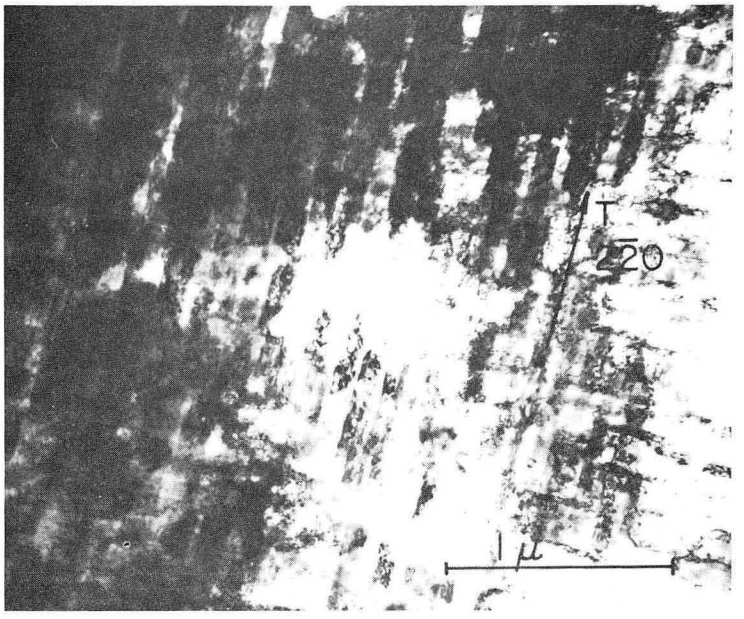

(a)

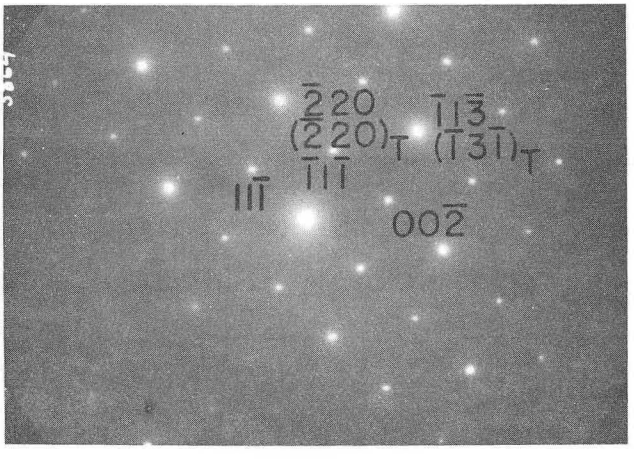

(b)

ZN-3923

Fig. IIA. 7-3 Diffraction pattern of micrograph showing no extra spots due to twinning.

8. THE FORMATION OF DIAMOND-SHAPED PRISMATIC LOOPS IN QUENCHED fcc METALS*

Alf Eikum and Gareth Thomas

The concept of dissociated prismatic dislocation loops is proposed to explain the formation of diamond-shaped loops observed in several metals after quench aging. The dissociated prismatic loop is composed of parallel segments on {111} planes having $\frac{a}{6}\langle 112\rangle$ Burger's vectors, as shown in Fig.IIA.8-1. The segment along AB cannot dissociate, but can climb in the (011) plane. The resultant diamond shaped loop can form as shown in Fig.IIA.8-1c, and an example is given in Fig. IIA.8-2. It is shown that diamond-shaped loops form from either a triangular or hexagonal Frank loop, and once formed can rotate on the glide cylinder to any orientation between and including {111} and {110}.

Climb kinetics are qualitatively discussed in terms of the equilibrium separation of partials. The separation is approximately equal to the core radius ($2|\bar{b}|$) in Al, but in Cu is large enough ($\approx 12|\bar{b}|$) to be experimentally detected. These considerations may explain why large loops are not often observed in metals other than aluminum.

* Extract from paper in J. Appl. Phys. 34, 3363 (1963) (UCRL-10814, May 1963).

9. FACTORS AFFECTING DISLOCATION SUBSTRUCTURES IN DEFORMED COPPER*

Om Johari and Gareth Thomas

Studies on substructures in plastically deformed copper have been reported by a number of workers[1-4] as a function of strain and temperature. Warrington gave a relation between the temperature and cell size.[2] Our work was carried on to study the relation of cell size to grain size, temperature, and strain rate for a given deformation.

This work was performed on copper of 99.999% purity. Two grain sizes (single crystals and polycrystals-- 70 to 100 grains/cm), two strain rates (10^{-3} in./in./min and 1 in./in./min), and three temperature (77°K, 196°K, and 273°K) were selected. After 20% tensile deformation the specimens were prepared and examined by thin-foil electron microscopy.

Our results showed no systematic correlation between observed substructure and deformation conditions. The substructures varied widely in the

* Condensation of paper in Acta Metallurgica, in press (UCRL-10932 Rev., October 1963).

1. G. Thomas and J. Washburn, Eds., Electron Microscopy and Strength of Crystals (Interscience Publishers, New York, 1963), pp. 131-183.
2. D. H. Warrington, in Proceedings of the European Regional Conference of Electron Microscopy, Delft, 1960, pp. 354-357.
3. A. Howie, in Direct Observations of Imperfections in Crystals, ed. by J. D. Newkirk and J. K. Wernick (Interscience Publishers, New York, 1962), p. 283
4. Z. S. Basinski, Symposium on the Role of Substructure in the Mechanical Behavior of Metals, Technical Document Report No. ASD-TDR-63-324, 1963.

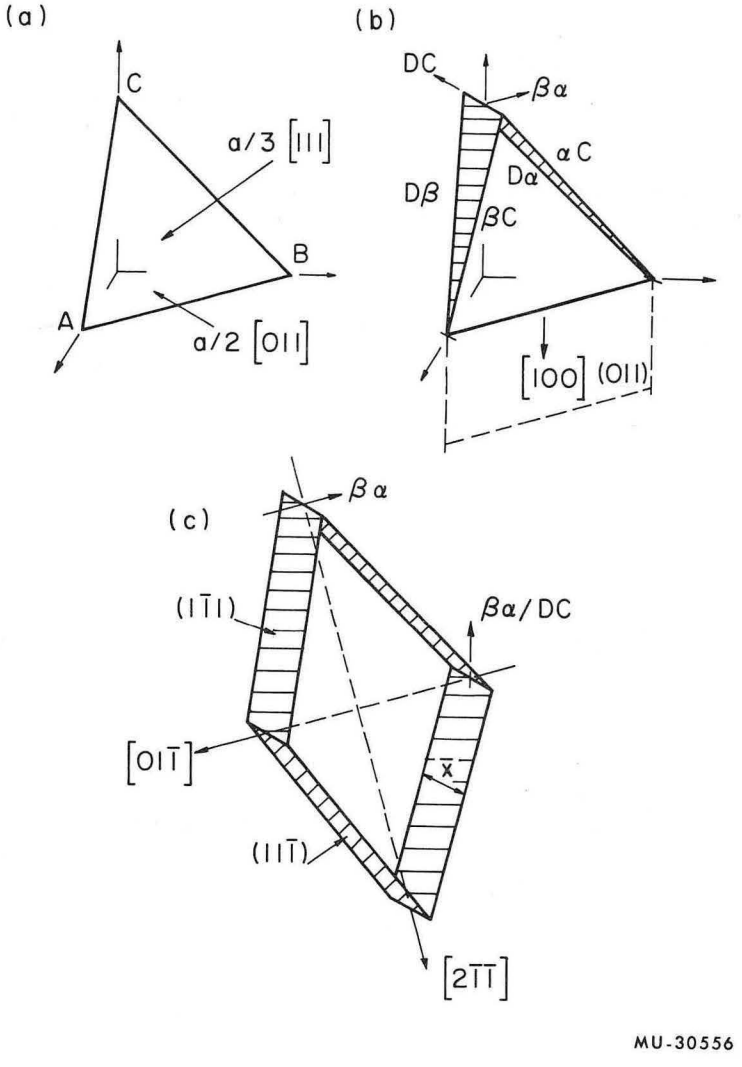

Climb geometry of the $\frac{a}{2}$ [011] prismatic loop; (a) perfect triangular loop, (b) after dissociation of two segments into $\frac{a}{6}$ <112> orientation, (c) equilibrium diamond shape.

Fig. IIA. 8-1 Climb geometry of the $\frac{a}{2}$[011] prismatic loop; (a) perfect triangular loop, (b) after dissociation of two segments into $\frac{a}{6}$ <112> orientation, (c) equilibrium diamond shape.

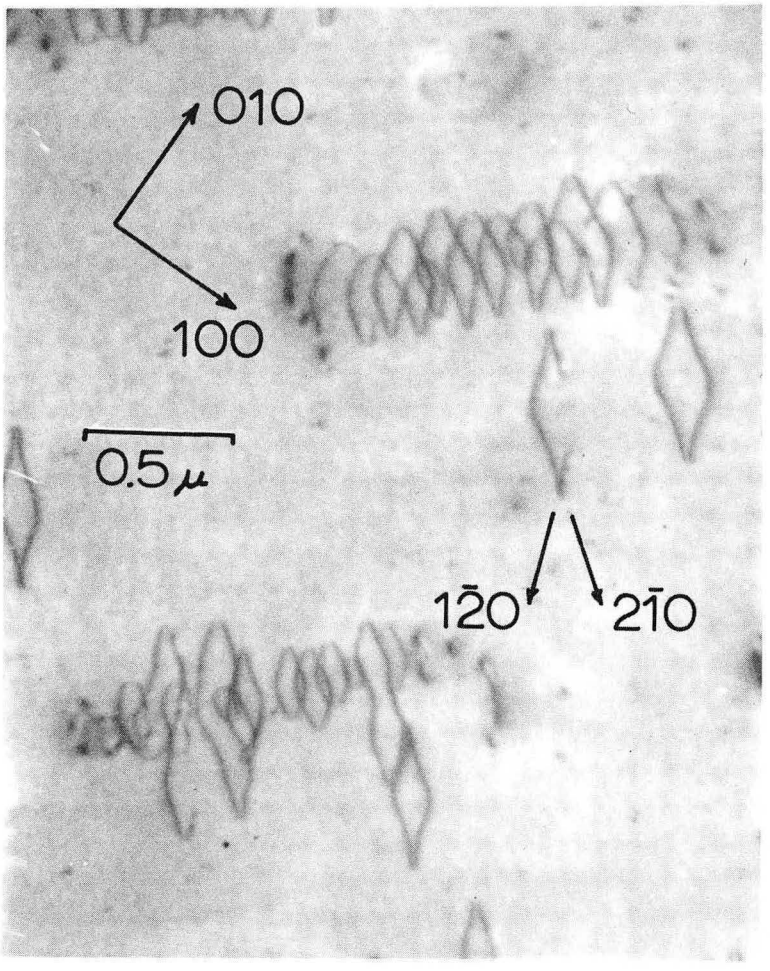

ZN-3629

Fig. IIA. 8-2 Diamond-shaped prismatic loops in Al-5.6 at. % Mg quenched from 520°C and aged 94 h at 100°C. The most probable plane of the loop is (111) or ($\bar{1}\bar{1}$1).

same specimen from one region to another--between the extremes of areas showing cells and areas showing only dislocation tangles. Some of these varied structures are shown in Figs.IIA.9.-1 and 2.

Although our results did not enable us to carry out quantitative analyses, it was possible to arrive at the following general conclusions:
(a) Cell formation is favored when two or more independent slip systems operate.
(b) Cell size decreases for increasing strain rate.
(c) Cell size decreases for decreasing temperature of testing.
(d) The dislocation density is a function of grain size, being greater in polycrystals than in single crystals. The effect can be understood if boundary sources are operating during plastic flow.
(e) In single crystals, the dislocations tend to lie very close to the active glide plane. This is not usually true for polycrystals.
(f) After explosive deformation, unlike conditions after static deformation, a uniform cell structure is observed; the cell sizes decrease with increasing pressure until after a critical size of 0.15 μ is attained (28 kbars or higher), deformation occurs by microtwinning.

10. ORIGIN AND MULTIPLICATION OF DISLOCATIONS*

Gareth Thomas

A review is presented of the current knowledge concerning the origin and multiplication of dislocations, with illustrations obtained by transmission electron microscopy. It seems unlikely that formation of dislocations from collapsed vacancy disks occurs during solidification, but stress may be the most important factor. Heterogeneous nucleation from impurities or grain boundaries has been observed, and an example of the latter is shown in Fig.IIA.10-1. A new kind of dislocation source--viz., the Bardeen-Herring climb source--has been observed, and is discussed fully in another paper.[1] An example is shown in Fig.IIA.10-2.

Almost all models for the multiplication of dislocations involve the Frank-Read mechanism or modifications thereof. Any barrier to a moving dislocation may cause cross-slip and multiplication. Another possible general mechanism of multiplication is that of dislocation cross over, which initially involves formation of dipoles separated by more than a critical distance. Figure IIA.10-3 shows examples of dipoles and dislocation cross over.

---

*Extract from paper in J. Metals, in press (UCRL-10714, March 1963). Presented at Western Metals Congress, L. A., 1963.
1. A. Eikum and G. Thomas, Acta Met., in press (UCRL-10968, October 1963).

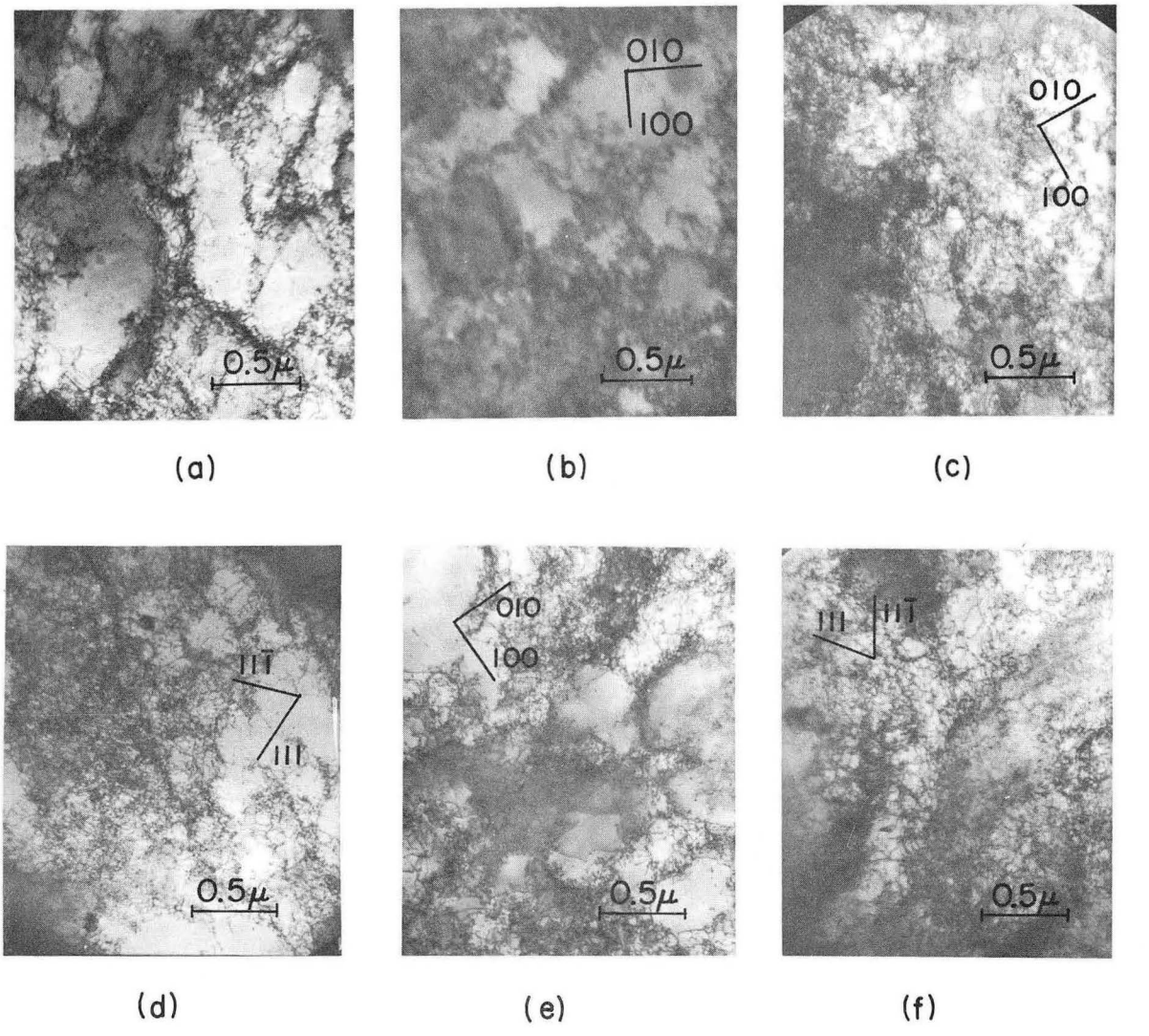

Fig. IIA. 9-1 Transmission Electron Micrographs from polycrystals deformed 20% in tension at:

(a) 273°K and 1 per min strain rate
(b) 273°K and 10^{-3} per min strain rate
(c) 196°K and 1 per min strain rate
(d) 196°K and 10^{-3} per min strain rate
(e) 77°K and 1 per min strain rate
(f) 77°K and 10^{-3} per min strain rate

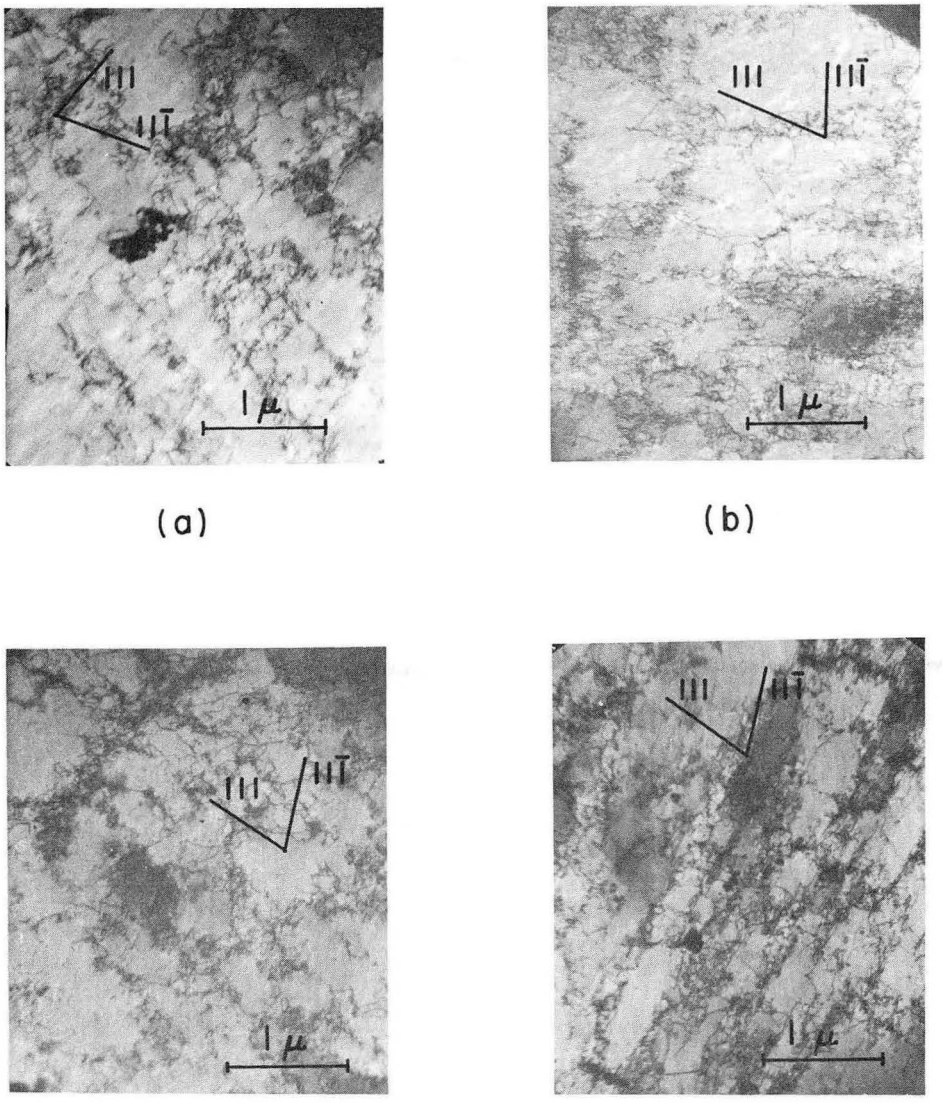

ZN-4036

Fig. IIA. 9-2 Electron micrograph showing dislocation structure in single crystals after 20% tensile deformation at
(a) 273°K and 1 per min strain rate
(b) 273°K and 10^{-3} per min strain rate
(c) 196°K and 1 per min strain rate
(d) 77°K and 10^{-3} per min strain rate

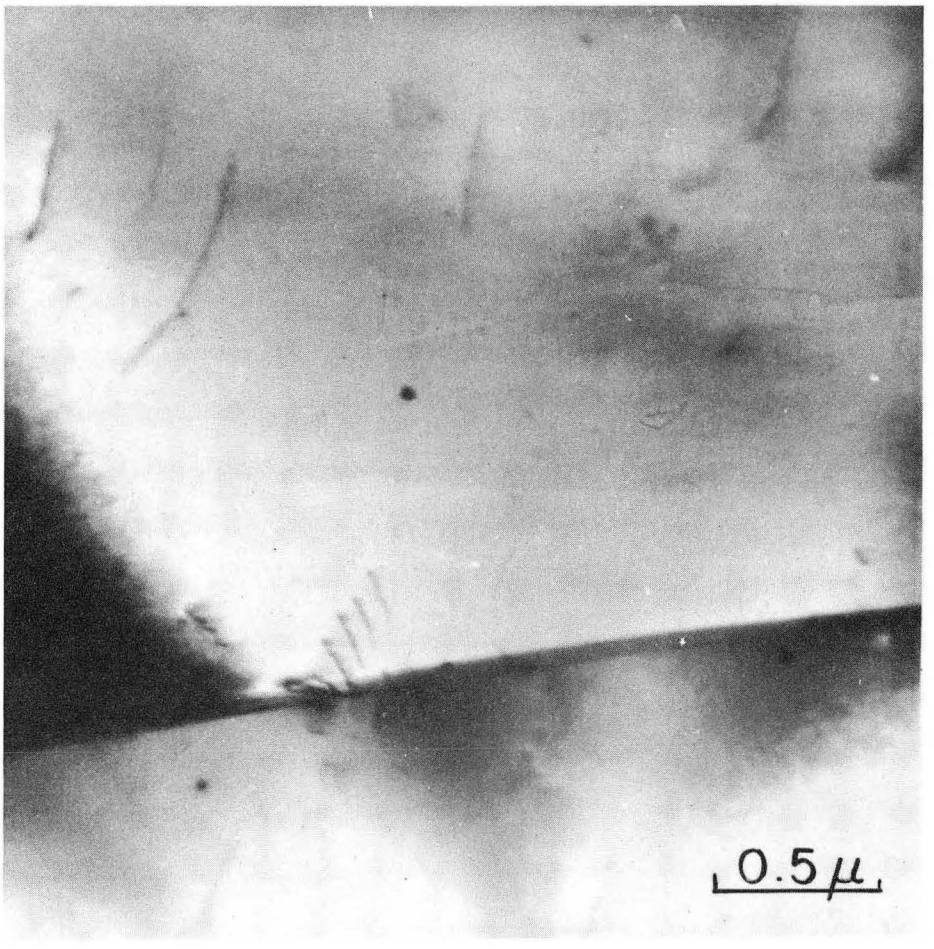

ZN-4255

Fig. IIA. 10-1 Showing the operation of a dislocation source at a high angle grain boundary in Nb.

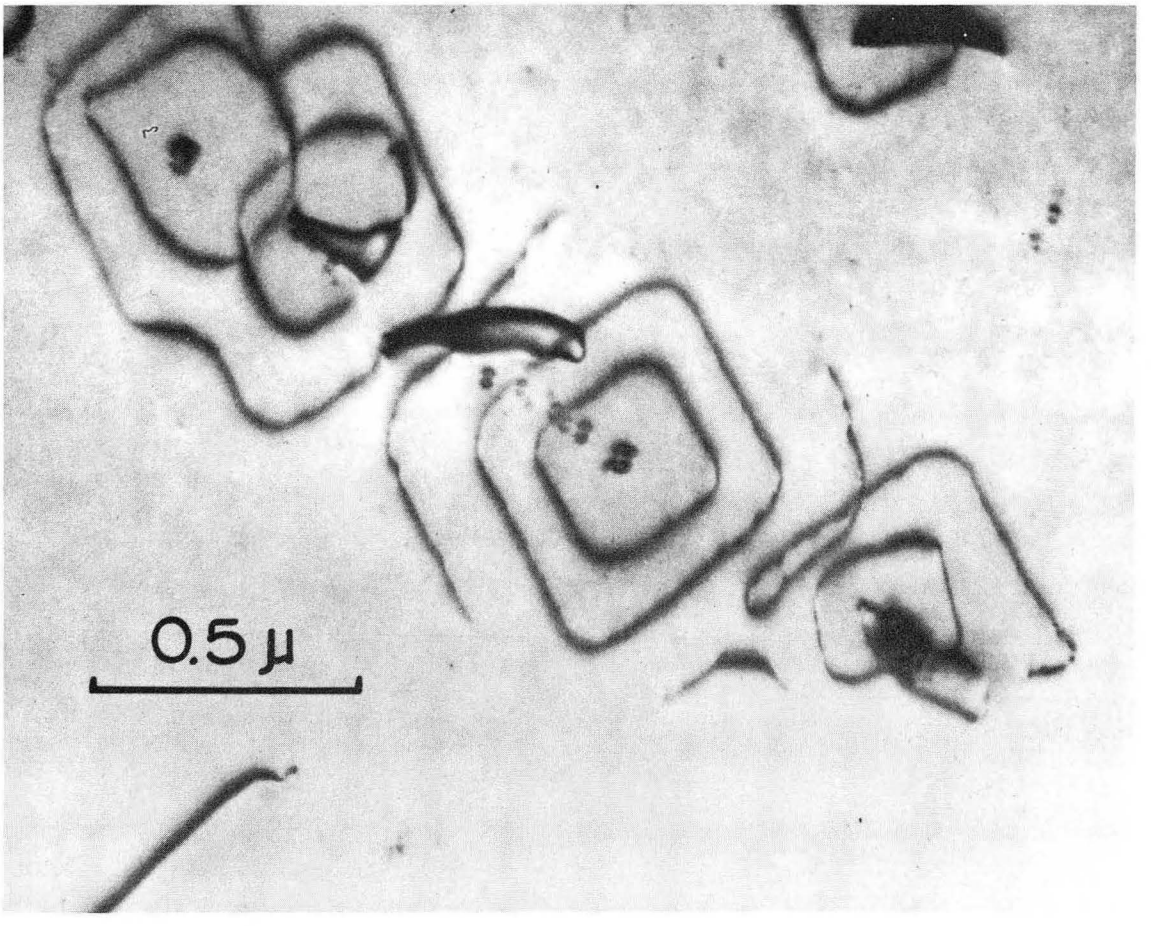

ZN-4254

Fig. IIA. 10-2 Showing precipitate contrast and multiple sources in Al-6.5 wt % Mg, quenched from 550°C into iced brine, aged 100 h at 100°C.

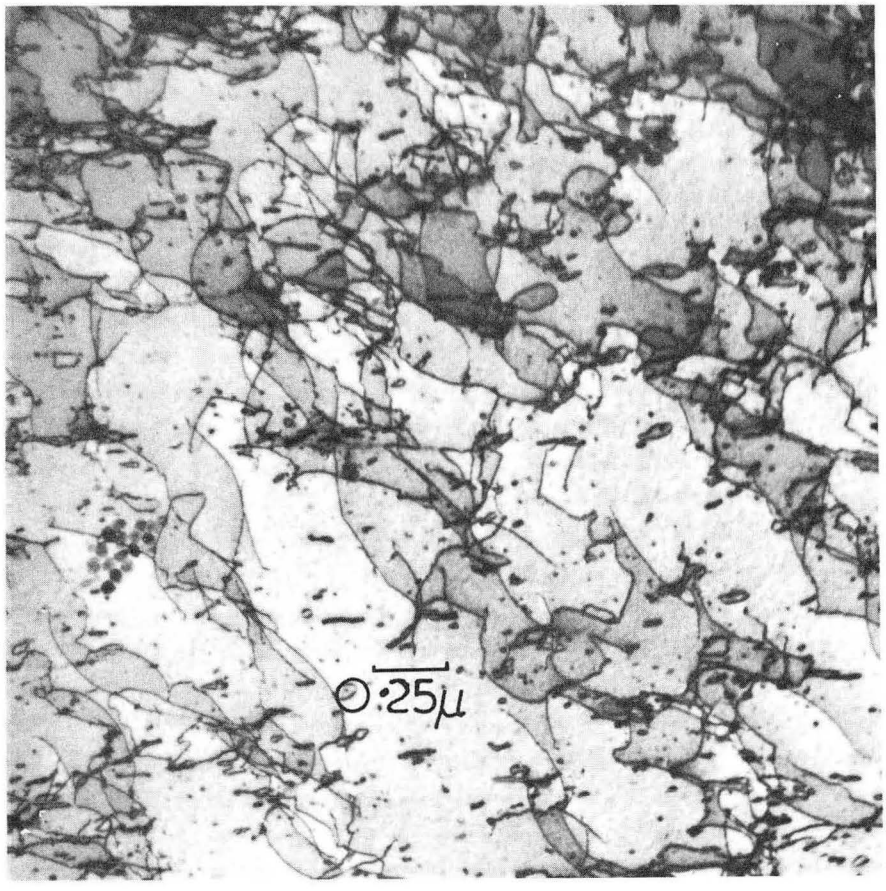

ZN-3686

Fig. IIA. 10-3 Examples of profuse dislocation interactions in Nb after 10% tensile strain. The cross-overs produce local tilts in the crystal leading to changes in contrast. Many of the dislocations are of opposite sign.

11. NUCLEAR MAGNETIC RESONANCE AND ELECTRON MICROSCOPE OBSERVATION OF STACKING FAULTS IN COBALT*

Louis E. Toth,† S. F. Ravitz,† Tom R. Cass, and Jack Washburn

The nuclear magnetic resonance spectrum of cobalt contains satellite peaks that can be explained if a high density of stacking faults is assumed to exist in the face-centered cubic phase.[1,2] From an analysis of the relative intensities of the various peaks and from an estimate of the probable interplanar-spacing in the neighborhood of stacking faults based on the spacing of close packed planes in the hexagonal and face-centered cubic structures of cobalt, it can even be predicted that the majority of the faults are of the intrinsic type. Small amounts of plastic deformation were found to increase the relative intensities of peaks associated with intrinsic faults. This result substantiates the interpretation, because intrinsic faults can be created by the glide of a single Shockley partial dislocation. Extrinsic faults can be formed by glide only if the right combination of Shockley partials glide on two successive close-packed planes. This is highly unlikely.

To further substantiate the interpretation of NMR results, the nature of the stacking faults (Fig. 1) produced during the diffusionless allotropic phase transformation from hexagonal close-packed to face-centered cubic was determined independently by transmission electron microscopy, making use of the theory of electron diffraction contrast at stacking faults.[3,4] According to this theory it is possible to distinguish between intrinsic and extrinsic stacking faults by comparing the bright-field and dark-field images. (Fig. 2).

---

* Extract from paper in Phil. Mag., in press (UCRL-11038, October 1963).

† This research was a cooperative project, the nuclear magnetic resonance experiments being carried out by L. E. Toth and S. F. Ravitz under a National Science Foundation Contract, and the Transmission Electron Microscopy being supported by the Inorganic Materials Research Laboratory

1. W. J. Hardy, Appl. Phys. 32, 122S (1961).
2. L. W. Toth and S. F. Ravitz, J. Phys. Chem. Solids 24, 1203 (1963).
3. H. Hashimoto, A. Howie, and M. J. Whelan, Proc. Roy. Soc. A 264, 80 (1962).
4. A. Art, R. Gevers, and S. Amelinckx, Phys. Stat. Solidi 3, 697 (1963).

12. DEFECTS IN ALUMINUM QUENCHED FROM THE LIQUID STATE*

Gareth Thomas and R. H. Willens†

High purity aluminum was quenched from the liquid state and specimens were examined by transmission electron microscopy. Very high densities of

---

* Extract of paper in Acta Metallurgica, 42, 191 (1964) (UCRL-10822 May 1963).

† W. M. Keck Laboratory, California Institute of Technology, Pasadena, California.

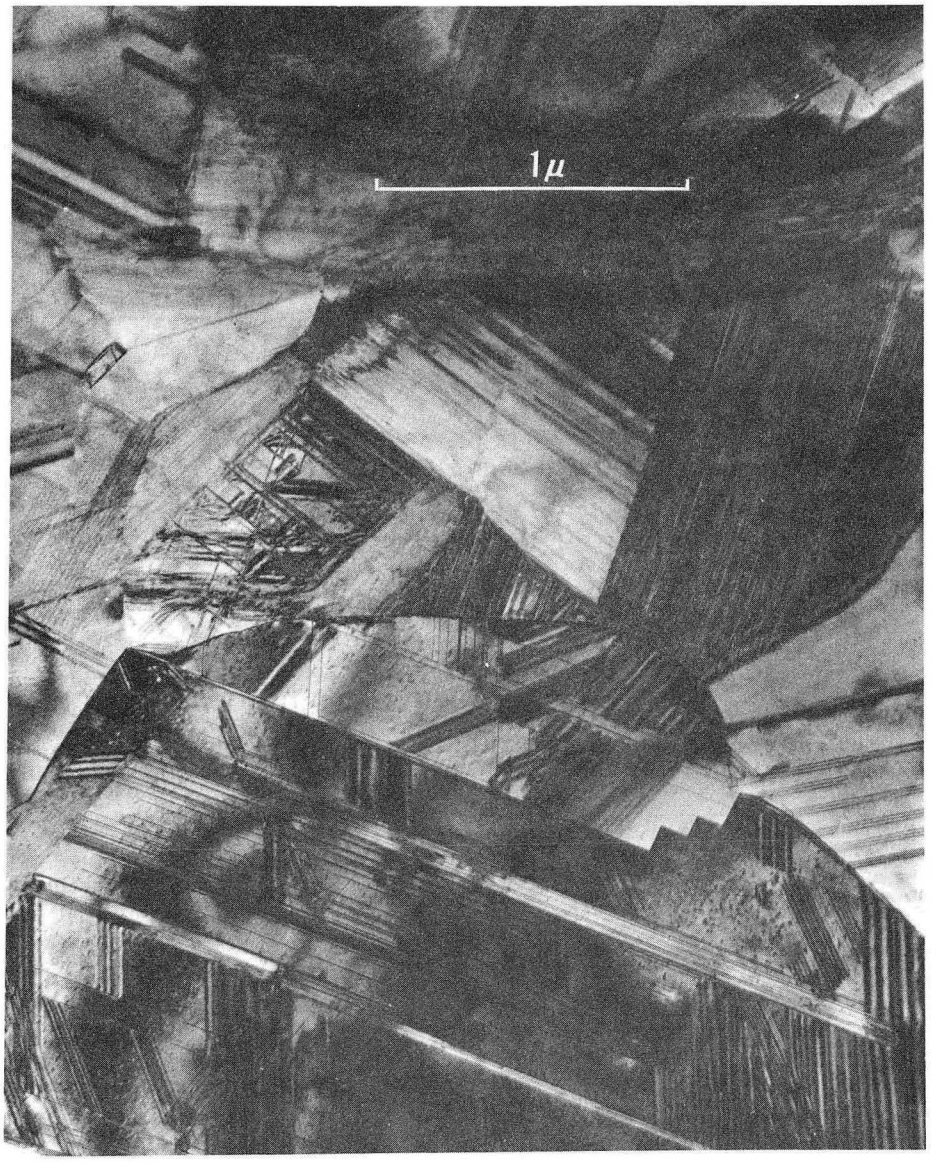

ZN-4237

Fig. IIA. 11-1 Electron micrograph of a cobalt strip annealed 20 minutes at 600°C in hydrogen and air-cooled.

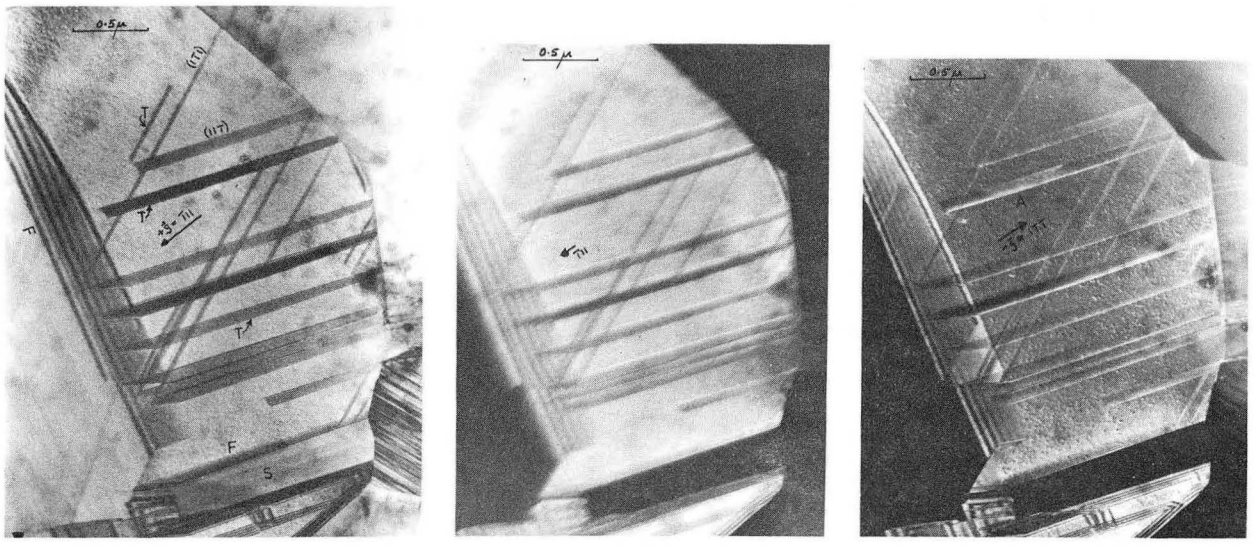

(a) (b) (c)

ZN-4019

Fig. IIA. 11-2 Stacking faults in fcc cobalt,

a. bright-field image with $\bar{1}11$ operating.

b. dark-field image of (a), using $\bar{1}11$.

c. dark-field image of (a), using $11\bar{1}$.
Foil orientation (431). T represents the top surface of the foil.

defects in the form of perfect loops, imperfect loops, and small black spots were observed. The vacancy concentration, as deduced from the number and size of defects in foils quenched from various temperatures, increased with increasing temperature at a much slower rate in the liquid than in the solid. As shown in Fig. IIA.12-1, both the vacancy formation energy and the entropy factor appeared to be considerably reduced above the melting point. Also a discontinuity in the vacancy concentration was found at the melting point.

13. EXTRINSIC-INTRINSIC STACKING-FAULT PAIRS IN EPITAXIAL SILICON*

Jack Washburn, Gareth Thomas, and H. J. Queisser+

Previous work has shown that most of the faults in epitaxially grown Si start at the original surface of the crystal and grow through the deposited material, usually forming closed figures. Because faults always lie on {111} planes, triangular figures are observed for {111} and {110} surface orientations and square figures for {100} surfaces. It has been shown that deliberate contamination of the starting surface with oxide greatly increases the number of faults.[1] This suggests that each stacking fault figure results from the inclusion at the original surface of some foreign atoms or particle. If the thickness of such a foreign particle is not equal to an integral multiple of Si unit cell dimensions, then coherence with the particle can be maintained only by a small upward or downward translation (relative to the surrounding lattice) of the Si lattice directly above the particle. This may result in the nucleation of stacking faults at the edges of the patch of foreign atoms. When symmetrical closed stacking fault figures are formed by this mechanism (i.e., three-sided or four-sided pyramids), it can be shown that the faults must all be of the same type, i.e., all extrinsic or all intrinsic. However, if a closed figure of faults is formed, two sides of which lie on parallel planes, and the material inside the faults has simply been translated upward or downward relative to the surrounding crystal, then the two parallel faults must be of the opposite type, provided they are joined by low energy $\frac{a}{6}\langle 110\rangle$ stair rod dislocations.

Figure IIA.13-1 shows two parallel faults in a (110) expitaxial layer that are joined at one end by a third fault. This appears to be an example of an extrinsic-intrinsic pair.

---

* Summary of a letter to J. Appl. Phys. 3, 44 (1963)(UCRL-10908, July 1963).

+ Shockley Transistor, Unit of Clevite Transistor, Palo Alto, California. Present Address: Physikalisches Institut der Universität, Frankfurt am Main, R. Mayerstr. Str. 2-4, Germany.

1. R. H. Finch, H. J. Queisser, G. Thomas, and J. Washburn, J. Appl. Phys. 34, 406 (1963).

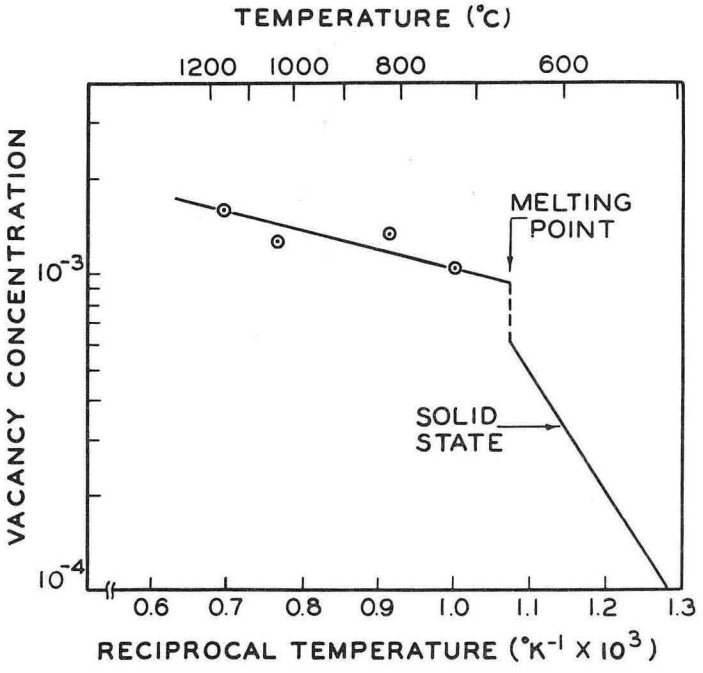

Fig. IIA. 12-1 Relationship between vacancy concentration and reciprocal temperature.

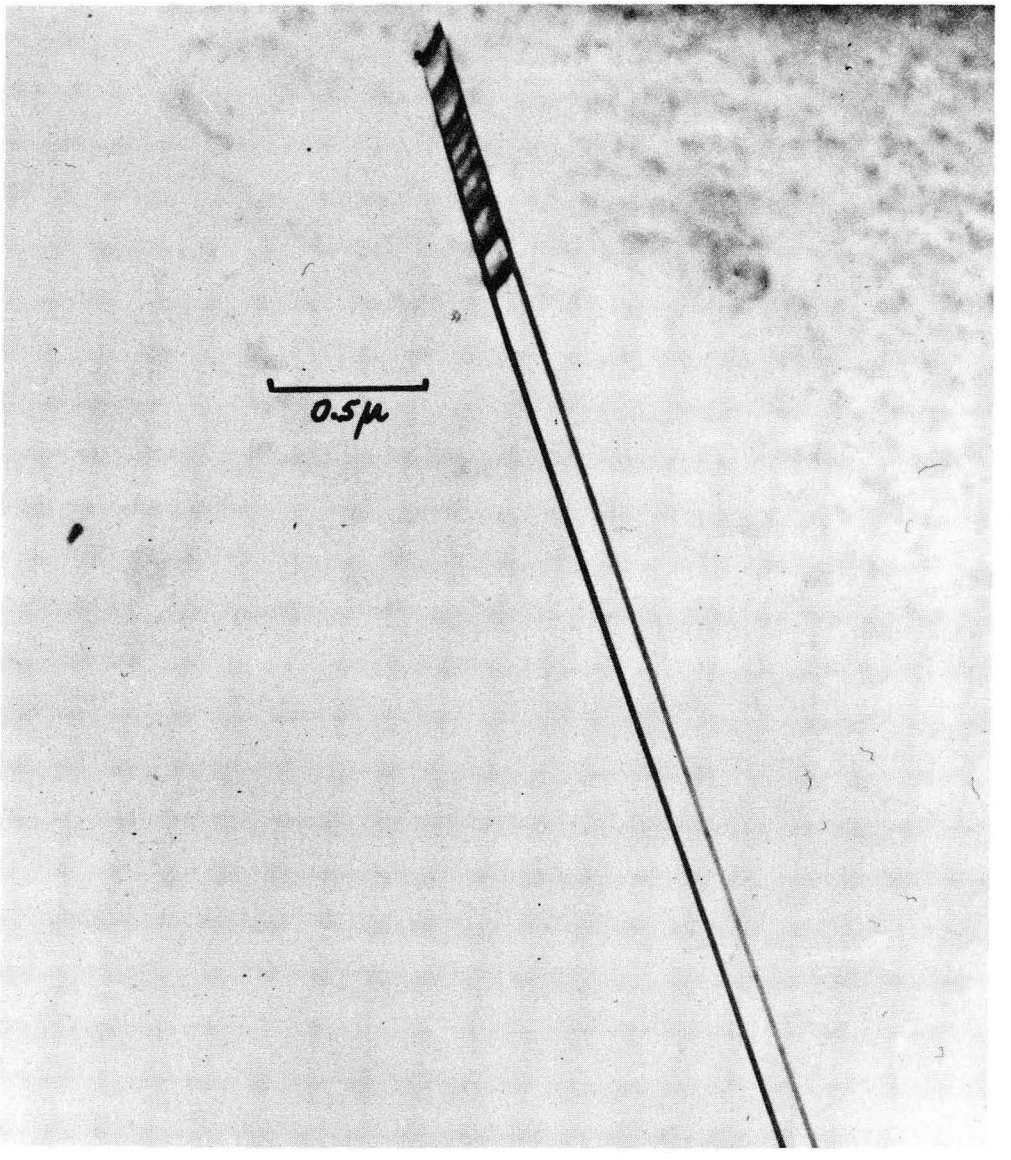

ZN-4253

Fig. IIA. 13-1 A probable example of an extrinsic-intrinsic pair of stacking faults. Transmission electron micrograph shows two parallel faults joined by a connecting fault at one end in epitaxially grown (110) silicon.

14. DIFFUSION-INDUCED DISLOCATIONS IN SILICON*

Jack Washburn, Gareth Thomas, and H. J. Queisser†

In silicon, diffusion treatments with boron or phosphorus cause lattice parameter changes in the surface layers. For high concentrations of solute the resulting stresses are relaxed by plastic deformation.[1] The resulting arrays of dislocations have been studied by transmission electron microscopy in an attempt to clarify the mechanism by which the dislocations move into the crystal during the diffusion.

For these experiments a special stage[2] was used in a Siemens electron microscope. It allowed the normal to the specimen surface to be tilted ±6° in any direction away from the axis of the microscope. This made possible the achievement of several different single diffraction conditions for the same field of view, as illustrated by Fig.IIA.14-1. From an analysis of the diffraction contrast experiments it was possible to determine unambiguously the Burgers vectors of the various kinds of dislocations in the array. The following are the main conclusions:

(a) The dislocation network consisted primarily of a crossed grid of very long edge dislocations with Burger's vector $\frac{a}{2}[110]$ and $\frac{a}{2}[\bar{1}10]$ parrallel to the (001) surface of the specimen.
(b) The dislocations did not all lie at exactly the same depth. Two or more edge dislocations of the same sign often lay one above the other.
(c) The long edge dislocations ended at nodes. The presence of these nodes suggested that the crossed grid was formed by dislocation reactions. In this way it would be possible for the array to move into the crystal at least in part by glide of dislocations having Burger's vectors that were not parallel to the surface.
(d) There was also evidence for precipitation--both homogeneous and preferentially along dislocation lines. When dislocations were out of diffraction contrast, strings of precipitates were often still visible. Although these precipitates were not identified they were assumed to contain phosphorus.

---

* Extract from paper submitted to J. Appl. Phys. (UCRL-11102, January 1964).
† Clevite Semiconductor Division, Palo Alto, California. Present address: Physikalisches Institut, Universität Frankfurt, Germany. There experiments were conducted in cooperation with the Clevite Semiconductor Division Laboratories.

1. H. J. Queisser, J. Appl. Phys. 32, 1776 (1961).
2. G. V. Patser and P. R. Swann, J. Sci. Instr. 39, 58 (1962).

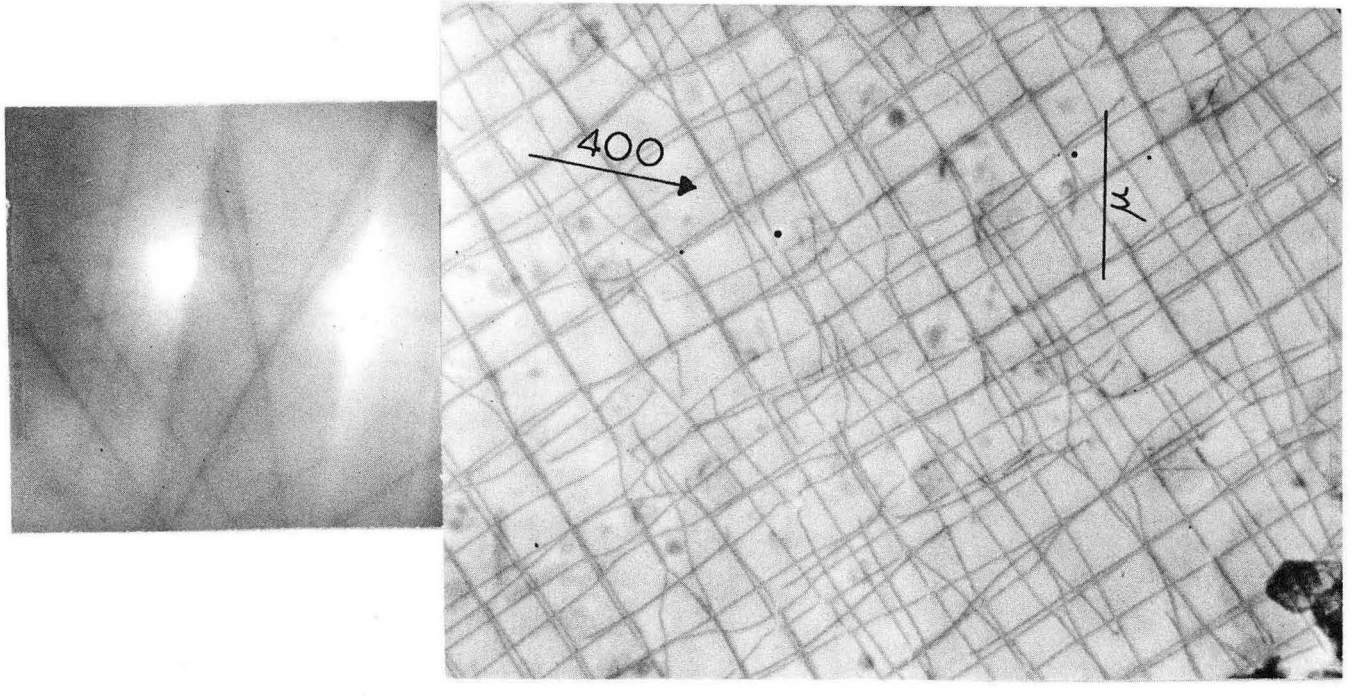

ZN-4142

Fig. IIA. 14-1 Diffusion-induced dislocation array in silicon, shown for 400 diffraction.

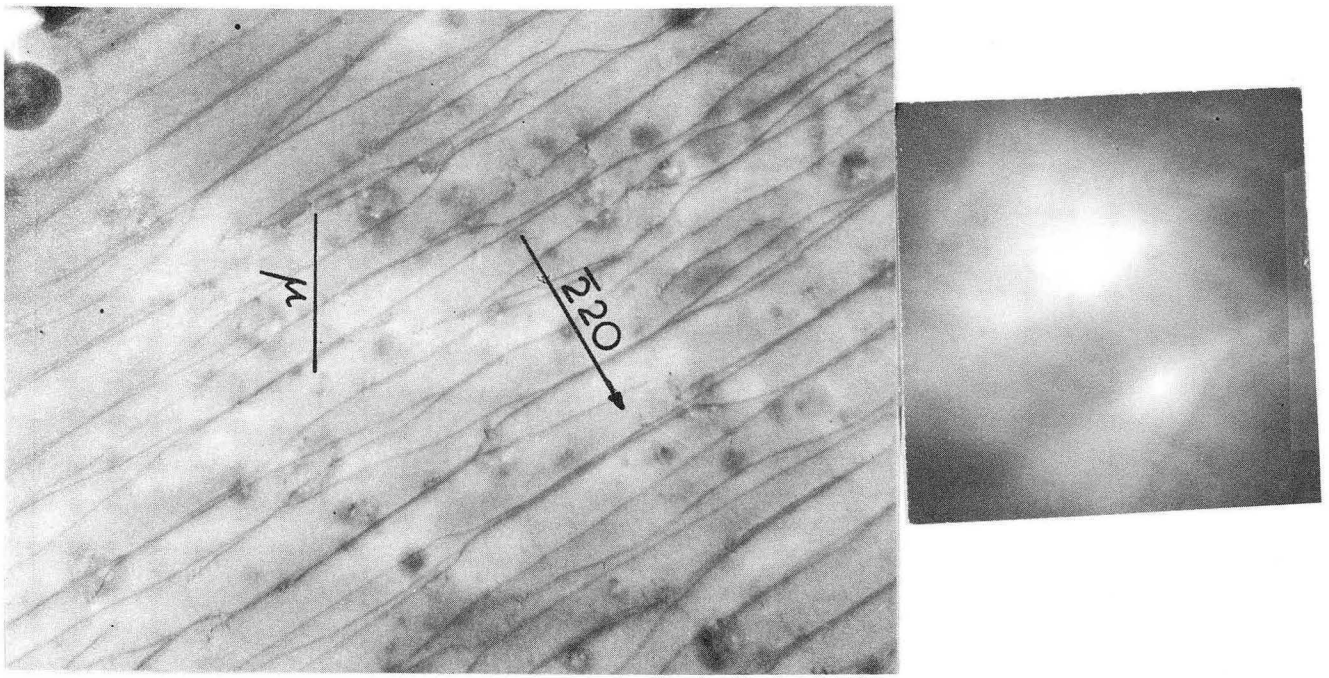

ZN-4143

Fig. IIA. 14-2 Diffusion-induced dislocation array in silicon, shown for 220 diffraction.

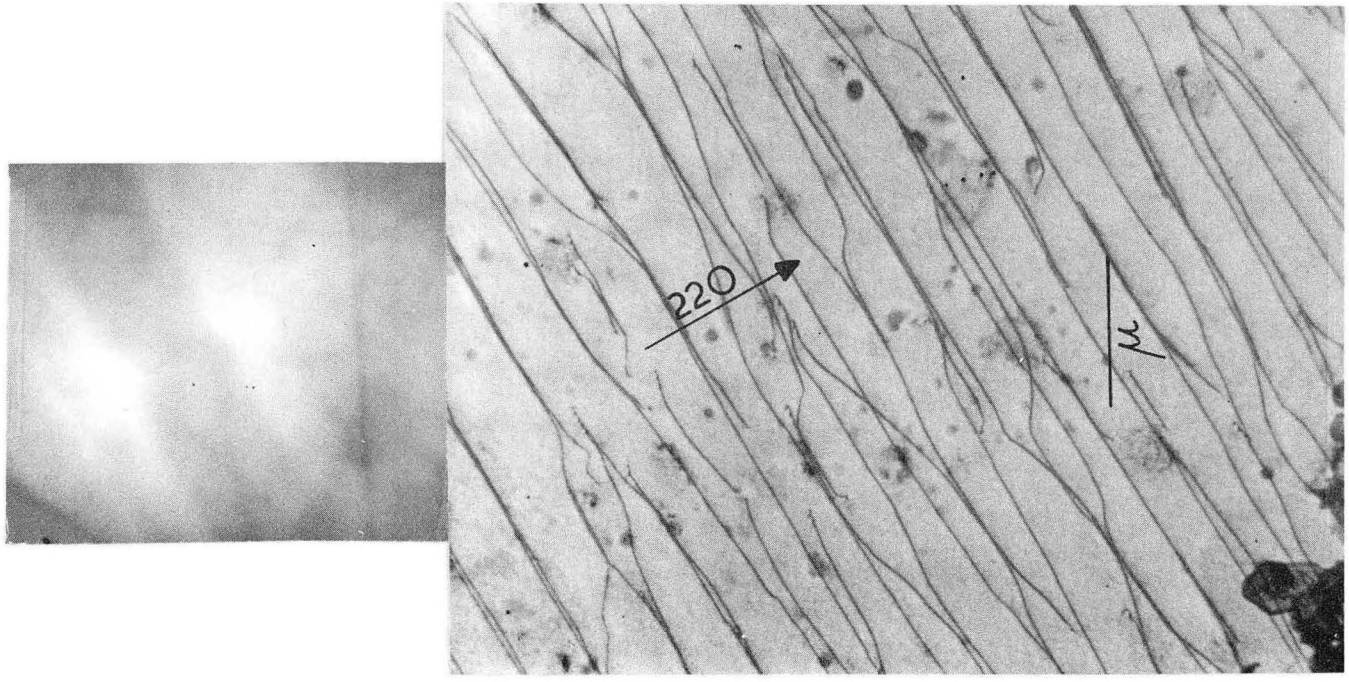

ZN-4144

Fig. IIA. 14-3 Diffusion-induced dislocation array in silicon, shown for $\bar{2}20$ diffraction.

15. EFFECT OF QUENCHING CONDITIONS ON THE VACANCY SUBSTRUCTURE IN ALUMINUM*

Gobinda Das and Jack Washburn

In a quenched metal, excess vacancies cluster. At some stage during the growth of clusters dislocation loops are formed, but it is not clear exactly how or when the collapsed defects are formed. In aluminum two different kinds of dislocation loops are observed: (a) stacking-fault loops consisting of an intrinsic stacking fault surrounded by an $\frac{a}{3}\langle 111\rangle$ dislocation, and (b) perfect $\frac{a}{2}\langle 110\rangle$ dislocation loops.

By investigating the factors that affect the type of collapsed defect formed in aluminum it may be possible to further elucidate the mechanism by which a cluster of vacancies becomes a dislocation loop.

It has been reported[1,2] that in 99.99% purity aluminum the common type of defect is the perfect dislocation loop, but that in zone refined aluminum stacking-fault loops predominate. This suggests that the presence of certain impurities favors formation of $\frac{a}{2}\langle 110\rangle$ loops.

In these experiments it has been found that in 99.999% purity aluminum slight changes in the quenching conditions can cause marked changes in the ratio of imperfect to perfect loops. The quenching conditions were changed by varying the thickness of the specimen to be quenched within the range 25 to 400 μ. The results are illustrated by Fig. IIA.15-1 a,1b. Both specimens were quenched from 540°C into water at 40°C, the only difference being the thickness at the time of quenching. For the 125-μ specimen almost all the loops contain a stacking fault, whereas for the 300-μ specimen nearly all the loops are perfect and diamond-shaped, with all four sides lying on {111} planes.

Changes in both cooling rate and quenching stresses are thought to accompany a change in thickness of the specimen being quenched. It has been found that to a first approximation the total number of excess vacancies that finally appear as loops is the same in thick and thin specimens. Therefore, the changes in loop substructure seem most likely to be due to changes in the amount of quenching deformation or to the stress.

---

* Condensation from Gobinda Das, Influence of Quenching Conditions on Vacancy Loops in Aluminum (M.S. Thesis), UCRL-11188, Jan. 1964.

1. S. Yoshida, M. Kiritani, and Y. Shimomura, J. Phys. Soc. Japan 18, 175 (1963).
2. R. M. J. Cotterill and R. L. Segall, Phil. Mag. 8, 1105 (1963).

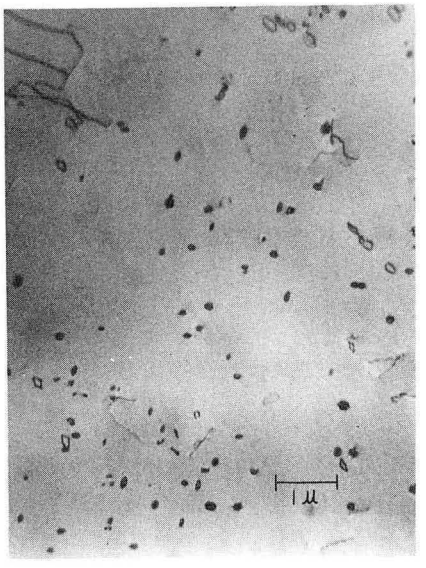

FIG. 3a

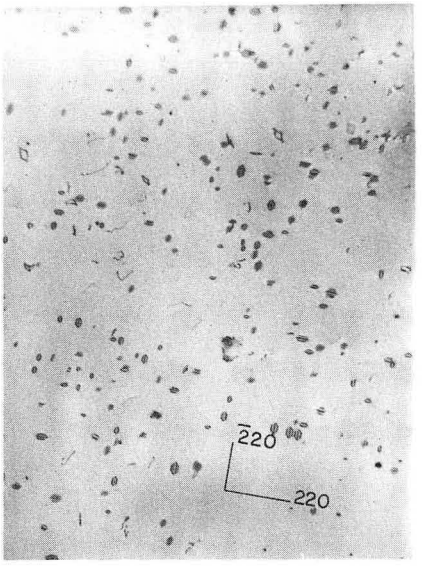

FIG. 3b

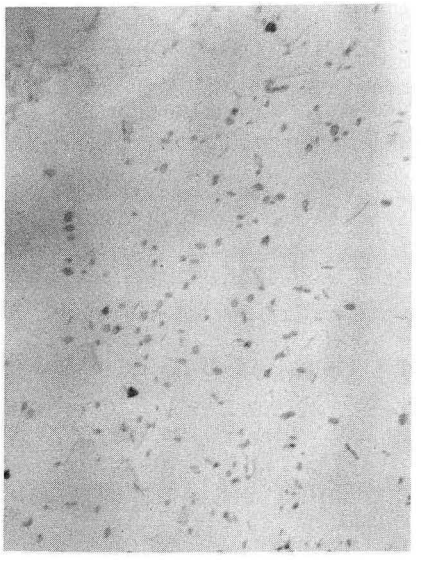

FIG. 3c

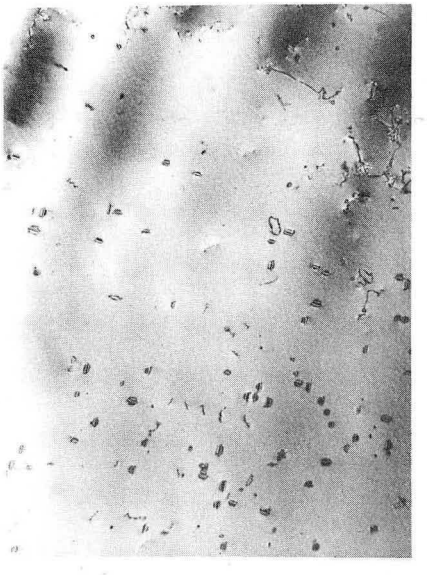

FIG. 3d

ZN-4162

Fig. IIA.15-1a (a),(b),(c),(d): The substructures of 125 μ thick specimens. Note all Frank sessile loops contain stacking fault fringes. The average diameter of the loops is 1750 Å.

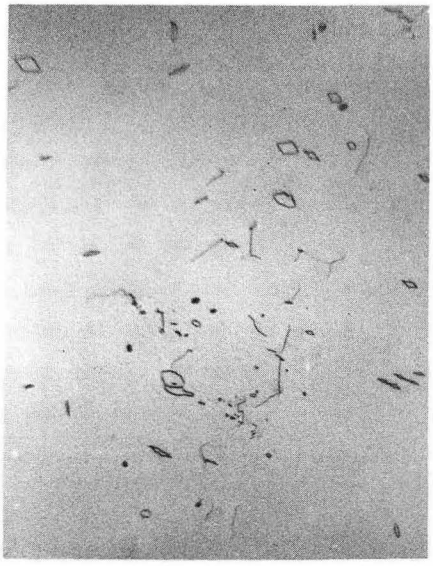

FIG. 6a

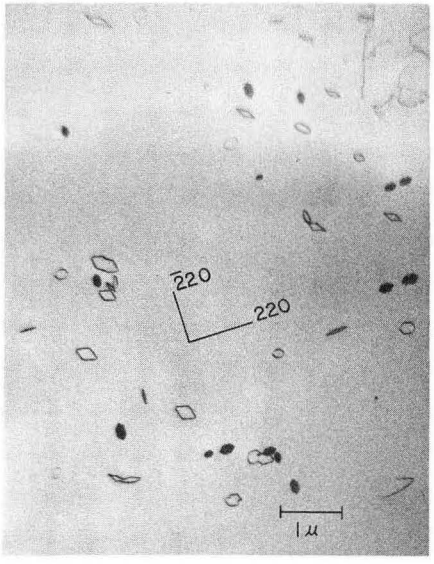

FIG. 6b

FIG. 6c

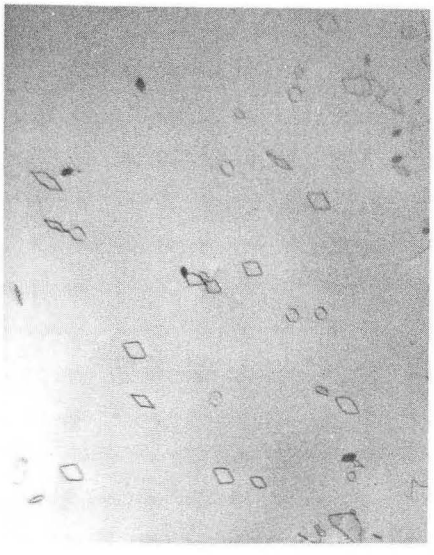

FIG. 6d

ZN-4165

Fig. IIA.15-1b (a),(b),(c),(d): The substructure of 400μ thick specimens. Note well developed diamond shaped loops of average diameter of 4100 Å.

16. DIRECT OBSERVATIONS OF INTERACTIONS BETWEEN IMPERFECT LOOPS AND MOVING DISLOCATIONS IN ALUMINUM*

Jean L. Strudel and Jack Washburn

Observations have been made by transmission electron microscopy on the interactions between faulted dislocation loops and moving dislocations in 99.999% aluminum. Single crystals of (110) orientation were grown; this particular orientation facilitated the determination of the Burger's vector of loops and moving dislocations. Quenching from 650°C into 20°C water followed by 10 hours' aging at 20°C produced a high density of small imperfect loops (Fig. IIA.16-1). Lowering the quenching temperature to 540°C produced a lower density of larger imperfect loops (Fig. IIA.16-2).

Most of the dislocation lines that were seen moving in the thin foils had relatively high velocity ($> 5 \times 10^{-3}$ cm/sec). Hence the interpretations of interaction with imperfect loops were deduced from the special features exhibited by slip traces left behind these moving dislocations (note the indentations on slip traces on Figs. IIA.16-1 and IIA.16-2).

Interpretations mostly based on this method led to the following conclusions:

1. When the imperfect loop does not lie on either glide plane of the moving dislocation the stacking fault is removed by a single Shockley partial that sweeps across the whole area of the loop and reaches the edge, where it combines with the Frank sessile dislocation. One turn of a helix is formed on the dislocation line (Fig. IIA.16-3). This portion that does not lie on the original glide plane hinders further motion of the dislocation, and hence is generally eliminated, either uniquely by glide to the surfaces of the foils (leaving indentations E'N'Q' as on Fig. IIA.16-1) or in part by glide, in part by leaving behind a smaller perfect loop (F is changed into P+I on Fig. IIA.16-2). 2. When the imperfect loop lies on a plane parallel to the Burger's vector of the moving dislocation two Shockley partials are emitted by the dislocation and remove the stacking fault each on its side. Two nodes are created and then eliminated by glide when the dislocation passes the loop. Examples of this type of interaction can be seen in Fig. IIA.16-1, where M is changed to a new Burger's vector at M' and in Fig. IIA.16-2, where S is changed at S'.

These observations suggest that whenever a moving dislocation intersects an imperfect loop in aluminum the stacking fault is always completely destroyed. In the bulk crystal when dislocations cut across colonies of imperfect loops, perfect loops are left behind and helical dislocation segments are swept into the subgrain boundaries or into regions of higher dislocation density.

---

* Condensed from paper in Phil. Mag., 9, 491 (1964) (UCRL-10959, Oct. 1963).

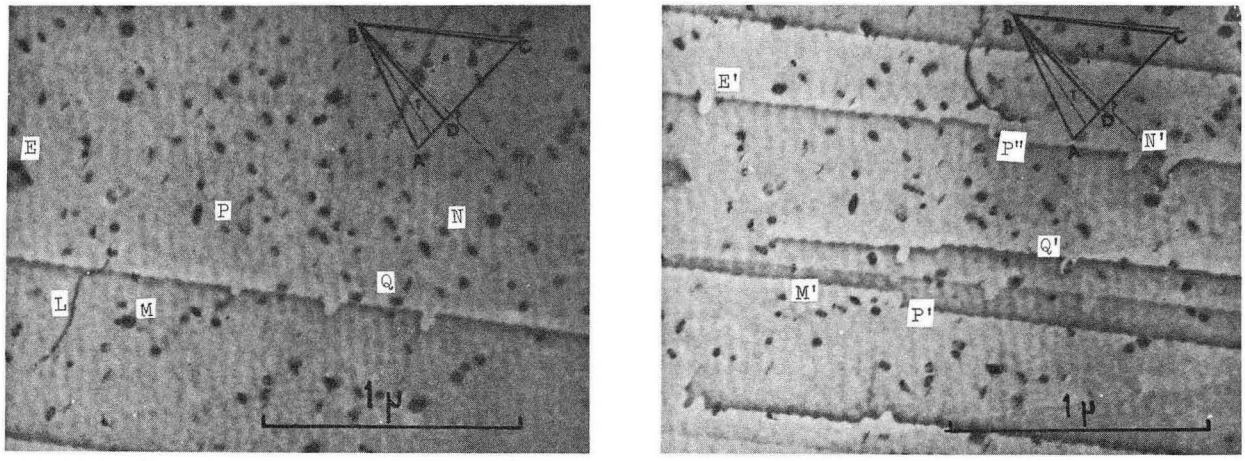

(a) (b)

ZN-3982

Fig. IIA. 16-1 a,b. Specimen quenched from 650°C into 0°C water. Interactions with small loops.

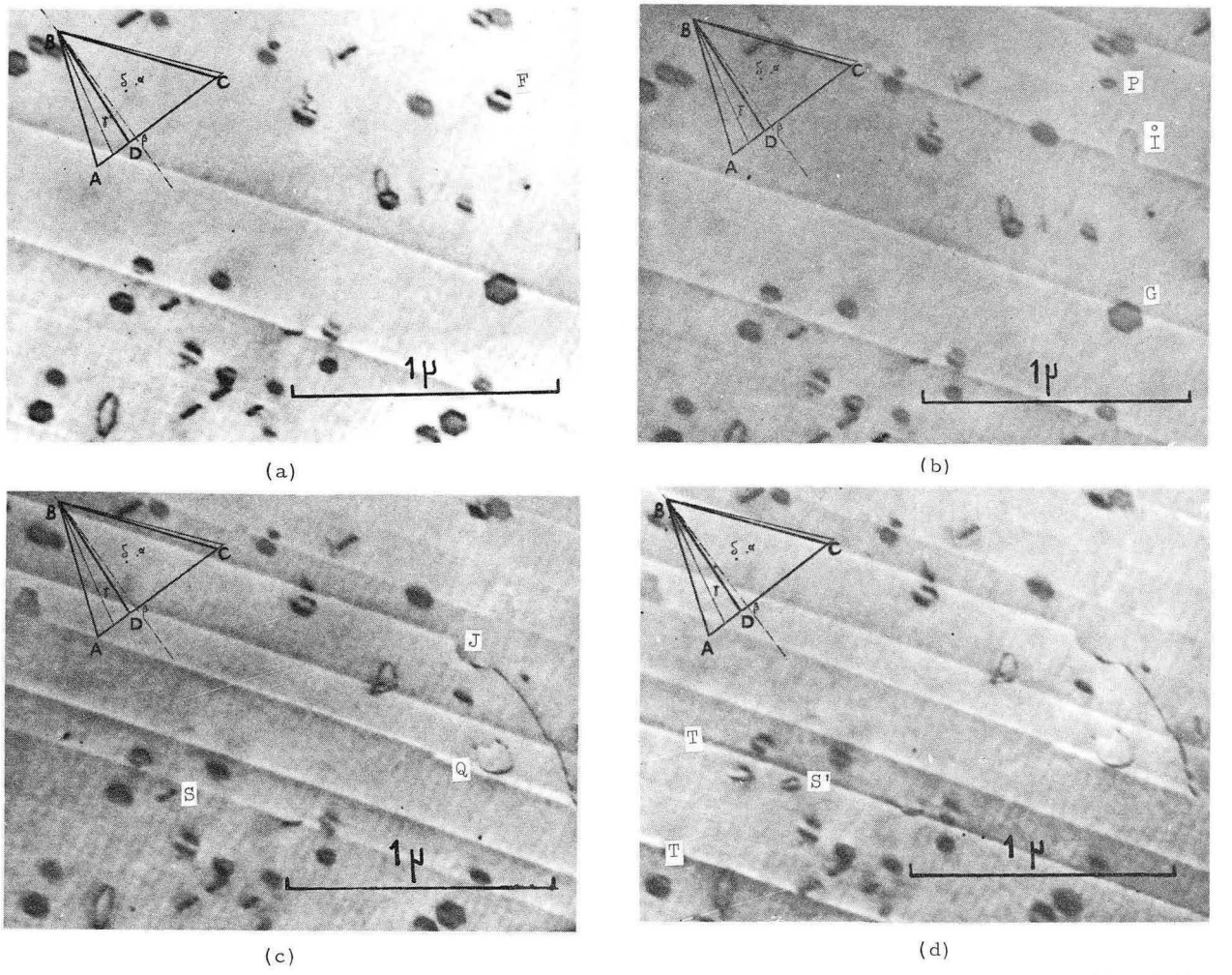

Fig. IIA. 16-2 a,b,c,d. Specimen quenched from 540°C into 0°C water. Interactions with large loops result in partial destruction of the loop.

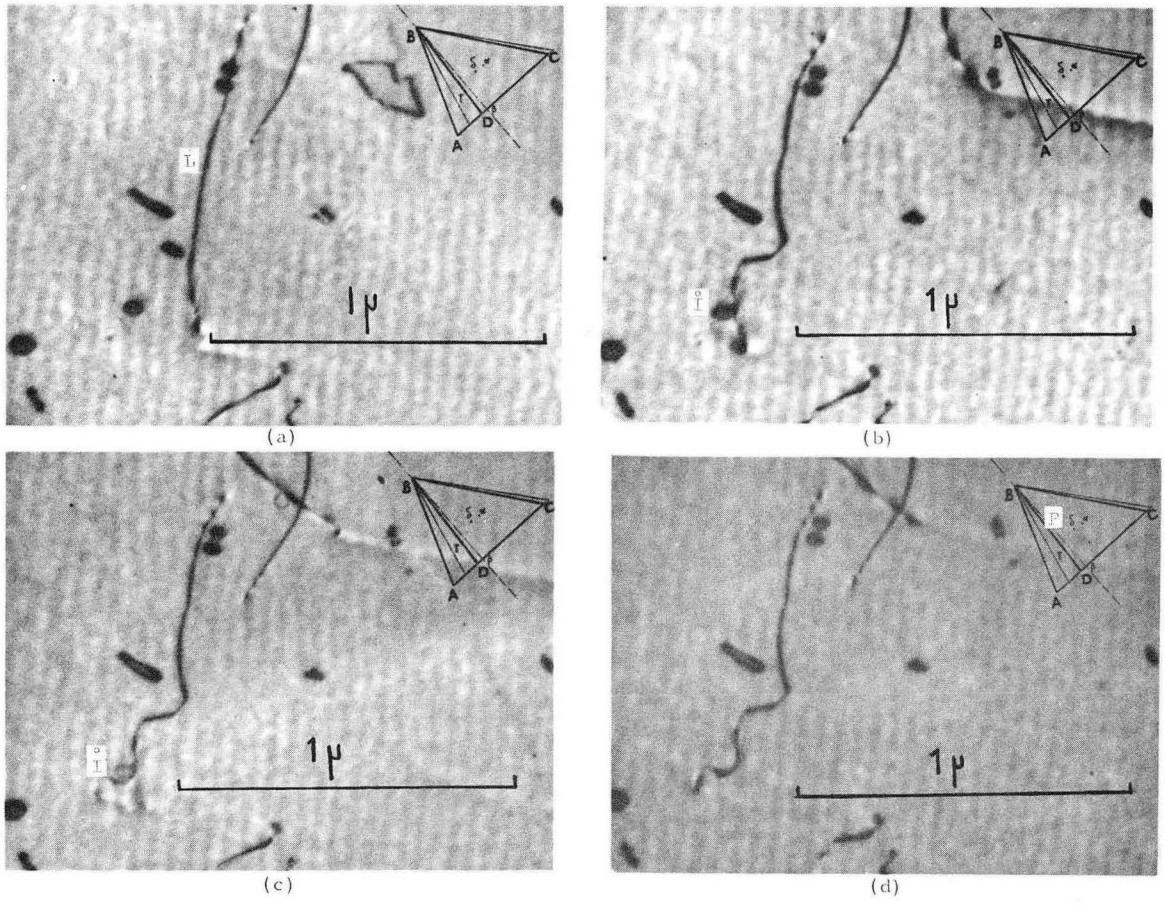

ZN-3979

Fig. IIA. 16-3 a,b,c,d. Successive stages of interactions between dislocation line L, perfect loop P and imperfect loop I.

17. ELECTRON MICROSCOPY OF THIN FOILS*

Gareth Thomas

This paper reviews the present state of knowledge regarding the application of the theory of diffraction contrast to the interpretation of electron micrographs, and is illustrated with many examples of contrast experiments. The topics discussed are listed below.

(1) Theory of diffraction contrast, including extinction and absorption.
(2) Geometrical treatment of diffraction contrast, the correct sense of $\vec{g}$.
(3) The deviation parameter s; determination of its sign.
(4) Determination of "habit planes" of lattice defects.
(5) Visibility of dislocations, dislocation loops, and stacking faults.
(6) Determination of the sign of displacement vectors.
(7) Determination of the sense of stacking faults (i.e., intrinsic or extrinsic).
(8) Determination of foil thickness.
(9) Contrast from small precipitates.
(10) Reliability of transmission electron microscopy.

* Extract from paper presented at ASM Symposium, Cleveland, 1963; to be published in a book, Structure and Properties of Thin Films (ASM). (UCRL-11009, Oct. 1963).

18. MODERN METALLOGRAPHIC TECHNIQUES*

Gareth Thomas

A review is presented of metallographic methods for analyzing the structure of materials. The following topics are discussed.

(1) Microscopic examination.
(2) Light metallography.
(3) X-ray microscopy.
(4) Thermionic emission microscopy.
(5) Field ion microscopy.
(6) Electron microscopy.
(7) Electron probe microanalysis.

* Extract from paper presented at a special Symposium on Metallurgy in Aerospace Technology, UCLA, 1963. To be published in a book of the conference proceedings (UCRL-11067, Oct. 1963).

19. DISLOCATION MOTION IN CRYSTALS CONTAINING VACANCY CLUSTERS

Jack Washburn

When dislocations move during plastic deformation, clusters of vacancies are left behind as part of the damage that causes strain hardening. Similar defects are also the cause of radiation hardening, and are produced by quenching a crystal from elevated temperature so as to trap thermal vacancies. Moving dislocations can also destroy some of these defects. An understanding of the detailed interactions between moving dislocation and vacancy clusters of all sizes, from a divacancy up to voids or dislocation loops consisting of $> 10^3$ individual vacancies, is fundamental to any real understanding of yielding and slip-band growth in crystals.

Research in this general field during the year 1964 will be concentrated on (a) a study of the growth of vacancy clusters or small voids in quenched copper during low-temperature aging (small-angle x-ray scattering techniques will be used) (b) Quantitative measurement of dislocation mobility in copper crystals containing vacancy clusters of known size.

20. THE THEORY OF STRAIN HARDENING

Jack Washburn

Quantitative theories of strain hardening, the most successful of which has been that due to Seeger,[1] have concentrated on an explanation of the second-stage linear hardening of face-centered cubic crystals--in particular those that have been carefully annealed so as to produce initially a small density of dislocations. So far it has not been possible to propose more general theories because of the complexity of the changes in defect substructure that take place during plastic deformation. The shape of a stress-strain curve depends on so many variables that in spite of the vast amount of work in this field there are important aspects of the problem that have not been quantitatively studied.

Our research in this area during 1964 will consist of the following specific investigations.

(a) The effect of initial dislocation substructure on yielding, on the hardening rate during stage I, and on the transition to stage II, studied with pure copper single crystals.
(b) Experiments utilizing surface observations of slip bands in an attempt to find out whether or not changes in the shape of stress-strain curves can be correlated with changes in the distribution of strain.

1.A. Seeger, S. Mader, and H. Kronmuller, Electron Microscopy and Strength of Crystals (Interscience, New York, 1963), p. 665.

21. THE GROWTH OF DEFORMATION TWINS

Jack Washburn

Although the formal crystallography of twinning is well established, the mechanism of deformation twinning when considered on an atomic scale is far from being understood. In this respect our knowledge of twinning lags far behind our knowledge of deformation by slip.

The reasons for this lack of knowledge are:

1. Deformation twinning occurs only under special conditions of temperature and strain rate in cubic structures. In hexagonal metals these conditions are less rigorous, but here the crystallographic orientation for twinning is more critical. The result is that, in practice, deformation by twinning is less commonly observed than deformation by slip.

2. Detailed quantitative information about the stresses required for twin nucleation and growth is difficult to obtain because the twin nucleation and initial growth process under a uniform stress is very rapid (occurring in a time of the order of 10^{-5} to 10^{-4} sec). This rapid formation leads to the production of an almost instantaneous strain resulting in a large load drop and, often, the nucleation of additional twins.

3. Although dislocation mechanisms have been proposed to account for twinning in the three common metal structures, the strain rates and temperature required by the cubic structures preclude direct observation of the process by transmission electron microscopy. Observations on hexagonal metals, admittedly made under conditions of nonuniform stress, do not support any proposed mechanism.

Deformation twinning is nevertheless an important phenomenon in deformation studies because the presence of small twinned regions may change the properties of metals, either by producing favorable orientations for slip or else by acting as a barrier to dislocations resulting in pile-ups and possible crack nucleation.

Experiments are at present in progress to study the thickening of twin lamellae in zinc specimens deformed in tension. Normally this process cannot be studied closely because it occurs immediately after nucleation, under a rapidly decreasing load, and is accompanied by the nucleation of other twins.

A technique has been developed for producing properly oriented cylindrical zinc tensile specimens the gauge section of which is traversed by a single twin lamella. On deforming such a specimen at 20°C with the tensile axis in the basal plane, the only process observed is the thickening of the twin lamella. This occurs by the smooth propagation of the two parent-twin interfaces at a constant load.

It is hoped to study the effect of shear stress and temperature on the rate of twin boundary propagation and to investigate the effect of grown-in or introduced dislocation structures on the mobility of these boundaries. Present experiments are using specimens of 99.999% pure zinc.

22. THE INFLUENCE OF OXYGEN ON THE INTERNAL FRICTION OF HIGH-PURITY (99.9999%) SILVER*

Michael W. Guinan and Larry Himmel

Measurements of the temperature dependence of the internal friction and elastic modulus of high-purity (99.9999%, $\rho_{296°K}/\rho_{4.2°K} > 2000$) oxygen-free (< 1ppm) silver and silver containing approximately 20 to 40 ppm of oxygen have been made on single crystals at frequencies of the order of 25 kc by the resonant-bar technique. Measurements were made over the range from 4.2°K to 1000°K at low strain amplitudes (approximately 10^{-8}). In addition, the dependence of the damping on strain amplitude was measured at various fixed temperatures throughout the same range.

The procedure followed was essentially the same for all specimens. After suitable annealing to insure that no additional changes in the dislocation structure occur during the course of the measurement (we found, for example, that cycling the specimen between 800°K and 1000°K reduced the damping in this range by an order of magnitude below that obtained by long anneals at 1000°K), the damping and modulus were measured at low strain amplitudes over the entire temperature range. Measurements were taken both on heating and cooling at rates from 15 to 30°K/h in steps of 200 to 300°K, with the specimen remaining for approximately 12 hr between steps. A second run was then made stabilizing the temperature every 50 to 100°K and measuring the strain-amplitude dependence of the damping and modulus. The specimen was then saturated with oxygen (up to 40 ppm) in place in the apparatus and the above set of measurements was repeated.

Although a detailed analysis of the data is not yet completed, we have made the following observations:

(a) The addition of as little as 20 ppm of oxygen reduces the damping to less than 3% of its initial value over the entire temperature range. The initial value can be completely recovered by a vacuum anneal. This provides us with a modulus base from which we can obtain the modulus defect associated with the damping in the oxygen-free silver.
(b) In the temperature range above 100°K, the experimental results for the oxygen-free silver are consistent with an interpretation based on the vibrating-string model.
(c) Oxygen (or some configuration of oxygen) can act as an effective pinning agent for dislocations in silver. Preliminary calculations also indicate that the binding energy associated with this pinning is considerably larger than that associated with substitutional impurities.

---

* Extract from Michael W. Guinan's Ph.D. Thesis, in preparation.

23. THE EFFICIENCY OF DISLOCATIONS AS SINKS FOR VACANCIES IN KIRKENDALL EXPERIMENTS*

Dennis M. Maher and Larry Himmel

The nature and extent of the porosity that forms during chemical interdiffusion at 900°C in the Cu-Ni system has been studied metallographically, and the accompanying dimensional changes have been measured in massive, sandwich-type diffusion couples prepared from two different grades of copper-OFHC and spectroscopically pure (99.999%, American Smelting and Refining Co.). Estimates of the relative fraction of the excess vacancies that condense to form pores on the copper-rich side have been obtained in two ways: (a) from the ratio of the overall expansion of the couple to the normal Kirkendall shift, and (b) from the ratio of the measured pore volume to that associated with the net vacancy flux, as derived from the concentration-distance profiles. Both estimates are in reasonable agreement and indicate that upwards of 90% of the excess vacancies agglomerate as pores rather than being annihilated at jogs on dislocations or other sinks; in spectroscopically pure copper, about 50% of the excess vacancies end their lives at pores. It is concluded that, contrary to the usual assumption, dislocations are not very effective sinks for vacancies under the conditions (e.g., relatively low vacancy supersaturations) which prevail within the diffusion zone. The observed differences in the extent of porosity in the two grades of copper are believed to be due to differences in the number or potency of nucleating sites available for vacancy condensation rather than to differences in the ease with which dislocation climb can take place in these two materials.

* Abstract of paper presented at the 1963 fall meeting of The Metallurgical Society, Cleveland, Ohio. See Dennis M. Maher, The Formation of Porosity During Diffusion Processes in Metals (M.S. Thesis), UCRL-10383, Sept. 1962.

24. RECOVERY OF INTERNALLY OXIDIZED SILVER MAGNESIUM ALLOYS*

Raymond A. Busch and Larry Himmel

The low-temperature annealing behavior of a cold-worked internally oxidized silver-0.1 at. % magnesium alloy has been investigated and compared with the annealing response exhibited by the corresponding unoxidized alloy and by pure silver. Wire specimens of each material were deformed in tension at 78°K and the recovery was followed by measuring the electrical resistivity and the flow stress at 78°K after suitable isochronal and isothermal anneals at temperatures between 78° and 550°K. It has been found that both point defect and dislocation annealing processes are markedly retarded by the presence of the dispersed oxide phase. The effect of internal oxidation on the annealing behavior is broadly explained in terms of defect-solute atom

* Abstract of paper presented at the AIME Annual Meeting, February 17-20, New York, N. Y. See Raymond A. Busch, Recovery of Internally Oxidized Silver-Magnesium Alloys (M.S. Thesis), UCRL-10816, July 1963.

cluster interactions. It is suggested, for example, that point defect annealing may be inhibited because vacancies and interstitials generated during plastic deformation are trapped in the strain fields surrounding Mg-O atom clusters.

25. INTERNAL FRICTION PEAKS DUE TO OXYGEN IN SILVER*

John M. Papazian and Larry Himmel

The addition of oxygen to high-purity silver ($\rho_{293°K}/\rho_{4.2°K}$ ~ 2000) is found to give rise to three separate low-temperature internal friction peaks. In single-crystal specimens, these relaxation peaks occur at about 130°, 180°, and 270°K at a frequency of 2 cps. The activation energies associated with these peaks are 8.5±1.0, 11.5±1.0, and 15.5±1.0 kcal/mole respectively. A study has been made of the orientation dependence of the peaks, the variation in the peak heights with oxygen concentration, and the response of these peaks to various thermal and mechanical treatments. It is shown that, for both the 130° and 180°K peaks, the relaxation strength is proportional to the square of the oxygen concentration over the range from about 100 to 300 ppm. For both peaks, the maximum relaxation strength is observed when crystals are tested in torsion about a <111> axis, whereas torsion about <100> results in minimum values of the peak heights. On the basis of these observations and others, the 180°K peak has been assigned to the stress-induced reorientation of interstitial oxygen atom pairs. It is proposed that the defect responsible for the 130°K peak consists of a pair of oxygen atoms residing in a vacant silver lattice site. The peak at about 270°K, which is considerably broader and less reproducible than the lower-temperature peaks, is tentatively ascribed to an oxygen-dislocation interaction.

* Abstract of paper presented at the AIME Annual Meeting, February 17-20, New York, N.Y. See John M. Papazian, The Internal Friction Due to Oxygen in Silver (M.S. Thesis), UCRL-11017, Sept. 1963.

26. THE ELASTIC CONSTANTS OF CADMIUM*

A. Y. Chang and Larry Himmel

The temperature dependence of the elastic constants of cadmium has been measured over the interval from 78°K to the melting point of cadmium (320°C). The elastic constants were determined from measurements made on suitably oriented single-crystal specimens by the pulse-echo technique. Single crystal spheres 1 in. in diam. were grown in high-purity graphite molds from 99.999% cadmium by a modified Bridgman technique. A 0.5-in.-thick center section of the desired orientation was then cut from the sphere by spark erosion and the ends were lapped. Measurements were made utilizing a Sperry ultrasonic attenuation comparator operating at 10 Mc.

* Extract from paper in preparation.

27. TEMPERATURE DEPENDENCE OF FLOW STRESS IN INTERNALLY OXIDIZED SILVER BASE ALLOYS*

Subhash Gupta and Larry Himmel

There is convincing evidence[1-3] that dilute alloys of Cu and Ag with Mg, Si, Be, Al, etc. harden considerably on internal oxidation. The various theories which have been proposed to explain the increase in yield strength in dispersion-strengthened materials predict different temperature sensitivity of the flow stress. Accordingly, the study of temperature dependence of flow stress in these materials may provide possible information about dislocation-particle interaction.

Since previous experience has shown that polycrystalline samples of Ag-1 at%Mg and Ag-1 at%Cd alloys specimens were embrittled as a result of internal oxidation, all the specimens used in this work were in the form of single crystals. The mechanical tests carried out were of three general types: (a) conventional stress-strain curve determination at a fixed temperature and strain rate, (b) measurements of the temperature dependence of the flow stress at a constant strain rate, and (c) determination of the strain-rate dependence of the flow stress as a constant temperature.

A detailed analysis of the data has not been completed, but we would like to comment that a very strong temperature dependence of the flow stress was observed in Ag-Mg-O and Ag-Cd-O systems. This suggests that neither Orowan's mechanism nor shearing of particles is responsible for hardening in these materials; cross slipping of dislocation around the particles may be the cause of strengthening.

* Extract from Subhash Gupta's Ph.D. Thesis, in preparation.

1.J. L. Meejering and M. J. Dryvesteyn, Philips Research Report 2, 81-102 (1947).
2.E. Gregory and G. C. Smith, J. Inst. Metals 85, 81-87 (1956-57).
3.M. F. Ashby and G. C. Smith, J. Inst. Metals 91, 182 (1962-63).

28. THERMAL CHARACTERISTICS OF A 150-kW ARC IMAGE SYSTEM*+

Ira Pratt, Mark Davis,
T. H. Hazlett and R. Eberhart

The arc image as a source for high thermal flux irradiation studies of materials has received considerable attention in recent years. The objective in this program was to develop an efficient tungsten to tungsten argon plasma for use as an intense thermal source for irradiation materials, and avoid the difficulties associated with carbon arcs. Theoretical heat

* Abstract of paper presented at The Asilomar High Temperature Symposium, September 8-11, 1963 (UCRL-11007).

+ Principal support for this program was provided by the U.S. Air Force, initially by the Office of Scientific Research, and later by the Aeronautical Systems Division, Wright-Patterson Air Force Base.

transfer and preliminary studies in a pressurized chamber indicated the way toward development of a tungsten cathode and a composite tungsten-copper anode structure suitable for currents to 3000 amperes as supplied by a three-phase silicon rectifier power supply at a nominal 70 volts.

The electrical characteristics at three different environmental pressures are plotted in Fig. IIA.28-1. The thermal flux intensity at the image plane is illustrated in Fig. IIA-28-2 and flux intensity distribution is shown schematically in Fig. IIA.28-3. High speed motion pictures, taken during arc initiation and shutdown, indicate that with the present power supply, it takes approximately 5 milliseconds for the plasma to grow to equilibrium size, and about the same time to decay.

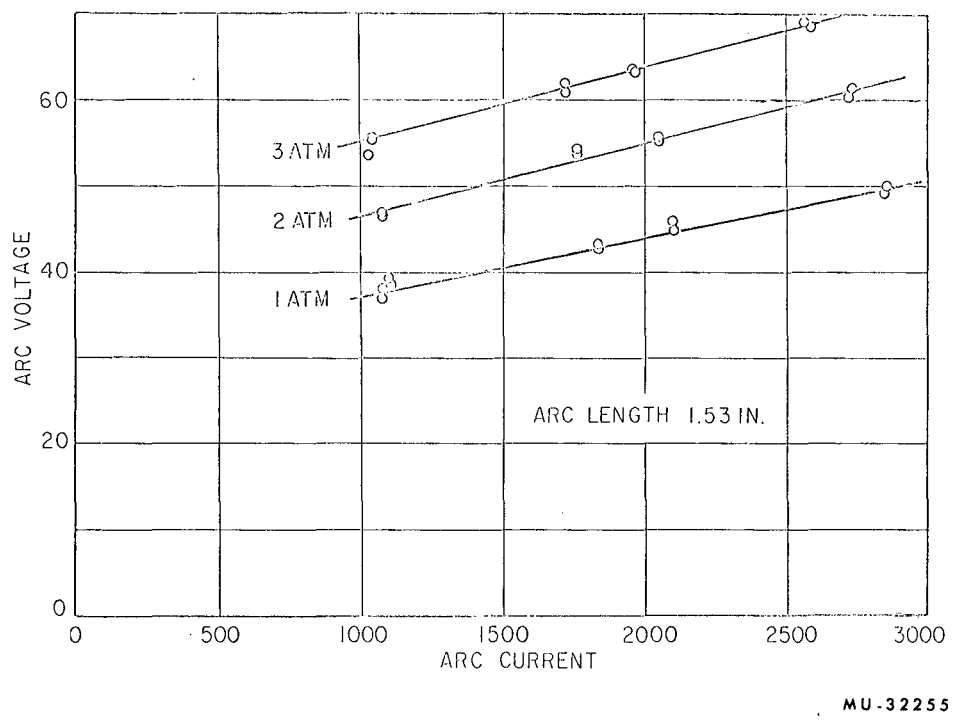

Fig. IIA. 28-1 Electrical characteristics of the argon arc.

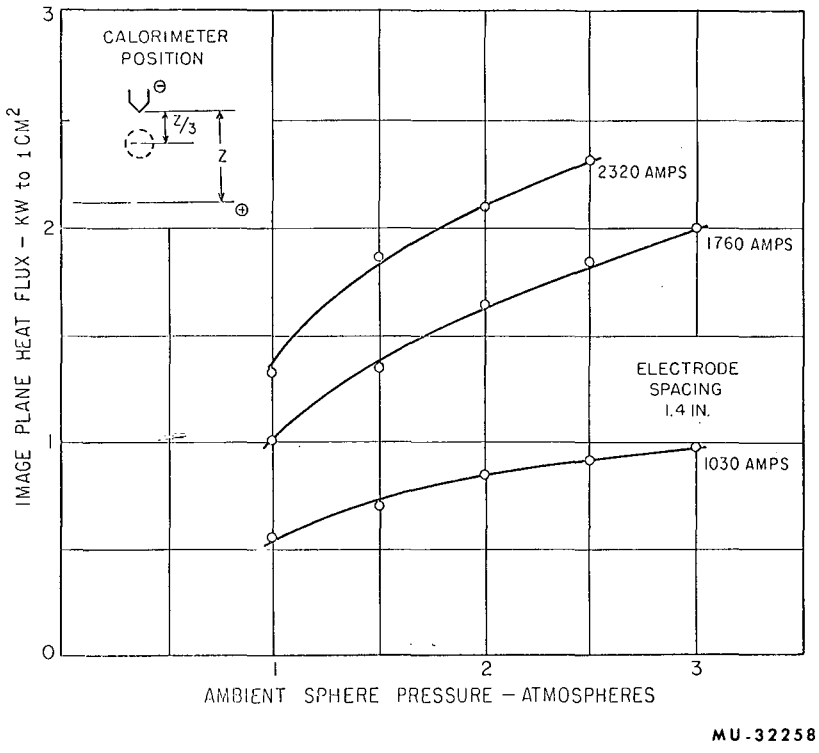

Fig. IIA. 28-2 Thermal flux at the image plane as measured with continuous flow calorimeter.

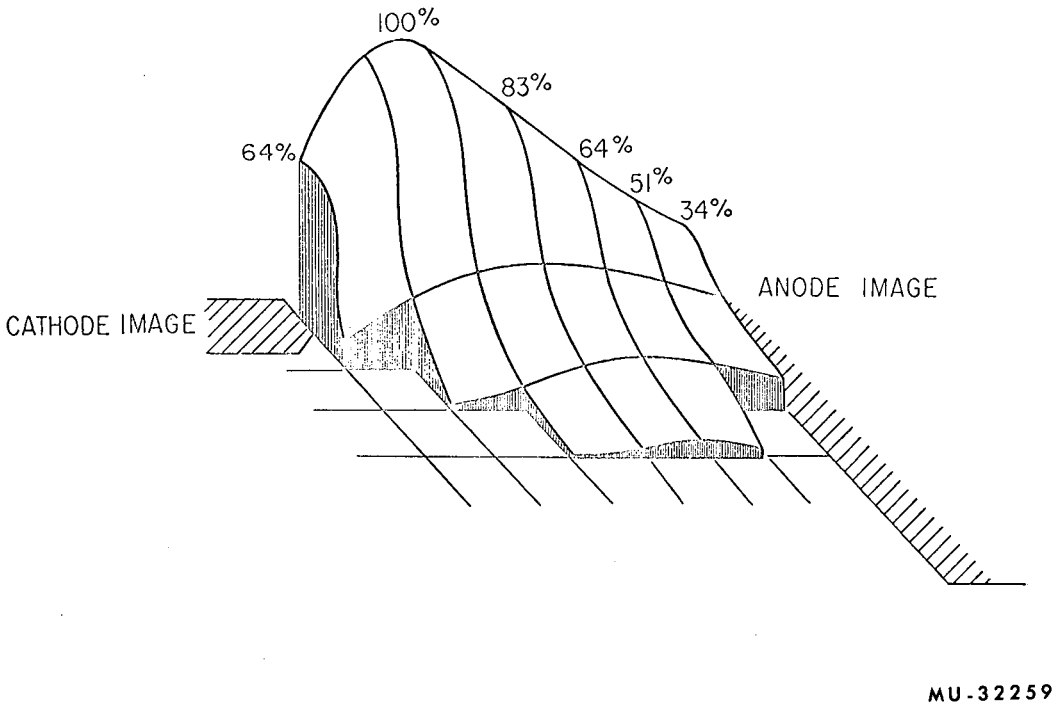

Fig. IIA. 28-3 Image-zone flux distribution in a 1.5-inch argon arc as measured with the 0.25-cm^2-aperture adiabatic calorimeter. The grid spacing is 0.25 inch.

B. SUPERCONDUCTIVITY

1. SUPERCONDUCTIVITY OF Mo_3Al_2C

Jean Johnston, Louis Toth, Kurt Kennedy, and Earl R. Parker

An investigation of ternary compounds of the form M_3Al_2C (M = Mo, Nb, Ta, V, Ti, or Cr), recently found by Jeitschko et al.[1,2] has led to the discovery of a new superconductor, Mo_3Al_2C, which crystallizes in β-Mn (A13) structure.[1]

The samples, with the exception of V_3Al_2C, were prepared by hot-pressing the metal powders in graphite molds; V_3Al_2C was made by arc-melting powder compacts in an argon atmosphere. In addition, sintered samples of Nb_3Al_2C and Ta_3Al_2C were prepared from powder compacts. All samples were annealed at 1000°C in vacuum and furnace cooled.

A superconducting transition was observed at 10.0°K for the compound Mo_3Al_2C. The lattice parameter for the β-Mn cubic cell was a = 6.867Å, which is in good agreement with the value reported by Jeitschko et al.[2] These investigators also found that β-Mn structure at the compositions Nb_3Al_2C and Ta_3Al_2C, but reported that the phase crystallized with a second phase, the "H phase," which has a hexagonal subcell. In the present investigation, the "H phase" could be identified in both hot-pressed and sintered samples; lattice parameters for the hexagonal subcell of the H phase are shown in Table IIB.1-1. The β-Mn structure could not be detected in any of the samples of Nb_3Al_2C or Ta_3Al_2C and none were superconducting above 4.2°K. Only the H phases were observed for the compounds V_3Al_2C, Ti_3Al_2C, and Cr_3Al_2C, and no transitions were found above 4.2°K. The lattice parameters for the hexagonal subcells of these compounds are also given in Table IIB.1-1.

To our knowledge, this is the second compound of the β-Mn type found to show a superconducting transition, the first being $Al_{0.5}Ge_{0.5}Nb_3$,[3] which has transition temperature of 12.6°K. The occurrence of superconductivity in both compounds at 10°K or higher indicates that the β-Mn structure is favorable for the occurrence of superconductivity at relatively high temperature.

We are grateful to Dr. Erwin Rudy of Aerojet-General Corporation, Sacramento, California for his assistance in making the hot-pressed samples.

1. W. Jeitschko, H. Nowotny, and F. Benesovsky, Monatshefte für Chemie 94, 247 (1963).
2. W. Jeitschko, H. Nowotny, and F. Benesovsky, Monatshefte für Chemie 94, 332 (1963).
3. T. B. Reed, H. C. Gatos, W. J. La Fleur, and J. T. Roddy, Superconductors (Interscience Publishers, Inc., New York, 1962), p. 143.

Table IIB.1-1 H phase lattice parameters for hexagonal subcell

Compound	Parameters
Nb_3Al_2C	a = 2.67 c = 8.02
Ta_3Al_2C	a = 2.68 c = 7.97
V_3Al_2C	a = 2.52 c = 7.52
Ti_3Al_2C	a = 2.63 c = 7.87
Cr_3Al_2C	a = 2.47 c = 7.39

2. THE NIOBIUM-RICH CORNER OF THE Nb-Al-C SYSTEM

Jean Johnston, Louis Toth, and Victor F. Zackay

Recently found ternary compounds of the form Me_3Al_2C (where Me is Mo, Nb, or Ta), which crystallize in the β-Mn structure,[1,2] have led to the study of the Nb-rich corner of the Nb-Al-C ternary system in an attempt to combine the superconducting carbides with the superconducting intermetallics.

The samples were prepared by hot-pressing metal powders in graphite crucibles or arc-melting cold pressed compacts. All samples were annealed at 1000°C and furnace cooled.

The work completed to date indicates a partial ternary phase diagram as shown in Fig. IIB.2-1. The compound Nb_3Al_2C showed a hexagonal structure (a = 2.674 Å, c = 8.020 Å) and, although several heat treatments were tried, the reported β-Mn structure could not be identified. The superconducting transition temperatures in the binary system and for the compound Nb_3Al_2C are noted in Fig. IIB.2-1.

Further work on solubility extents and transition temperatures within the ternary system are in progress.

We are grateful to Dr. Erwin Rudy of Aerojet General Corporation for his assistance in making the hot-pressed samples.

1. W. Jeitschko, H. Nowotny, and F. Benesovsky, Monatshefte für Chemie 94, 247 (1963).
2. W. Jeitschko, H. Nowotny, and F. Benesovsky, Monatshefte für Chemie 94, 332 (1963).

3. PHASE RELATIONSHIPS AND SUPERCONDUCTIVITY IN THE TERNARY SYSTEM Nb-V-Al

Jean Johnston, Louis Toth, and Earl R. Parker

Compounds with the A15 (or β-tungsten) crystal structure have the highest critical temperatures of any known superconductors. The critical temperature is being determined for the (as yet unevaluated) metastable A15 compounds V_3Al, Ta_3Au, $(Nb,V)_3Si$, and Nb_3Pb. In addition, the sigma phase, also a favorable structure for superconductivity, is being investigated in the unexplored Nb-V-Al ternary system.

Recently, Holleck et al.[1] have reported the existence of the compound V_3Al with an A15 structure. This compound was not found in earlier investigations of the V-Al binary system.[2-4] Since most compounds of this structure are

1. H. Holleck, F. Benesovsky, and H. Nowotny, Monatshefte für Chemie 94, 477 (1963).
2. C. B. Jordan and P. Duwez, Trans. Am. Soc. Metals 48, 789 (1956).
3. W. Rostoker and A. Yamamoto, Trans. Am. Soc. Metals 46, 1136 (1954).
4. O. N. Carlson, D. J. Kenney, and H. A. Wilhelm, Trans. Am. Soc. Metals 47, 520 (1955).

Superconducting Phases

Compound	Structure		T_c (°K)
Nb(S.S.)	BCC	Nb-rich Al-rich	9 6
NbC	B1	Nb-rich C-rich	6 11
Nb_3Al	A15	Nb-rich Al-rich	12.5 17.5
Nb_2Al	σ	Nb-rich Al-rich	13.5 <4.2

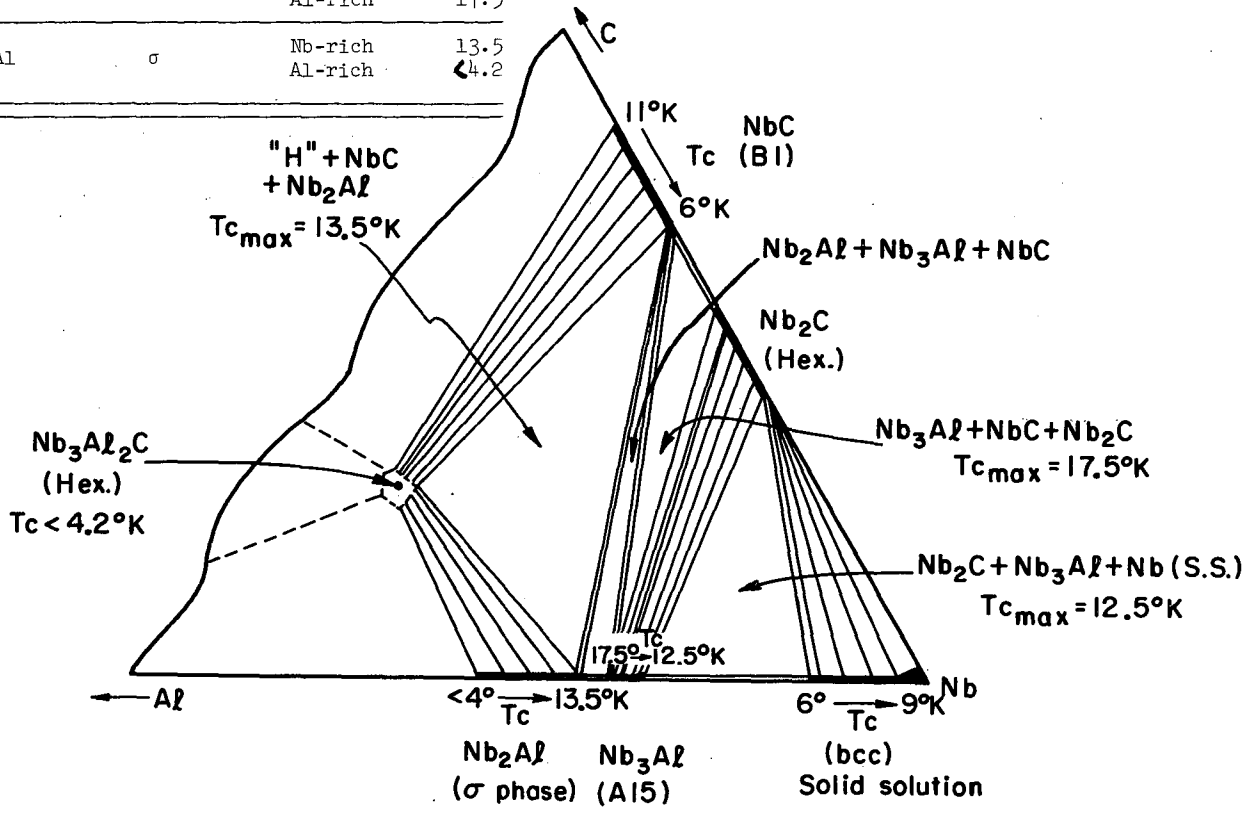

MUB-2839

Fig. IIB. 2-1 Nb-rich corner of the Nb-Al-C ternary system.

superconductive and a substantial fraction of these have critical temperatures above 10°K, it would be of considerable interest to obtain V_3Al with an A15 structure.

In the present investigation we studied the pseudo-binary $Nb_{0.73}Al_{0.27}$ - $V_{0.73}Al_{0.27}$ in an effort to stabilize the A15 structure on the vanadium-rich side. The samples were made in a helium arc furnace to remove most of the danger of impurity contamination. Each sample was melted four times and homogenized for 80 hours at 1250°C in vacuum.

X-ray analysis of the samples thus obtained show a bcc solid solution (a = 3.055 Å) at the composition $V_{0.73}Al_{0.27}$, which is in good agreement with results of earlier investigators.[2,4] Further heat treatment at 800°C produced no observable change in structure. The bcc structure was found to exist as far as the composition $(Nb_{0.5}V_{0.5})_3Al$. The variation of the lattice parameter for this solid solution is shown in Fig. IIB.3-1. These samples showed no superconducting transition above 4.2°K.

On the Nb-rich side we obtained the A15 structure, which showed a transition temperature of 17.5°K at the composition $Nb_{0.73}Al_{0.27}$ (a = 5.185 Å), in good agreement with results as shown in the literature.[5-7] In the binary system Nb-Al the critical temperature was observed to decrease to 12°K with addition of Nb, while the lattice parameter increased to a = 5.196 Å. The transition temperature of the A15 structure at the composition $Nb_{0.73}Al_{0.27}$ remains essentially constant with addition of up to 10% vanadium, and then begins to decrease rapidly as shown in Fig. IIB.3-2.

The sigma phase in the binary Nb-Al system showed a lattice parameter change from a = 9.318 Å, c = 4.813 Å to a = 9.295 Å, c = 4.819 Å, while the transition temperature decreased from 13.5°K to less than 4.2°K with the addition of aluminum. The maximum critical temperature obtained is higher than the 12°K reported by Corenzwit,[5] but is considerably lower than that reported by Raetz and Saur.[6] Addition of vanadium to these compounds decreased the transition temperature to less than 4.2°K.

An investigation shows that the A15 structure V_3Al cannot be formed by arc melting with the limited heat treatments tried. Similar results were obtained by Geballe.[8] According to Nowotny,[9] the phase V_3Al is probably stabilized by small amounts of impurities (C, N, O). We are undertaking an investigation of the ternary system V-Al-C to determine if the A15 phase can be stabilized with carbon.

---

5. E. Corenzwit, J. Phys. Chem. Solids 9, 93 (1959).
6. K. Raetz and E. Saur, Z. Physik 169, 315 (1962).
7. P. S. Swartz, Phys. Rev. Letters 9, 448 (1962).
8. T. H. Geballe (Bell Telephone Laboratories, Murray Hill, N.J.), private communication.
9. H. Nowotny, University of Vienna, Vienna, Austria, (private communication).

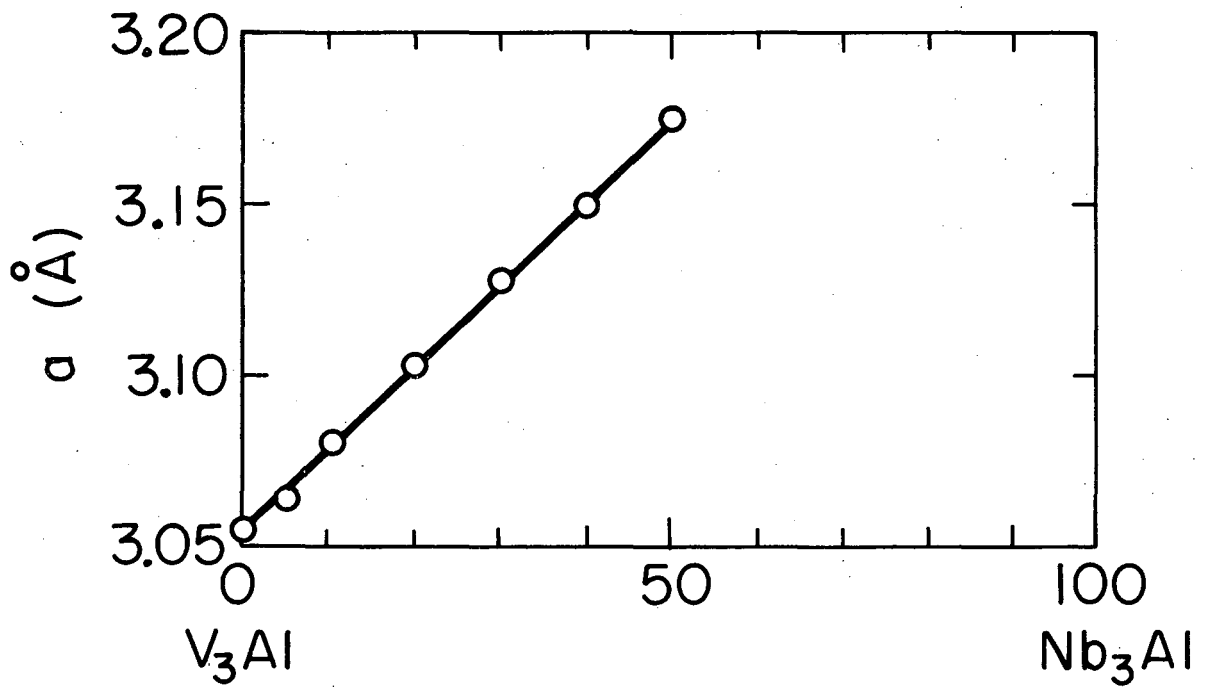

Fig. IIB. 3-1 Variation of lattice parameter with composition.

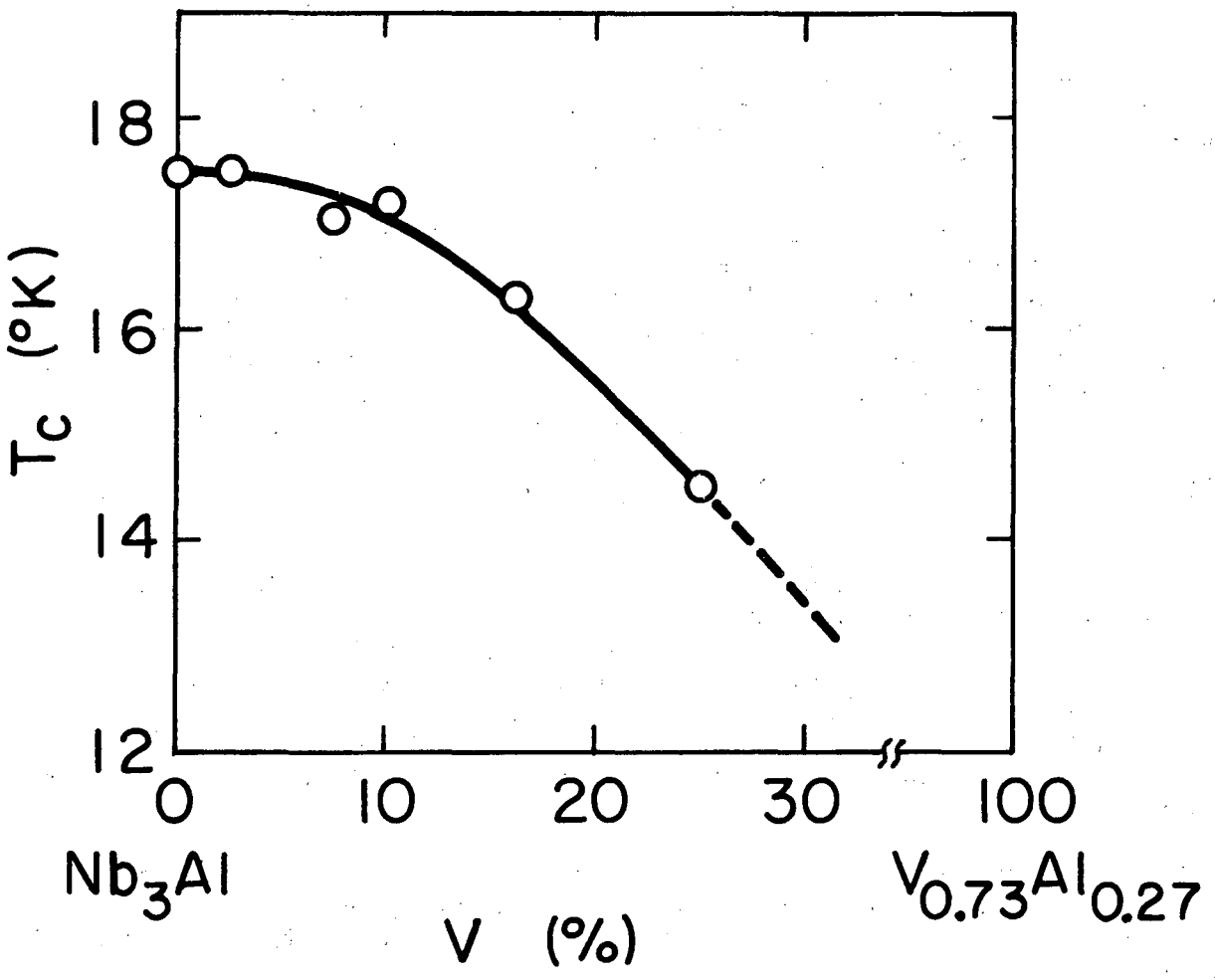

Fig. IIB. 3-2 Variation of T_c with composition.

THE SUPERCONDUCTIVITY OF SOLID SOLUTIONS OF TaC AND NbC

Molly Wells, Milt Pickus, Victor F. Zackay

The critical temperatures of ternary systems consisting of two metals and one nonmetal are being studied as a function of composition. Examples of unevaluated pseudo-binary systems of this type under investigation are: NbC-TaC, NbC-WC, NbC-VC, and NbC-MoC.

Work is in progress on a study of critical temperature of solid solutions of niobium carbide and tantalum carbide. Previous work has been done by Mathias et al.[1] who studied solutions of MoC in various other transition metal carbides. All these solutions were of the NaCl structure. Although MoC is normally hexagonal, it forms a cubic solid solution with the cubic carbides up to 80% MoC when quenched. When Tc was plotted as a function of per cent MoC, the only curve showing a maximum was that for MoC in NbC, where NbC was the only solute studied which was known to be superconductor. All other curves extrapolated up to hypothetical critical temperature for cubic MoC.

From these results it was assumed that solid solutions of NbC and TaC would have an optimum composition for maximum Tc. NbC and TaC are both known superconductors whose critical temperatures are highly dependent on stoichiometry. The stoichiometry of the carbides used was determined by lattice parameter measurements,[2,3] and the expected Tc obtained from a graph of Tc versus per cent carbon.[4] Results confirmed those of Giorgi et al., who had studied critical temperature as a function of stoichiometry in the pure carbides.

Solutions of NbC and TaC did have a maximum Tc, as expected. Although the pure carbides began the superconducting transition at 11.5°K for TaC and 10.7°K for NbC, the best solid solution began the transition at 14°K.

Work has been initiated on solutions of vanadium carbide in tantalum carbide and niobium carbide in order to complete a pseudo-ternary system.

---

1. B. T. Matthias, J. Phys. Chem. Solids 1, 188-190 (1956).
2. A. L. Bowman, J. Phys. Chem. 65, 1596-1598 (1961).
3. E. K. Storms and N. H. Krikorian, "The Niobium-Niobium Carbide System", to be published in Phys. Rev. Letters.

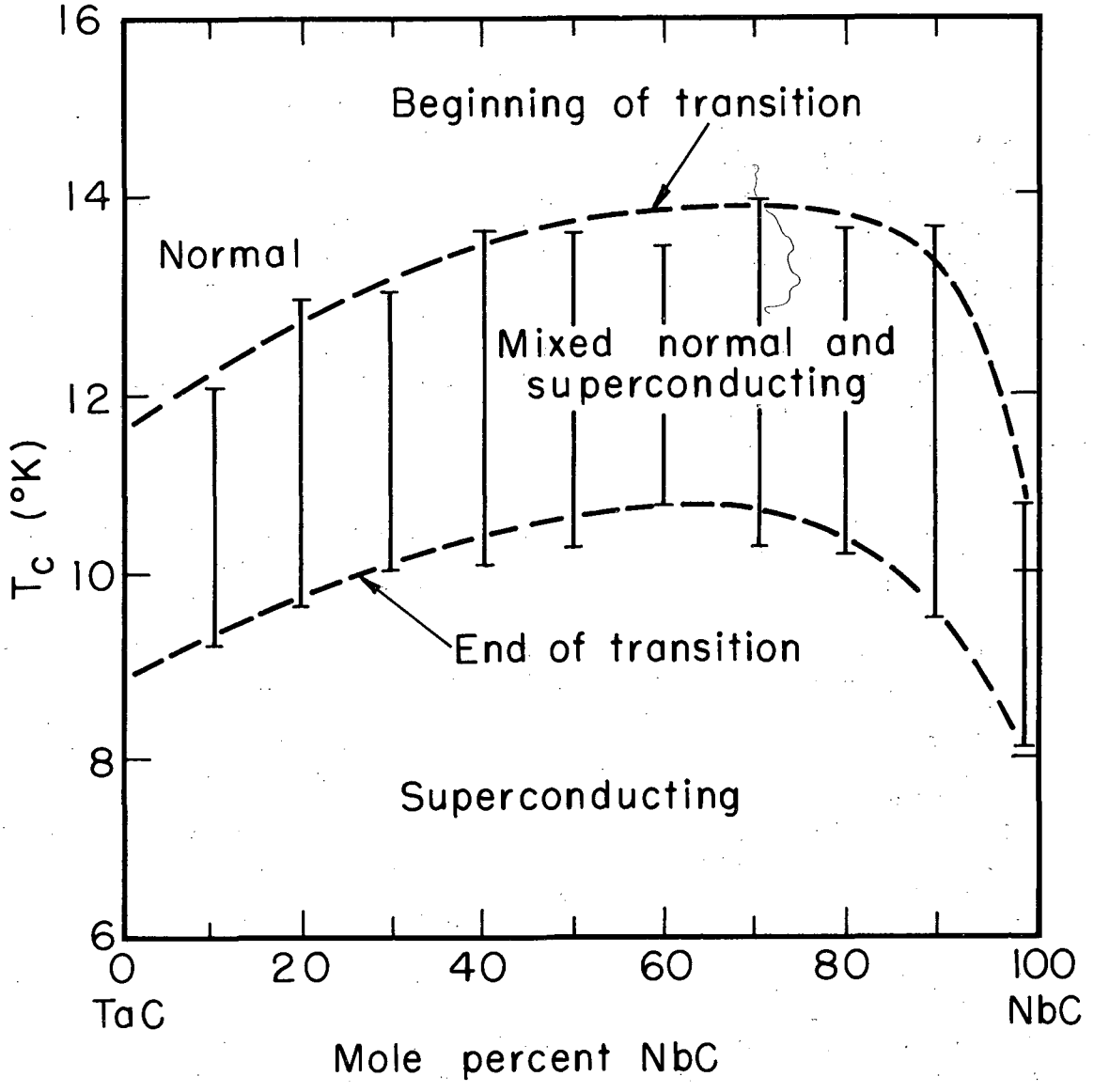

MUB-2840

Fig. IIB. 4-1 Variation of the superconducting critical temperature, T_c, with composition in solid solutions of NbC in TaC.

5. ELECTROMAGNETIC PROPERTY MEASUREMENTS

Ira Pratt

Electromagnetic induction techniques for the measurement of the electrical and magnetic properties of materials have long been useful. There has been some question,[1] however, of the interpretation of the results in terms of the basic properties of the material being examined. The classical concepts of resistivity (attributed to conduction electron density and scattering) and permeability still represent a most convenient means for designating electrical properties. The concept of permeability is a little more evasive than is resistivity, since it involves the conduction electrons with associated scattering terms, the bound electrons of the atom core, and--on a fine scale-- the nucleus itself. It is clear that resistivity and permeability as used in electrical calculations are not independent variables, although they are usually treated as such for convenience.

Of interest here are the susceptance (or permeability) and the resistivity of a metallic specimen as deduced from alternating-current induction measurements; and the effect on these measurements of a change in the specimen, or a change in the frequency of the applied magnetic induction field, or both.

A metallic material, sitting in an alternating magnetic field, is represented as a single-turn current loop with three characteristics: (a) physical size with and effect cross-section area A_2 normal to the exciting field; (b) resistivity ρ, based upon free electron density, mean free path ℓ, and the thermal (Boltzmann) electron velocity v; and (c) permeability μ_o, where the subscript of the μ_o indicates the component of the complex permeability in phase with the induced current in the specimen. Also the term μ_H is used to represent the complex component in phase with the exciting field H. The effective cross section of the specimen A_2 is equal to the actual cross section area multiplied by a constant g, for a particular frequency.

For a cylindrical specimen, the inductive reactance may be written as $X = 4\pi\mu_o \omega A_2/\ell_2$, where ω is the radial frequency of the applied magnetic field. The resistance may be written as $R = 2\pi\rho/\ell_2$. With an induced voltage in the specimen e_2, current in the specimen may be calculated:

$$i_2 = \frac{e_2}{R+jX} = \frac{j\omega\mu_H A_2 H}{\frac{2\pi\rho}{\ell_2} + j\frac{4\pi\omega\mu_o A_2}{\ell_2}}. \qquad (1)$$

This specimen current will develop a magnetic field which will, in turn, generate a voltage in the sense coil $\dot{e}_3$. Upon making the substitution[2] $\alpha = \rho/2\mu_o A_2$, the ratio of the difference voltage $\dot{e}$ to the reference voltage $\dot{e}_o$ becomes

$$\frac{\dot{e}}{\dot{e}_o} = \frac{\omega\mu_H A_2/A_3}{\omega - j\alpha}, \qquad (2)$$

where A_2/A_3 is the ratio of specimen effective cross section to actual

1. E. Maxwell and M. Strongin, Phys. Rev. Letters 10, 212 (1963).
2. This is similar to the usual penetration depth δ equation with frequency α, and $\delta^2 = \sqrt{A/\pi}$.

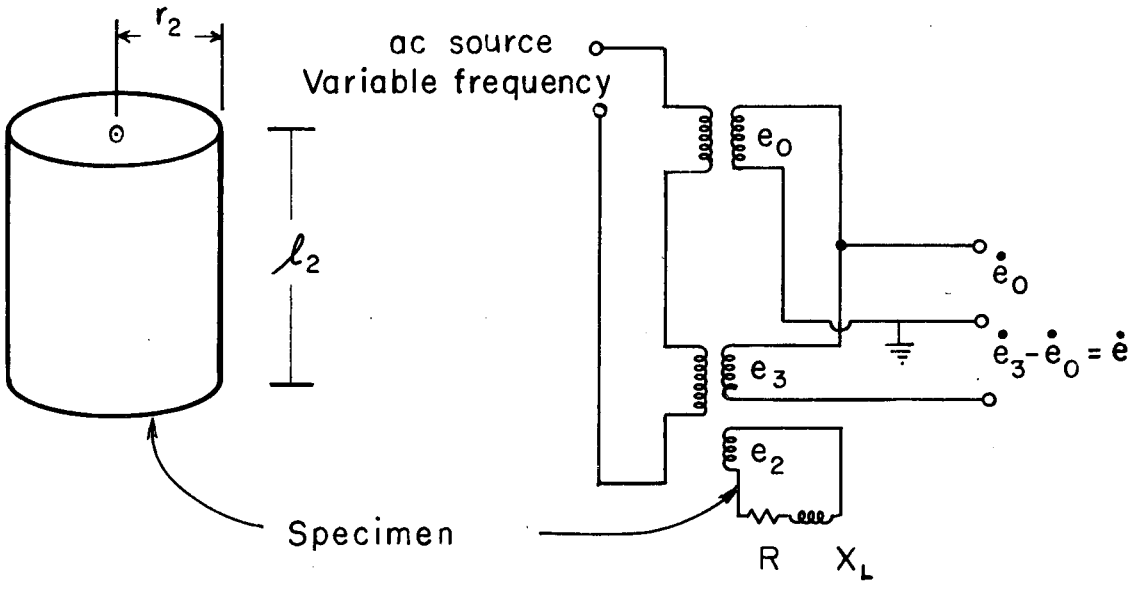

Fig. IIB. 5-1 Specimen geometry and measuring circuit.

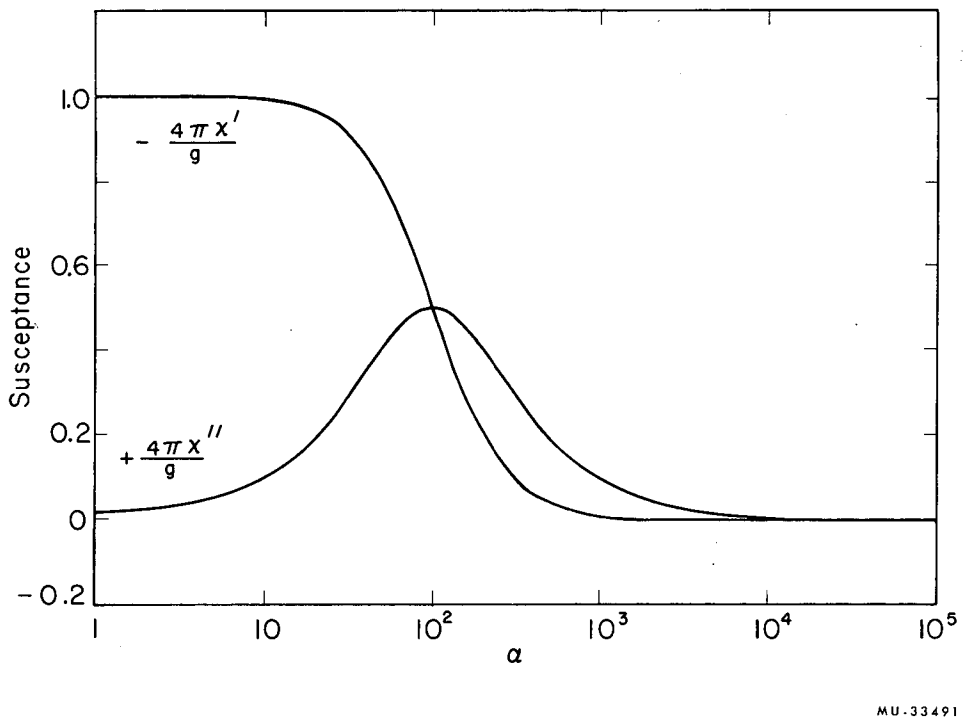

Fig. IIB. 5-2 A.C. Susceptance. Plot of Eq. (5) for g = 2, at a measuring frequency of 100 cps.

$$\alpha = \frac{\rho}{2\mu_o A_2}, \text{ and } \frac{4\pi\chi_H}{g} = \frac{4\pi\chi'}{g} + j\frac{4\pi\chi''}{g}.$$

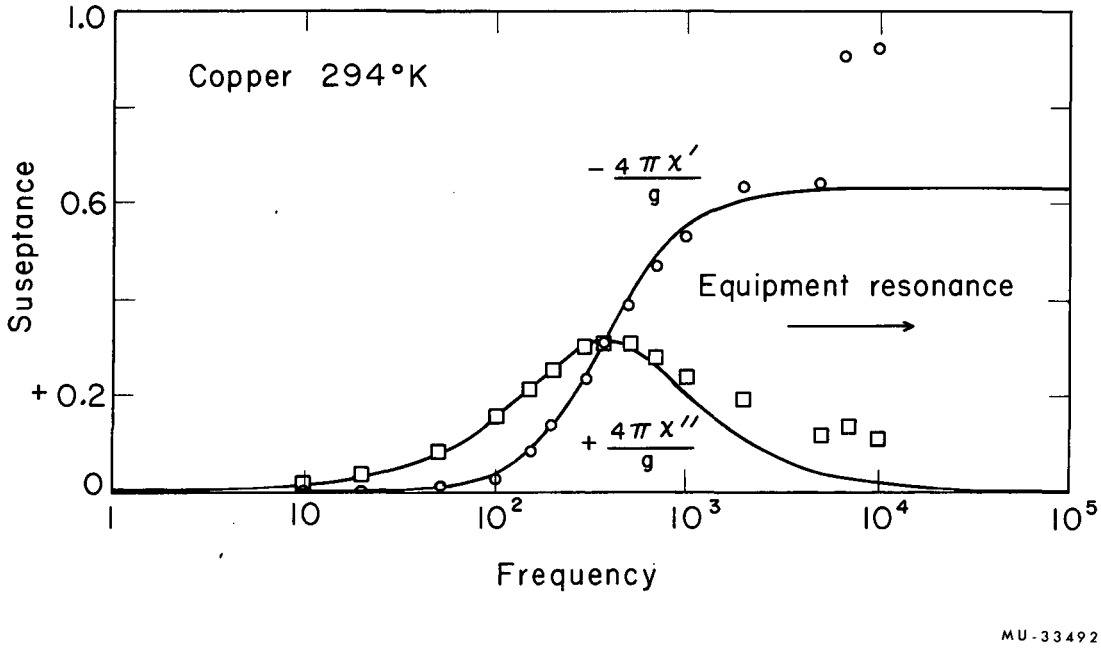

Fig. IIB. 5-3 Calculated susceptance curve for copper. The superimposed points are experimental values. $A_2 = g_o A = 3.25\ cm^2$, where $g_o = 2.58$.

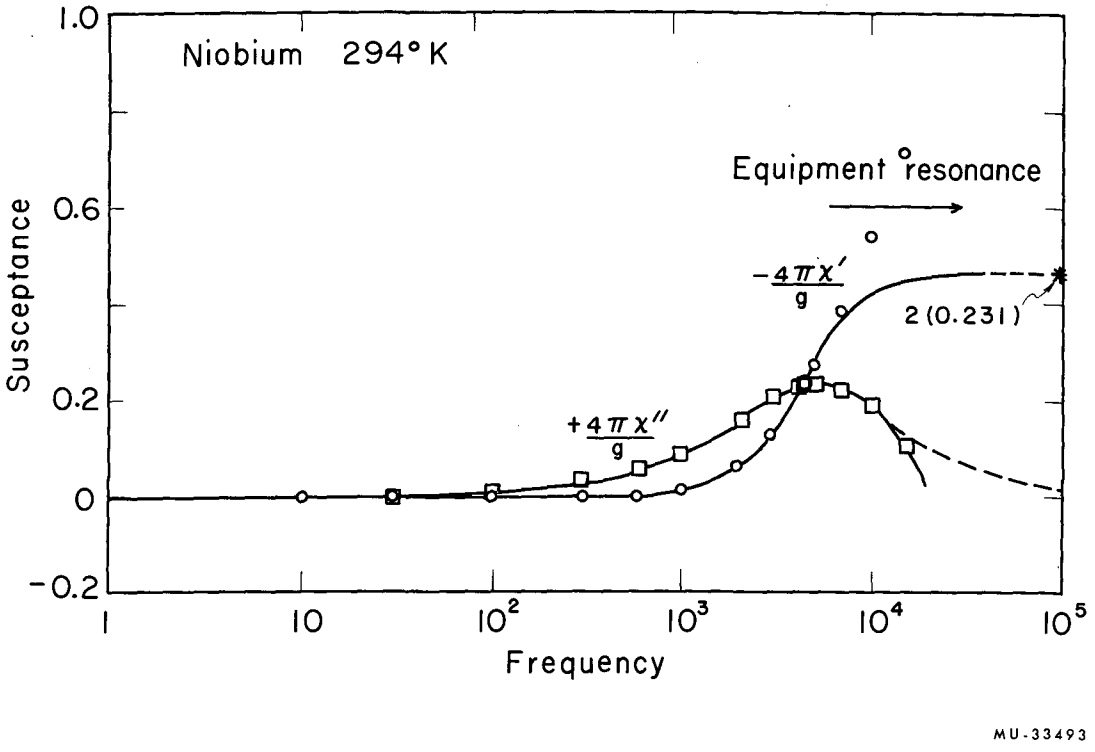

Fig. IIB. 5-4 Niobium susceptance. The transition giving "flux exclusion" occurs at a field frequency of 4,400 cps. $A_2 = g_o A = 2.37$ cm^2, where $g_o = 3.16$.

6. COMPOSITION FLUCTUATIONS IN HARD SUPERCONDUCTORS

Louis E. Toth and Ira P. Pratt

It is well knwon that the critical magnetic field and critical current density are structure-sensitive properties. The interaction of imperfections with the magnetic field, however, is now well understood. According to Anderson flux penetration in the mixed state is a thermally activated process with an activation energy resulting from inhomogeneities, strains, dislocations, and other physical defects.[1] An external field in effect, aids the motion of "bundles" of flux over these energy barriers and plays a crucial role in determining the critical current density. Recently Webb has analyzed the pinning forces due to forests of screw dislocations on fluxoids and single screw dislocations on coaxial and parallel superconducting filaments.[2] Webb's model is based on the small differences in elastic compliances and moduli between the normal and superconducting phases; these differences result in a small free-energy density difference and a pinning force. Evidence for a dislocation-stabilized filamentary network has been found.[3]

It has been suggested on the basis of experiments with heat-treated niobium-zirconium alloys[4] and age-hardened alloys[5] that the stress field around precipitation zones is important in determining critical current densities and hysteresis effects. Because of the importance of Nb-Zr as a high-field superconductor, we determined the general equations for the pinning forces due to any array of isolated composition fluctuations.[6] We show here that an array of isolated composition fluctuations can result in localized stress fields capable of pinning a continuous filamentary phase.

Our model material contains "regions of composition fluctuations" which are represented as spheres of radius a separated from the other similar spheres by an average distance of 40 a. The superconducting filaments (or the fluxoids) are present in the form of cylinders with an effective radius c, and the cylinders extend from the region of one sphere to the next. A stress field will necessarily surround regions of composition fluctuation when the types of atoms composing the alloy are of different sizes. Precipitation of a second phase would tend to relieve this stress. Although we are primarily interested in the effects of the stress field, it is also necessary to distinguish between three types of composition fluctuations: those with a localized critical temperature equal to, greater than, or less than that of the material in the matrix. For the first two types, the superconducting filaments are most stable when the center of the sphere coincides with the

1. P. W. Anderson, Phys. Rev. Letters 9, 309 (1962).
2. W. W. Webb, Phys. Rev. Letters 11, 191 (1963).
3. E. Maxwell and M. Strongin, Phys. Rev. Letters 10, 212 (1963).
4. M. S. Walker, R. Stickler, and F. E. Werner, Metallurgy of Advanced Electronic Materials, G. Brock, editor (Interscience Publishers, New York, 1963), p. 49.
5. R. E. Mould and D. E. Mapother, Phys. Rev. 125, 33 (1962).
6. In a single-phase inhomogeneous alloy certain microscopic regions contain more of one kind of atom than the other. We shall call these "regions of composition fluctuation" and the surrounding material the matrix.

axis of the superconducting filament. In the last type the region of composition fluctuation tends to trap flux, while the strain field tends to trap superconducting filaments in the same region. To approximate the last type we shall determine the pinning force on a superconducting filament when its axis is separated from the center of the sphere by a distance b = a + c.

The elastic energy density in the matrix surrounding a spherical inclusion is given by Eshelby[7] as

$$6\mu a^4(a-r_s)^2/r^6. \tag{1}$$

Here μ is the shear modulus and r_s is defined as the radius the sphere would assume if it contained an equal number of stress-free atoms of the same composition as the matrix. For the case $b \geqslant a + c$ the interaction energy U between a superconducting filament and a stress field surrounding a spherical imperfection is

$$U = 24\,\Delta S_{44}\,\mu^2 a^4 (a-r_s)^2 \int_0^{\infty} \frac{dZ}{(r^2+z^2)^3} \int r\,dr \int_0^{\theta_{max}} d\theta, \tag{2}$$

where the limits on r are given by $b\cos\theta \pm (c^2 - b^2\sin^2\theta)^{1/2}$ and θ_{max} is given by $\sin\theta_{max} = c/b$. The integration is over the superconducting volume. Here ΔS_{44} is the change in elastic compliance between the normal and superconducting state. Integrating with respect to z and r gives

$$U = 3\pi\,\Delta S_{44}\,\mu^2 a^4 (a-r_s)^2 \int_0^{\theta_{max}} \frac{(c^2-b^2\sin^2\theta)^{1/2}(3b^2+c^2-4b^2\sin^2\theta)}{(b^2-c^2)^3}\,d\theta. \tag{3}$$

Substituting $k = c/b$ and $\sin\theta = k\sin\phi$ yields

$$U = 3\pi\,\Delta S_{44}\,\mu^2 a^4 (a-r_s)^2 \int_0^{\pi/2} \frac{[(k^2-1) + 4(1-k^2\sin^2\phi)]\cos^2\phi\,d\phi}{(1-k^2\sin^2\phi)^{1/2}}, \tag{4}$$

or

$$U = \frac{\pi\,\Delta S_{44}\,\mu^2 a^4 (a-r_s)^2 b^3}{(b^2-c^2)^3} \left\{(3k^4-2k^2-1)\,F(\pi/2,k) + (7k^2+1)\,E(\pi/2,k)\right\} \tag{5}$$

Here F and E are Legendre normal forms of the complete elliptic integral. The pinning force $F_c = \partial U/\partial b$ is

$$F_c = 3\pi\,\Delta S_{44}\,\mu^2 a^4 (a-r_s)^2 \left\{\frac{b^2+7c^2}{(b^2-c^2)^3}\,F\left(\frac{\pi}{2},\frac{c}{b}\right) - \frac{b^4+14b^2c^2+c^4}{(b^2-c^2)^4}\,E\left(\frac{\pi}{2},\frac{c}{b}\right)\right\}. \tag{6}$$

---

7. J. D. Eshelby, Solid State Physics, edited by F. Seitz and D. Turnbull (Academic Press, New Yor, 1956) p. 115.

For the region $b \geq a + c$, F_c has its maximum value at $b = a + c$. The magnitude of F_c can be estimated by using typical values of $a = 10^{-5}$ cm, $c = 10^{-5}$ cm, $|(a-r_s)/a| = 0.02$, $\mu = 3 \times 10^{11}$ dyne cm^{-2}, and $\Delta S_{44} = 4 \times 10^{-16}$ dyne^{-1} cm^2. The values of μ and ΔS_{44} are the values of Nb at 4.2°K reported by Alers and Waldorf.[8] Substitution of these values into Eq. (6) yields $F_c = 2.2 \times 10^{-2}$ dyne cm^{-1} when the spacing of these spheres is 40 a. The larger the sphere and the greater the difference in atomic size, the larger F_c becomes.

For the case in which a = c and b = 0, we find

$$U = 3.3\pi \Delta S_{44} \mu^2 a(a-r_s)^2 + \frac{6\pi a(a-r_s')^2}{\chi'} \frac{\Delta\chi'}{\chi'} . \qquad (7)$$

Here χ' is the compressibility within the sphere, $\Delta\chi' = \chi_n' - \chi_s'$ and r_s' is the is the radius the sphere would assume in its stress-free state. The first term on the right is the difference in strain energy contained in the matrix and the last term is the difference in the sphere.[9] To avoid geometric complications, we underestimate the pinning force and define

$$\bar{F}_c = \frac{U(b=2a)-U(b=0)}{2a} .$$

Setting $\chi' = 2 \times 10^{-12}$ cm^2 dyne^{-1} $\Delta\chi'/\chi' = -1 \times 10^{-6}$ (Alers and Waldorf's values for Nb at 4.2°K), and $|(a - r_s')/a| = 1/2|(a - r_s/a|$ yields $F_c = 1.6 \times 10^{-2}$ dyne/cm.

These values for F_c are of the same order of magnitude as those found for dislocations.[2] Here the regions of composition fluctuations are separated from one another by 4 microns, while in the dislocation model the dislocations and filaments are coaxial.

Pinning of fluxoids in the critical state results from their repulsion from the stress barriers of the imperfections. Webb estimates that the value of the pinning force on fluxoids by a "forest" of dislocations is of the same order of magnitude as that due filament pinning by a single screw dislocation. Although we expect the pinning by the stress field due to groupings of these regions of composition fluctuations to be of comparable value, there is, however, a significant difference. The fluxoid may become trapped on the region of composition fluctuation when the T_c of the material in this region is less than that of the matrix. Livingston[10] has explained his magnetization results on the Pb-Sn system in this manner.

8. G. A. Alers and D. L. Waldorf, Phys. Rev. Letters 6, 677 (1961).
9. J. Friedel, Advan. Phys. 3, 446 (1954).
10. J. D. Livingston, Phys. Rev. 129, 1943 (1963).

C. HIGH-STRENGTH MATERIALS

1. A STUDY OF STRENGTHENING MECHANISMS IN NITROGEN MARTENSITE

Ray Busch and Earl R. Parker

Carbon and nitrogen-free austenite single crystals are being used in the study of strength in martensite. Martensite can be formed in the austenite single crystals by cooling them to liquid nitrogen temperature. The resulting change in hardness and yield strength can then be measured and compared. This has been done; the increase was relatively small, being less than a factor of two.

The martensite structure is stable upon reheating to several hundred degrees above room temperature (because of the large hysteresis in transforming back to austenite). It is possible, therefore, to diffuse nitrogen--an effective martensite strengthener--into the martensite. The nitrogen cannot form a supersaturated solid solution within the martensite, as it could if it had been dissolved in the austenite prior to quenching, and must therefore be restricted in its actions to dissolving in the lattice defects, or in forming particles of a second phase. In experiments completed to date, second-phase particles have formed and the hardness has increased severalfold. It is hoped that by these experiments it will be possible to identify and to evaluate the various possible hardening mechanisms.

2. THE NATURE OF MARTENSITE

Aziz Ahmadieh and Earl R. Parker

One of the strongest of the useful metallurgical structures is martensite--the supersaturated solid solution of carbon in the low-temperature form of iron. The importance of the martensitic structure has led to numerous and extensive investigations concerned with the mechanism of its formation, the location of the carbon atoms, and the reason for its great strength. There is general agreement that the atomic processes involved when the face-centered cubic phase transforms into a body-centered tetragonal structure during quenching are well understood, and it is genearlly accepted that the carbon atoms are located along the cube edge midway between the iron atoms, but there is no agreement about the nature of the strengthening process. Since the structure of martensite is presumably well understood, and yet the accepted picture of the structure has not led to an understanding of the strengthening mechanism, it seemed appropriate to question the validity of the accepted structural picture. A re-examination of the role of carbon has led to a new insight into the nature of martensite. A picture has evolved which has made it possible to predict, with a high degree of accuracy, the effect of carbon on the lattice parameters of austenite and martensite, and to forecase that the first carbide to form from martensite should have a hexagonal crystal structure with predictable lattice constants.

If the assumption is correct, that carbon atoms in solution in the austenite are randomly distributed it should be a straightforward procedure to calculate the lattice parameter as a function of the carbon content.

This was done as follows: For a steel containing 1 wt % carbon, there are 21.66 iron atoms per atom of carbon, or 5.41 unit cells. If the one carbon resides at the center of one of these unit cells, its lattice parameter will be increased by 0.513 Å, the amount that a crabon atom would expand a unit cell. The average increase in lattice parameter is therefore 0.513/5.41, or 0.0948 Å. This figure is twice the experimentally determined value. The simplest explanation for this discrepancy is that the carbon atoms are paired. This explanation is reasonable, because the lattice around a single carbon atom is so expanded that a second carbon atom can find a lower-energy site in an adjacent expanded position (e.g., if the first atom is at $[\frac{1}{2}, \frac{1}{2}, \frac{1}{2}]$, the second one will fit without effort into the $[\frac{1}{2}, 0, 0]$ position). A calculation based on elastic distortion of the lattice for two atoms separated vs two atoms paired showed clearly that from the strain-energy point of view, pairing was favored. From the kinetic point of view, it is easily possible for carbon atoms to pair. Internal friction measurements have shown that, even at room temperature, carbon atoms jump from one location to an equivalent site about once each second.

Models with paired atoms were constructed, and from these as well as from lattice distortion calculations it was evident that the second carbon could easily fit into an expanded neighboring site without causing any significant additional distortion. It was concluded, therefore, that the theoretical lattice parameter should be $a = 3.548 + 0.047\ C$, where C is the wt % of carbon. This theoretical line is in excellent agreement with experimental data, as Fig. IIC.2-1 shows.

The concept of carbon pairs was extended to studies of the behavior of carbon in ferrite and martensite. The assumption that carbon atoms reside at the midpoint of the long edges of the martensite (or ferrite) unit cell has been accepted as "factual" since the work of Petch two decades ago. The octahedral sites were selected for the location of carbon atoms because the tetragonality of martensite could apparently be explained only if carbon atoms were located therein. It was thought that if the carbon atoms resided in the larger tetrahedral sites, (e.g., $[\frac{1}{2}, \frac{1}{4}, 0]$ only uniform expansion of the bcc lattice should result. However, the validity of this assumption is highly questionable. The tetrahedral site is 1.9 times as large as the adjacent octahedral site. The $[\frac{1}{2}, 0, 0]$ location is, therefore, highly unfavorable from the viewpoint of elastic strain energy.

The only objection of "allowing" the carbon to reside in the energetically favorable site was that it did not seem possible to explain the tetragonality of martensite if carbon atoms were located in the tetrahedral sites. When the problem was re-examined on the basis that pairs of carbon atoms should reside in adjacent tetrahedral sites (e.g., $[\frac{1}{2}, \frac{1}{4}, 0]$ and $[\frac{1}{2}, \frac{1}{4}, 0]$), then the objection disappeared, because carbon pairs so located produce a tetragonal distortion of the structure in much the same way as a single carbon atom would if it were located midway along the cube edge (i.e., at $[\frac{1}{2}, 0, 0]$). Furthermore, from the elastic strain-energy point of view, the pairing of carbon atoms in adjacent tetrahedral sites is strongly favored over the single-atom state. Thus, the objection to carbon atoms' occupying tetrahedral sites is invalid, and the role of carbon in martensite can be re-appraised.

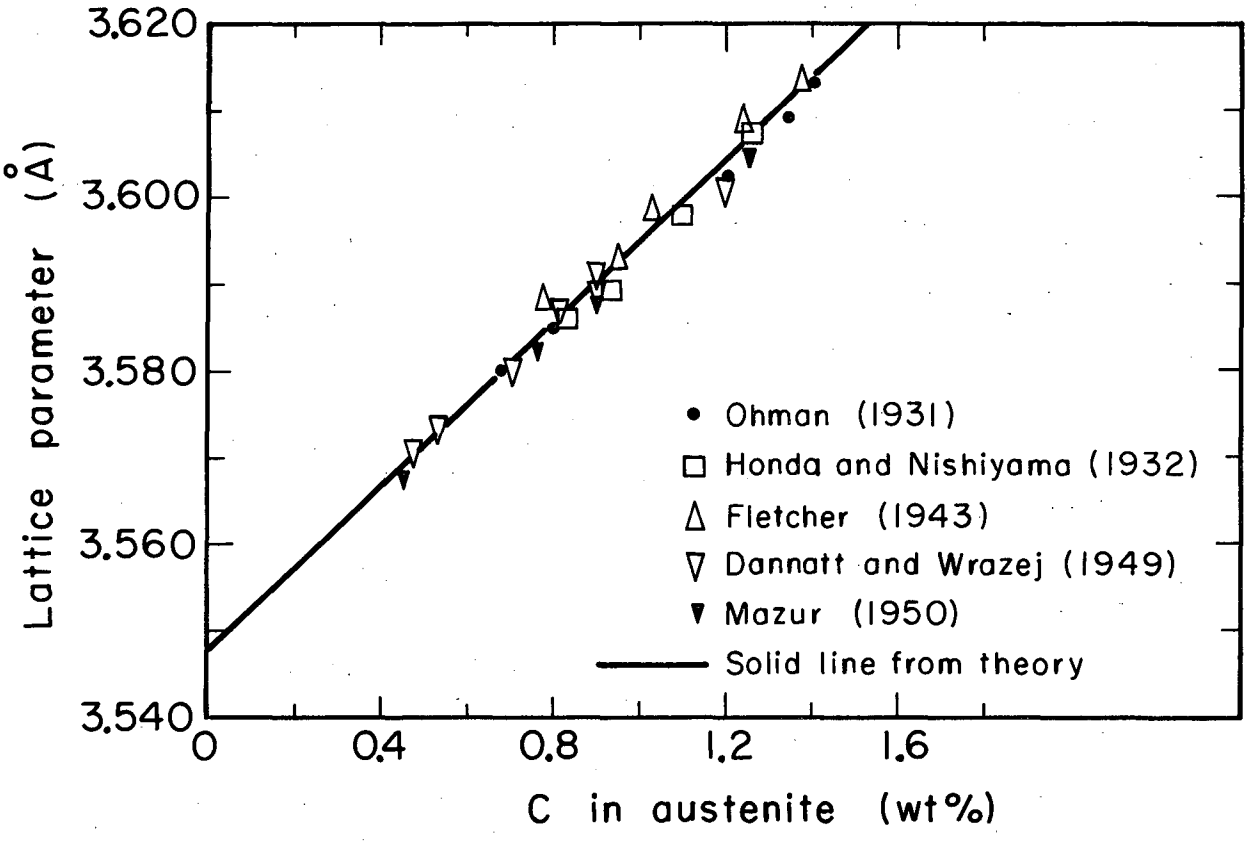

MUB-2790

Fig. IIC. 2-1 Comparison of experimentally determined room-temperature lattice parameters of austenite containing various amounts of carbon with values calculated from carbon-pair theory.

From geometric considerations and a study of scale models of tetragonal martensite with carbon pairs in tetrahedral sites, it became evident that a single carbon pair would cause about 17 pairs of the iron atoms located along the crystal axes to move farther apart. Calculations showed that the lattice constant of the unit cell containing the carbon pair was increased from 2.8605 to 3.7180. For 1 wt % of carbon alloy, there are 21.66 iron atoms per carbon atom, or 43.32 iron atoms per carbon pair. Each iron atom forms three Fe-Fe pairs--one along each crystallographic axis. The average increase in lattice constant in the c-axis direction of the tetragonal structure is given by

$$\Delta a = \frac{17}{(3)(43.32)} \quad (3.7180 - 2.8605),$$

where $\Delta a = 0.1126$ for 1 wt % of carbon.

The c-axis lattice constant for a 1% carbon martensite should thus be

$$2.8605 + 0.1126 = 2.9731 \text{ Å},$$

which is exactly what many past measurements have shown it to be. The almost perfect agreement between the predicted values and those obtained by measurements for various carbon contents is shown in Fig.IIC.2-2.

Calculations were also made for the a-axis lattice constants, and the results are also shown in Fig.IIC.2-2. In the tetragonal structures, as the atoms along the c axis are moved apart by the carbon pairs, the pairs of iron atoms located along the two a axis move closer together. The number of Fe-Fe pairs involved is 34, which is twice as many as for the c-axis iron atom pairs, because of the two a axis that are mutually perpendicular to the c axis. The Poisson's-ratio type of contraction is to be expected in the a axis directions, but because of the large c axis strains (i.e., 0.8575 / 2.8605, or 30%) it is unreasonable to expect the normal value of 0.3 for Poisson's ratio to apply for such large strains. The repulsive forces between atoms increases inversely at a high power of the distance that separates them. Poission's ratio would therefore vary as the atomic distance decreased, and would approach zero as the outer electron shells of the atoms began to overlap. Ther is no exact way of determining a precise value of Poisson's ratio for strains as large as those involved in this case. From the measured values of a axis lattice constants, a figure of 0.05 for Poisson's ratio seems appropriate. The value of Δa for a 1% carbon martensite would thus become

$$\Delta a = \frac{(2)(17)}{(3)(43.32} \quad (3.7180 - 2.8605)\ (0.05),$$

$$\Delta a = 0.0113 \text{ Å}.$$

The agreement between experimentally determined values of a axis lattice constants for various carbon contents and those calculated are shown in Fig.IIC.2-2.

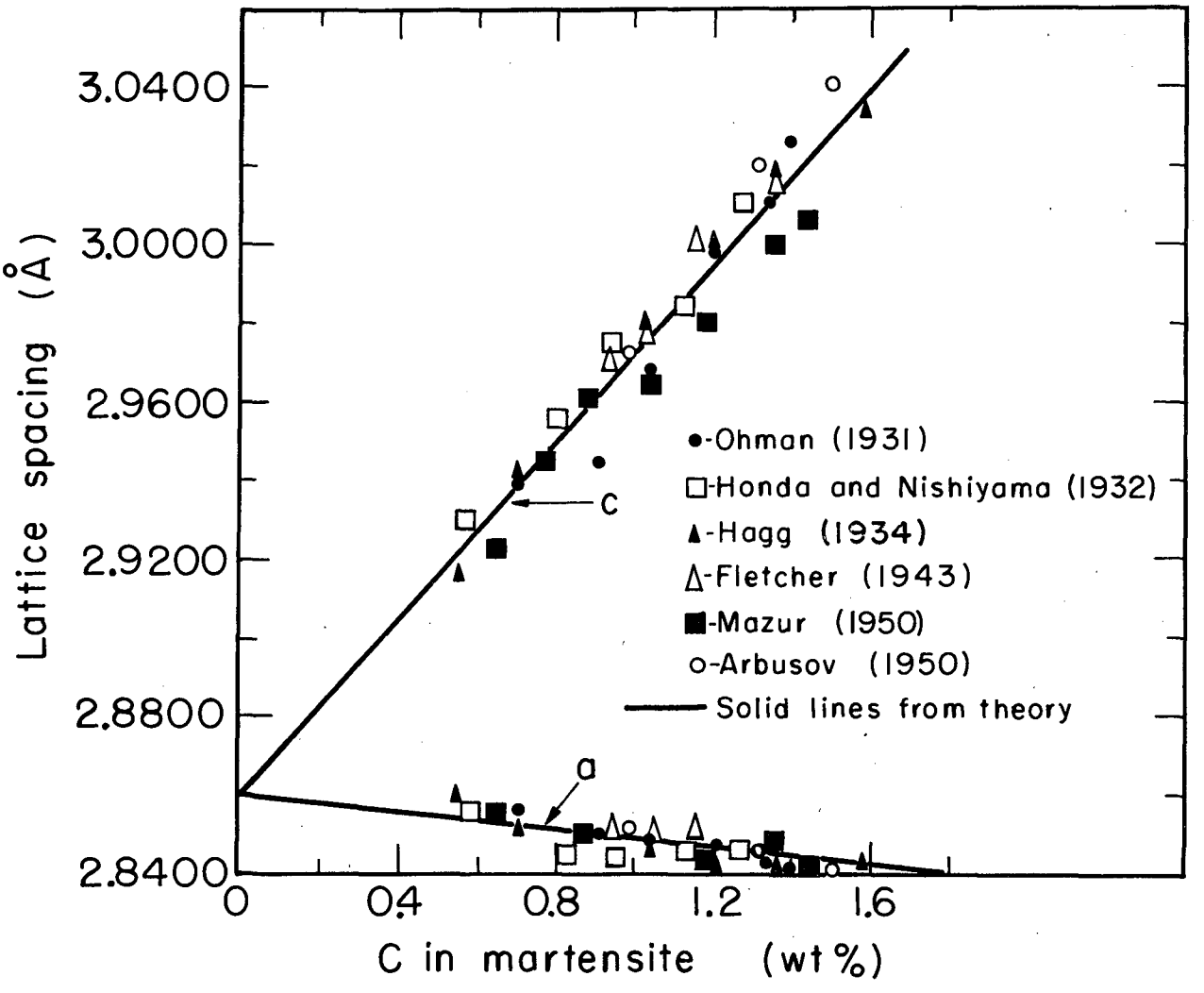

MUB-2793

Fig. IIC. 2-2 Comparison of experimentally determined room-temperature lattice constants of martensite containing various amounts of carbon with values calculated from carbon-pair theory.

From the concept of carbon pairs comes a potent mechanism of strengthening of martensite that has not heretofore been proposed. Slip would separate some of the C-C pairs into single atoms. This would require a high value of stress because of the strong C-C interaction (preliminary calculations have set the value of this interaction energy at more than 10 kcal/mole).

During the tempering of martensite, the first carbide to form is the metastable ϵ-Fe_2C, which has a hexagonal unit cell. From preliminary studies it now appears that the formation of this carbide is a natural consequence of the C-C pair formation. These studies are continuing.

3. THE STRAIN HARDENING OF IRIDIUM

Victor Zackay, T. Trozera,* Jack Washburn, and Gareth Thomas

The precious metal iridium has been reported to have an exceptionally high rate of work hardening, i.e., 300 000 psi with 5% uniform elongation for a 50% deformed polycrystalline sample. This combination of strength and ductility is equivalent to that of a conventional high-strength steel. The exceptionally high rate of work hardening at both small and large strain prompted a basic study of its properties. Single crystals of zone-refined and high-temperature vacuum-annealed iridium were prepared and mechanically tested. It became readily apparent that impurities, especially those in the grain boundaries, influenced the rate of work hardening, the tensile strength, and the mode of fracture. The shear stress of the iridium decreased from 23 000 psi (polycrystalline) to 2000 psi (single crystal) to 900 psi (single crystal) with zero, one, and two zone passes, respectively. However, the rate of work hardening of the doubly zoned crystal remained high. For example, it is five times as high as that of Fe-Si single crystals. In addition, a high degree of twinning is observed as well as an usual type of growth face which appears after zone refining. Further zone purification of the single crystals is under way, in addition to preparation of thin foils for electron transmission microscopy.

* General Atomics, San Diego, California

4. CYCLIC PHASE TRANSFORMATIONS IN STEELS

Victor Zackay and David Dickson

For the achievement of high strength in complex multiphase systems, dislocation theory suggests a size and distribution of hard particles in a ductile matrix that hitherto has not been attained in real alloy systems. For example, in conventional high-strength steels the particle spacing is two to three orders of magnitude greater than the ideal. Microstructures closer to the ideal have been obtained in this investigation by a process involving solid-state transformations coupled with control of composition, plastic deformation and temperature. The process consists of cycling a cold-worked high-carbon austenitic steel between room temperature and progressively decreasing

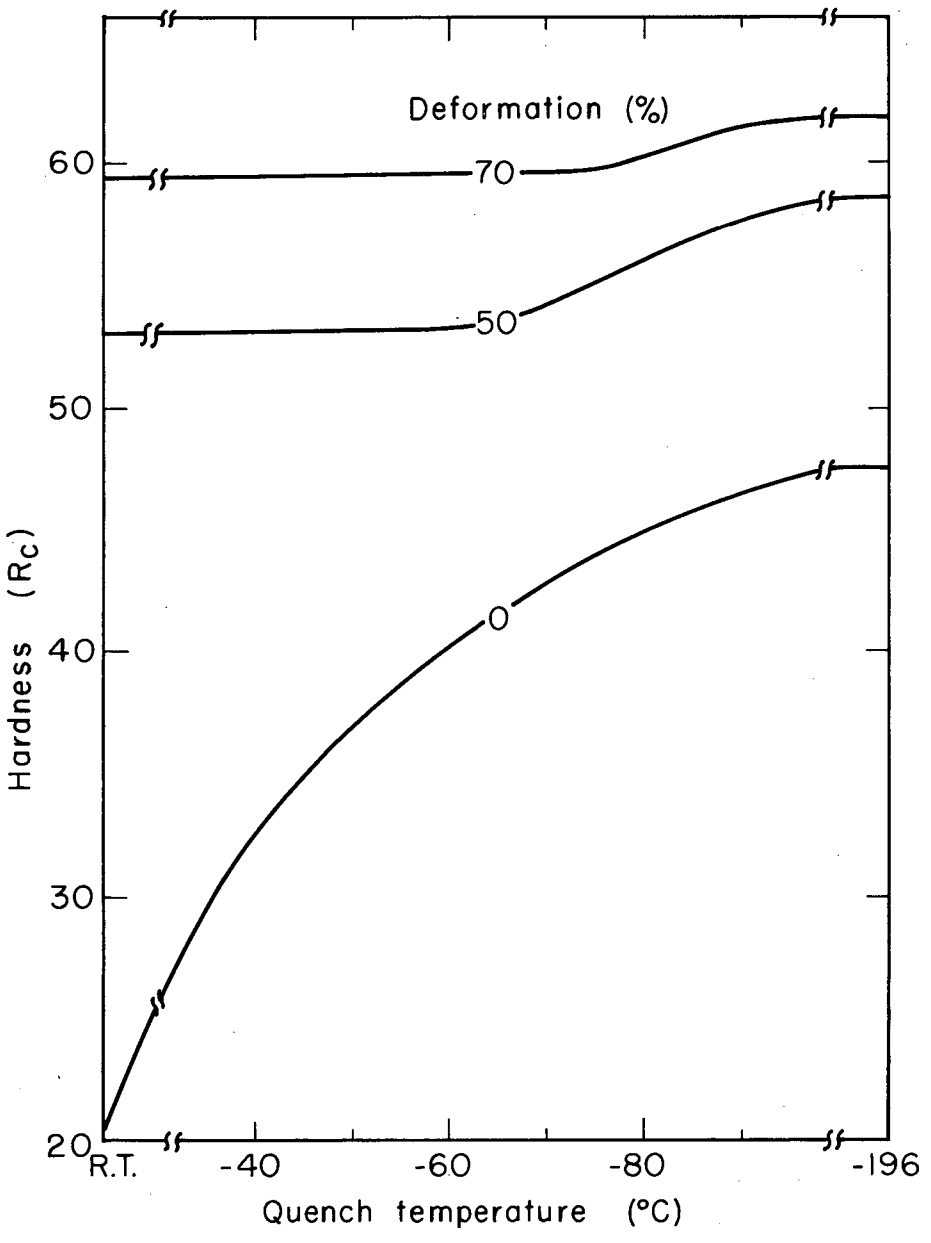

MUB-2797

Fig. IIC. 4-1 The hardness of a deformed austenitic steel progressively transformed to martensite by a thermal cycling, i.e., quenching below M_s temperature followed by a tempering treatment.

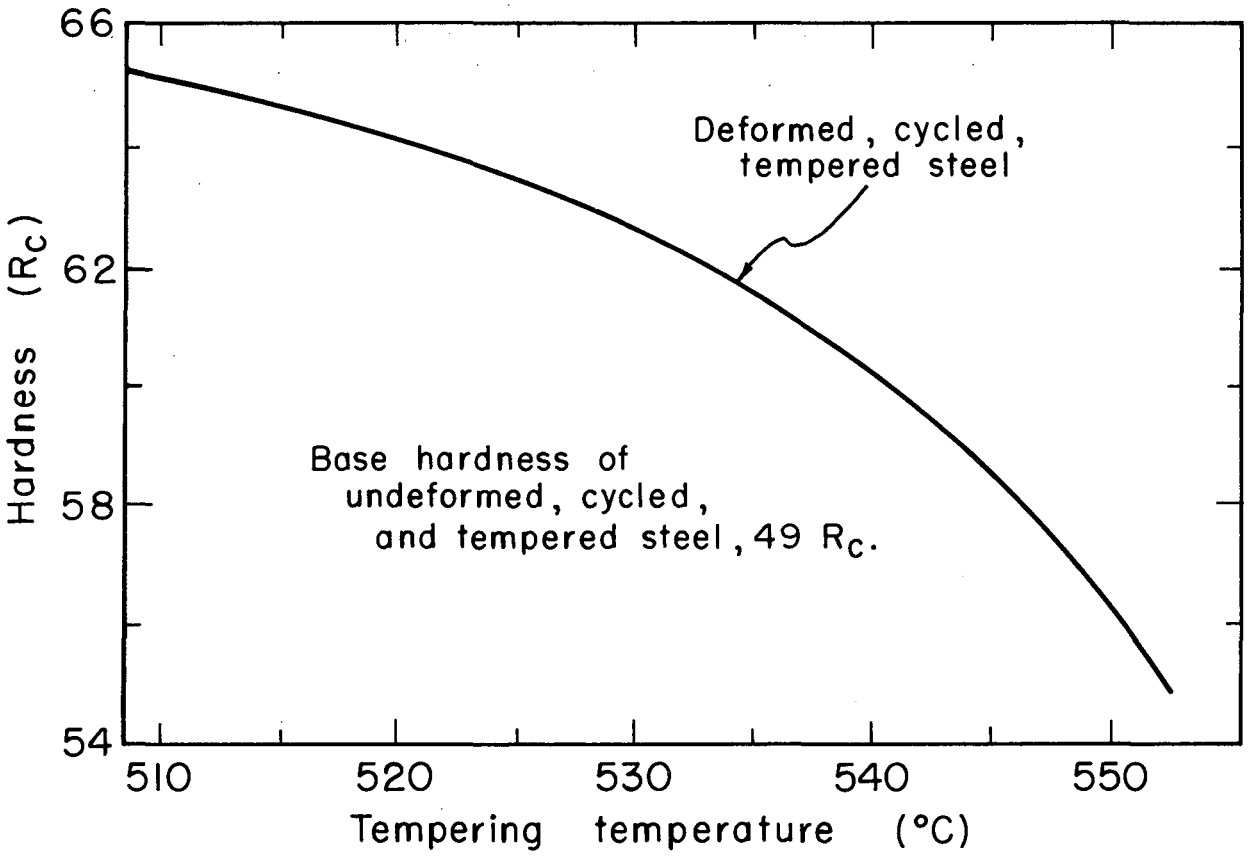

MUB-2789

Fig. IIC. 4-2 Comparison of the hardness of a deformed and cycled martensitic steel with that of the same steel conventionally heat treated.

temperatures such that with each cycle a greater volume of a hard phase (martensite) appears, which causes large numbers of dislocations to be produced. After each low-temperature cycle the steel is annealed, causing precipitation of carbides on the dislocations. The resulting precipitation renders the austenitic steel susceptible to further transformation during the next cycle. The process is continued until all the austenite is transformed to a dispersion of fine carbides in martensite. By this type of cyclic transformation the hardness of the steels is increased from 49 to 65 (Rockwell "C" scale). As shown in Fig. IIC.4-1, the hardness of the cycled steel is primarily determined by the degree of cold-work of the austenite. The hardness of the deformed and cycled steel is about 15 points Rockwell "C" greater (at low tempering temperatures) than the conventionally quenched and tempered steel, as shown in Fig. IIC.4-2. Optimum processing cycles have been established by metallographic, magnetic, and hardness measurements. Attempts to correlate the microstructures obtained and their associated mechanical properties with the predictions of theory are currently under way.

D. KINETICS OF DISLOCATION MECHANISMS

1. PHYSICAL ASPECTS OF CREEP*

John E. Dorn and Jimmy D. Mote+

This constitutes a summary and analysis of the physical theories and pertinent experiments on high-temperature creep. Several newly developed concepts are presented as follows:

1. Whereas Nabarro and Herring assumed that creep in polycrystalline aggregates occurs by stress-directed diffusion of vacancies through the volume of the grain, there is a finite probability that this diffusion may occur preferentially in the grain boundary. An approximate kinetic analysis has been made which suggests that for

$$\frac{g_f - g_{f_b} + g_m}{kT} < 30$$

diffusion preferentially occurs in the grain boundary. The values of g_f, g_{f_b}, and g_m refer to the free energy of formation of a vacancy in the volume of a crystal (f), the free energy of formation of a vacancy in the grain boundary (fb), and the free energy of activation of a vacancy for motion (m), respectively, where kT has its usual meaning. This suggests that volume diffusion will be the preferred mechanism in most metals, whereas grain-boundary diffusion may predominate in some ceramic materials. An equation for creep by grain-boundary diffusion of vacancies has also been developed. Whereas the appropriate experimental creep data for Al_2O_3 suggest that Nabarro creep is controlled by anion volume diffusion, data for BeO and UO_2 suggest the process may be controlled by anion grain-boundary diffusion.

2. Although experimental results on dislocation-promoted creep have revealed that high-temperature creep results from the formation and migration of vacancies, no completely satisfactory formulation of the theory has yet matured; it can be shown that creep of bcc and fcc metals with high-stacking-fault energy can be well rationalized in terms of the motion of jogged screw dislocations. The critical issue concerns the fact that the distance between jogs in these metals is very small and therefore the activation energy is only mildly reduced as a result of stress. The short jog length arises from facile cross-slip of screw segments. The observed activation energy for creep coincides well (as has been experimentally demonstrated) with that for self-diffusion. This also accounts for the insensitivity of the activation volume to temperature. A second major issue concerns the fact that dipoles, entanglements, and subgrains are formed during primary creep. The entire change in creep rate over the primary stage can be ascribed to the decreasing density of moving jogged screw dislocations.

---

*Short form of a presentation to the International Conference on Elevated Temperature Structural Mechanics, held at Columbia University, New York City, January 23-25, 1963.

+Now at Sandia Corp., Albuquerque, New Mexico.

3. A secondary creep rate was assumed to arise when the generation of dislocations by climb from dipoles and entanglements equals the rate of formation of these substructural details as controlled by the motion of jogged screw dislocation. Thus the creep in this region can be analyzed by either the motion of jogged screw dislocations or the climb of edge dislocations.

4. The major advantage of this theoretical approach is that for the first time the primary stage of creep may be explained in some detail. It follows from the theory that the total creep strain γ can be given by

$$\dot{\gamma} = f\ (te\ \frac{-\Delta H_d}{RT}),$$

where t = duration of the test and ΔH_d is the enthalpy for self-diffusion. This equation has been experimentally verified in our laboratory.

5. A more accurate equation describing the equilibrium distribution of solute atoms in a Cottrell atmosphere has been developed, taking into consideration the problem of occupancy of lattice sites and, for the first time, the effect of non-ideality of the solution.

6. The qualitative formulation for a better theory of creep in dispersion-strengthened alloys has been developed. This analysis suggests that the high-temperature creep resistance in these alloys is due to the low rate at which dislocations are released by climb from high-density dislocation entanglements resulting from the presence of the dispersed particles and particularly to the short distances they move before they again become entrapped.

2. DISLOCATION CONCEPTS OF STRAIN RATE EFFECTS*

John E. Dorn and Frank E. Hauser

Whereas von Karman and Taylor independently based their analyses for plastic wave propagation on the deformation concept, which assumes the deformation stress is exclusively a function of the plastic strain, Malvern believed that a viscoelastic type of behavior is more realistic, assuming the flow stress is a function of the strain rate as well as the strain. With relatively few exceptions, current investigators of plastic wave propagation phenomena are rather sharply divided into two camps, those who insist on the von Karman-Taylor type of formulation and those who adhere to the Malvern approach. It is the thesis of this paper that both concepts are substantially correct under appropriate circumstances. This thesis will be upheld not only in terms of new experimental evidence but also in terms of deductions arrived at from elementary dislocation theory.

---

* A shortened version of paper in Proceedings of Symposium on Structural Dynamics Under High Impulse Loading, ASD-TDR-63-140, May 1963, pp. 173-178.

3. ON THE NATURE OF STRAIN HARDENING IN POLYCRYSTALLINE ALUMINUM AND ALUMINUM-MAGNESIUM ALLOYS*

Sandip K. Mitra+ and John E. Dorn

By applying experimental techniques involving changes in temperature and strain rate during the low-temperature plastic deformation of polycrystalline Al and several Al-Mg α solid solutions, it was possible to deduce--from an appropriate extension of Seeger's theory for thermally activated intersection of dislocations--the mean force-displacement diagram for the thermally activated intersection, the mean distance between the dislocations being intersected, and the contribution of the athermal processes to the flow stress. The force-displacement diagram for pure polycrystalline Al agreed precisely with that previously obtained for pure single Al crystals, revealing that intersection is the rate-controlling mechanism.[1,2] Whereas the initial effective dislocation spacing was found to be identical in polycrystalline Al and in single crystals of Al, the dislocation density increased much more rapidly with straining in the polycrystalline material. This behavior was attributed to the polyslip that must take place when polycrystalline metals are deformed. Furthermore, in the polycrystalline metal, the athermal contributions to the flow stress increased much more rapidly with strain. The principal factor causing this was shown to be the greater long-range back stresses due to blockage of dislocations at the grain boundary. The theoretical ratio calculation predicting that the flow stress of a polycrystalline aggregate is 3.10 times the resolved shear stress for slip, as suggested originally by G. I. Taylor, was not confirmed. When the strains were identical, the ratio did hold if the effective dislocation density was the same in the polycrystalline and single-crystal specimen.

Theoretically, many factors such as short-range-order hardening (Fisher), dislocation-solute atom locking (Cottrell), and chemical interaction due to stacking faults (Suzuki), can account for solid solution strengthening. In this investigation it was found that the thermally activated mechanism for deformation of Mg α solid solutions of Al was also ascribable to intersection. The force-displacement diagram deduced from the the plastic behavior was only slightly different from that for pure Al, as expected when the stacking-fault energy is decreased slightly. The major factor, however, in accounting for the increased strength on alloying was the greater initial density of dislocation and the more rapid increase in dislocation density with strain. The back stress due to various athermal processes was also increased as a result of

*Short version of published paper, Trans. AIME 227, 1015-24 (1963).

+Now at National Physical Laboratories, Teddington, Middlesex, England.

1. S. K. Mitra and J. E. Dorn, On the Nature of Strain Hardening in fcc Metals, Trans. AIME 224, 1062-1071 (1962).
2. S. K. Mitra, P. W. Osborne, and J. E. Dorn, On the Intersection Mechanism of Plastic Deformation in Al Single Crystals, Trans. AIME 221, 1206-14 (1961).

alloying. Undoubtedly the various locking mechanisms are responsible for the retention of high dislocation densities following annealing of the cold-worked specimens. This effect of alloying on increasing the density of dislocations was overlooked in all previous investigations on solute-atom strengthening. Since this effect was observed to be much greater than those attributed to the Fisher, Cottrell, and Suzuki contributions to alloy hardening, the entire field of solid solution strengthening should be re-explored.

4. ON THE THERMALLY ACTIVATED MECHANISM OF PRISMATIC SLIP IN THE Ag-Al HEXAGONAL INTERMEDIATE PHASE*

Eugenia M. Howard, Willis L. Barmore, Jimmy D. Mote,+ and John E. Dorn

Previous research results have revealed that the prismatic slip of Ag-Al (33 at. %) hexagonal intermediate phase from 170° to 475°K was athermal and could be ascribed only to short-range-order strengthening.[1,2] From the mechanical data, and assuming chemical equilibrium at 475°K, the short-range order energy was determined to be 730 cal/mole, and Cowley's degree of order was about $\chi = 0.30$. Above 475°K, however, thermally activated creep was observed.

Both the activation energy for creep and the stress laws for creep have been determined in order to assist in identifying the thermally activated mechanism for creep. Following a short inverted transient, a steady-state creep rate, γ, given by

$$\gamma = 1.4\ \tau^{3.6}\ e^{-33\ 000/RT},$$

there τ is the applied shear stress, was obtained. The activation energy of 33 000 cal/mole was independent of the applied stress and about equal to the estimated value for diffusion. Since the stress level for creep was much below that necessary to overcome short-range ordering, the process could not be ascribed to either the motion of jogged screw dislocations or the climb of edge dislocations. Equally it could not be attributed to viscous drag of a Cottrell atmosphere, since such an atmosphere does not form in this alloy because of the identity of the atomic radii of Ag and Al. A theory in qualitative agreement with the facts was proposed, based on local disordering by diffusion due to relaxation in the near vicinity of the cores of moving dislocations.

---

* Trans. AIME 227, 1061-68 (1963).

+ Now at Sandia Corporation, Albuquerque, New Mexico.

1. J. D. Mote, K. Tanaka, and J. E. Dorn, Effect of Temperature on Yielding in Single Crystals of the Hexagonal Ag-Al Intermetallic Phase, Trans. AIME 221, 858 (1961).

2. K. Tanaka and J. D. Mote, The effect of Temperature on the Yield Strength of Polycrystalline Hexagonal Ag-Al Intermetallic Phase (UCRL-9992, Dec. 1961), submitted for publication in Trans. ASM.

5. THERMODYNAMICS OF STACKING FAULTS IN BINARY ALLOYS*

John E. Dorn

Distribution of solute atoms between the matrix and stacking faults is significant to the mechanical behavior of alloys as a result of Suzuki locking of dislocations. A more complete and sophisticated analysis of the distribution coefficient was established by use of classical thermodynamics, for any solid solution (not just regular solutions) and the final results were expressed in terms of experimentally measurable quantities.

* Extract from paper in Acta Met. 11, 3, 218-19 (1963).

6. DISPERSED-PARTICLE STRENGTHENING AT LOW TEMPERATURES*

Jack B. Mitchell, Sandip K. Mitra,+ and John E. Dorn

Current thoughts on the effect of dispersion strengthening are based on the Fisher-Hart-Pry extension of Orowan's concept that dislocations can extrude past particles spaced a distance λ apart when the applied stress is $\tau = 2\Gamma/b\lambda$, where Γ is the line energy and b is the Burger's vector. Fisher, Hart, and Pry suggested that the dislocation loops left around the particles provide high back stresses that are responsible for the high rates of strain hardening observed in the initial stages of straining. Finally, fracturing of the dispersed phase as a result of the high stress concentration due to the dislocation loops results in very low final rates of strain hardening.

By use of the same techniques as described in the preceding investigation, it was shown that the thermally activated mechanism of plastic deformation in polycrystalline aggregates of Al containing dispersions of $CuAl_2$ is again intersection of dislocations. The force-displacement diagrams for intersection of dislocations in these alloys differed only slightly from those for pure Al, in a manner suggesting that the alloys had a slightly lower stacking-fault energy than pure Al. The great increase in flow stress in the early stages of deformation was principally attributable to the great increase in dislocation density. The mean dislocation spacing deduced from the mechanical data coincided closely with that observed in the entanglements by transmission-electron microscopy. No circular dislocation loops as postulated by Fisher, Hart, and Pry were observed. This suggests that the dislocation mechanics for dispersion-hardened alloys are similar to those of solid solutions. Extensive polyslip and cross-slip in the vicinity of the particles causes the formation of high-density entanglements rather than loops. The low rates of strain hardening after extensive deformation were not due to fracturing of the precipitate, and probably are ascribable to cross-slip.

* Extract from paper in Trans. ASM 56, 2, 236-48 (1963).

+ Now at National Physical Laboratories, Teddington, Middlesex, England.

7. PLASTIC WAVE PROPAGATION IN RODS*

Stanley Rajnak and Frank E. Hauser

A recent determination of the relation between stress, strain, and strain-rate for polycrystalline pure aluminum under impact loading permits precise theoretical predictions to be made of the behavior of thin bars using a "Malvern" type system of equations. Two types of computations and experiments were carried out. One was a check on the validity of Kolsky's "thin wafer" technique for determining the relation between stress, strain, and strain rate. In the second experiment a long tubular bar was impacted and the final strain distribution was predicted by using the experimentally determined strain-rate function.

---

* Extract from paper in Proceedings of ASTM Symposium on Dynamic Behavior of Materials, held at the University of New Mexico, Albuquerque, September 27, 1962, ASTM Special Technical Publication 336 , 167 (1963).

E. PHYSICAL CERAMICS

1. CERAMIC COMPOSITES*

Donald O. Nason, Didericus P. Hasselman, and Richard M. Fulrath

Glass matrices have been used to fabricate well-characterized composite systems by introducing metal microspheres or spherical porosity. When the glass was chosen so that the thermal expansion of the dispersed metal spheres was greater than the matrix, a system without interfacial bonding was produced which had a characteristic decrease in strength with increasing volume fraction of the dispersed phase. When an interfacial bond was present between the dispersant and the matrix, an increase in strength with increased dispersed phase was attained. Interfacial bonding did not appear to change the behavior of a composite system when the glass had a higher thermal expansion than the dispersed phase, however, the fracture-propagation path changed significantly between systems with and without interfacial bonds. Without interfacial bonding, the fracture plane bisected the spherical particles. When interfacial bonding was present, the fracture plane appeared to avoid the dispersed phase.

The elasticity of a glass containing less than 2.5% spherical porosity was shown to follow the relationship

$$E = E_o (1 - \alpha P),$$

where E_o represents the Young's modulus of pore-free material, P the volume fraction porosity, and α is a constant.

* This summarizes portions of the results presented in UCRL-11011, UCRL-11027, UCRL-10973, and UCRL-10846.

2. FIRST-STAGE DENSIFICATION OF CaF_2 UNDER PRESSURE AND TEMPERATURE*

Yasuo Hashimoto and Richard M. Fulrath

The initial densification of spherical CaF_2 powders was determined by dilatometric and microscopic observations. The experiments consisted of heating the powder to a fixed temperature at a constant rate under a load and then releasing the load and quenching. Further experiments were performed by heating to a fixed temperature without load application, rapidly applying the load and holding for 40 sec or 1 h, and releasing the load and quenching.

The initial stages of hot pressing were divided into three regions. Region I exhibited little densification. Region II showed densification by limited plastic flow and fracturing. Region III above a pressure-dependent critical temperature exhibited extensive densification due to plastic flow, fracturing of particles, and their subsequent rearrangement. After this

* Abstracted from Yasuo Hashimoto, First-Stage Densification of CaF_2 Under Pressure and Temperature (M.S. Thesis), UCRL-11214, Jan. 1964.

initial densification, the densification rate was consistent with the equations proposed by Murray et al.[1]

1 P. Murray, D. T. Livey, and J. Williams, Hot Pressing of Ceramics, in Ceramic Fabrication Processes, W. D. Kingery, Ed. (Technology Press and Massachusetts Institute of Technology and John Wiley & Sons, Inc., New York, 1958), pp. 147-171.

3. THE EFFECT OF TENSILE STRAIN ON HELIUM PERMEATION OF GLASS AND SEVERAL REFRACTORY CERAMICS*

Orlin M. Stansfield† and Richard M. Fulrath

A mass spectrometer was used to measure helium permeation through the walls of tubes made of Pyrex glass, fused silica, refractory mullite, and high-alumina ceramics. Application of tensile strains near the breaking point gave an instantaneous and reversible increase in steady-state helium permeation, on the order of 1%. The strain dependence of the permeation in Pyrex, fused silica, and mullite could be expressed as

$$K_\epsilon = K \exp[M\epsilon/RT] ,$$

where K_ϵ and K are the strained and unstrained permeability coefficient, respectively, M is the strain coefficient of the activation energy of permeation, ϵ is the total strain, and R and T are respectively the universal gas constant and absolute temperature. The observed strain dependence of permeation in these materials was similar and presumably due to aniaxial strain in the glassy phase with a resultant decrease in the activation energy of helium permeation. The high-purity alumina showed no detectable helium permeation in the stressed or unstressed state within the temperature range investigated.

* Abstracted from Orlin M. Stansfield, The Influence of Tensile Stress on Gaseous Permeation in Glassy-State and Complex Ceramics, (M.S. Thesis), UCRL-10755, April 1963.

† Now at Solar Aircraft Company, San Diego, California

4. LIQUID-SOLID TRANSFORMATION KINETICS IN Al_2O_3*

Amio R. Das and Richard M. Fulrath

A dc arc plasma torch was used to subject sized particles of synthetic sapphire in the range of 9 to 104 μ to rapid melting and resolidification.

* Abstracted from Amio R. Das and Richard M. Fulrath, Liquid-Solid Transformation Kinetics in Al_2O_3, UCRL-11166, Dec. 1963.

In order to study the formation of metastable phases of alumina, the size and apparent density of spheroidized particles were used as parameters in determining quenching rates. A hypothesis based on the kinetics of nucleation of the crystalline solid phases from the supercooled liquid droplets was proposed to explain the ratio of the metastable phases to the stable α phase. Experimental data relating this ratio with quench rates of the liquid droplets have been shown to give good agreement with the proposed hypothesis.

5. DEFORMATION AND FRACTURE OF POLYCRYSTALINE LITHIUM FLUORIDE*

William D. Scott and Joseph A. Pask

Techniques for the fabrication of polycrystalline LiF test specimens were developed and evaluated with single-crystal LiF as a control. An etch was developed which revealed dislocations on all crystallographic faces of LiF. Large-grained polycrystalline specimens tested in four-point loading underwent 0.076 to 0.798% plastic strain before fracture. In most cases their yield stress was similar to that for single crystals favorably oriented for flow on {110}⟨110⟩slip systems. Deformation was inhomogeneous among the grains because of differences in orientation with respect to the applied stress and within individual grains because of interactions at grain boundaries. Grain boundaries were barriers to slip, but stresses resulting from slip in one grain were transmitted to neighboring grains and often caused local deformation near the boundary. In one case, local boundary slip occurred on a (010) plane. Three-grain junctions were areas of high residual stresses, and fractures originated at boundaries at or near three-grain junctions. Fractures were mixed transgranular and intergranular.

* Abstract of published paper, J. Am. Ceram. Soc. 46, [6], 284 (1963).

6. EFFECT OF TEMPERATURE ON THE FLOW STRESSES ON THE {100} and {110} PLANES, AND ON THE PLASTICITY OF POLYCRYSTALLINE LITHIUM FLUORIDE*

David W. Budworth and Joseph A. Pask

Stress-strain data were obtained in four-point bending at temperatures up to 500°C for large-grained specimens of polycrystalline lithium fluoride. A marked increase in ductility and decrease of work hardening was observed to occur between 350°C and 400°C, and to coincide with the appearance of wavy slip lines on the specimen surface. It was suggested that these changes were due to the additional movement on {100} slip planes above this temperature range, supplementing the movement on the {110} planes. Failure above 400°C was of the grain-boundary type, while at lower temperatures it was principally

* Extract from published papers, Trans. Brit. Ceram. Soc. 62 [9], 763 (1963); J. Am. Ceram. Soc. 46 [11], 560 (1963).

of the cleavage type. It was suggested that this difference was due to the decreased ease of cleavage.

Compression studies were then made on single crystals to determine the flow stress on the {110}⟨110⟩and {100}⟨110⟩families of slip systems (Fig. IIE.6-1), and on polycrystalline specimens (Fig. IIE.6-2) as a function of temperature up to 700°C. The stress-strain curves for the polycrystalline specimens at 400°C and higher exhibited a sharp yield, lower work hardening, and considerably more strain at fracture. It was thus substantiated that plastic deformation cannot be expected until it is possible to activate the {100}⟨110⟩family of slip systems almost as easily as the {110}⟨110⟩family. Also, it appears that the stress-vs-temperature curves, obtained in compression at a constant loading rate, for both single crystals and polycrystals of LiF tend to extrapolate to zero or a very low stress at the melting point.

7. INDEPENDENT SLIP SYSTEMS IN CsCl-TYPE CRYSTALS*

Stephen M. Copley

Rachinger and Cottrell[1] showed that slip occurs on the {110}⟨001⟩ slip systems in CsCl-type crystals which tend toward ionic bonding, and on the {110}⟨111⟩slip systems in crystals in which bonding is of metallic character. Johnson and Pask[2] have shown that in CsBr slip occurs on the {110}⟨001⟩family of slip systems. This family yields three independent slip systems and, thus, a general deformation is not possible by this mechanism. Extensions parallel to the crystal axes cannot be produced.

* Extract from published correspondence, Phil. Mag. 8 [93], 1599 (1963).
1.W. A. Rachinger and A. H. Cottrell, Acta Met. 4, 109 (1956).
2.Lawrence D. Johnson and Joseph A. Pask, Mechanical Behavior of Single-Crystal and Polycrystalline Cesium Bromide, UCRL-10468 Rev., July 1963.

8. EFFECT OF CRYSTAL ORIENTATION ON PLASTIC DEFORMATION OF MAGNESIUM OXIDE*

Charles O. Hulse†, Stephen M. Copley and Joseph A. Pask

Stress-strain data for single crystals of MgO tested in compression with⟨100⟩and ⟨111⟩loading axes and polycrystalline MgO were obtained for temperatures ranging from 26° to 1250°C. Single crystals with a⟨111⟩loading axis were found to deform plastically on the {100}⟨110⟩slip systems at temperatures above 350°C. The total strain at fracture for polycrystalline specimens at temperatures above about 600°C was about 2%. The general inability of the {110}⟨110⟩slip system to satisfy the Taylor requirement--i.e.,

* Abstract of published paper, J. Am. Ceram. Soc. 46, [7], 317 (1963).
† Now at United Aircraft Corporation, East Hartford, Connecticut.

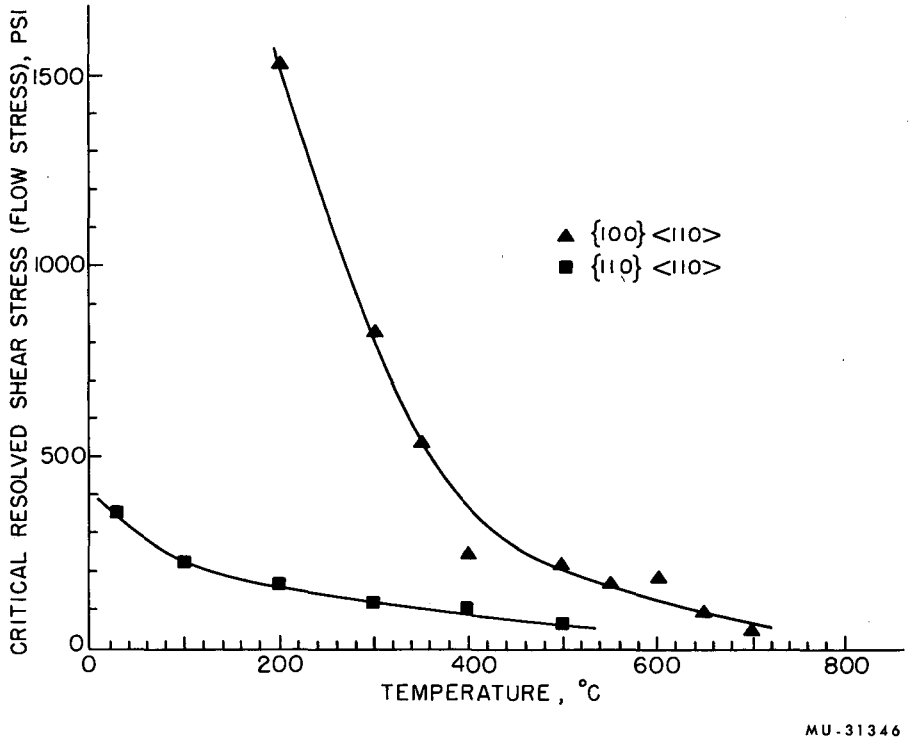

Fig. IIE. 6-1 Flow stress on the {100} ⟨100⟩ and {110} and ⟨110⟩ families of slip systems as a function of temperatures.

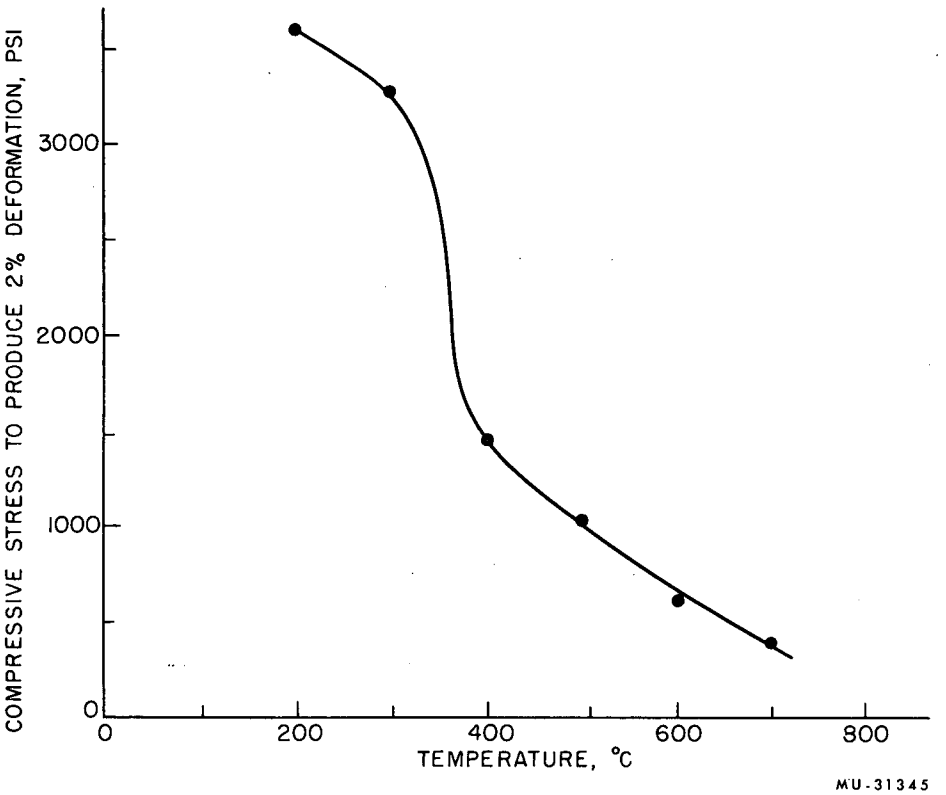

Fig. IIE. 6-2 Compressive stress needed to produce 2% deformation of polycrystalline LiF as a function of temperature.

the necessity of five independent slip systems, ease the cleavage, and slip nonuniformity--all act to limit polycrystalline ductility at low temperatures. At higher temperatures the additional flow on {100}⟨110⟩slip systems provides the additional slip systems necessary to satisfy Taylor's criterion, and stress-induced climb and high dislocation mobility inhibit cleavage fracture.

9. HIGH-TEMPERATURE REACTIONS.

THE KINETICS AND MECHANISM OF THE ANATASE-RUTILE TRANSFORMATION*

Robert D. Shannon and Joseph A. Pask

The mechanism of the transition has been analyzed in detail from pole figures obtained from transformed single crystals of anatase. Both the anatase and rutile structures can be represented as sodium chloride structures with half the cations removed. The difference in the two structures lies in the distribution of the cations in the pseudo-close-packed planes. The cations lie in rows along [001] in the rutile (100) close-packed plane, while they form zig-zag chains along [221] in the anatase (112) close-packed plane. Because the spacings of these two planes are nearly identical in both structures ($d_{ana}^{112} = 2.33$; $d_{rut}^{100} = 2.297$), the reaction mechanism was assumed to occur by retention of these planes and rearrangement within the planes. Because it was also assumed that the mechanism would occur with the least spatial disturbance of the ions, a distribution of cations similar to that in the rutile (100) was sought in the anatase (112) plane. Of the several possible configurations, the one corresponding to the least distortion of the oxygen ions and the smallest change in titanium ion distribution was found to result in a pole figure closely approximating the experimental pole figures. The mechanism for this structural change was determined to be a cooperative movement of the oxygen ions and titanium ions whereby three-fourths of the titanium atoms break two Ti-O bonds in reaching their new sites while the remaining fourth retained their original six neighbors. This movement is in contrast to diffusion, in which the cations would move in an essentially fixed anion structure.

The nucleation and growth of rutile was observed in anatase single-crystal sections under a hot-stage microscope. Nucleation occurred at temperatures of 1000° to 1100°C at inclusions, at the corners and edges of the crystals, and at surface scratches. Growth occurred at inclusions and edges and corners at 950° to 1050°C. The growth was generally found to spread from several discrete sites rather than to spread instantaneously over the surface. The significance of this observation is that it enables the exclusion of the shrinking-sphere model for application of rate laws to powder reactions.

---

* Abstracted from Robert D. Shannon, The Kinetics and Mechanism of the Anatase-Rutile Transformation (Ph.D. Thesis), UCRL-11001, March 1964.

Our report of last year included data on the kinetics of transformation of several TiO_2 powders. Additional studies have been made on the effect of CuO on the kinetics of R163 powder. The reaction temperatures were lowered by 200° to 300°C and the activation energy increased from 100 to 180 kcal. It was evident that the kinetics of another process, probably the diffusion of Cu into TiO_2, were being measured. The formation of a CuO-TiO_2 solid solution at a level of 0.3% CuO were indicated by a typical error-function distribution of Cu in a pressed disc of anatase which had been heated in CuO powder.

The influence of CuO on the transformation rate suggested that the concentration of oxygen vacancies was important in determining the rate of transformation. The rate in various mixtures of H_2 -N_2 was also found to be greatly accelerated. Optical reflection spectra showed a direct correlation between the amount of reduction and the amount of transformed material. These observations combined with the CuO data confirmed the conclusion that the accelerating effect of both CuO and a hydrogen atmosphere can be explained on the basis of an increased vacancy concentration. Conversely, the reaction should be inhibited by a decrease in vacancy concentration. This conclusion is supported by the fact that impurities such as S^{+6}, P^{+5}, and F^- have all been observed to raise the transformation temperature, and that it appears reasonable, as the cooperative movement of the oxygen and titanium atoms during transformation would be expected to occur more easily with increase of the oxygen vacancy concentration.

10. THE KINETICS OF THE HIGH TEMPERATURE HYDROLYSIS OF MAGNESIUM FLUORIDE*

Donald R. Messier† and Joseph A. Pask

The rate of the hydrolysis of magnesium fluoride was investigated by a gravimetric method as a function of temperature and water vapor pressure over the ranges from 745 to 835°C and 1 to 20 mm Hg, respectively.

Single-crystal and polycrystalline specimens were investigated with regard to their suitability for use in rate determinations. Because of orientation effects and a limited supply of single-crystal material, heat-treated slabs of hot-pressed MgF_2 were chosen for the final rate determinations.

A linear rate law was found, and it was concluded that the rate-determining process was chemical reaction at the MgF_2-MgO interface. A three-step reaction mechanism was postulated. The first step involves the chemisorption of water vapor,

---

* Abstracted from Donald R. Messier, The Kinetics of the High-Temperature Hydrolysis of Magnesium Fluoride (Ph.D. Thesis) UCRL-11103, Jan. 1964.

† Now at Argonne National Laboratories, Metallurgy Division, Argonne, Illinois.

$$MgF_2(c) + H_2O(g) \underset{k_2}{\overset{k_1}{\rightleftharpoons}} MgF_2 \cdot H_2O(ads). \qquad (1)$$

The second step, formation of a hydroxyfluoride complex, can be represented by

$$MgF_2 \cdot H_2O(ads) \underset{k_4}{\overset{k_3}{\rightleftharpoons}} Mg(OH)F(c) + HF(g). \qquad (2)$$

The third step, decomposition of the hydroxyfluoride complex to form products can be written as

$$Mg(OH)F(c) \underset{k_6}{\overset{k_5}{\rightleftharpoons}} MgO(c) + HF(g). \qquad (3)$$

With the assumptions that the chemisorption step was in equilibrium and that the HF pressure was negligible, an expression was developed which showed that the rate was proportional to the concentration of chemisorbed water vapor. It was possible to express the rate dependence on water vapor pressure in terms of the Langmuir adsorption isotherm equation.

Values of -16.9 kcal/mole and -4.2 eu were obtained for the enthalpy and entropy of chemisorption. The activation enthalpy and frequency factor for decomposition of the chemisorbed intermediate, $MgF_2 \cdot H_2O(ads)$, were 46.4 kcal/mole and 1.75×10^{10} sec^{-1}. The low value for the entropy of chemisorption was attributed to possible oversimplification in the interpretation of the reaction mechanism.

11. KINETICS OF THE HIGH-TEMPERATURE HYDROLYSIS OF CALCIUM FLUORIDE

Donald R. Messier* and Joseph A. Pask

The rate of the hydrolysis of calcium fluoride single-crystal slabs was gravimetrically investigated as a function of temperature and water vapor pressure in the ranges from 1000 to 1120°C and 1 to 20 mm Hg, respectively. The curves of weight loss vs time were found to be paralinear, in agreement with the results of Bontinck (1958), who investigated the kinetics by a chemical analysis method at a single water vapor pressure.

Reaction rates for both the initial, parabolic portion and final, linear portion of the weight-loss curves were found to be pressure-dependent. The parabolic rates, which apparently may be identified with the process of dissolution and diffusion of oxygen and fluoride ion vacancies in the

* Now at Argonne National Laboratories, Metallurgy Division, Argonne, Illinois.

fluorite structures,[1] showed a strong tendency toward saturation values. The linear rates were approximately proportional to the square root of the water vapor pressure, and may represent a surface reaction step. Both rates also showed significant temperature dependencies.

1 W. Bontinck, The Hydrolysis of Solid CaF_2, Physica 24, 650-658 (1958).

12. DIFFUSION OF IRON INTO SINGLE-CRYSTAL MgO*

Stuart L. Blank and Joseph A. Pask

Magnesium oxide single crystals were placed in iron powder and heated in a vacuum furnace at 1150, 1250, and 1350°C for various times. Concentration-vs-penetration profiles were determined by using the electron microprobe analyzer. The interdiffusion coefficient D was determined from these concentration-vs-penetration curves by using a computer program designed for these calculations. The interdiffusion coefficient D was found to be concentration-dependent in the range 1 to 22 at.%Fe. At 1150°C,

$$D = 8.1 \times 10^{-12} \exp (0.150Fe) \text{ cm}^2/\text{sec};$$

at 1250°C,

$$D = 1.60 \times 10^{-11} \exp (0.173Fe) \text{ cm}^2/\text{sec};$$

and at 1350°C,

$$D = 2.40 \times 10^{-11} \exp (0.190Fe) \text{ cm}^2/\text{sec}.$$

The apparent activation energy for the diffusion process was found to increase with increasing iron concentration in the composition range studied. At an iron concentration of C = 5 at.%,

$$D = 6.34 \times 10^{-7} \exp(-29{,}600/RT);$$

at C = 10,

$$D = 4.49 \times 10^{-6} \exp(-32{,}900/RT);$$

at C = 15,

$$D = 5.04 \times 10^{-5} \exp(-37{,}700/RT);$$

and at C = 20,

$$D = 8.40 \times 10^{-4} \exp(-43{,}500/RT).$$

An electron paramagnetic resonance study was made to determine if the concentration of trivalent iron increased as the divalent iron concentration was increasing.

* Abstracted from Stuart L. Blank, (M.S. Thesis), UCRL-11073, Nov. 1963.

13. DIFFUSION OF IRON INTO SODIUM DISILICATE GLASS*

Marcus P. Borom and Joseph A. Pask

Diffusion couples of elemental iron and degassed sodium disilicate glass rod were prepared under neutral to reducing conditions at several temperatures and at varying times. The various diffusion profiles were analyzed by use of electron microprobe techniques. Diffusion-coefficient calculations and activation energy plots indicated that a change in mechanism occurs between 1000°C and 1050°C. Transmission spectroscopy and magnetic susceptibility measurements were employed as an aid in determining the diffusing species at the various temperatures. Magnetic susceptibility measurements indicate that elemental iron is the diffusing species at 900°C and that ferrous iron is the diffusing species at 1050°C under the test conditions. These observations are supported by transmission spectroscopy measurements and by theoretical thermodynamic considerations.

A furnace has been designed and built for the preparation of iron oxide disks by controlled oxidation of iron. These oxide samples will be used in the further studies of the diffusion of iron into sodium disilicate glass, with the various oxides of iron used as the substrate material.

---

* Abstracted from Marcus P. Borom, Diffusion of Iron Into Sodium Disilicate Glass, (M.S. Thesis), UCRL-11116, Nov. 1963.

14. DEHYDRATION OF CRYSTALLINE ALUMINUM HYDROXIDES AND ALUMINUM OXIDE HYDROXIDES

Robert B. Langston and Joseph A. Pask

The decomposition path the trihydrates of alumina follow can be represented by

$$Al_2O_3 \cdot 3H_2O \rightleftharpoons Al_2O_3 \cdot (3-n)H_2O + nH_2O.$$

Uncertainty exists in the literature as to the effect of the reaction variables of temperature, water vapor pressure, and particle size. Also, it has been observed that dehydration reactions proceed to a series of different levels as a function of temperature, which in some cases has been interpreted as the existence of intermediate compounds. Preliminary results do not indicate the existence of any intermediate compounds, and suggest that a diffusion mechanism controls the dehydration.

F. THERMODYNAMICS AND HIGH-TEMPERATURE REACTIONS

1. HEATS OF FORMATION OF α-PHASE Cu-Zn ALLOYS

Raymond Orr, Ralph Hultgren, and Bernard Argent+

Measurement of the heats of formation of twenty α-phase Cu-Zn alloys, X_{Zn} = 0.010 to 0.335, at 573°K has been completed. The variation of heat of formation with composition was studied in close detail in an effort to find further evidence for the existence of ordering in α brass which has been inferred from other types of measurement. Anomalies have been found in measurements of Cp[1] and zinc vapor pressure[2] and in thermal analysis studies,[3] which have been interpreted as resulting from the occurrence of considerable amounts of short-range order at certain compositions.

Measured heats of formation show an unusual amount of scatter above X_{Zn} = 0.20, which might result from differences in the initial ordered states in the alloys. The heat of formation becomes markedly more exothermic at about X_{Zn} = 0.33. Resistivity measurements being conducted on these same alloys by Argent[4] at Sheffield University show an anomalous increase in this same composition range. Further analysis and correlation of the data are necessary before definite conclusions can be drawn.

---

† Sheffield University, Sheffield, England.

1. H. Masumoto, H. Saito, and M. Sugihara, J. Japan Inst. Metals (Sendai) 16, 359 (1952).
2. B. B. Argent and D. W. Wakeman, Trans. Faraday Soc. 54, 799 (1958).
3. L. M. Clarebrough, M. E. Hargreaves, and M. H. Loretto, Proc. Roy. Soc. (London) A-261, 500 (1961).
4. B. B. Argent, private communication.

2. HEAT CAPACITY OF THE LIQUID EQUIATOMIC Bi-In ALLOY

Raymond Orr, Marc Onillon, and Ralph Hultgren

The heat capacity of the liquid equiatomic Bi-In alloy has been measured from its melting point, 383°K, to 750°K, with experimental methods and apparatus previously developed for similar measurements on a liquid In-Sn alloy.[1] As in In-Sn and the pure metals studied, Cp was found to decrease rapidly with increasing temperature for about 250° above the melting point, from 7.8 cal/deg g-atom at 383°K to 6.85 cal/deg g-atom at 650°K; above this temperature the heat capacity appears to level off. This behavior is believed to be the result of either (or both) of two primary mechanisms: (a) the breakup of quasi-crystalline atomic associations remaining in the liquid or (b) changes in the vibrational-translational energy distributions with increasing temperature. Because of the rather extended temperature range over which the decrease occurs, the latter mechanism is thought to be more likely.

---

1 Raymond L. Orr, Henri J. Giraud, and Ralph Hultgren, Trans. ASM 55, 853 (1962).

Above the melting point of Bi, a negative deviation from Kopp's law was found. This is in qualitative accord with the existence of an intermediate solid Bi-In phase and the exothermic character of the system.[2] The heat content with respect to 298°K and the heat of fusion of $Bi\text{-}In_{(s)}$ (1.65 kcal/g-atom) have been determined also.

2.Ralph Hultgren, Raymond L. Orr, Philip D. Anderson, and Kenneth K. Kelley, Selected Values of Thermodynamic Properties of Metals and Alloys (John Wiley and Sons, Inc., New York, 1963), pp. 527-9.

3. THERMODYNAMIC AND ELECTRICAL STUDIES ON SEMICONDUCTING PHASES

Barry Lichter and Ralph Hultgren

A diphenyl ether, Bunsen-type calorimeter has been constructed for measurements of the heat content of solid and liquid semiconducting phases up to a temperature of 1500°K. Several sources of error have been analyzed, and the heat content of platinum has been used as a secondary calibration standard. An ultimate precision of the order of ±1 cal in the measured heat is indicated for measured amounts of heat up to 700 cal and for temperatures up to 1000°K.

The heats of fusion of GaSb (ΔH_m = 7.94 ± 0.08 kcal/g-atom, T_m = 980°K) and of InSb (ΔH_m = 5.82 ± 0.06 kcal/g-atom, T_m = 798 °K) have been determined. The heat content ($H_T - H_{298}$) of solid GaSb has been determined from 400° to 800°K, and measurements are presently continuing up to the melting point. Several measurements of the heat content of liquid InSb in the vicinity of the melting point have been made, and these measurements are being continued in order to check for a reported higher-order transition in liquid InSb.[1]

Apparatus has been constructed for determination of the electrical conductivity of liquid In-Sb alloys by means of a four-probe dc potentiometric technique. The "probe" has been calibrated at room temperature by use of the known conductivity of mercury. The conductivity of liquid indium has been measured in the temperature range 500° to 900°K, extrapolating to good agreement with previous measurements between 430° and 500°K.[2] Measurements on In-Sb alloys are in progress.

1.A. Schneider and R. Blachnik, Naturwiss. 49, 1 (1962).
2.Alexis I. Kaznoff, Raymond L. Orr, and Ralph Hultgren, Thermal Properties of Indium, Second Technical Report, Series 155, Issue No. 2, Contract Nonr-222(63), April, 1961.

4. THE ACTIVITY OF Mn IN Fe-Mn ALLOYS FROM VAPOR PRESSURE MEASUREMENTS

Prodyot Roy and Ralph Hultgren

Measurements of the equilibrium vapor pressures of Mn above Fe-Mn alloys with compositions between $X_{Mn} = 0.09$ and 0.70 have been made in the temperature range 1300° to 1500°K for the purpose of determining the activities of Mn in the alloys. Measurements were made by both the Knudsen-effusion and torsion-effusion methods.

Activities determined from Knudsen measurements showed a slight negative deviation from ideality for $X_{Mn} < 0.35$. However, torsion-cell data indicate a slight positive deviation from ideality over the range from $X_{Mn} = 0$ to $X_{Mn} = 0.70$, at which composition γ_{Mn} approaches unity. This discrepancy is believed to result from the effect of depletion of Mn from the alloy surface in the Knudsen measurements, which require a much longer time at the temperature of measurement in order to get a sufficient weight loss. The rate of diffusion of Mn in the lower Mn content alloys ($X_{Mn} < 0.50$) does not appear to be sufficient to replace the Mn vaporized from the surface. This conclusion was also indicated by torsion measurements on these same alloys in which a gradual decrease in apparent Mn vapor pressure was found if the torsion cell was held at temperature for extended times. For alloys of compositions above $X_{Mn} = 0.50$, however, this effect was not found, suggesting that diffusion is not the rate-controlling step for the alloys with higher Mn content.

5. APPLICATIONS OF THE BORELIUS EQUATION FOR HEATS OF FORMATION OF BINARY ALLOYS

Marian Smith and Ralph Hultgren

Borelius[1] has proposed a zeroth approximation for the heat of formation of a binary alloy based on the bonding energies of groups of four atoms in the combinations A_4, A_3B, A_2B_2, and B_4. For a random solid solution, this leads to the expression

$$\Delta H = 4\,ax^3y + 6bx^2y^2 + 4cxy^3 ,$$

where ΔH is the heat of formation, x and y are the atom fractions of the components, and a, b, and c are constants.

Selected values[2] for the heats of formation of 74 binary alloy systems were fitted to the Borelius equation using a method of least squares with the aid of an IBM 7090 computer. For all cases, the data fit the equation very well, the average deviation for each system being less than the estimated uncertainty in the data.[2] The usual quasi-chemical treatment in which

1. G. Borelius, Ann. Physik 24, 32 (1935); 28, 507 (1937).
2. Ralph Hultgren, R. L. Orr, P. D. Anderson, and K. K. Kelley, Selected Values of Thermodynamic Properties of Metals and Alloys (John Wiley and Sons, Inc., New York, 1963).

nearest-neighbor bonds are considered (i.e., atoms are counted two at a time) yields one empirical constant and a symmetric dependence of ΔH on composition, which is not followed by the majority of alloy systems. The three empirical constants contained in the Borelius equation provide the flexibility for a much better fit.

The Borelius equation is useful because it provides a means of comparing different alloy systems even when the experimental results do not cover the same compositions. Attempts to demonstrate physical significance for the constants--e.g., in connection with ordered states--have not been encouraging.

6. EVALUATION OF THERMODYNAMIC DATA FOR METALS AND ALLOYS

Marian Smith, Raymond Orr, and Ralph Hultgren

The results of the first phase of the project for the compilation and critical evaluation of published thermodynamic data for metals and alloys has been published in book form.[1] Included are tables of selected values and critical discussions of data for 63 metallic elements and 168 binary alloy systems. The project has been continued and extended to include several nonmetallic elements, e.g. B, C, Si, Ge, As, Se, and Te. Limited data available for the actinide series elements have also been evaluated. The appearance of new data, especially for alloys, requires continuing additions to and revisions of the evaluations already completed.

A new Termatrex system of bibliography coding and searching has been installed. The entire reference file has been transferred to the new system, which permits all references in the file to a specific system or topic to be quickly located. On a trial basis, limited bibliographies of references to thermodynamic or phase diagram data for specified systems are being provided to responsible laboratories which require them. The bibliographies consist of Xerox copies of file cards which often include abstracts.

---

1. Ralph Hultgren, R. L. Orr, P. D. Anderson, and K. K. Kelley, Selected Values of Thermodynamic Properties of Metals and Alloys (John Wiley and Sons, Inc., New York, 1963).

7. HIGH-TEMPERATURE HEAT CONTENT OF NIOBIUM*

Donald Hawkins, Raymond Orr, and Ralph Hultgren

Growing interest in niobium as a high-temperature refractory metal plus the availability of a sample of high purity (99.99+ %) material made it desirable to determine the high-temperature thermal properties of niobium by means of heat content measurements. Previously reported data of the high-temperature thermal properties by Jaeger and Veenstra,[1] (H_T-H_{295}, 670°-1828°K), Lowenthal,[2] (Cp, 1471°-2259°K) and Gel'd and Kusenko,[3] (H_T-H_{298}, 433-1840°K), are not in agreement. The present heat content measurements (H_T-H_{298}) were made over the temperature range 298° to 1415°K with a diphenyl ether Bunsen-type drop calorimeter,[4] designed expressly for studying small metallic specimens.

The results are well represented by the analytical expressions

$$H_T - H_{298.15} = 6.564\ T - 1.81 \times 10^{-4} T^2 + 5.12 \times 10^{4}\ T^{-1} - 2113 \quad (298°\text{-}500°K),$$

$$H_T - H_{298.15} = 5.672\ T + 5.06 \times 10^{-4} T^2 - 1736 \quad (500°\text{-}1400°K).$$

The data join smoothly in both Cp and (dCp/dT) with reported low-temperature Cp data.[5] Heat content values of Jaeger and Veenstra are about 0.5% lower than those found here, while those of Gel'd and Kusenko are from 1% to 3% high. Cp values of Lowenthal obtained from optical-emission measurements appear to be about 3% high.

---

* Extract from paper submitted to J. Chem. Eng. Data.

1. F. M. Jaeger, and W. A. Veenstra, Rec. Trav. Chem. 53, 677 (1934).
2. G. C. Lowenthal, Australian J. Phys. 16, 47 (1963).
3. P. V. Gel'd and F. G. Kusenko, Izv. Akad. Nauk SSSR, Otd. Tekhn. Nauk Met. i. Toplivo, 2, 79 (1960).
4. Ralph Hultgren, Peter Newcomb, Raymond Orr, and Linda Warner, Phys. Chem. Metallic Sol., Natl Phys. Lab. Symposium, Teddington, Middlesex, England, No. 9, Vol. 1, Paper 1H, 8pp., 1959.
5. K. P. Clusius, P. Franzosini, and V. Piesbergen, Z. Naturforsch. 15, 728 (1960).

8. THE ACTIVATION ENERGY FOR THE SUBLIMATION OF GALLIUM NITRIDE*

Zuhair A. Munir+ and Alan W. Searcy

In 1932, Johnson et al.[1] reported that gallium nitride sublimes without decomposition at temperatures in excess of 800°C. Recently, Sime and Margrave[2] measured the vapor pressure of gallium nitride by a transpiration

---

* Abstracted from Zuhair A. Munir, The Activation Energy for the Sublimation of Gallium Nitride (Ph.D. Thesis), UCRL-10702, March 1963.

+ Now at San Jose State College, San Jose, California.

1. W. Johnson, J. Parsons, and M. Crew, J. Phys. Chem. 36, 2651 (1932).
2. R. Sime and J. Margrave, J. Phys. Chem. 60, 810 (1956).

method and concluded from their experimental results, estimated free-energy functions, and the heat of formation, that the vapor species above the solid is a polymer (GaN) (g).

The present research has proved that no gallium nitride molecules are present. However, the kinetics of sublimation of gallium nitride proved to be extremely interesting and we have measured the heat of activation and entropy of activation for sublimation.

Gallium nitride was prepared by the action of ammonia gas on liquid gallium at temperatures between 900 and 1000°C. Preliminary vapor pressure measurements were made by using a torsion-effusion cell with 2.5-mm-diam orifices. X-ray analysis showed that under these conditions, only gallium nitride remained in the cell after heating, indicating that the gallium nitride sublimed consequently. The total pressures obtained in these runs with 2.5-mm effusion holes lay slightly below the vapor pressure of elemental gallium, and far below the nitrogen pressures reached in the gallium nitride decomposition studies of Lorenz and Binkowski.[3] Thus, the pressures measured in the cell with 2.5-mm-diam holes must be nonequilibrium values. Theoretical calculations show that the effusion holes would have to be impracticably small in order to approach equilibrium pressures in the cell.

The vapor species above gallium nitride were identified with an Inghram-type mass spectrometer at several temperatures corresponding to the temperature range of the proposed vapor pressure measurements. The principal ions detected were N_2^+ and Ga^+ with minor amounts of Ga_2^+ and Ga_2O^+. The latter were usually less than 2% of the total Ga^+ intensity. No peaks that could be attributed to gallium nitride molecules were observed.

Solid gallium nitride wafers were prepared at room temperature under pressures of 1.5×10^6 psi. Using these wafers in place of orifices in the side walls of the torsion-effusion cells, free surface sublimation was studied. This method may be designated as the torsion-Langmuir method. Microscopic examination of the wafers under 200 X magnification showed no pores. Similarly, no discernible change in the contour of the surface was observed when a sample wafer was heated at 1200°C for 1 hour.

Deflection measurements on the torsion-Langmuir cell were made at temperatures from 1166 to 1428°K. Figure IIF.8-1 shows the free surface vapor pressure as a function of 1/T. Least-square treatment yielded the expression (P in atm.)

$$\log P = 5{,}28 - 15{,}400/T.$$

3. M. Lorenz and B. Binkowski, J. Electrochem. Soc. 109, 24 (1962).

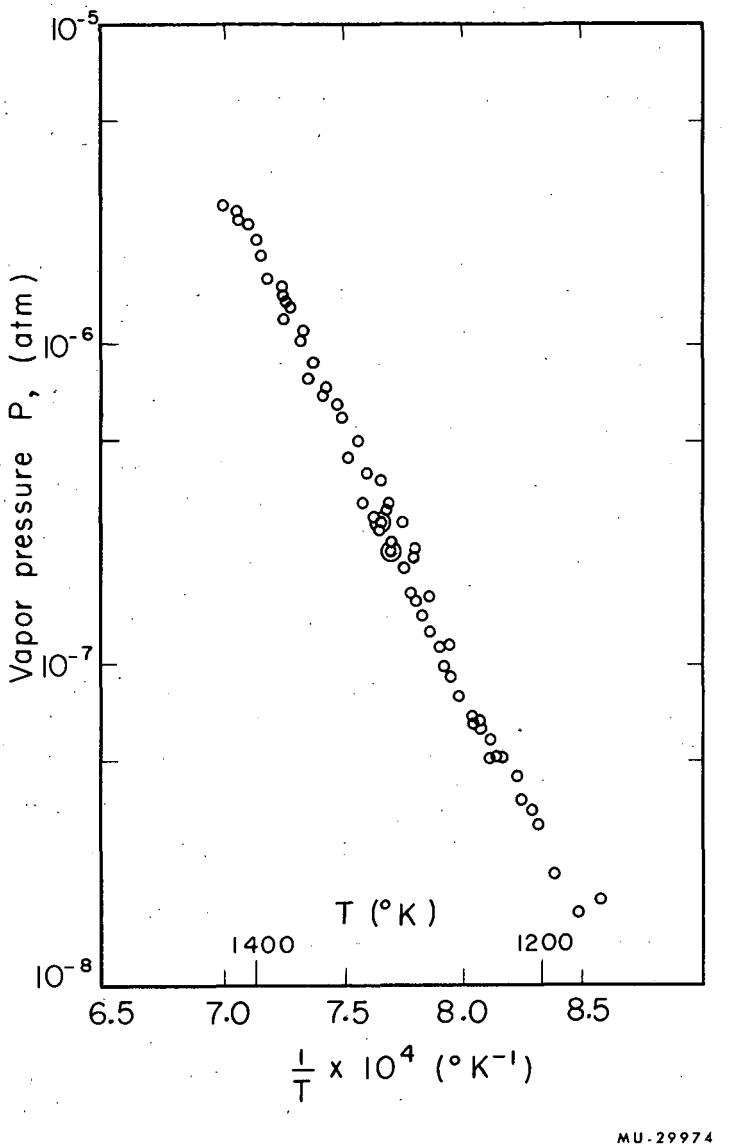

Fig. IIF. 8-1 Vapor pressure of gallium nitride: torsion-Langmuir method.

The data led to the expression

$$\text{Log } Q = 7.92 - 23\,100/T$$

for the reaction $GaN(s) = 1/2\ N_2(g) + Ga(g)$, where Q is $P_{N_2}^{1/2} \cdot P_{Ga}$. The activation energy for the sublimation of gallium nitride was calculated by using both the second-law and third-law methods. The second-law heat of activation was calculated to be $\Delta H_{298} = 106$ kcal/mole, and the entropy was calculated to be 54.85 eu. Third-law calculations based on the assumptions that the activated complex was the free vapor species and that the free energy function for GaN(s) is the same as that of ZnO(s) gave $\Delta H_{298} = 127.50$ kcal/mole for the heat of activation and $\Delta S_{298} = 52.92$ eu for the entropy of activation.

The equilibrium constant for the reaction $GaN(s) = Ga(g) + 1/2N_2(g)$ as calculated from thermodynamic data is about 5×10^{-5} at 1400°K. The apparent equilibrium constant calculated from our Langmuir data is only 3×10^{-9}. The marked difference between the apparent equilibrium constants for sublimation measured under Langmuir conditions and those measured in Knudsen cells demonstrates the existence of a high free-energy barrier to the sublimation process.

9. THE SUBLIMATION OF INDIUM SESQUISULFIDE

Alan R. Miller[+] and Alan W. Searcy

Sublimation pressures were measured for indium sesquisulfide between 950 and 1130°K by the Knudsen effusion method, and the composition of the vapor was investigated with a mass spectrometer. The solid sublimes almost exclusively by the reaction $In_2S_3(s) = In_2S(g) + S_2(g)$, for which ΔH_{298} is calculated to be 147.4±3 kcal. The equilibrium constant is given in the experimental range by the equation - log K = 30 600/T - 17.94. The heat of formation of $In_2S(g)$ at 298°K is calculated to be + 14.5±5 kcal. The free-surface sublimation rate is above 0.01 times the equilibrium rate at 1000°K.

---

* Extract from Alan R. Miller and Alan W. Searcy, J. Phys. Chem. 67, 2400 (1963).

+ Now at Aerojet General Nucleonics, San Ramon, California.

10. IONIC MODEL CALCULATIONS OF THE STABILITIES OF GASEOUS ALKALINE EARTH MONOHALIDE MOLECULES

Gary D. Blue

Recent thermochemical investigations[1-3] have yielded values for the dissociation energies of the gaseous alkaline earth monofluoride molecules. These values are, with one possible exception,[4] much greater than the old values based on rather unreliable extrapolations of spectral data.[5,6]

A previous attempt to determine the binding energies of these monofluoride molecules by use of an ionic model due to Rittner[7] was very encouraging, especially for the monofluorides of the heavier alkaline earth metals. In the research presented here an attempt has been made to improve the values of the metal ion polarizabilities used in the calculations and to extend the method to the remainder of the alkaline earth monohalides for the purpose of predicting the stabilities of these molecules, which may be of importance in some high-temperature systems, especially under reducing conditions.

The alkaline earth metal ion polarizabilities were improved by correcting the previously calculated values[3] by comparison with the ratio of the known values[8] to the calculated values (obtained from the same approximation formula) for the isoelectronic alkali metal atoms. Values of most of the other parameters needed for the calculations were available in standard sources. However, it was necessary in many cases to estimate the bond distance in the monohalides as being 97% of the distance in the corresponding dihalides.[9,10]

---

1. M. A. Greenbaum, R. E. Yateo, M. L. Arin, M. Arshadi, J. Weiher, and M. Farber, J. Phys. Chem. 67, 703 (1963).
2. G. D. Blue, J. W. Green, R. G. Bautista, and J. L. Margrave, J. Phys. Chem. 67, 877 (1963).
3. G. D. Blue, J. W. Green, T. C. Ehler, and J. L. Margrave, Nature 199, 804 (1963).
4. M. M. Novikov, and L. M. Tunitskii, Opt. Spectr. (USSR) 8, 396 (1960).
5. A. G. Gaydon, Dissociation Energies (Chapman and Hall, Ltd., London 1953).
6. G. Herzberg, Molecular Spectra and Molecular Structure, I. Spectra of Diatomic Molecules (D. Van Nostrand Co., Inc., New York, 1953).
7. E. S. Rittner, J. Chem. Phys. 19, 1030 (1951).
8. A. Dalgano, Advan. Phys. 11, 281 (1962).
9. E. Morgan and R. F. Barrow, Nature 185, 754 (1960); 192, 1182 (1961).
10. Leo Brewer, G. R. Somayajulu, and Elizabeth Brackett, Thermodynamic Properties of Gaseous Metal Dihalides, UCRL-9840, Sept. 1961.

The dissociation energies obtained from the ionic model are shown in Table IIF.10-1. Values from several other methods are shown for comparison. The stabilities predicted by the ionic model show the expected trends and are in excellent agreement with the thermochemical results for the monofluorides. It is felt that an upper limit on the dissociation energy is set by the average bond energy in the dihalide and that a lower limit is given by the ionic model calculation, which probably closely approximates the true dissociation energy for the more ionic molecules.

11. SUBLIMATION AND THERMODYNAMIC PROPERTIES OF ZINC OXIDE*

Donald F. Anthrop† and Alan W. Searcy

Brewer and Mastick[1] concluded in 1951 that under neutral conditions zinc oxide sublimes congruently by decomposition to the gaseous elements according to the reaction,

$$ZnO(s) = Zn(g) + \tfrac{1}{2}\, O_2(g) \ . \qquad (1)$$

Brewer calculated a limit of $\Delta H_0^\circ < 92$ kcal/mole for ZnO(s).[2] Several investigators studied the rate of sublimation of zinc oxide in various environments and reported general agreement with the rate calculated from the thermodynamic data for Reaction (1), except in an atmosphere of zinc vapor.[3-5] Two of these investigators proposed that the sublimation of zinc oxide by Reaction (1) is catalyzed by zinc vapor. Since this proposal is at variance with accepted theory and with experimental evidence for other systems, the study reported here was undertaken.

Knudsen Effusion Studies

Zinc oxide was shown in a mass spectrometric study (see below) to sublime only to zinc atoms and oxygen molecules. Since the ratio of zinc atoms to oxygen molecules in the vapor must therefore be 2/1, the partial pressures of oxygen and zinc in equilibrium with zinc oxide can be calculated from Knudsen weight-loss determinations. Measurements were made in alumina and silica effusion cells. The effusion cell assembly was inductively heated in a glass vacuum system.

---

*Abstracted from Donald F. Anthrop, Vaporization and Thermodynamic Properties of Zinc Oxide (Ph.D. Thesis), UCRL-10708, May 1963.

† Now at Avco Corporation, Wilmington, Massachusetts.

1. L. Brewer and D. F. Mastick, J. Chem. Phys. 19, 834 (1951).
2. L. Brewer, Chem. Revs. 52, 1-75 (1953).
3. W. J. Moore and E. L. Williams, J. Phys. Chem. 63, 1516 (1959).
4. E. A. Secco, Can. J. Chem. 38, 596 (1960).
5. T. C. M. Pillay, paper presented at Electrochem. Soc. Symposium on High-Temperature Chemistry, Los Angeles, May 1962.

Table II F.10-I. Dissociation energies of gaseous alkaline earth monohalides

Gaseous molecule MX	Repulsive constant (a) ρ (Å)	Coulomb term (b) $\frac{e^2}{re}$ - I,+E(ev)	Ionic model (This work) D(MX)(ev)	Valence-state hypothesis (c) D(MX)(ev)	Avg. bond energy (d) $\frac{1}{2}\Delta H_A(MX_2)$(ev)	Spectroscopic D(MX)(ev)	Thermochemical D(MX)(ev)
BeF	0.192	4.76	6.24	4.81	6.50	4.0[e],5.4[f],8.0[g]	6.29[i]
BeCl	0.238	2.97	4.20	3.13	4.81	3.0[e],4.3[f],5.9[h]	
BeBr	0.264	2.02	2.94	2.42	4.11		
BeI	0.295	0.88	1.53	1.57	3.26		
MgF	0.243	4.18	4.64	3.92	5.50	3.2[e],4.2[f]	4.60[j]
MgCl	0.291	2.72	3.04	2.64	4.21	2.7[e],3.2[f]	
MgBr	0.309	2.21	2.49	1.94	(3.51)	<3.35[f]	
MgI	0.337	1.44	1.68	1.17	2.75		
CaF	0.274	4.63	5.44	4.73	5.81	<3.15[f]	5.44[j,k]
CaCl	0.318	3.60	4.10	3.68	4.75	<2.76[f]	
CaBr	0.332	2.96	3.39	3.08	4.15	2.9[f]	
CaI	0.353	2.21	2.59	2.32	(3.40)	2.8[f]	
SrF	0.287	4.67	5.46	4.73	5.75	2.7[e],3.5[f]	5.45[j]
SrCl	0.329	3.69	4.18	3.85	(4.86)	2.5[e],3.0[f]	
SrBr	0.344	3.08	3.49	3.21	4.22	2.8[f]	
SrI	0.367	2.39	2.75	2.47	(3.48)	2.2[f]	
BaF	0.299	4.88	5.84	5.16	6.05	3.8[f]	5.80[j]
BaCl	0.337	3.87	4.45	4.21	5.09	2.7[f]	
BaBr	0.348	3.27	3.77	3.57	4.45	2.8[f]	
BaI	0.369	2.62	3.06	2.86	(3.75)		

(The superscript lower case letters refer to references for this table)

[a] Ref. 7

[b] J. L. Margrave, J. Phys. Chem. 58, 258 (1954); different values of re are used in many instances in calculating these values.

[c] H. A. Skinner, Trans. Farad. Soc. 45, 20 (1949).

[d] Ref. 10

[e] Ref. 5

[f] Ref. 6

[g] V. M. Tateuskii, L. M. Tunitskii, and M. M. Novikov, Opt. Spectr. (USSR) 5, 521 (1958).

[h] Ref. 4

[i] Ref. 1

[j] Ref. 3

[k] Ref. 2

Data obtained with the alumina cell are shown in Fig. IIF.11-1. Pressures inside the cell were calculated from the weight loss through an orifice by means of the Knudsen equation.[6,7] The last four measurements were made with some silica mixed with the zinc oxide sample, because it had been observed that silica, present as particles or as the container, reduced the evaporation rate of zinc oxide. The Knudsen studies proved that under neutral conditions the vaporization rate for zinc oxide is exactly that expected from thermodynamic data on the assumption that Reaction (1) is the only vaporization reaction.

Mass Spectrometric Investigation

A high-temperature mass spectrometer was used to determine the vapor species in equilibrium with solid zinc oxide at background pressures below 10^{-6} torr. The cells from the weight-loss studies were used in the spectrometer as well.

Determination of the rate of effusion from the cells by means of the weight-loss experiments, coupled with the knowledge that the oxide sublimes congruently at a Zn/O_2 ratio of 2/1, allowed calibration of the spectrometer intensities vs pressures for zinc and oxygen with an uncertainty of less than 20%. No gaseous zinc oxide molecules of any kind were detected. Upper limits were calculated for the pressures of $Zn_2O(g)$ and $ZnO(g)$. From these limits dissociation energies of $D^o_{298} \leq 127$ and ≤ 66 were calculated for $Zn_2O(g)$ and $ZnO(g)$, respectively. To investigate the effect of zinc vapor on the dissociation of zinc oxide, zinc oxide was heated with a 40% zinc-60% gold alloy in the mass spectrometer. The results showed no change in evaporation rate of ZnO due to the presence of zinc vapor.

Transport Studies

Re-examination of zinc oxide sublimation in a tube furnace in a dried helium carrier gas, sometimes with liquid zinc and sometimes with iron wire present in the furnace, at 1056°C resulted in the data shown in Table IIF.11-1.

The explanation of the conflicting data reported by other investigators was revealed by the tube furnace experiments with the iron wire. Cubicciotti had suggested that water vapor, present despite normal drying procedures, might produce the observed zinc oxide volatilization.[8] Our substitution of iron wire for zinc was designed to test this hypothesis. Iron has a negligible volatility at the temperatures of the tube furnace experiments, but can reduce water to hydrogen, and carbon dioxide to carbon monoxide. The evaporation rates of zinc oxide obtained when iron wire was heated in the gas stream were comparable to those obtained when liquid zinc was present.

6. Joos, Theoretical Physics (Blackie and Son, Ltd., London, 1958), Chap. 34.
7. Leo Brewer, in Chemistry and Metallurgy of Miscellaneous Materials: Thermodynamics, L. L. Quill, Ed. (McGraw-Hill Book Co., Inc., New York, 1950).
8. D. D. Cubicciotti (Stanford Research Institute), private communication.

Table IIF. 11- I. Summary of tube furnace experiments

System studied	Time (h)	Temp (°C)	He flow rate (cm^3/min)	Wt. of Zn transported (g)	P_{Zn}	Wt. loss of ZnO (mg)	Wt. loss of ZnO (g/hr)	Calc. rate of loss of ZnO (g/hr)
ZnO	44.4	1056	77.0	-	-	3.8	8.56×10^{-5}	1.31×10^{-4}
ZnO + Zn	19.97	1019	64.8	3.0046	1.45×10^{-2}	387.6	1.94×10^{-2}	3.7×10^{-12}
ZnO + Fe	22.8	1019	75.8	-	-	128.7	5.64×10^{-3}	5.79×10^{-5}
ZnO + Fe	26.3	1006	65.2	-	-	152.8	5.81×10^{-3}	3.72×10^{-5}

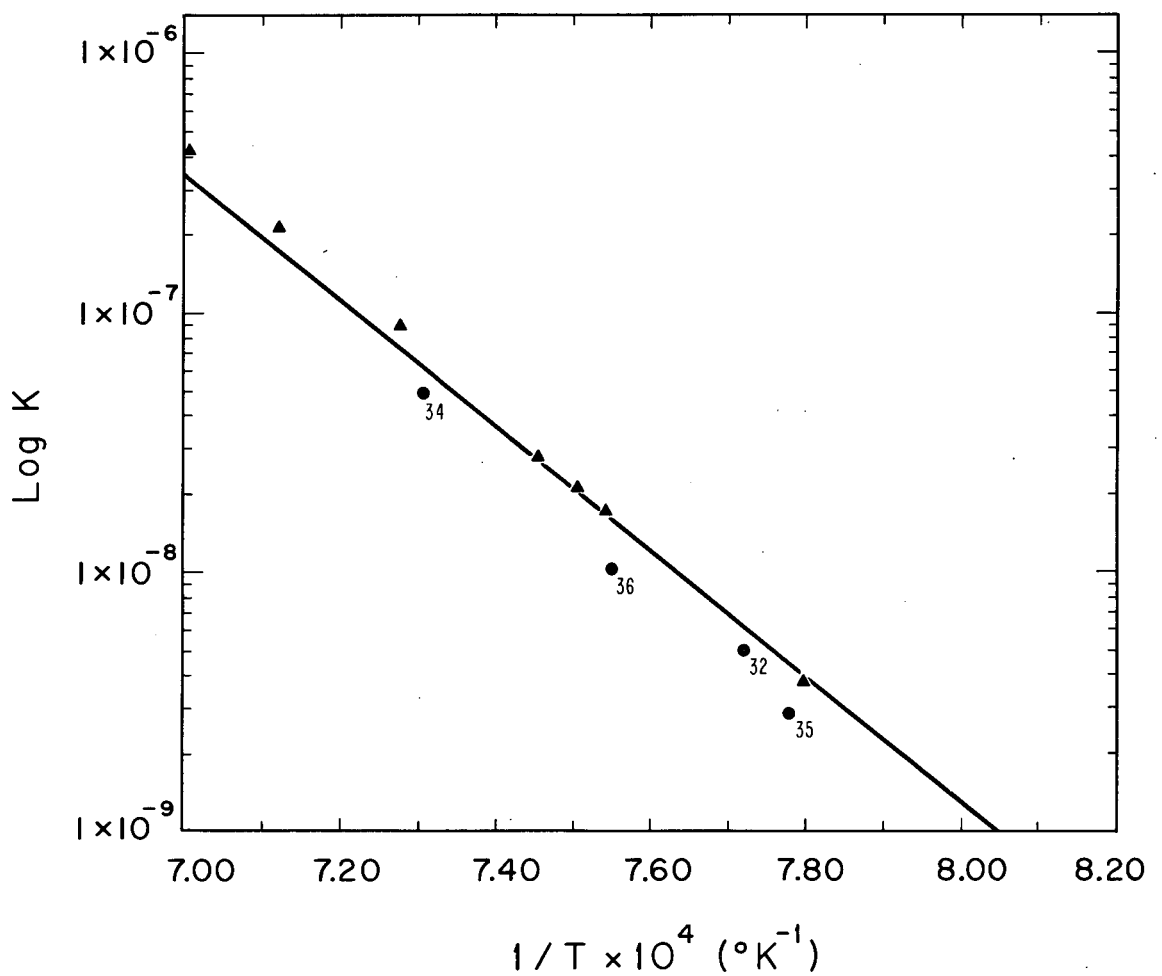

Fig. IIF. 11-1 The equilibrium constant for the reaction ZnO(s) = Zn(g) + $\frac{1}{2}$ O_2(g) measured in alumina cells. The solid triangles are experimental determinations on zinc oxide alone. The line is plotted from the free energy of the reaction ZnO(s) = Zn(g) + $\frac{1}{2}O_2$(g) that was calculated by Coughlin from the heats of formation of zinc oxide, the heat of vaporization of zinc, and from entropies and heat capacities. The numbered points were obtained when silica was added.

We conclude that when zinc is present in the cooler region of the furnace the reaction taking place is $H_2O + Zn(\ell) = ZnO(s) + H_2(g)$ or $CO_2 + Zn(\ell) = ZnO(s) + CO(g)$, or both, whereas in the hot region the hydrogen gas or CO (or both) reacts with the zinc oxide sample to yield zinc vapor and to regenerate $H_2O(g)$ or CO_2 (or both). Zinc vapor in the absence of a readily reducible gas and of a temperature gradient has no unusual effect on the rate of vaporization of zinc oxide.

12. TORSION-EFFUSION STUDY OF THE VAPOR PRESSURE AND HEAT OF SUBLIMATION OF GALLIUM*

Zuhair A. Munir† and Alan W. Searcy

Measurements of the vapor pressure of gallium have been reported by Harteck[1] and by Speiser and Johnston[2] who employed the Knudsen effusion method using quartz effusion cells. Recently, Cochran and Foster investigated the apparent vapor pressure of gallium in alumina Knudsen cells with and without added silica or magnesia.[3] Apparent pressures obtained with silica present agreed well with the pressures of Harteck and of Speiser and Johnston, but pressures measured when only gallium was present were four-to fivefold lower. Cochran and Foster concluded that the previous studies in quartz were erroneous because of the reaction $2Ga(\ell) + SiO_2(c) = SiO(g) + Ga_2O(g)$, and further concluded that the vapor pressure of gallium is lower by about a factor of 4 than previously reported.

We here report a redetermination of the vapor pressure of gallium by the torsion effusion method,[4] using a graphite container. Drowart and Honig have demonstrated that gallium atoms are the only major vapor species when gallium is heated in graphite.[5] Our results are in disagreement with the results of Cochran and Foster.

Figure IIF.12-1 shows the data measured with two orifices (25 mm and 10 mm diam). The least-square method gave a second-law heat of sublimation of $\Delta H_{s,298} = 64.3$ kcal/mole. Third-law calculations using free-energy functions selected by Hultgren[6] yielded $\Delta H_{s,298} = 65.44 \pm 0.23$ kcal/mole. The third-law analysis gave the following expression for the vapor pressure of gallium, in atmospheres, between 1174 and 1603°K,

$$\log P = 5.458 - 13,743/T \ .$$

Our third-law value of $\Delta H^\circ_{s,298} = 65.44$ kcal/mole is significantly lower than the value of 68.96 kcal/mole reported by Cochran and Foster.[3]

It is not possible to explain the discrepancy between this work and that reported by Cochran and Foster as resulting from the presence of volatile impurities in our present investigation. Mass spectrometric studies conducted

*Abstracted from Zuhair A. Munir, The Activation Energy for the Sublimation of Gallium Nitride (Ph.D. Thesis), UCRL-10702, March 1963; submitted for publication in J. Electrochem. Soc.

† Now at San Jose State College, San Jose, California

1. P. Harteck, Z. Physik. Chem. 134, 1 (1928).
2. R. Speiser and H. L. Johnston, J. Am. Chem. Soc. 75, 1469 (1952).
3. C. N. Cochran and L. M. Foster, J. Electrochem. Soc. 109, 144 (1962).
4. M. Vollmer, Z. Physik. Chem., Bodenstein Festband 863 (1931).
5. J. Drowart and R. E. Honig, Bull. Soc. Chim. Belges 66, 411 (1957).
6. R. Hultgren, R. L. Orr, P. D. Anderson and K. K. Kelley, Selected Values of Thermodynamic Properties of Metals and Alloys (John Wiley and Sons, Inc., New York, 1963).

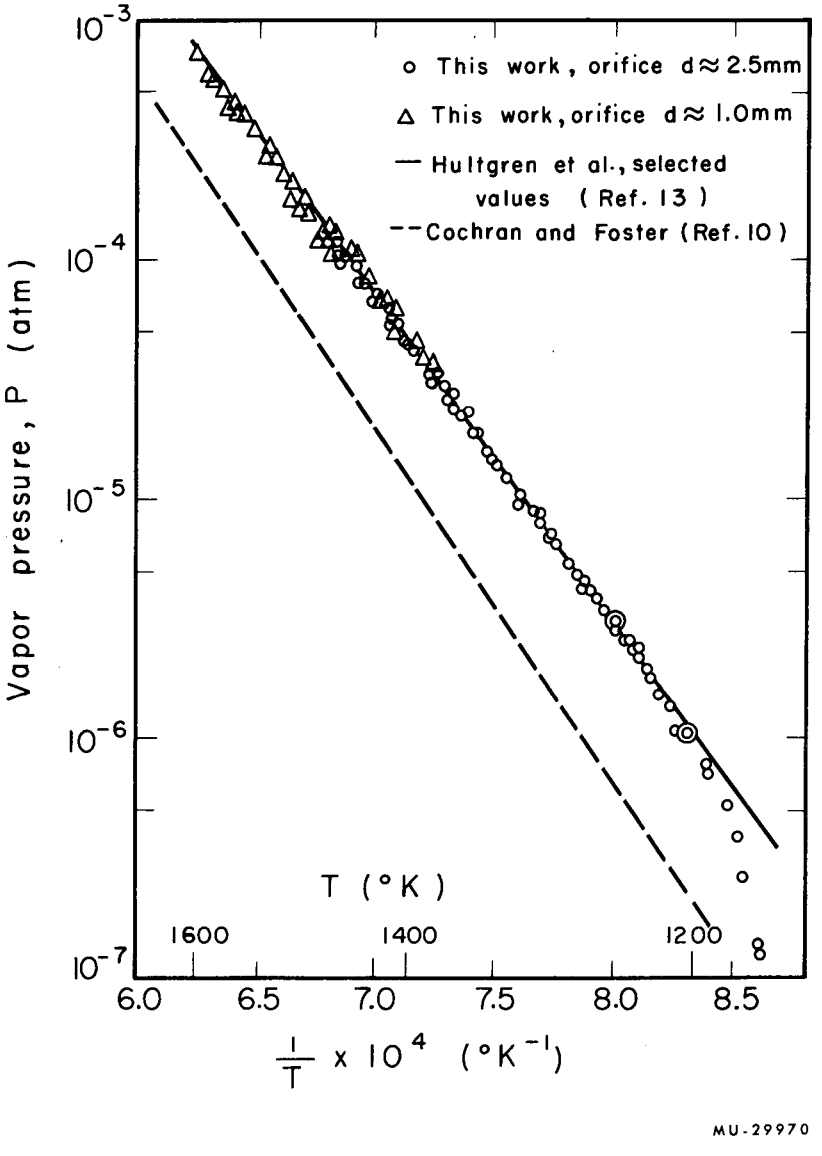

Fig. IIF. 12-1 Vapor pressure of gallium (ℓ).

in a graphite cell under conditions very similar to the conditions during the torsion-effusion pressure studies showed that the ratio of Ga/Ga_2O is greater than 50. No other impurities were found. The possibility of a systematic error was checked by redetermining the vapor pressure of tin in the temperature range used for the gallium measurements. The results were in excellent agreement with the best literature values.[6,7]

7.D. A. Schultz (Ph.D. Thesis), University of California, Berkeley, 1961.

13. VAPOR PRESSURE AND HEAT OF SUBLIMATION OF BARIUM FLUORIDE

Patrick E. Hart and Alan W. Searcy

Only limited vapor pressure data have been available for barium fluoride. Ruff and LeBoucher[1] obtained pressures between 1960 and 2206°K by use of a dynamic method. Blue et al.[2-4] used a mass spectrometer to obtain vapor pressure data by the Knudsen method at temperatures between 1232 and 1505°K. The mass spectrometer pressures were normalized to agree with free-surface weight loss studies. The normalized pressures were used to calculate the heat of sublimation at 298°K by the third-law method. Pressures were calculated from the weight loss study by means of the Langmuir equation with the assumption that the sublimation coefficient was unity. Therefore, the pressures calculated in neither the Langmuir study nor in the mass spectrometer study would be equilibrium values if the sublimation coefficient of barium fluoride were less than unity. It therefore seemed desirable to measure pressures for barium fluoride in the temperature range of the Langmuir study by a method that clearly gives equilibrium data.

Experimental Procedure

The vapor pressure of barium fluoride was determined by the torsion effusion method that has been described by Schulz and Searcy[5] and others.[6,7]

*Abstracted from Patrick E. Hart, Vapor Pressure and Heat of Sublimation of Barium Fluoride (M.S. Thesis), UCRL-11124, Jan. 1963.

1.O. Ruff and L. LeBoucher, Z. anorh. Chem. 219, 376 (1934).
2.G. D. Blue, J. W. Green, E. C. Ehler, and J. L. Margrave, paper presented to the Eleventh Annual Conference of Mass Spectrometry and Allied Topics, May 19-24, 1963, San Francisco.
3.J. W. Green, Ph.D. Thesis, University of Wisconsin, 1963.
4.R. G. Bautista and J. L. Margrave, private communication.
5.D. A. Schulz and A. W. Searcy, J. Phys. Chem. 67, 103 (1963).
6.H. Mayer, Z. Physik 67, 240 (1931).
7.M. Vollmer, Z. Physik. Chem., Bodenstein Festband, 863 (1931).

The graphite torsion cell was of match-box shape. Two different sets of orifices were used to measure pressures over a range of 10^{-7} to 10^{-4} atmosphere. For this work barium fluoride of optical quality was used. The cell was heated in a resistance furnace. The configuration of the hair-pin-shaped heating elements eliminated any residual deflection of the cell due to a directional magnetic field. Such fields have been troublesome in other work of this type.[5]

The pressures obtained are shown in Fig. IIF.13-1.

Results and Discussion

Molecular flow equations only apply when the mean free path, λ, is greater than the effusion orifice d. Therefore, pressures for which $\frac{\lambda}{d} < 0.5$ were excluded from the final calculation of $\Delta H°_{298}$ (Fig.IIF.13-1). A least-squares calculation for the data gives an expression of the form

$$\log P(\text{atm}) = \left(-\frac{78.70}{45.76} \pm 1.42 \right) \times \frac{10^4}{T} + 6.94 \pm 0.23$$

between 1261 and 1548°K. The heat of sublimation of barium fluoride at 298°K by both the second-law (sigma plot) and third-law method were calculated. In all calculations BaF_2 is considered to be the major vapor species. A least-squares calculation yields $\Delta H°_{298} = 87.06 \pm 1.45$ kcal/mole. A third-law calculation yields $\Delta H°_{298} = 90.29$ kcal/mole.

The results of this and earlier vapor studies are shown in Fig.IIF.13-1. Brewer et al.[8] suggest $\Delta H°_{298} = 88$ kcal/mole based on the earlier work of Ruff and LeBoucher. Blue, in the mass spectrometer study, found $\Delta H°_{298} = 92.3$ kcal/mole by the third-law method, using the same free-energy functions as were assumed in this work. Nearly the same temperature ranges were employed in the two studies. Therefore, the differences in the calculated heats of sublimation at 298°K reflect only the systematic differences in measurements and not possible errors in the free-energy functions. Apparently, a significant discrepancy exists between the results of this and the previous study of barium fluoride sublimation.

The difference in results obtained by the two techniques may indicate a systematic error in measurement of temperature, or may indicate that the Langmuir data with which Blue's measurements were normalized were not equilibrium measurements. A low sublimation coefficient for barium fluoride would cause Langmuir pressures to be less than the equilibrium pressures.

The best way to identify the source of the discrepancy appears to be to conduct Langmuir free-surface sublimation experiments in our torsion effusion apparatus. Errors in temperature measurements and other systematic errors will largely cancel when pressures are measured by effusion and by free-surface sublimation in the same apparatus. If lower apparent pressures are obtained in free-surface sublimation experiments than have been obtained in effusion experiments, a low sublimation coefficient can be concluded to characterize barium fluoride sublimation.

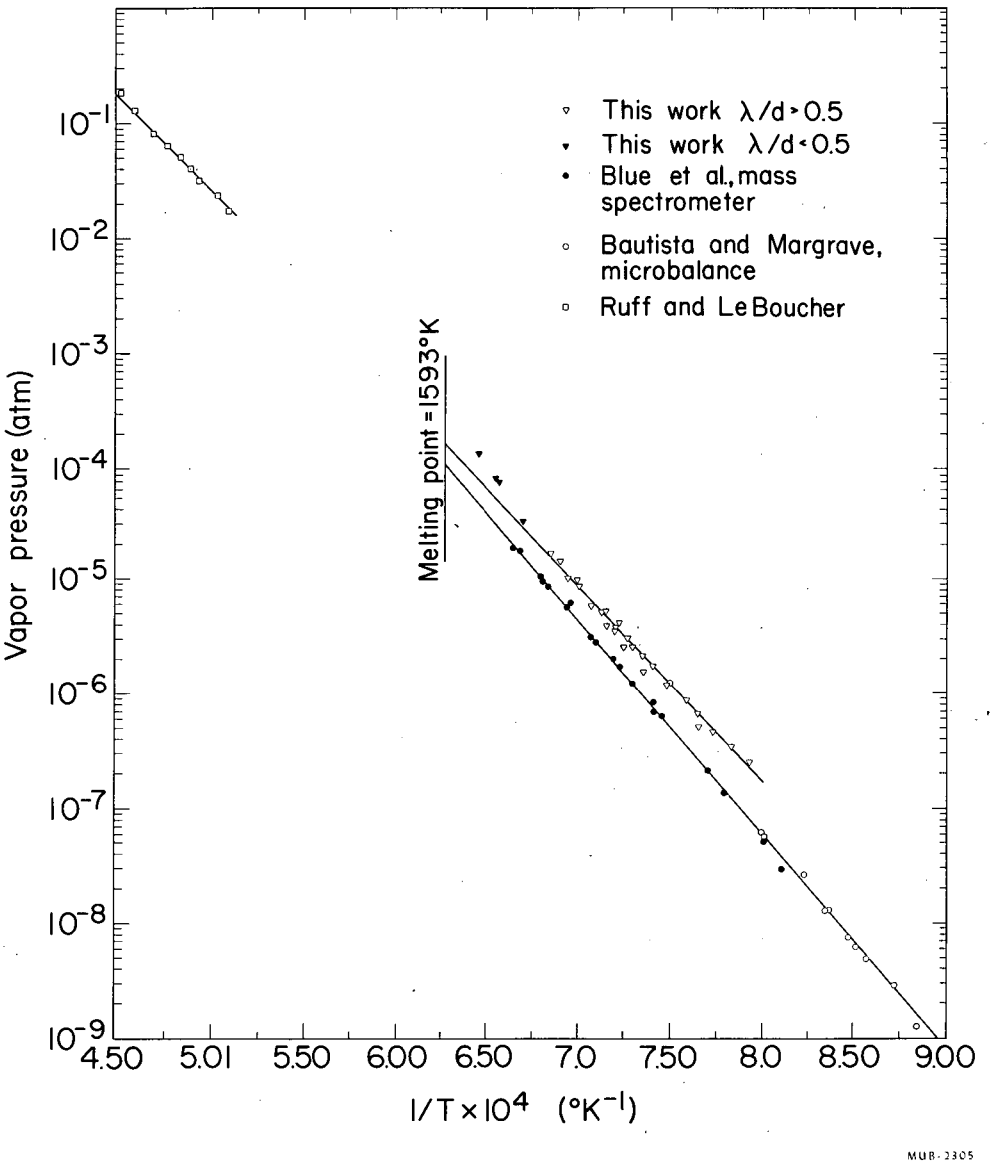

Fig. IIF. 13-1 Vapor pressure of barium fluoride.

14. THE VAPOR PRESSURE OF INDIUM SULFIDES AS A FUNCTION OF COMPOSITION AND TEMPERATURE*

Alan R. Miller† and Alan W. Searcy

It is usually essential for the determination of the partial pressures of vapor species in multicomponent phase systems by a dynamic method (such as the Knudsen effusion method) to choose conditions that yield pressures which do not change with time at constant temperature. Time-independent pressures for a two-component system can be obtained by bringing two condensed phases into equilibrium with the vapor. Some two-component single-phase systems have particular compositions that sublime congruently and that can also be studied by dynamic-pressure-measurement techniques. However, the pressures that characterize other single-phase compositions are not readily studied.

The major purpose of this study was to determine whether or not ion intensity-vs-time data obtained with a mass spectrometer can be used for continuous determination of composition-vs-pressure data in composition ranges in which compositions change with time of heating at constant temperature.

Indium sesquisulfide was chosen for the study because (a) we had previously obtained, as a function of temperature, reliable measurements of the total vapor pressure at the composition of congruent sublimation,[1] (b) the vapor pressure range is a convenient one for study with a high-temperature mass spectrometer, and (c) our preliminary investigations revealed the indium sesquisulfide phase to have a relatively wide solid solution range at high temperatures (this fact had not been recognized in previous investigations).

In this study the partial pressures of In_2S and S_2, the major vapor species, were measured as a function of temperature in the two-phase region on the indium-rich side of the indium sesquisulfide phase, and as a function of composition and temperature in the solid-solution region of the indium sesquisulfide phase.

X-Ray Diffraction Studies

Samples of composition between 41.5 and 42 at.% showed that x-ray diffraction pattern after heating to 600°C of a single phase with the known In_2S_3 pattern[2] but with a contraction in the unit-cell volume. The patterns of samples containing 43 to 45% indium indicated that two phases were present, one of which had the contracted In_2S_3 pattern. The other pattern matched that obtained from the sample quenched in the mass spectrometer at a time

---

* Abstracted from Alan R. Miller, (Ph.D. Thesis) UCRL-10857, Oct. 1963.
† Now at Aerojet General Nucleonics, San Ramon, California
1. A. R. Miller and A. W. Searcy, J. Phys. Chem. 67, 2400 (1963).
2. H. Hahn and W. Klingler, Z. anorg. Chem. 260, 97 (1949).

when the ion intensities were rapidly changing (46.5% In). From the diffraction-vs-composition studies, the maximum solubility of indium in the phase of ideal-composition In_2S_3 appears to occur at 42 at.% indium at the temperature of our experiments. The diffraction pattern of the sample of 46.5 at.% indium agreed in position and approximate intensities with the pattern of a phase previously reported to have the approximate formula In_5S_6.[3] For convenience in subsequent discussions, this phase will be designated InS_{1+}. The x-ray diffraction pattern of the 50 at.% indium sample (nominally InS) appeared to be that of a third single phase, and patterns of samples ranging from 46.5 to 50 at.% indium contained lines of both InS and InS_{1+}. The InS pattern, however, did not agree with the one reported by Schufle.[4] A sample of overall composition In_2S yielded the diffraction patterns of indium and of InS as found in this study.

Mass Spectrometer Studies

Indium-rich samples were heated at 600°, 650°, 700°, 750°, and 800°C; the sulfur-rich samples were heated at 600°, 650°, 700°, and 750°C. Several 40-at.% samples were heated to between 880° and 950°C. During each run the intensities of the ions In_2S^+ and S_2^+, the major vapor species, were alternately recorded on a strip chart until the ion intensities became constant with time.

Several samples, initially 50-at.% indium, were heated in the temperature range 600° to 750°C; all showed constant ion intensities at first, then a rapid change in intensities in a very short time period. The rapid change indicated that a narrow, single-phase region at 46.7 at.% In.

If the intensity of an ion that is produced from each major vapor species can be followed as a function of time at constant temperature, a pressure-vs-composition plot can be derived. The necessary constants can be evaluated for In_2S and S_2 by taking advantage of the circumstance that the partial pressure of each of these species is known at known compositions of congruent sublimation.

The Free Energy of Formation of In_2S_3 and InS_{1+}

The pressure-vs-composition curves derived from intensity-vs-time data were used to calculate the free energy of Reaction (1) as a function of composition for the indium sesquisulfide phase. Calculations were performed for the reaction

$$\frac{1-x}{2}\ In_2S(g) + \frac{3x-1}{4}\ S_2(g) = In_{1-x}S_x(s), \qquad (1)$$

where x is the atom fraction of sulfur. The results are shown in Fig. IIF.14-1 as solid lines.

In Reaction (1) the slope of $\Delta F°$ vs composition for In_2S_3 between 40 and 44 at.% should change smoothly with temperature and must always have

3. American Society for Testing Materials x-ray card 5-0429.
4. American Society for Testing Materials x-ray card 5-0722.

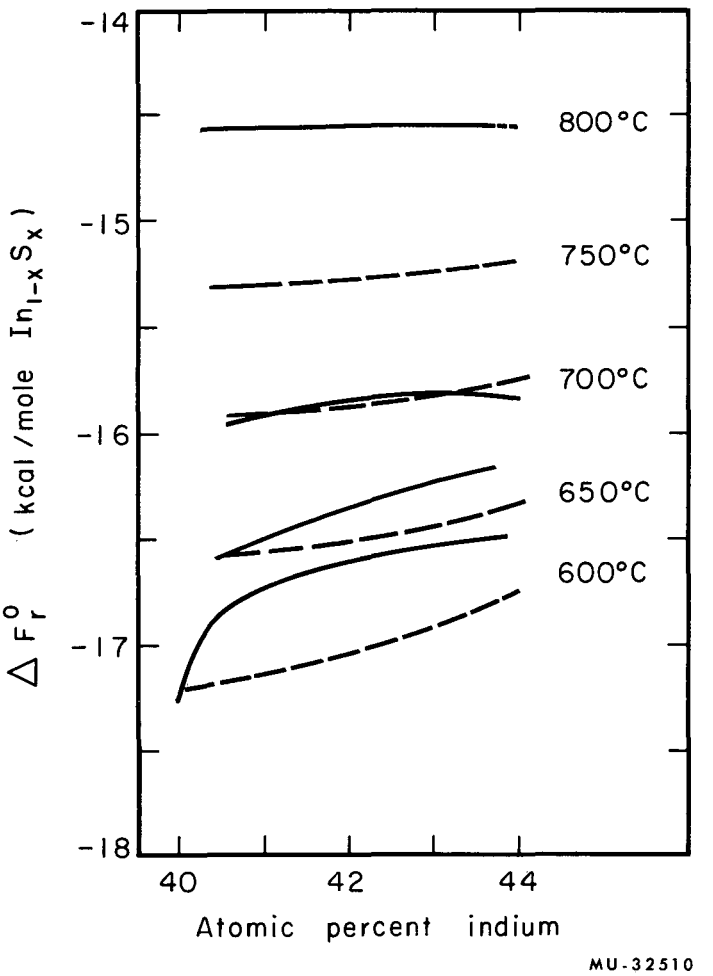

Fig. IIF. 14-1 Free energy of formation of indium sesquisulfide as a function of composition and temperature. Solid line calculated from experimental data. Dashed line calculated from solid curve at 800°C and the assumption of a single model described in text.

a positive curvature, instead of the negative curvature indicated by the experimental data at 600° and 650°C. In order to determine more definitely the change in slope with temperature, $\Delta F°$ was calculated at 600°, 650°, 700°, and 750°C and at various compositions between 40 and 44 at.% indium, from the experimental value at 800°C and with the assumption of a simple model for the entropy of formation (See Fig. IIF.14-1).

The calculated curves are, within the experimental error, in agreement with the curves of negative curvature that were calculated directly from the experimental data. These new calculated curves probably represent the true composition dependence of $\Delta F°$ for formation more correctly than the curves of negative curvature.

The heat and free energy of formation of InS_{1+} (approximately $In_{0.467}S_{0.533}$) were determined at 600°, 650°, 700°, and 750°C at the sulfur-rich boundary. Since the phase is only a few tenths of an atomic percent wide, ΔF and ΔH per gram atom must be essentially constant with composition across the phase. The results are shown in Table IIF.14-I.

Table IIF.14-I. The heat and free energy of formation of InS_{1+} (kcal/g atom).
$0.467\ In(\ell) + 0.266\ S_2(g) = In_{0.467}S_{0.533}(s)$

T(°C)	$-\Delta H°_f$	$-\Delta F°_f$
600	27.3	16.6
650	27.3	16.1
700	27.5	15.7
750	27.8	15.5

This study demonstrated that a mass spectrometer can be used for measurement of pressure-vs-composition data and for determination of variation in thermodynamic quantities with temperature as well as for determination of composition limits at high temperatures.

III. REACTOR MATERIALS

1. THE SOLUBILITY OF HELIUM IN UO_2

Firooz Rufeh, Donald R. Olander, and Thomas H. Pigford

An investigation of the diffusion of helium in UO_2 would provide a useful comparison to the more plentiful data on xenon and krypton diffusion in the same material. Although helium cannot be generated in the solid by uranium fission, it exhibits sufficient solubility in UO_2 at high gas pressures to permit study. In order to study the diffusion process, the solubility must be known, since this parameter constitutes one of the boundary conditions of the diffusion equation. Conversely, the quantity of helium absorbed by a sample in a finite time is less than the solubility, by an amount depending upon the diffusivity. In principle, a set of experiments can be designed to measure both the solubility and the diffusivity. In the work reported here, the former was measured with considerably greater precision than the latter.

A weighed amount of UO_2 (4 to 5 g) was held in a resistance furnace capable of helium pressures up to 100 atm and temperatures of 2000°C. The UO_2 was in the form of a powder consisting of ≈ 4-μ particles. The system was pressurized for times long enough to attain between 70 and 99% saturation. The samples were kept under vacuum for 2 months to remove any helium in open pores, then annealed at 300°C for several hours to remove adsorbed helium from the UO_2 surface. The sample was dissolved in a molten salt flux to release the contained helium (He^4), and a measured amount of He^3 was added to the gas. The gas mixture was analyzed mass spectrometrically for the ratio of He^3 to He^4, from which the average helium concentration in the solid could be determined. The measured helium content is less than the solubility by the factor

$$f = 1 - \frac{6}{\pi^2} \operatorname{erg}\left(-\pi^2 \frac{Dt}{a^2}\right), \qquad (1)$$

where f is the fractional saturation, D is the diffusivity of helium in UO_2, as is the particle radium (assumed spherical), and t is the time of pressurization. Equation (1) is the two-term approximation to the infinite-series solution of Fick's second law for spherical geometry.[1] For $f > 0.7$, neglecting the remaining terms introduces an error of less than 1%. The results are shown in Table III.1-I.

The precision of the data is estimated as ± 2%. The difference in the amount of dissolved helium in 46.9-hr Run 4 and 71.4-hr Run 6 is of this order of magnitude, and these two experiments represent the solubility of helium in UO_2 at 1200°C. The average of Runs 4 and 6 is 6.7×10^{-4}, which is

1. H. S. Carslaw and J. C. Jaeger, Conduction of Heat in Solids (Oxford University Press, London, 1959).

nearly an order of magnitude greater than the results of Bostrum extrapolated to 1200°C.[2] Comparison of Runs 4 and 5 shows that He-UO_2 obeys Henry's law within experimental precision. The heat of solution from Table III.1-I is ≈ 34 kcal/mole.

The diffusivity at 1200°C was roughly estimated by plotting the data of Table III.i-I and fitting the points with curves of the form of Eq. (1) for various values of D. The best estimate of the diffusivity is 1.5 ± 0.4 x 10^{-13} cm^2/sec.

Several experiments at 1500°C and 1800°C were attempted, but sintering of the UO_2 powder resulted in nonreproducible and anomalously high apparent solubilities, probably due to inclusion of helium during sintering.

Table III.1-I Helium dissolution in UO_2.

Run	T(°C)	P (atm)	Time (hr)	He dissolved[a]
1	1200	100	6.0	5.16×10^{-4}
2	1200	100	8.9	5.39×10^{-4}
3	1200	100	5.2	6.06×10^{-4}
4	1200	100	46.9	6.61×10^{-4}
5	1200	50	48.9	6.71×10^{-4}
6	1200	100	71.4	6.80×10^{-4}
7	1300	100	30.1	3.23×10^{-4}

[a] cc(STP) per g UO_2-atm

2. Bostrum, WAPD-183

2. PARTICLE-VOLTAIC EFFECT IN SEMICONDUCTORS

Allen R. Kirkpatrick, John G. Poksheva,
Lawrence D. Posey, and Thomas H. Pigford

An experimental study has been undertaken of the use of silicon and gallium arsenide large-area junction diodes as α-particle energy converters. The diodes under study are commercially available IRC p on n and n on p silicon solar cells, Hoffmann p on n solar cells, and RCA p on n gallium arsenide solar cells.

Irradiations have been performed with the IRC S0510E11 p on n cells at temperatures of 200°K and 275°K with α-particle energies of approximately 2.6 MeV, 3.3 MeV, and 4.3 MeV. The α particles are obtained from a 1.3-millicurie americium-241 source. Under irradiation the silicon solar cells yielded, initially, short-circuit currents of approximately 10^{-7} A, decreasing to values below 5×10^{-8} A at exposure times in excess of 3000 minutes at 275°K. The resulting decrease in short-circuit current at 200°K is less than at 275°K. Similar changes in performance during exposure are observed for the various α-particle energies employed. The energy-conversion efficiency of these cells is generally found to increase with decreasing temperature. The effect of α-particle radiation damage on these large-area junction devices is obtained from the changes in cell performance during exposure.

The effects of radiation damage are also obtained from observing exposure-induced changes in the dark-current-voltage characteristic of a cell. These characteristics are found to deviate from existing theoretical predictions; the deviation becomes more pronounced as the cell temperature is decreased.

Also under study is the energy loss mechanism for high-energy charged particles in semiconductors. The energy required to produce an electron-hole pair has been measured for α particles in silicon. The value obtained at 275°K, 3.5 eV, is in good agreement with previous measurements and theoretical predictions. Measurements at lower temperatures show that the existing theory cannot adequately explain the experimentally observed temperature dependence of the energy per electron-hole pair in silicon.

3. RELEASE OF FISSION GAS BY SIMULTANEOUS DIFFUSION AND EVAPORATION

Stephen D. Lowe, Paul L. Chambre, and Thomas H. Pigford

Isothermal postirradiation anneal experiments have been extensively used to determine diffusion coefficients for fission gases in nuclear fuel bodies. Several of these experiments have been carried out at temperatures sufficiently high for the fuel body to show an appreciable evaporation rate, but the effect of this evaporation upon the release of fission gas and upon the determination of diffusion coefficients has heretofore been neglected. We have carried out an analysis of the release rates to be expected when evaporation and diffusion occur simultaneously; this analysis permits a proper determination of the Fick's Law diffusion coefficient under such conditions.

For simplicity, we describe herein the analysis and results for slab geometry. A similar analysis for spherical geometry has also been completed.[1]

The rate of decrease in fission gas concentration C(x,t) within the sample is given by

$$\frac{\partial C(x,t)}{\partial t} = D\frac{\partial^2 C(x,t)}{\partial x^2}, \tag{1}$$

where D is the diffusion coefficient. The sample is exposed to vacuum in these experiments, so that the resulting boundary condition is

$$C\,[\,\pm(a-bt),t\,] = 0, \tag{2}$$

where a is the initial half-thickness of the sample and b is a constant rate of decrease in the half-thickness resulting from evaporation. For a spatially uniform initial (t=0) concentration of the diffusing species, the fraction f(t) of the initial amount of fission gas which has been released by time t due to simultaneous diffusion and evaporation is obtained by solving Eqs. (1) and (2):

$$f(t) = \beta\tau + 2\tau^{1/2}\,\mathrm{ierfc}\,\frac{\beta\tau^{1/2}}{2} + \tau^{1/2}\sum_{m=1}(4)^{m-1}\left(\frac{\beta\tau^{1/2}}{2}\right)^{m-1} i^m\mathrm{erfc}\frac{\beta\tau^{1/2}}{2}, \tag{3}$$

where $\beta = \frac{ba}{D}$,

and $\tau = \frac{Dt}{a^2}$.

Equation (3) has been obtained by restricting the general solution of $\tau < 0.01$ and $\beta\tau < 0.5$, which are the regions of interest in most postirradiation anneal experiments. The integral error functions are tabulated in Reference (2).

As shown in Fig. III.3-1, the fractional release is a linear function of $\tau^{1/2}$ for no evaporation ($\beta=0$). A very small but finite rate of surface evaporation can result in a more rapid increase of f with increasing $\tau^{1/2}$, which is consistent with observations in some high-temperature postirradiation anneal experiments.[3,4]

---

1. Stephen D. Lowe, Fractional Release of a Tracer Element Through a Moving Boundary (M.S. Thesis), UCRL-11097, Oct. 1963.
2. H. S. Carslaw and J. C. Jaeger, Conduction of Heat in Solids (Oxford University Press, London, 1959).
3. Hagai Shaked, Diffusion of Xenon in Uranium Monocarbide (Ph.D. Thesis), UCRL-10462, Nov. 1962.
4. G. Long, D. Davies, and J. R. Findlay, Diffusion of Fission Products in Uranium Dioxide and Uranium Monocarbide, TID-7610, Oct. 1960.

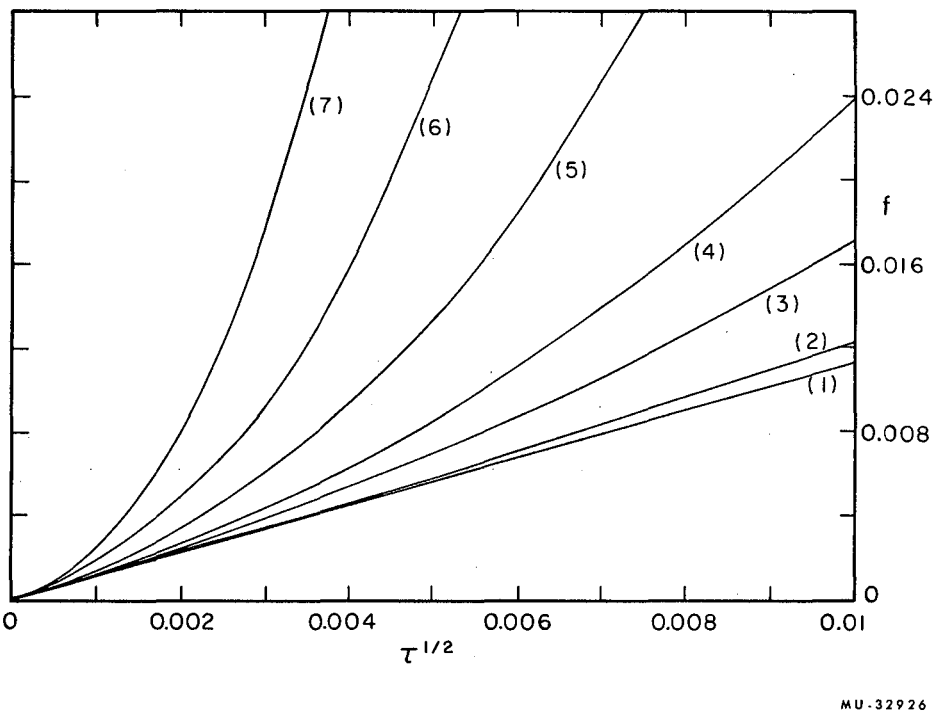

(1) β = 0 (no evaporation)
(2) β = 20
(3) β = 100
(4) β = 200
(5) β = 500
(6) β = 1000
(7) β = 2000

Fig. III. 3-1 Fractional release vs $\tau^{1/2}$ for various rates of evaporation.

For values of $\frac{\beta\tau^{1/2}}{2}$ less than ≈ 0.2, Eq. (3) may be further simplified to

$$f(t) = \tfrac{1}{2}\,\beta\tau + \frac{2}{\sqrt{\pi}}\,\tau^{1/2}, \qquad (4)$$

which is a form easily adaptable to predicting D from postirradiation anneal experiments. An equivalent equation for spherical geometry, where a now represents the initial radius, is found to be

$$f(t) = 3/2\ \beta\tau + \frac{6}{\sqrt{\pi}}\,\tau^{1/2}.$$

For example, the diffusion coefficient for zenon in uranium monocarbide at 2040°C has been determined from a measured fractional release f of 5.2×10^{-3}, corrected for initial release, after an anneal time of 2.25×10^{4} sec.[3] Thermodynamic data[5] for uranium monocarbide at this temperature lead to a predicted surface disappearance rate b of 0.015 cm/hr if the sample is exposed to vacuum. The evaporation rate in the experiment cited was estimated to be only 3×10^{-5} cm/hr, because the sample was contained in a Knudsen effusion cell of small aperture. These data lead to a diffusion coefficient D of 4.1×10^{-12} cm^2/sec, as predicted from Eq. (5), which is 60% less than the value obtained if evaporation effects are not considered.

As a more extreme case, if the sample had been directly exposed to vacuum for the same period as above, a fractional release of 0.76 would be predicted from an equation equivalent to (3) which we have obtained for spherical geometry. If surface evaporation were ignored, the diffusion coefficient so predicted would be erroneously high by more than four orders of magnitude.

These examples illustrate the importance of either minimizing evaporation experimentally or taking it into account analytically, using the theory and equations summarized herein.

---

5. C. B. Alcock and P. Grieveson, A Study of Uranium Borides and Carbides by Means of the Knudsen Effusion Technique, IAEA, Vienna, May, 1962.

IV. CURRENT RESEARCH INTERESTS

Summaries of current research interests, as of January, 1964 under the direction of each principal investigator.

1. Leo Brewer

HIGH TEMPERATURE CHEMISTRY AND THERMODYNAMICS

a. The available data for nitrides, carbides, sulfides and halides of molybdenum have been critically evaluated, and estimated values have been tabulated when no data were available.[1,2] During the next two years, it is planned to consolidate these previous compilations, to bring them up to date, and to compile complete thermodynamic tables for molybdenum and its compounds.

b. The radiative lifetime apparatus is being used with various atomic light sources to excite different rotational and vibrational levels of the $^3\pi$ state of I_2 to determine the variation of lifetime with rotational and vibrational excitation and to measure the lifetimes of various electronic states of the alkali metals. Similar work is planned for LaO.

c. Studies of electronic spectra of Se_2 and Te_2 are continuing. Various sources of emission spectra of alkaline earth oxides are being investigated in an effort to analyze several known but uncharacterized bands of MgO and CaO which are predicted to be triplet systems. The Si_2 spectrum is also being examined for triplet systems.

The spectra of the alkaline earth monohalides are being examined in the infrared for evidence of predicted low-lying electronic states. The third group oxides are being examined for low-lying electronic states and in an effort to establish the group states of transition metal oxides.

d. An attempt will be made to develop new methods of analyzing electronic spectra. Absorption spectra of high-temperature molecular beams have been obtained in an effort to establish the ground states. The polarization of fluorescence from molecular beams will be examined in an effort to detect Q branches and heads. The possibility of exciting and studying electronic Raman spectra of molecular beams is being considered.

e. It has been found that sharp electronic spectra of high-temperature atoms and molecules trapped in rare gas matrices at liquid helium and liquid hydrogen temperatures can be obtained. Forbidden transitions such as the infrared vibration spectrum of S_2 can be seen in matrices.[3] The spectra of a variety of high-temperature molecules in rare gas as well as polar matrixes are being studied.

---

1. L. Brewer, L. A. Bromley, P. W. Gilles and N. L. Lofgren, National Nuclear Series, Vol. 19B, Ed. by L. L. Quill (McGraw-Hill, New York, 1950), Papers 4 and 8.
2. L. Brewer, ibid, Paper 7.
3. B. Meyer, J. Chem. Phys. 37, 1577 (1962).

f. A bibliography of papers dealing with high-temperature vaporization processes and high-temperature spectra is being prepared for quarterly distribution by the National Bureau of Standards as an IUPAC function.

2. Robert E. Connick

KINETICS AND STOICHIOMETRIC STUDIES OF HYDRATED METAL IONS

The observation of the broadening of the O^{17} NMR resonance of water has yielded measures of very rapid rates of water exchange in and out of the first coordination sphere of a number of paramagnetic ions [Swift and Connick, J. Chem. Phys. 37, 307 (1962)]. This type of measurement will be extended to other magnetic cations and the temperature range covered by the original measurements will be broadened to yield additional information on exchange kinetics and the relaxation process. An extensive set of data should reveal the primary factors controlling these rates of exchange. The change in the water exchange rate brought about by complexing of the metal ion by ligands other than water is also being investigated.

Work has started on measuring the number of water molecules in the first coordination sphere of diamagnetic cations whose exchange is sufficiently slow to yield a separate O^{17} resonance for the bound water. In certain cases it will be possible to obtain rates of exchange from studies of temperature dependence.

Time permitting, determinations of oxygen bridging in hydrolyzed cationic polymers and poly acids will be attempted with the O^{17} NMR resonance.

3. John E. Dorn

KINETICS OF DISLOCATION MECHANISMS

The major objective of this research program in mechanical behavior is determination of the various dislocation mechanisms responsible for the plastic behavior of crystalline materials. This study requires consideration and development of suitable theories of dislocation mechanics, critical investigations of mechanical behavior of crystalline materials (particularly the determination of activation energies and volumes for deformation) complimented with auxiliary x-ray, metallographic, and electron microscope evidence so directed as to provide documentation, and identification of the strain-rate-controlling deformation mechanisms. Specific areas of current interest include:

a. Mechanisms of low-temperature prismatic slip in alpha solid solutions of Li in Mg.

b. The low-temperature deformation of polycrystalline aluminum

c. High-temperature creep of iron and iron alloys

d. Recovery of creep-induced substructures

e. The effect of crystal orientation on strain hardening of aluminum

f. The mechanism of deformation of AgMg at elevated temperature

g. The dynamic behavior of crystalline materials and plastic wave theory

h. The rate-controlling mechanism of slip in the intermetallic compound AgMg at low temperatures

i. The mechanism for thermally activated slip in Ag_2Al

j. The theory of dislocation constriction processes

k. The role of dislocations in the recovery of cold-worked aluminum

l. The impact of dislocation theory on engineering

m. The nucleation of kink pairs and the Peierls mechanism of plastic deformation

n. The recovery of creep-resistant substructures

4. Richard M. Fulrath

PHYSICAL CERAMIC RESEARCH

This project is concerned with a study of the properties of polycrystalline and multiphase ceramic materials. A major effect is directed toward characterization of the microstructure of ceramic materials and understanding how specific microstructures are formed. The mechanical properties and diffusional characteristics of polycrystalline and multiphase ceramics are strongly dependent on the microstructure and are of primary concern.

Specific areas of interest include:

a. Studies of composite systems with emphasis on alumina spherical particles dispersed in a glass matrix. The effort will concentrate on establishing the effect of the particle size of the dispersed phase on the mechanical properties of the composite.

b. Studies of the final densification in hot pressing Al_2O_3. Preliminary studies indicate that pretreatment of the alumina powders has a marked effect on the rate of densification and on the final density achieved. The effects of pretreatment will be studied in detail.

c. Study of the permeation of gas through ceramics under stress, with emphasis on increasing the temperature at which the permeation is determined.

d. Studies on the electrical and mechanical property changes induced in poling ferroelectric ceramics. The poling of a ferroelectric can induce

considerable strain at grain boundaries in a polycrystalline body. These strains are believed to be responsible for loss of dielectric strength and the failure of these materials when exposed to large electrical fields.

5. Edward A. Grens II

ELECTROCHEMISTRY

a. Experimental studies of current distribution in electrodes with fissure-type pores. This work involves measurement of a redox reaction as a function of depth in a single fissure (of micron-order width) which serves as one electrode of a laboratory cell.

b. Measurements of rates of dissolution of porous metal anodes undergoing electrolysis, and the dependence of these rates upon position and pore depth in the electrodes.

COMBUSTION

Investigation of the initiation and course of the reaction of liquid droplets (or solid particles) suspended in gaseous atmosphere, including components with which they react. Effects of the composition and temperature of the atmosphere are to be investigated.

6. Ralph Hultgren

THERMODYNAMICS OF THE METALLIC STATE

a. The relative partial molar heat contents of Au and Sn in a liquid Au-Sn alloy will be measured in the liquid metal solution calorimeter. The change with composition of $\Delta\bar{H}_{Au}$ and $\Delta\bar{H}_{Sn}$ in the equiatomic region will be studied at a temperature just slightly above that of the melting point of solid AuSn, 691°K.

b. Heat capacity measurements on liquid alloys will be continued to determine whether the rapid decrease in Cp above the melting temperature found previously for Bi-In and In-Sn alloys is shown by other representative systems.

c. High temperature heat contents ($H_T - H_{298}$) and heats of fusion of the solid phases AlSb and InAs will be determined. Heat contents of liquid In-Sb alloys will be determined and combined with phase-equilibrium data in order to determine the partial molar enthalpies and free energies for the liquid alloys. Electrical-conductivity studies of In-Sb alloys presently in progress will be continued.

d. Galvanic cell studies will be made at elevated temperatures with a solid oxide, ThO_2 (containing 8% Y_2O_3), as the electrolyte. It is planned

to determine the standard free energy of formation of some oxides, to measure the oxygen activity in dilute metallic solid solutions, and to determine the activity of the oxygen-saturated metal in some binary alloyws. Systems with oxygen activities as low as 10^{-34} can be investigated at temperatures up to 1600°K. The refractory metal-oxide systems selected for study are those of Ti, Zr, V, Nb, and Ta.

e. The heats of formation of the ordered and disordered phases of CuPt and thus the heat of ordering will be determined by liquid-tin solution calorimetry.

f. The compilation and evaluation of published thermodynamic data for metals and alloys and possibly a few nonmetallic systems will be continued.

7. Harold Johnston

STUDY OF GAS-PHASE CHEMICAL REACTIONS

Principal interest is the detection of intermediates in gas-phase reactions and measurement of their lifetimes. Usually in chemical reactions, one measures the rate of disappearance of reactants and the rate of appearance of products, but most of the chemical change is carried out by fast-reacting intermediates in very low concentrations. These intermediates include atoms, free radicals, and excited electronic states. By utilizing recently developed techniques in optics and electronics and the data-taking computer, we are developing new methods to see these intermediates and to measure their lifetimes in reacting systems.

The first stage in utilizing optical cavities as an analytical chemical tool for following reactive intermediates is to set it up for a free radical of known spectrum, to measure its absorption spectrum, and to measure its decay time after quenching the exciting light. The first radical to be studied is the photochemically produced HO radical. The radical will be followed by the absorption of HO emission lines produced from a water discharge lamp. The photochemical reaction will be activated by a square-wave low-pressure mercury-vapor lamp, and the decay of the HO radical sampled at a series of times up to 0.01 sec duration after quenching the light. The output per cycle will be stored by the College of Chemistry's computer and a large number of cycles averaged to reduce the problem of noise. The wave length is just above 3000 A, and special multilayer dielectric narrow-band coatings will be used to give mirrors of high reflectivity--perhaps better than 96%. The first chemical process to be studied will be photolysis of hydrogen peroxide.

8. William L. Jolly

INORGANIC CHEMICAL SYNTHESIS

A. Sulfur-Nitrogen Compounds

The chemistry of compounds containing sulfur-nitrogen bonds represents a large, although little understood, branch of inorganic chemistry. We are attempting to systematize the reactions of these compounds.

Recently we reported four new methods for preparing NSCl and new improved methods for the preparation of $S_3N_2Cl_2$, S_3N_2Cl, $S_3N_3Cl_3$, and S_4N_3Cl. As an offshoot of these studies, we are presently investigating the nature of the reaction of HCl with S_4N_4. The reaction of ammonia with S_2Cl_2 to produce, among other things, S_4N_4, S_7NH, and S_8 is being studied to determine the optimum conditions for the preparation of S_4N_4 and S_7NH. It appears that various sulfur-nitrogen-chlorine compounds are formed as intermediates in this reaction, and perhaps some of these can be isolated.

We have found that solutions of S_4N_4 in tetrahydrofuran can be titrated with solutions of sodium naphthaleneide to form a series of species, probably of the type $S_4N_4^-$, $S_4N_4^{2-}$, etc. We plan to follow the course of the reaction by measuring the uv absorption spectra and ESR spectra of the solutions. Other species, such as the $S_4N_3^+$ ion, will also be titrated.

The reactions of atomic nitrogen with a variety of sulfur-containing compounds are being systematically studied. So far we have found that sulfur vapor reacts to give S_4N_2, that S_2Cl_2 reacts to give NSCl, and that H_2S reacts to give S_4N_4.

B. Hydrides

We have found that it is possible to prepare the higher hydrides of silicon and germanium, as well as their phosphorus- and arsenic-substituted derivatives, by the action of a silent electric discharge on the simple hydrides. We plan to compare these new compounds with the structurally analogous hydrocarbons, organo-phosphines, and organo-arsines in order to determine which properties are similar and which are markedly different.

We are currently studying the NMR and infrared spectra of trisilane and both isomers of tetrasilane. We are now engaged in preparing the isomers $SiH_3SiH_2PH_2$ and SiH_3PHSiH_3 in large enough quantities to permit the measurement of their physical and chemical properties. By studying the effect of the electric discharge on mixtures of SiH_4 and SiH_3PH_2, and of Si_2H_6 and PH_3, we hope to get an insight to the mechanism of the discharge tube reaction.

We plan to study the reactivity of species such as germane and digermane with the borohydride ion. Preliminary data suggest that it is possible to prepare the ion GeH_3BH_3.

Practically nothing is known of the mechanism whereby the borohydride ion reduces inorganic species in aqueous solution. As a start toward obtaining this information, we are studying the kinetics of the reduction of

ferricyanide to ferrocyanide.

C. Liquid Ammonia Synthesis

We have recently completed studies of the absorption spectrum of calcium in liquid ammonia and the calcium-ammonia phase diagram. Projected studies in liquid ammonia chemistry include:

a. A study of the kinetics of the reactions of the electron with various species such as NH_4^+, ROH, NO_2^-, MuO_4^-, etc. It will be interesting to compare the rate constants for these reactions with the rate constants for the corresponding reactions in aqueous solution.

b. A study of the rates of proton exchange reactions in liquid ammonia by means of NMR measurements. Such rates are often acid- or base-catalyzed, so it may be possible to establish a relative acidity scale in liquid ammonia. This would be extremely useful in other physical chemical studies in this solvent.

c. A direct measurement of the equilibrium constant of the reaction

$$NH_2^- + \frac{1}{2}H_2 = NH_3 + e^-.$$

9. George Jura

ULTRAHIGH PRESSURE RESEARCH

A study of the chemical and physical properties of materials under high pressure.

Future program plans include the following studies:

a. The two determinations of the Mössbauer effect under pre ssure, for Dy^{161} and Fe^{57}, show that this tool can be as important and useful under pressure as at one atmosphere. For iron the experiments became impossible when the data became the most interesting—when the iron started to transform to the high-pressure phase. The first experiments did not permit us to decide the magnetic nature of the high-pressure phase.

b. Studies of the geometry and containing rings are under progress. These studies will enable us to make the determinations up to higher pressures. Other physical methods--namely heating-- will enable us to determine the spectrum of iron after it has been completely transformed to the high pressure phase. This in turn will enable us to determine the magnetic properties of the high pressure form. These determinations will also be attempted as a function of temperature as well as of pressure. In general, when a Mössbauer nucleus is available, it will be possible in many cases to determine the magnetic properties of the material under study as a function on interatomic distance. These results could be important in the understanding of the ferromagnetic state.

c. One of the objectives of the high pressure program is the determination of the thermodynamic properties of materials under high pressures. At 1 atmosphere, the usual measurements are of the volume and thermal properties. Except for very special cases, namely hydrogen at helium temperatures, no direct measurement of a thermal property of any solid at high pressures has been made. The difficulty in these measurements is that the heat capacity of the container is much larger than the heat capacity of the system under consideration. As a further complication, the heat leak is very large. We plan to solve these difficulties by using a pulsed heating technique, with the sample resistance used as an indicator of sample temperature.

10. Bruce Mahan

GASEOUS MOLECULAR ION REACTIONS

The principal portion of this program is concerned with the study of elementary reactions of molecular and atomic ions in the gas phase, by means of vacuum ultraviolet photon excitation. The work includes studies of:

a. The nature of ionized gases.

b. Photosensitized ionization.

c. The kinetics of electron reactions by microwave techniques.

d. The kinetics of atomic reactions by paramagnetic resonance.

Future program plans include the following studies:

a. Nature of ionized gases. In order to understand the magnitude of the rate constants associated with mutual charge neutralization in gaseous ions, it is important to know what fraction of the ions are held in complexes with inert neutral molecules. Construction has begun on a mass spectrometer which will be used to determine equilibrium constants as a function of temperature. This investigation will give information about the magnitudes of ion-neutral binding energies, as well as the data necessary to understand ion neutralization rates.

b. Photosensitized ionization. Measurements of the threshold of photosensitized ionization, in combination with direct photo-ionization measurements, will be used to study the one-electron bond energies of Cs_2^+, Na_2^+, K_2^+, and Rb_2^+.

c. Microwave cavity resonance. This technique will be used to measure the concentration of gaseous thermal electrons. The method can be used to study the kinetics of reactions such as

$$e^- + NO_2 + Ar \longrightarrow NO_2^- + Ar.$$

d. Electron paramagnetic resonance permits direct observation of gaseous free radicals, and can be used to study the rates of their chemical reactions. Rate constants for O + O, N + H, and H + H will be determined first. They are of particular interest because their potential energy surfaces are well known so that rate data can be interpreted theoretically.

11. Rolf H. Muller

ELECTRODE-ELECTROLYTE INTERFACES

Studies will be conducted on the preparation and characterization of solid-fluid interfaces. Of special interest are the properties of electrolytically prepared metal surfaces and the influence of adsorbed or reacted interfacial layers on kinetic parameters. Ellipsometry, which is sensitive to transitional layers of atomic dimensions, promises to be a powerful tool for this work. Later studies will include the electrolytic crystal growth on surfaces of defined characteristics, preferably single crystal faces. Optical, electron and field ion microscopy are being considered as experimental techniques.

Electrolyte films on gas-consuming electrodes will be investigated in detail, and theoretical reasons for the observed phenomena will be sought. Refraction and adsorption indices for light reflected at the solid-liquid interface will be measured with an ellipsometer to determine the exact value of the optical phase retardation. Knowledge of these quantities is needed to ascertain the position of the zero point in film thickness measurements.

Efforts to measure current distributions in pore models of realistic critical dimension will be continued. In a new high precision assembly under construction, the width of each electrode section is being decreased to provide a better resolution of current distribution. At the same time, the width of the separating insulation between sections is being decreased and its construction revised so as to reduce dead surface and chance of cold flow.

12. Rollie J. Myers

STRUCTURE AND CHEMISTRY OF MOLECULES

The general program includes studies in

a. High-temperature microwave spectroscopy.

b. Paramagnetic resonance of free radicals.

c. Power saturation in paramagnetic resonance.

d. The microwave spectra of unusual molecules.

e. The paramagnetic resonance of transition metal complex ions.

Future program plans include:

Improvement in the design of a high-temperature microwave spectrometer so that triatomic molecules like $PbCl_2$ can be studied.

Continuation of work in paramagnetic resonance, including both radical-anions and radical-cations. The paramagnetic resonance work will be extended to include studies of triplet-state molecules. Line-width studies of the effect of anions on Mn^{+2} will be extended to SO_4^{-2} and similar anions. Triplet-state work will include both phosphorescent and ground-state triplet in molecules such as C_2O in a frozen matrix.

Extension of power saturation measurements both to direct studies of relaxation times and to electron-nuclear double resonance studies.

13. John Newman

FLUID DYNAMICS: STEADY, LAMINAR EDDIES

This program is concerned with an investigation of the formation of eddies for fluid flow past bluff bodies and for fluid flow past reentrant corners.

Plans are being prepared for the construction of a suitable flow channel. In order to obtain a uniform velocity profile in the test section, the upstream section will have moving walls. The construction techniques for moving the wall will require preliminary development.

The velocity distribution in the eddy formed by flow past a square notch will be studied, with particular attention to the possible existence of secondary eddies in the corner.

The principal investigator has proposed a procedure for predicting the flow pattern past bluff objects. Preliminary consideration will be given to the extensive numerical calculations involved in this method.

14. Donald R. Olander

PHYSICAL CHEMISTRY: INTERPHASE DIFFUSION AND GAS-SOLID REACTIONS

This program involves research on several physicochemical problems associated with nuclear reactor technology. Some of the areas under investigation are: theoretical and experimental studies of the diffusional kinetics of interphase mass transfer; the transport properties of liquid metals; and the development of equipment for studying reactions between a gas phase and a fused salt. Current experimental work is concerned with high temperature gas-solid reactions, with emphasis on systems which are subject to diffusion-limited kinetics.

Current and future plans of this program include:

a. Liquid Metal Extraction

The kinetics of extraction of cerium-144 from a molten uranium-chromium eutectic drop into liquid magnesium is being studied. The rate of fall of the drop will be measured by radioactive detection at various intervals along the column. The amount extracted will be determined by gamma analysis of the drop before and after extraction.

b. Kinetics of the Chlorination of UCl_4 in UCl_4-LiCl-KCl Melts with Elemental Chlorine

The solubility of chlorine in the LiCl-KCl eutectic salt has been investigated. Results indicate that the equilibrium concentration of chlorine

in the melt is below the limits of detectability, or $< 10^{-9}$ mole Cl_2 per liter.

The reaction $UCl_4(\ell) + Cl_2(g) \longrightarrow UCl_6(g)$ will be studied in the recently completed laminar jet apparatus. A theoretical study of diffusion-limited surface reactions in this system is under investigation.

c. The Graphite-Hydrogen Systems

The primary heterogeneous reactions between hydrogen and graphite are to be studied by a modulated molecular beam technique.

A modulated molecular beam of hydrogen effuses from an oven source at a prescirbed temperature through a collimating slit into the main reaction chamber, maintained at approximately 10^{-6} mm Hg, where it impinges upon a heated graphite surface. A small fraction of the hydrocarbon reaction products (CH, CH_2, CH_3, and higher hydrocarbons) enters the ionization chamber of a mass spectrometer, and the resulting ion currents are mass-analyzed and measured by an electron multiplier.

d. Diffusion Controlled Oxidation of the Refractory Metals

The kinetics of the oxidation of the refractory metals will be studied at temperatures in the neighborhood of the sublimation point of the principal oxide in a device which permits accurate estimation of the diffusional resistance.

e. Elastic Scattering of Crossed Alkali Metal Beams

The differential elastic scattering cross sections of the alkali metals are to be measured by scattering of crossed atomic beams. From these measurements the interatomic potentials can be obtained by the usual kinetic theory methods. In addition, the transport properties of the gas phase, which are difficult to measure at elevated temperatures, can be computed directly from the differential cross sections.

f. Chemical Reactions Induced by Fission Fragment Irradiation

The purpose of this research is to measure the buildup of unstable products and unstable intermediates in the radiation-induced conversion of ammonia to hydrazine. This system has been chosen because of the relatively small number of stable species (H_2, H_2, NH_3, and N_2H_4) and free radicals (H, N, NH, and NH_2).

15. Edwin F. Orlemann

ELECTRODE REACTION MECHANISMS

Current interest is centered around a study of the mechanism of oxidation and reduction of the In, In(+3) couple at a mercury electrode. Specifically, the electrode processes will be investigated below room temperature. An investigation of the species present in In(+3) perchlorate solutions in the pH range 1 to 4 will be undertaken. The In(+3) species present in acid perchlorate solution containing 10^{-3} to 1 M chloride ion will be investigated.

16. Earl Parker

THEORETICAL AND EXPERIMENTAL STUDY OF HIGH-STRENGTH MATERIALS

In general high-strength materials tend to be brittle. From theoretical considerations, however, it has been concluded that high strength and ductility are not incompatible. Dislocation theory, in conjunction with alloy theory and control of process variables, can lead to an understanding of factors that control ductility in high-strength alloy systems. The following areas of experimental research are intended to elucidate flow and fracture processes in complex multiphase alloy systems:

a. Nitrogen martensite.

b. Theory of the strength of martensite.

c. Internal oxidation of silver alloys.

Future program plans include the following studies:

Homogeneous Nucleation in Precipitation Hardening Systems

Homogeneous nucleation of precipitates is nearly impossible to obtain in precipitation hardening alloys because of heterogeneous nucleation at defect sites. Common nucleation sites are grain boundaries and dislocation networks. The finest network developable by cold work has a spacing of about 0.5 μ. This limits the interparticle spacing in alloy systems to about 0.5 μ. Theoretical considerations lead to the conclusion that considerably finer dispersions can be produced by unique combinations of thermal and mechanical treatments. Substantial improvements in strength and toughness could be obtained if the finely dispersed precipitates could be produced. This principle is applicable to many different alloy systems, and a number of base materials, including aluminum, copper and iron, will be used.

Internal Oxidation of Silver Alloys

Preliminary work on Ag-1 at. % Mg-O with a transmission electron microscope revealed no discrete particles in this system, even though the yield strength was increased 75-fold by oxidation. The reasons for this very large increase in strength are not known, but efforts to disclose the nature of the hardening mechanism are continuing. The principles governing strengthening in this case should be applicable to other systems.

Aluminum Alloys

High-strength precipitation hardening aluminum alloys are to be reexamined in view of the latest concepts of controlled dispersions. Alternating short aging periods with plastic deformation treatments should produce finer dispersions than ever before attained. If the concepts prove correct, alloys with superior strength and toughness will result.

Nickel Alloys

Age-hardening systems, such as Ni-Ta, are to be subjected to cyclic heating and straining in an effort to produce finer structures than have heretofore been attainable.

17. Joseph A. Pask

HIGH-TEMPERATURE REACTIONS, AND MICROSTRUCTURE AND PHYSICAL PROPERTIES

The objective of this program is a fundamental understanding of the factors responsible for microstructure of ceramic materials, and of the relationship of such microstructures to mechanical behavior at room and high temperatures. The research program may be divided into two principal areas: One is concerned with studies of the kinetics and mechanisms of reactions involving at least one nonmetallic inorganic solid phase which play a part in the development of microstructure; the second with studies of the mechanisms responsible for the mechanical behavior of single crystals and subsequent application of such knowledge to a similar understanding of polycrystalline ceramic materials.

Specific areas of interest include:

a. The diffusion of iron into single-crystal MgO at temperatures up to 1600°C.

b. The diffusion of iron into sodium disilicate glass. Experiments will also be extended to include iron oxide-sodium disilicate glass diffusion couples.

c. The kinetics and mechanism of the dehydration of aluminum hydroxide.

d. The stress-strain behavior of polycrystalline MgO in relation to its microstructure, including such variables as pore size and distribution, nature and amount of impurity, and nature of grain boundaries. The deformed specimens are being examined to determine the relative effects of dislocation movements and grain boundary sliding.

e. Plastic deformation of single-crystal specimens of a number of compounds with NaCl-type structures.

18. Norman E. Phillips

LOW-TEMPERATURE CALORIMETRY

Experimental work in this area currently covers the temperature interval between 0.07°K and 20°K, with emphasis on the relatively unexplored regions below 1°K and from 4 to 15°K. The calorimeters used are of two distinct types. The first employs the technique of adiabatic demagnetization to cover the region from 1°K to the lowest temperatures. Experiments are in progress to improve the accuracy of temperature measurements below 0.1°K and to extend the measurements to lower temperatures. The second type of calorimeter exmploys liquid H_2 and liquid He^4 to produce temperatures between 1°K and 20°K and in some cases a He^3 stage is added to extend the range to 0.3°K. A special apparatus for the calibration of germanium thermometers between 0.3°K and 20°K is being made.

Measurements in progress or planned for the next year include

a. Magnetic hyperfine heat capacities in ferromagnetic and antiferromagnetic metals. In some cases it should be possible to determine the sign of the hyperfine field by making measurements in a magnetic field.

b. The heat capacity of solid rare gases at pressures up to 10 000 atmospheres.

c. Spin wave heat capacities of ferromagnets and antiferromagnets.

d. Comparison of elastic constants and lattice heat capacity in superconducting and normal metals.

19. Ira P. Pratt

ELECTRONIC PROPERTIES OF MATERIALS

The specific properties of materials that are directly attributable to density of conduction electrons or bound electrons (those under the Fermi surface), and electron excitational levels, are being examined on a semiclassical basis. An attempt will be made to extend ac relationships describing resistivity and complex permeability to include Larmor frequency in a static magnetic field, and perhaps to include description of the normal-to-diamagnetic transition associated with superconductors.

Photoexcitation in nonmetals by ultraviolet photons is being experimentally studied to gain information on electron trapping and metastable excitation levels.

20. Otto Redlich

EQUATION OF STATE AND CRITICAL PROPERTIES

An equation of state for gases and a rule of parameter combination for mixtures have been developed. A convenient computer program is being set up which requires only the critical temperatures and pressures, and the accentric factors of the components. It furnishes compressibility factors, mean and individual fugacity coefficients, heat contents, and entropies. The arrangement allows the prescription of any desired set of temperatures, pressures and compositions.

The extension of the equation to liquids is progressing. At the same time, various problems concerning critical lines, region of retrograde condensation, stability of two phases, and so on, become interesting. Although the equation of state is primarily intended to be a practical tool, thought is given to the possibility of using it for the elucidation of some fundamental problems never discussed before.

21. Alan W. Searcy

HIGH TEMPERATURE REACTIONS, MASS SPECTROMETRY

As part of a general effort to investigate the evaporation coefficient of alkaline earth dihalides, torsion furnaces will be used for measurements of equilibrium pressures of SrF_2 by the torsion-effusion method, and for measurements of the free-surface apparent pressures of SrF_2 and BaF_2 by the torsion-Langmuir method.

Nitrides studied to date--GaN, AlN, and Be_3N_2-- have high free energies of activation for vaporization. Measurements of the vapor pressure and free surface sublimation kinetics for Mg_3N_2 as functions of temperature will be initiated. Attempts will be made to correlate surface structure, porosity, and impurity level with variations in sublimation kinetics in order to obtain not only a free energy of activation for the vaporization process but also more detailed understanding of the factors that influence rates of evaporation.

A technique of determining the multiplicities of ground and low-lying electronic states by use of an inhomogeneous field magnet attached to the mass spectrometer will be tested and perfected on known species such as oxygen. The technique, if successful, will then be applied to the problem of establishing the ground electronic states for vapor molecules.

The theory of purification of metals by removal of carbon by use of controlled oxygen pressures will be explored for a variety of metals. A new method, which would remove carbon and nitrogen simultaneously as HCN, will also be theoretically evaluated.

The reactions of water vapor and nitrogen dioxide gas with tungsten will be studied at chlorine pressures of 10^{-6} to 10^{-3} Torr over a temperature range of 1900 to 2600°K.

Oxidation reactions of various metals, such as tungsten, tantalum, etc., will be studied at low pressures and high temperatures in the presence and absence of other gases such as nitrogen and halogens.

22. Charles H. Sederholm

THE STRUCTURE OF MOLECULES, AS STUDIED BY NMR TECHNIQUES

High-resolution NMR techniques are being used to study the structure of molecules. Such techniques make available information about electronic configurations, geometric structures, and barriers to changes in the geometric configurations. In addition, various instrumental techniques are being developed which will substantially increase the amount of information available from NMR measurements.

An investigation is being started to determine the role that solvent effects have on NMR coupling constants between fluorine atoms.

Computer programs have been written to describe the NMR spectra due to internal rotation of AB, ABX, and ABC spin systems. These programs are currently being used to obtain the barriers to internal rotation in CF_2BrCCl_2Br and $CF_2BrCFBr_2$. In CF_2BrCCl_2Br, all the barriers are approximately 10.5 kcal/mole. In $CF_2BrCFBr_2$, the barrier between the two dl rotamers is about 7.8 kcal/mole, and the other two barriers are about 9.3 kcal/mole. Work is also in progress on $CF_2BrCHBrCl$ to see if there is a correlation between the barrier heights and the size of the halogen substituents.

Geminal proton-proton coupling constants are very difficult to measure. A few constants have been determined in four-membered ring compounds. Several of these constants have been unexpectedly low. An effort is being made to determine the proton-proton-geminal coupling constants in a variety of four-membered ring compounds and to determine the factors that influence these constants. This effort involves special experimental techniques such as double resonance and requires extensive calculations.

By accurately measuring chemical shifts of both protons and deuterons in a series of perchloric acid solutions in which both the acid concentration and the hydrogen to deuterium ratio are varied, we hope to determine the ionization constant of perchloric acid as well as the extent of hydration of protons in solutions of varying acid strengths.

In addition, it is hoped to connect two NMR spectrometers directly to an SDS 910 computer. By using the computer's data retrieval possibilities, a substantial improvement in the signal-to-noise ratio of the spectrometer should be obtained. It should also be possible to improve the effective resolution of the spectrometers by mathematical decomposition of the experimental spectra into a superposition of several Gaussian-shaped resonances.

23. Gareth Thomas

RELATION OF SUBSTRUCTURE TO PROPERTIES OF CRYSTALLINE MATERIALS: ELECTRON MICROSCOPY

The relation of substructure and in particular lattice defects (dislocations, stacking faults, vacancies, solute atoms) to properties can be conveniently studied by transmission electron microscopy. The general areas of research are as follows:

a. Body-Centered Cubic Materials

The effect of interstitial impurities upon dislocation arrangements of bcc metals and solid solutions and their effect upon mechanical properties will be studied.

b. Stacking-Fault Energy

The stacking-fault energy of fcc solid solutions is a function of composition and solute atom distribution. Estimates of SFE can be made from node measurements on electron micrographs. At present the following factors in relation to SFE are under investigation: (i) short-range order; (ii) mechanical twinning in shock-loaded metals; (iii) temperature.

c. Impurity-Vacancy Interactions

The concentration of quenched-in vacancies is a function of solute atom kind and concentration. The important parameter is the binding energy between vacancies and solute atoms. Estimates of this parameter can be made from dynamic measurements of dislocation climb rates, using hot-stage microscopy.

The data will also be useful in understanding phenomena such as recovery and creep.

d. Defects in Silicon

The types and origin of lattice defects in undoped and doped epitaxial silicon are under study.

24. Charles W. Tobias

STUDIES OF CHARGE AND MASS TRANSPORT IN ELECTROCHEMICAL SYSTEMS, NONAQUEOUS SOLVENT MEDIA, AND UNCOMMON ELECTRODE REACTIONS

These studies include the following problems.

a. Development of precise numberical techniques for the evaluation of current distribution in two-dimensional enclosures.

b. Experimental studies of current distribution, and the distribution of rates of dissolution in a porous metal electrode.*

c. Experimental and theoretical studies of transport properties in concentrated electrolytes.+

d. Experimental and theoretical studies of the effect of mass transport on current distribution on "rough" surfaces.

e. Studies of the anodic oxidation of liquid phosphorous in aqueous media.

f. Determination of physical properties and of the electrochemical behavior of metallic solutions of calcium in liquid ammonia.

g. Exploration of the nature of the electromotive series in dimethyl sulfoxide.

h. The mechanism of electrodes of the second kind in nonaqueous solvents.

---

* Partially supported by NASA Research Grant NsG 150-61 during 1964-5.

+ Partially supported by Contract No. DA36-039-SC-89153 during 1964-5.

25. Jack Washburn

INFLUENCE OF CRYSTAL IMPERFECTIONS ON MECHANICAL PROPERTIES

The central them of the research program is an attempt to achieve a more fundamental understanding of the behavior of dislocations in crystals so as to be able to make more accurate correlations between crystal structure, the crystal imperfections that are always present, and important mechanical and physical properties. The emphasis is on simple experiments with single-crystal specimens and direct observation of individual dislocations. Most of the experimental work involves etch pit or transmission electron microscopy observations of dislocations in single-crystal specimens of carefully controlled crystallographic orientation. Specific research topics include:

a. The effect of quenching conditions on the type of vacancy defects that form during aging in pure aluminum.

b. Interaction between moving dislocations and large faulted loops in the FCC structure.

c. Dislocation multiplication in magnesium oxide.

d. Mechanism of mechanical twinning.

e. Correlation between nuclear magnetic resonance and transmission electron microscopy determinations of the type of stacking faults in cobalt.

f. Diffusion-induced plastic deformation of silicon.

Future program plans include the following studies:

a. Study of Dislocation Motion in Crystal Containing Vacancy Clusters

When dislocations move during plastic deformation, clusters of vacancies are left behind as part of the damage that causes strain hardening. Similar defects are also the cause of radiation hardening, and of hardening produced by quenching a crystal from elevated temperature so as to trap thermal vacancies. Moving dislocations can also destroy some of these defects. An understanding of the detailed interactions between moving dislocation and vacancy clusters of all sizes, from a divacancy up to voids or dislocation loops consisting of 10^3 individual vacancies, is fundamental to any real understanding of yielding and slip band growth in crystals.

Research in this general field during the year 1964 will be concentrated on the following measurements: (i) a study of the growth of vacancy clusters or small voids in quenched copper during low-temperature aging. Small-angle x-ray scattering techniques will be used. (ii) Quantitative measurement of dislocation mobility in copper crystals containing vacancy clusters of known size.

b. Theory of Strain Hardening

(i) The effect of initial dislocation substructure on yielding, on the hardening rate during stage I, and on the transition to stage II will be

studied, with pure copper single crystals. (ii) Experiments utilizing surface observations of slip bands will be conducted in an attempt to find out whether or not changes in the shape of stress-strain curves can be correlated with changes in the distribution of strain.

c. Growth of Deformation Twins

A technique has been developed for producing properly oriented cylindrical zinc tensile specimens the gauge section of which is traversed by a single twin lamella. On deforming such a specimen at 20°C with the tensile axis in the basal plane the only process observed is the thickening of the twin lamella. This occurs by the smooth propagation of the two parent-twin interfaces at a constant load.

It is hoped to study the effect of shear stress and temperature on the rate of twin boundary propagation, and to investigate the effect of grown-in or introduced dislocation structures on the mobility of these boundaries. Present experiments are using specimens of 99.999% pure zinc.

26. Victor F. Zackay

THE DESIGN OF HIGH-STRENGTH MATERIALS FROM FUNDAMENTAL PRINCIPLES, STUDIES OF MATERIALS FOR SUPERCONDUCTIVITY

The requirements for tough, ductile, high-strength solids can be deduced from dislocation theory. By combining a knowledge of the thermodynamics and kinetics of phase transformations in metals with the precise control of process variables such as temperature, composition, and deformation, "ideal" microstructures can be approximated and the associated properties compared with those predicted from theory.

The following programs comprise the effort currently being devoted to the study of complex high-strength solids.

a. Elevated-Temperature Strain Aging.

Highly alloyed martensitic steels are being strained varying amounts at different strain rates and temperatures. The volume fraction of finely dispersed carbides is significantly increased by this kind of processing.

b. The Spinodal Transformation.

A characteristic of the spinodal transformation is the formation of composition gradients in a single-phase solid. By appropriate choice of alloy systems, a ternary element can be diffused into the binary spinodal alloy. Compounds formed by this process are in a three-dimensional grid and the array can be closely controlled. The interaction of dislocations with grids of hard particles is being studied in both bulk and foil specimens.

c. The Liquid-Solid Transformation. The liquid-solid phase transformation can also be employed to produce controlled arrays of hard particles in ductile solids. One such system is that of aluminum and silicon with phosphorus added as an inoculant.

d. The Theoretical Strength of Solids.

A comparison of the theoretical and actual strength-weight ratios of the common structural metals over a wide range of temperature has been made. The discrepancy between the theoretical and the actual strength-weight ratios at room temperature were shown to vary by factors ranging from approximately 3 for Fe and Ti to about 40 for Be.

e. The Strain Hardening of Iridium.

The metal iridium has a high elastic modulus (74×10^6 psi), is chemically inert, oxidation-resistance to about 1000°C, and is reported to have an exceptionally high rate of work hardening.

f. Structure of A15.

The A15 structure consists of nonconnected orthogonal "chains" of close-packed atoms held apart by "spacer" atoms. There is reason to believe that the chains of these compounds do not extend continuously for long distances throughout the crystal, but that they end rather abruptly at the boundary of another "domain" of different orientation. The techniques of electron transmission microscopy are being used to study these domain structures.

g. Metal-Nonmetal Compounds.

In contrast to the behavior of intermetallic compounds with the A15 structure, the critical temperature of compounds composed of metals and nonmetals, such as the metal carbides and nitrides, is sometimes significantly increased by ternary additions. The variation of the superconducting transition temperature in the Nb-N-C system is being studied as a function of composition and nitriding pressure.

h. β-Mn Structure and Superconductivity.

Although compounds having the β-Mn structure have not been extensively investigated, it has been assumed that this structure is not a favorable one for superconductivity. However, current studies of the A15 structure of intermetallics and the B1 structure of the metal carbides suggested to us that compounds of the β-Mn structure, especially ternary systems containing nonmetals, would be good superconductors. We have found that the compound Mo_3Al_2C is a superconductor with critical temperatures of 10.0°K.

i. Mo-Tc System.

The critical temperature of compounds with the A15 structure usually decreases with increasing deviation from the ideal stoichiometry A_3B. In the system Mo-Tc, however, an A15 structure, perhaps $(A,B)_3B$, exists at the approximate composition 50% Mo, 50% Tc. It has a reported[3] transition temperature of 15°K. Further recent theoretical predictions by Leo Brewer indicate that the A15 structure should be stable in the ternary system, Mo-Tc-Nb. Studies are being made of the relation of the critical temperature to composition for the binary and ternary systems.

V. PUBLICATIONS, 1963

Publications, or papers issued, by the staff members of the Inorganic Materials Research Division that appeared during the 1963 calendar year are listed below. Most, but not all, of these publications received primary financial support from the U. S. Atomic Energy Commission.

Brewer and Associates

Brewer, L., "Prediction of High Temperature Metallic Phase Diagrams," UCRL-10701, July (1963).

Brewer, L., R. Berg, and G. Rosenblatt, "Radiative Lifetime of I_2 Fluorescence, $B^3\Pi_{0^+u} - X^1\Sigma_{0^+g}$," J. Chem. Phys. 38, 1381-88 (1963).

Brewer, L., G. Somayajulu, and E. Brackett, "Thermodynamic Properties of Gaseous Metal Dihalides," Chem. Rev. 63, 111 (1963).

Hagan, L., "Absolute Intensity of the C_2 Swan Bands" (Ph.D. Thesis), UCRL-10620, March (1963).

Meyer, C. B., "Unstable Solid Allotropes of Sulfur," UCRL-10768, August (1963).

Rosenblatt, G., "Harmonic-Oscillator Thermodynamic Functions for P_4," J. Mol. Spec. 10, 484-5 (1963).

Rosenblatt, G., "Interpretation of Knudsen Measurements on Porous Solids," UCRL-10271, July (1962), J. Electrochem. Soc. 110, 6 (1963).

Connick and Associates

Connick, R., "Chemical Kinetics in Laboratory and Classroom," J. Chem. Educ. 40, 587 (1963).

Connick, R., with R. Hasty and D. Fine, "Identification of Anionic Ru (III) Species," UCRL-10605, December (1962).

Connick, R., and D. Fiat, "The Coordination Numbers of Beryllium and Aluminum Ions," UCRL-10763, May (1963).

Dorn and Associates

Dorn, J., "Thermodynamics of Stacking Faults in Binary Alloys," UCRL-10487, September (1962), Acta Met. 11 [3], 218-9 (1963).

Dorn, J., "Impact of Dislocation Theory of Engineering," UCRL-10788, May (1963).

Dorn, J., and J. P. Andre, "Energies d'Activation pour le Fluage du Magnesium Polycristalline," Memoires Sc. Rev. Met. 60, 12 (1963).

Dorn, J., with J. Mitchell and S. Mitra, "Dispersed Particle Strengthening at Low Temperatures," UCRL-10469, August (1962), Trans. ASM, Quart. 56, 2 (1963).

Dorn, J., with E. Howard, W. Barmore, and J. Mote, "On the Thermally Activated Mechanisms of Prismatic Slip in the Ag-Al Hexagonal Intermediate Phase," UCRL-10588, December (1962), Trans. AIME, 227, 1061 (1963).

Dorn, J., and J. Mote, "Physical Aspects of Creep," UCRL-10598, January, (1963).

Dorn, J., and S. Rajnak, "Dislocations and Plastic Waves," UCRL-10627, March (1963).

Dorn, J., with A Rosen, "On the Role of Dislocations in the Recovery of Cold-Worked Aluminum," UCRL-10728, April (1963).

Dorn, J., with T. L. Larsen, S. Rajnak, and F. Hauser, "Slip Behavior of Single Crystals of Hexagonal Ag-Al Under Impulsive Loading," UCRL-10789, June (1963).

Dorn, J., and S. Rajnak, "Nucleation of Kink Pairs and the Peierls' Mechanism of Plastic Deformation," UCRL-10833, July (1963).

Dorn, J., and N. Jaffe, "Effect of Stress and Recovery of the Creep of High Purity Polycrystalline Aluminum at Intermediate Temperature," Trans. AIME, 227, 1314 (1963).

Dorn, J., and S. Mitra, "On the Nature of Strain Hardening in Polycrystalline Al and Al-Mg Alloys," Trans. AIME, 227, 1015 (1963).

Dorn, J., with A. Rosen and J. Mote, "On the Low-Temperature Thermally Activated Mechanism for Prismatic Slip in the Ag-Al Intermediate Hexagonal Phase," UCRL-10917, August (1963).

Dorn, J., with A. Mukherjee, "The Rate Controlling Mechanism of Slip in the Intermetallic Compound AgMg at Low Temperatures," UCRL-10916, August (1963).

Dorn, J., and L. Raymond, "Recovery of Creep Resistant Substructure," IER Report No. MT-63-4, April (1963).

Dorn, J., and F. Hauser, "Dislocation Concepts of Strain Rate Effects," ASD-TDR-63-140, pp. 173-178, May (1963).

Mote, J., with J. George, "Dislocation Etch Pits in Hexagonal Ag-Al Intermetallic Phase," UCRL-10871, July (1963).

Mukherjee, A., and J. Martin, "The Effect of Nitriding Upon the Creep Properties of Some Molybdenum Alloys," J. Less-Common Metals 5, 403-10 (1963).

Mukherjee, A., and J. Martin, "The Effect of Nitriding on the Elevated Temperature Tensile Properties of Some Molybdenum-Base Alloys," J. Less-Common Metals, 5, 117-127 (1963).

Mukherjee, A., and J. Martin, "Hot-Hardness of Dispersion-Hardened Molybdenum-Titantium and Molybdenum-Zirconium Alloys," J. Inst. Metals 91, 283-4 (1963).

Fulrath and Associates

Fulrath, R., "Controlled Microstructure of Refractory Bodies," UCRL-10846, September (1963), International Symposium on High-Temperature Technology at Asilomar, September 1963.

Fulrath, R., "Composite Materials Fabrication, Structure, and Properties," UCRL-10973, August(1963).

Fulrath, R., with O. Stansfield, "The Influence of Tensile Stress on Helium Permeation of Glass and Several Refractory Ceramics," UCRL-10755 Rev., June (1963).

Fulrath, R., and R. Rossi, "Epitaxial Growth of Spinel by Reaction in the Solid State," J. Am. Ceram. Soc. 46 [3], 145 (1963).

Fulrath, R., with D. Hasselman, "The Effect of a Small Fraction of Spherical Porosity on the Elastic Moduli of Glass," UCRL-11027, September (1963).

Fulrath, R., with A. Das, "Liquid-Solid Transformation Kinetics in Al_2O_3," UCRL-11166, December (1963).

Rossi, R., with R. Shannon, "The Definition of Topotoxy," UCRL-10957, August (1963).

Barner, J., "Design of a Differential Calorimeter Suitable for Measurement of High Temperature Heats of Solid-State Reactions" (M.S. Thesis) UCRL-10631, January (1963).

Nason, D., "Effect of Interfacial Bonding on Strength of a Model Two-Phases System" (M.S. Thesis), UCRL-11011, September (1963).

Herschbach and Associates

Herschbach, D., with R. Zare, "Doppler Line Shape of Atomic Fluorescence Excited by Molecular Photodissociation," UCRL-10411, , Proc. IEEE 51, 173-182 (1963).

Herschbach, D., with R. Zare, "Mechanics of Molecular Photodissociation," UCRL-10438, February (1963).

Herschbach, D. with J. Cashion, "Empirical Evaluation of the London Potential Energy Surface for the H + H_2 Reaction," UCRL-11171, December (1963).

Herschbach, D., and V. Laurie, "Influence of Vibrations on Molecular Structure Determinations. III. Inertial Defects," UCRL-11208, November (1963).

Cashion, J., "The Testing of Diatomic Potential Functions by Numerical Methods," J. Chem. Phys. 39, 1872 (1963). (From J. Cashion, "Applications of Numerical Solutions to the Radial Equation for Diatomic Molecules," UCRL-10643, May (1963)).

Cashion, J., "Vibration-Rotation Interaction Factors for Diatomic Molecules Calculated by Numerical Factors," UCRL-10644, July (1963).

Child, M., "Semiclassical Analysis of Weakly Inelastic Molecular Collisions," UCRL-11135, November (1963).

Norris, J., "Chemical Reactions in Crossed Molecular Beams" (Ph.D. Thesis), UCRL-10848, June (1963).

Zare, R., and J. Cashion, "The IBM Share Program D2 NU SCHR 1072," UCRL-10881, July (1963).

Zare, R., "Calculation of Intensity Distribution in the Vibrational Structure of Electronic Transitions," UCRL-11110, October (1963).

Himmel and Associates

Busch, R., "Recovery of Internally Oxidized Silver Magnesium Alloys" (M. S. Thesis), UCRL-10816, June (1963).

Papazian, J., "The Internal Friction Due to Oxygen in Silver" (M.S. Thesis), UCRL-11017, September (1963).

Hultgren and Associates

Hultgren, R., R. Orr, P. Anderson, and K. Kelley, Selected Values of Thermodynamic Properties of Metals and Alloys, (J. Wiley and Sons, New York, 1963).

Hawkins, D., M. Onillon, and R. Orr, "High Temperature Heat Content of Hafnium," UCRL-10729, March (1963), J. Chem. Eng. Data 8, 628 (1963).

Worrell, W., "The Free Energy of Formation of NbO_2 Between 1100° and 1700°K," UCRL-11037, October (1963).

Worrell, W., "Estimation of the Entropy of Formation for Some Refractory Metal Carbides," UCRL-11039 October (1963).

Jolly and Associates

Jolly, W., "The Symmetrical Deformation Frequencies of Methyl, Silyl, and Germyl Groups," UCRL-10733, March (1963), J. Am. Chem. Soc. 85, 3083 (1963).

Jolly, W., "The Use of Electric Discharges in Chemical Synthesis," in The Technique of Inorganic Chemistry (Interscience, New York, N.Y., 1963), pg. 179.

Jolly, W., "Electron Repulsions in Molecules," UCRL-10839, September (1963).

Jolly, W., "Electron Repulsions in Compounds of Nitrogen, Oxygen, and Fluorine," UCRL-10920, August (1963).

Jolly, W., "Some Compounds Prepared in Electric Discharges," UCRL-11106 Abs., November (1963), ACS Meeting December 1963.

Jolly, W., "An Introduction to the Chemistry of Complex Compounds, by A. A. Grinberg (Book Review)," Chem. Eng. News 41, [7], 98 (1963).

Jolly, W., and J. Drake, "Proton Magnetic Resonance Spectra of Silylphosphine, Silylarsine, Germylphosphine, and Germylarsine," J. Chem. Phys. 38, 1033 (1963).

Jolly, W., with C. Hallada, "Absorption Spectra of Calcium-Ammonia Solutions," UCRL-10815, May (1963), Inorg. Chem. 2, 1076 (1963).

Jolly, W., with C. Lindahl, "Some Reactions of Diphosphorus Tetrachloride," UCRL-10840, May (1963), ACS Meeting September, 1963.

Jolly, W., K. Maguire, and D. Rabinovich, "Convenient Methods for Preparing $S_3N_2Cl_2$ and S_4N_3Cl," UCRL-10877, June (1963), Inorg. Chem. 2, 1304 (1963).

Jolly, W., with K. Maguire and J. Smith, "Four New Methods for Preparing NSCl," UCRL-10876, June (1963), Chemistry and Industry, 1963, p. 1589.

Jolly, W., and K. Maguire, "Sulfur Nitrogen Chlorides," UCRL-10940, November (1963).

Jolly, W., with S. Gokhale, "Phosphine: $4H_3PO_3 \longrightarrow 3H_3PO_4 + PH_3$," UCRL-11177, December (1963).

Jolly, W., C. Hallada, and M. Gold, "The Absorption Spectra of Metal-Ammonia Solutions," UCRL-10960, November (1963).

Jolly, W., with S. Gokhale and K. Maguire, "The Higher Silanes and Germanes," UCRL-11078, November (1963).

Bloom, H., "Reductions Using Solutions of Calcium in Molten Salts," UCRL-11205, December (1963).

Villena-Blanco, M., "A Study of the Reactions Between Gaseous Ammonia and Sulfur-Chlorides" (M.S. Thesis), UCRL-11081, October (1963).

Jura and Associates

Jura, G., "Resistance Measurements at High Pressures," UCRL-11030, November (1963).

Jura, G., with P. Souers, "Semiconducting Region of Ytterbium," UCRL-10715, March (1963), Science, 140 [3566], 481-3 (1963).

Jura, G., with J. Stone, M. Nicol, and J. Rasmussen, "The Influence of High Pressures on the Mössbauer Effect in Dysprosium-161," UCRL-10630, Rev., April (1963).

Jura, G., with M. Nicol, "The Effect of Pressure on the Mössbauer Spectrum of Fe^{57} in Iron Metal," UCRL-10785 Rev., October (1963), Science, 141, [3585], 1035-38 (1963).

Jura, G., with P. Souers, "Semiconducting Region of Bismuth I," UCRL-10942, September (1963).

Jura, G., D. McWhan, P. Montgomery, and H. Stromberg, "Pressure-Temperature-Resistance Properties of La, Bi, Np, Pu, and Am to 450° and 30 KB," J. Phys. Chem. 67, 2308 (1963).

Nicol, M., "The Effect of Pressure on the Mössbauer Spectrum of Fe^{57} in Iron Metal" (Ph.D. Thesis), UCRL-10785, May 1963.

Mahan and Associates

Mahan, B., Elementary Chemical Thermodynamics (W. A. Benjamin, Inc., New York, 1963).

Mahan, B., "Temperature Dependence of Equilibrium. A First Experiment in General Chemistry," J. Chem. Educ. 40, 293 (1963).

Mahan, B., and J. Person, "Gaseous Ion Recombination Rates," UCRL-10987, August (1963).

Mahan, B., and J. Person, "Gaseous Ion Recombination Rates, II," UCRL-11084, December (1963).

Mahan, B., and T. Carlton, "Gaseous Ion Recombination Rates, III," UCRL-11134, November (1963).

Person, J., "Mutual Charge Neutralization of Gaseous Ions" (Ph.D. Thesis), UCRL-10904, July (1963).

Muller and Associates

Muller, R., "Discussion of 'A Simple Method for Detecting Microvariations in the Surfaces of Polished Flat Materials,' by M. V. Sullivan (Book Review)," UCRL-10721, March (1963), Electrochem. Tech. 1, 378 (1963).

Muller, R., "Optical Computations for Transparent Thin Films on Metal Surfaces," UCRL-10963, July (1963).

Muller, R., "'Kalte Verbrennung, Fuel Cells,' Book Review," Chem. Eng. News 42 [4], 132 (1963).

Myers and Associates

Myers, R., with J. B. Spencer, "The Exchange of CN^- with $Cr(NO)(CN)_5^{-3}$ as Followed by Electron Spin Resonances," UCRL-10725, March (1963), ACS Meeting, March (1963).

Myers, R., with R. Hayes, "The Effect of Cl^- and SO_4^{-2} on the Paramagnetic Resonance Line Width of Mn^{+2} in Aqueous Solution and the Rates of Formation of the Complex Ions," UCRL-10446, September (1963).

Myers, R., and N. Edelstein, "A Study of the Low Pressure Reactions of $H + O_2$ and the Lifetime of HO_2," UCRL-10997.

Myers, R., and R. U. Blukis and P. H. Kasai, "Microwave Spectra and Structure of Dimethyl Ether," J. Chem. Phys. 38, 2753 (1963).

Hayes, R. G., "On the Electron Paramagnetic Resonance Spectrum of the $Cr(CN)_5NO^{3-}$ Ion," J. Chem. Phys. 38, 2580 (1963).

Olander and Associates

Olander, D., "A Hydromatic Model of Mass Transfer in a Stirred Vessel Extractor," Chem. Eng. Sci. 18, 123 (1963).

Olander, D., "Mutual Diffusion in Dilute Binary Systems," AIChE Journal 9, 207 (1963).

Olander, D., "Analysis of Liquid Diffusivity Measurements to Account for Volume Changes on Mixing," J. Phys. Chem. 76, 1011 (1963).

Olander, D., and A. Emanuel, "Diffusion Coefficients of Copper Sulfate in Water and Water in N-Butyl Alcohol," J. Chem. and Eng. Data 8 [1], 31 (1963).

Olander, D., and M. Benedict, "Mechanism of Extraction by Tributyl Phosphate-n-Hexane Solvents, Part II, Nitric Acid Extraction," Nucl. Sci. Eng. 15 [4], 354 (1963).

Olander, D., H. Shaked, and T. Pigford, "Calculation of the Fractional Release of Fission Gas from Solid Specimens During Postirradiation Anneal Experiments," Trans. Am. Nucl. Soc. 6 [1], 130 (1963).

Olander, D., H. Shaked, and T. Pigford, "Diffusion of Xe^{133} in Uranium Monocarbide," Trans. Am. Nucl. Soc. 6 [1], 131 (1963).

Olander, D., J. Holmens, and C. Wilke, "Convective Mass Transfer in a Diaphragm Diffusion Cell," J. Phys. Chem. 67, 1469 (1963).

Olander, D., and L. Reddy, "The Effect of Concentration Driving Force on Liquid-Liquid Mass Transfer," Chem. Eng. Sci. 19, 67-73 (1963).

Orlemann and Associates

Orlemann, E., with C. Merideth and W. Mathews, "The Rate of Aquation of Dichlorotetraaquochromate Ion as a Function of pH in Chloride Media," UCRL-10787, May (1963).

Parker and Associates

Parker, E., in Materials for Missiles and Spacecraft, editor, University of California Eng. and Sci. Ext. Series (McGraw-Hill, New York, 1963).

Parker, E., "Plastic Flow and Fracture of Crystalline Solids," U.S. Dept. of Commerce, NBS Monograph #59, March (1963).

Parker, E., "Mechanical Behavior of Crystalline Solids," Perspectives in Materials Research ONR, Surveys of Naval Science, ACR-61, No. 10, March (1963).

Parker, E., and J. Bokros, "The Mechanism of the Martensite Burst Transformation in Fe-Ni Single Crystals," Acta Met. 11, 1291 (1963).

Bayce, A., with P. Osborne, "Film Deposits and Whisker Growth in the Electron Microscope," UCRL-10558, August (1963).

Pask and Associates

Pask, J., "Impact of Materials Science and Materials Engineering on Ceramic Engineering," Bull. Am. Ceram. Soc. 42 [1], 23 (1963).

Pask, J., "Summary of Viewpoints of the Materials Committee on the Teaching of Materials to Engineers," J. Eng. Educ. 53, 700 (1963).

Pask, J., "Objective Criteria in Ceramic Engineering," Bull. Am. Ceram. Soc. 42 [9], 503 (1963); J. Eng. Educ. 54, 41 (1963).

Pask, J., "Ceramics in Israel," Bull. Am. Ceram. Soc. 42 [12], 760 (1963).

Pask, J., and S. Copley, "Thermochemical Behavior of Ceramics," UCRL-10704, March (1963).

Pask, J., with D. Budworth, "Temperature Dependence of Flow Stresses on the {100} and {110} Planes in LiF and the Plasticity of Polycrystals," UCRL-10919, August (1963), J. Am. Ceram. Soc. 46, 11 (1963).

Pask, J., and W. Scott, "Deformation and Fracture of Polycrystalline Lithium Fluoride," J. Am. Ceram. Soc. 46, 284 (1963).

Pask, J., with L. Johnson, "Mechanical Behavior of Single-Crystal and Polycrystalline Cesium Bromide," UCRL-10468, Rev., July (1963).

Pask, J., with D. Budworth, "Effect of Temperature on the Plasticity of Polycrystalline Lithium Fluoride," UCRL-10490, October (1962), Trans. Brit. Ceram. Soc., 62 [9], 763-770 (1963).

Pask, J., C. Hulse, and S. Copley, "Effect of Crystal Orientation on Plastic Deformation of MgO," J. Am. Ceram. Soc. 46, 7 (1963).

Borom, M., "Diffusion of Iron Into Sodium Disilicate Glass" (M.S. Thesis) UCRL-11116, November (1963).

Copley, S., "Independent Slip Systems in CsCl-Type Crystals," UCRL-10918, July (1963), Phil. Mag. 8, 93, 1599 (1963).

Shannon, R., "Activated Complex Theory Applied to the Thermal Decomposition of Solids," UCRL-10791, July (1963).

Shannon, R., and R. Rossi, "The Definition of Topotoxy," UCRL-10957, August (1963).

Phillips and Associates

Phillips, N., J. Ho, and H. O'Neal, "Low Temperature Heat Capacities of Constantan and Manganin," Rev. Sci. Instr. 34 [7], 782-83 (1963).

Phillips, N., with W. Lien, "The Low Temperature Heat Capacities of Potassium, Rubidium, and Cesium," UCRL-9880 Rev., August (1963).

Ahlers, G., "Heat Capacity of Solid He^4 at the Density of the Gammas Phase," UCRL-10719, March (1963), Phys. Rev. Letters 10, 439 (1963).

Ahlers, G., and W. Orttung, "The Lambda Anomaly in the Heat Capacity of Solid Hydrogen at Small Molar Volumes," UCRL-10757 Rev., October (1963).

Ahlers, G., "Some Properties of Solid Hydrogen at Small Molar Volumes" (Ph.D. Thesis), UCRL-10757, September (1963).

Ahlers, G., "On the Ortho-Para Conversion in Solid Hydrogen," UCRL-11042, October (1963).

Ahlers, G., "The Lattice Heat Capacity of Solid Hydrogen," UCRL-11045, December (1963).

Lambert, M., "Nuclear Spin Ordering in Adsorbed He^3," Phys. Rev. Letters 12, 67 (1963).

Pitzer and Associates

Snelson, A., "Infrared Spectra by Matrix Isolation of Lithium Fluoride, Lithium Chloride, and Sodium Fluoride," J. Phys. Chem. 67, 882 (1963).

Brown, J., "Magnetic Resonance of Metals and Paramagnetic Ions in Solution," UCRL-9944 Rev. , J. Phys. Chem. 67, 2524 (1963).

Pratt and Associates

Pratt, I., M. Davis, and T. Hazlett, "Thermal Characteristics of a 150-kW Arc Image System," UCRL-11007, September (1963), Symposium at Asilomar, September (1963).

Pratt, I., and L. Toth, "Composition Fluctuations in Hard Superconductors," UCRL-11158, December (1963).

Redlich and Associates

Redlich, O., "The Molal Volume of Electrolytes," J. Phys. Chem. 67, 496 (1963).

Redlich, O., "Old and New Problems in the Field of Vapor-Liquid Equilibria," UCRL-10841, July (1963).

Redlich, O., and A. K. Dunlop, "Thermodynamics of Solutions. VIII. An Improved Equation of State," Chem. Eng. Progr. Symp. Series 59, 44 (1963).

Redlich, O., A. L. Jacobson, and W. H. McFadden, "On the Fractionation of Polypropylene by Coacervation," J. Polymer Sci. 1, 393 (1963).

Redlich, O., and F. Ackerman, "On the Thermodynamics of Solutions. IX. Critical Properties of Mixtures and Equation of Benedict, Webb, and Rubin," J. Chem. Phys. 38, 2740 (1963).

Redlich, O., "Wissenschaftliche Forschungserichte (Raman Spectroscopy)," Am. Chem. Soc. 85, 1213 (1963).

Ackerman, F., "The Efficiency of Equations of State for Gases and Mixtures at the Critical Locus" (M.S. Thesis), UCRL-10650, February (1963).

Searcy and Associates

Searcy, A., "Chemistry at High Temperatures: The Problem of Reducing Chemical Attack," UCRL-10821, June (1963).

Searcy, A., "High Temperature Reactions," Surv. Prog. Chem. 1, 35-79 (1963).

Searcy, A., and D. Schulz, "Vapor Pressure and Heat of Sublimation of Calcium Fluoride," J. Phys. Chem. 67, 103 (1963).

Searcy, A., with D. Meschi, "Some Aspects of the Chemistry of Solid Solutions," UCRL-10739, April (1963), Electrochemical Society Paper, April (1963).

Searcy, A., and D. Schulz, "Demonstration of Some Unrecognized Characteristics of Gas Flow Through Orifices," UCRL-10519, October (1962), J. Chem Phys. 38 [3], 772 (1963).

Searcy, A., with A. Miller, "Sublimation of Indium Sesquisulfide," UCRL-10782, May (1963), J. Phys. Chem. 67, 2400 (1963).

Searcy, A., with G. De Poorter, "Energy Exchange Between a Hot Tungsten Surface and Cold Gases," UCRL-10504 Rev., April (1963), J. Chem. Phys. 39 [4], 925 (1963).

Searcy, A., with L. Toth, "Activation Energies for Diffusion in Pure Metals and Concentrated Binary Alloys," UCRL-10581 Rev., July (1963).

Searcy, A., with Z. Munir, "Torsion-Effusion Study of the Vapor Pressure and Heat of Sublimation of Ga," UCRL-11062, October (1963).

Searcy, A., R. Newbury, and G. Barton, "A Demonstration of the Existence of Gaseous Barium Hydroxide," UCRL-11072, November (1963), ACS Meeting Paper, December (1963).

Searcy, A., and J. Carpenter, "The Decomposition Pressures of Alpha and Beta-Nb_5Ge_3 and the Thermodynamic Stability of $NbGe_2$," J. Phys. Chem. 67, 2144 (1963).

Anderson, H., "Determination of Ionization Pressure Gauge Sensitivity with a Mass Spectrometer," UCRL-10670, February (1963), Rev. Sci. Instr. 34 [6], 703 (1963).

Altman, R., "Vaporization of MgO and Its Reaction with Al," J. Phys. Chem. 67, 366-69 (1963).

Anthrop, D., "Vaporization and Thermodynamic Properties of Zinc Oxide" (Ph.D. Thesis), Ucrl-10708, May (1963).

Blue, G., J. Green, R. Bautista, and J. Margrave, "The Sublimation Pressure of Calcium(II) Fluoride and the Dissociation Energy of Calcium(I) Fluoride," J. Phys. Chem. 67, 877 (1963).

Blue, G., J. Green, T. Ehlert, and J. Margrave, "Dissociation Energies of the Alkaline Earth Monofluorides," Nature 199, 804 (1963); Bull. Am. Phys. Soc. 8, 112 (1963).

Blue, G., J. Green, T. Ehlert, and J. Margrave, "Mass Spectrometric Studies of Inorganic Fluorides," in Proceedings of 11th Conference on Mass Spectroscopy and Allied Topics, San Francisco, May (1963), pp. 344-49.

Miller, A., The Vapor Pressure of Indium Sulfides as Functions of Composition and Temperature" (Ph.D. Thesis) UCRL-10857, October (1963).

Munir, Z., "The Activation Energy for the Sublimation of Gallium Nitride" (Ph.D. Thesis) UCRL-10702, March (1963).

Washburn, C., "Vaporization of Iron Oxides" (M.S. Thesis), UCRL-10991, August (1963).

Sederholm and Associates

Sederholm, C., with R. Newmark, "The Time Weighted Average Approximation in the NMR Spectrum of $CF_2BrCFBrCl$," UCRL-10905, September (1963).

Sederholm, C., with S. Ng, "The Nuclear Magnetic Resonance Fluorine-Fluorine Coupling Constants," UCRL-11093, November (1963).

Thomas and Associates

Thomas, G., "Dislocation Substructures, Stacking Fault Energies, and Yield Stresses of Alpha Brasses," UCRL-10488, October (1962), J. Australian Inst. Metals 8, 80 (1963).

Thomas, G., "Origins and Multiplication of Dislocations," UCRL-10714, March (1963), AIME Western Metals Congress, May (1963).

Thomas, G., "The Effect of SRO on Stacking Fault Energy and Dislocation Arrangements in FCC Solid Solutions," UCRL-10751, April (1963), Acta Met. 11, 1369 (1963).

Thomas, G., "Heterogeneous Precipitation in Stainless Steel," UCRL-10596 January (1963), National Physical Laboratory Conference Proceedings, January (1963).

Thomas, G., "Electron Microscopy of Thin Films," UCRL-11009, October (1963), ASM Thin Film Conference Paper, October (1963).

Thomas, G., "Modern Metallographic Techniques," UCRL-11067, October (1963), Aerospace Materials Conference, Los Angeles, November (1963).

Thomas, G., with R. Nolder, "Mechanical Twinning in Nickel," UCRL-10646, January (1963), Acta Met. 8, 944-5 (1963).

Thomas, G., and J. Washburn, "Clustering of Vacancies and Hardening," UCRL-10674, February (1963), AIME Symposium on Point Defects, Rev. Mod. Phys. 35, 4, 992 (1963).

Thomas, G., and J. Washburn, Electron Microscopy and Strength of Crystals editor (Interscience Publishers, New York, 1963).

Thomas, G., with J. Hren, "Direct Observations of Precipitation in Thin Foils of Al-20% Ag Alloys," Trans. AIME 308, 227 (1963).

Thomas, G., with R. Finch, H. Queisser, and J. Washburn, "Structure and Origin of Stacking Faults in Epitaxial Silicon," J. Apply. Phys. 34, 406 (1963).

Thomas, G., with A. Eikum, "Effect of Solute Atoms Upon Vacancy Climb of Prismatic Dislocations in Al-5% Mg Alloy," J. Phys. Soc. Japan 18, III 98 (1963).

Thomas, G., with A. Eikum, "The Formation of Diamond-Shaped Prismatic Loops in Quenched FCC Metals," UCRL-10814, May (1963), J. Appl. Phys. 34, 3363 (1963).

Thomas, G., with J. Washburn and H. Queisser, "Extrinsic-Intrinsic Stacking Fault Pairs in Epitaxial Silicon," UCRL-10908, July (1963), Appl. Phys. Letters 3, 44 (1963).

Thomas, G., with W. Elkington, and J. Washburn, "On the Damage Produced by Moving Dislocations in MgO," UCRL-10354 Rev., January (1963), J. Am. Ceram. Soc. 6, 7 (1963).

Thomas, G., with L. Van Torne, "Yielding and Plastic Flow in Niobium," Acta Met. 11, 881 (1963).

Thomas, G. with O. Johari, "Substructure in Plastically Deformed Cu," UCRL-10932, Rev., October (1963).

Eikum, A., "Annealing of Vacancies in Quenched Aluminum Magnesium Alloy" (M.S. Thesis) UCRL-10879, September (1963).

Johari, O., "Substructures in Plastically Deformed Cu"(M.S. Thesis) UCRL-10932, September (1963).

Nolder, R., "The Substructure of Plastically Deformed Nickel," (Ph.D. Thesis) UCRL-10778, April (1963).

Roser, W., "Stacking Fault Energy, Ordering and Transgranular Stress Corrosion Cracking in Fe-Cr-Ni Alloys" (M.S. Thesis), UCRL-10890, June (1963).

Tobias and Associates

Tobias, C. W., with J. Klingert and S. Lynn, "Evaluation of Current Distribution in Electrode Systems by High-Speed Digital Computers," UCRL-10998, September (1963).

Newman, J., "Temperature Computed for Distillation," Hydrocarbon Process. Petrol. Refiner 42 [4], 141-144 (1963).

Grens, E., "'Fundamentals of Chemical Engineering,' by C. Thatcher: Book Review," Chem. Eng. News, pg. 65, March 25,(1963).

Grens, E., and R. McKean, "Temperature Maxima in Countercurrent Heat Exchangers with Internal Heat Generation," Chem. Eng. Sci 18, 291 (1963).

Washburn and Associates

Washburn, J., "Dislocation Multiplication," in Materials Science Research (Plenum Press, New York, 1963).

Washburn, J., "Sodium Chloride Structure," in Electron Microscopy and Strength of Crystals (Interscience Publishers, New York, 1963).

Washburn, J., with R. Finch, H. Queisser, and G. Thomas, "Structure and Origin of Stacking Faults in Epitaxial Silicon," J. Appl. Phys. 34, 406 (1963).

Washburn, J., with W. Elkington and G. Thomas, "On the Damage Produced by Moving Dislocations in MgO," J. Am. Ceram. Soc. 46, 7 (1963).

Washburn, J., with G. Thomas, "Clustering of Vacancies and Hardening," UCRL-10674, February (1963), AIME Symposium on Point Defects, February (1963).

Washburn, J., and G. Thomas, Electron Microscopy and Strength of Crystals (Interscience Publishers, New York, 1963).

Washburn, J., with W. Price, "On the Nature of the Dislocation Substructure in Deformed Copper," J. Australian Inst. Met. 8, 1 (1963).

Washburn, J., with J. Galligan, "Effect of Vacancy Clusters on Yielding and Strain Hardening of Copper," UCRL-10606 Rev., March (1963), Phil. Mag. 8, 93 (1963).

Washburn, J., G. Thomas, and H. Queisser, "Extrinsic-Intrinsic Stacking Fault Pairs in Epitaxial Silicon," UCRL-10908, July (1963), Appl. Phys. Letters 3, 44 (1963).

Washburn, J., with J. Strudel, "Direct Observations of Interactions Between Imperfect Loops and Moving Dislocations in Aluminum," UCRL-10959, October (1963).

Washburn, J., with J. Strudel and J. Vincotte, "Stacking Faults in Quenched Aluminum," UCRL-11025, October (1963), Appl. Phys. Letters 3, 148 (1963).

Washburn, J., with L. Toth, T. Cass, and S. Ravitz, "Determination of the Predominant Type of Stacking Fault in Cobalt by Nuclear Magnetic Resonance and Electron Microscopy," UCRL-11038, October (1963).

Washburn, J., and N. Subramanian, "Fatigue Deformation of Magnesium Oxide," UCRL-10749, March (1963), J. Appl. Phys. 34, 3394 (1963).

Galligan, J., "Effect of Vacancy Clusters on Yielding and Strain Hardening of Copper" (Ph.D. Thesis), UCRL-10606, January (1963).

Strudel, J., "Dislocation Substructure in Quenched Aluminum Single Crystals" (M.S. Thesis), UCRL-10793, June (1963).

Zackay and Associates

Zackay, V., "The Real and Ideal Strengths of the Common Structural Metals," UCRL-10811, June (1963).

Zackay, V., "Strength of Steel," Scientific American 209 [2], 72-82 (1963).

Zackay, V., "The Theoretical and Currently Attainable Strength-to-Weight Ratios of the Common Structural Metals and Alloys," AIChE Meeting, May (1963).

Zackay, V., F. Borik, and W. Justuson, "Fatigue Properties of an Ausform Steel," Trans. ASM (1963).

Pigford and Associates

Pigford, T., H. Shaked and D. Olander, "Calculation of the Fractional Release of Fission Gas from Solid Specimens During Post-Irradiation Anneal Experiments," Trans. Am. Nucl. Soc. 6 [1], 130-131 (1963).

Pigford, T., H. Shaked, and D. Olander, "Diffusion of Xe^{133} in Uranium Monocarbide," Trans. Am. Nucl. Soc. 6, [1], 131-132 (1963).

Pigford, T., with H. Shaked and D. Olander, "Diffusion of Xenon in Uranium Monocarbide," UCRL-10462, Rev.

Pigford, T., and J. de Ladonchamps, "Effective Concentration in Lumped Fuel for Reactivity Lifetime Analysis," Trans. Am. Nucl. Soc. 6 [2] (1963).

Pigford, T., and J. de Ladonchamps, "Effects of Flux Changes Upon Reactivity Lifetime and Burnup," Trans. Am. Nucl. Soc. 6 [2] (1963).

Lowe, S., "Fractional Release of a Tracer Element Through a Moving Boundary," (M.S. Thesis), UCRL-11097, October (1963).

REPORT INDEX